**Universidade de Aveiro** Departamento de Química
**Ano 2024**

**Mahtab Moradi**

# Modelação termodinâmica e experimental da separação de compostos quirais utilizando sistemas líquido-líquido compostos por solventes verdes

# Thermodynamic modeling and experimental study of chiral compounds separation using liquid-liquid systems based on green solvents

**Universidade de Aveiro** Departamento de Química
**Ano 2024**

**Mahtab Moradi**

# Modelação termodinâmica e experimental da separação de compostos quirais utilizando sistemas líquido-líquido compostos por solventes verdes

# Thermodynamic modeling and experimental study of chiral compounds separation using liquid-liquid systems based on green solvents

Dissertação apresentada à Universidade de Aveiro e Universidade de Tecnologia Amirkabi para cumprimento dos requisitos necessários à obtenção do grau de Doutor em Engenharia Química, realizada sob a orientação científica do Doutor Gholamreza Pazuki, Professor Associado do Departamento de Engenharia Química da Universidade de Tecnologia Amirkabir, coorientação do Professor João Manuel Costa Araújo Pereira Coutinho, Professor Catedrático do Departamento de Química da Universidade de Aveiro, e da Doutora Ana Maria da Conceição Ferreira Takahashi, Investigadora do Departamento de Química da Universidade de Aveiro.

*To my dearest mother, the source of my strength and the embodiment of unconditional love.*

**o júri**

Presidente

vogais

**agradecimentos**

In the culmination of this academic endeavor, I am filled with gratitude for the remarkable individuals who have played pivotal roles in shaping this journey. Their unwavering support, guidance, and kindness have been invaluable, and it is with immense appreciation that I express my thanks.

First and foremost, I extend my deepest gratitude to my mother, whose boundless love and unwavering support have been my constant source of strength. Your prayers and encouragement have been the bedrock upon which I have built my academic pursuits, and for that, I am truly grateful.

To my friends and Path members, your camaraderie has enriched this journey with laughter, shared experiences, and unforgettable moments. Thank you for being a source of joy and support, turning challenges into opportunities for growth.

To my supervisor, Dr. Pazuki, for his invaluable guidance and support. I am truly grateful for the opportunities to learn and grow under his mentorship.

I extend my sincere thanks to Prof. Joao for his mentorship, trust, and unwavering support. It has been a privilege to work under his mentorship, and the confidence he showed in my abilities has been a source of inspiration. His kindness has been a comforting beacon of light during challenging times in my life, making the journey not just educational but also enriching on a personal level.

Dr. Ana Maria deserves special appreciation for her continuous support and kindness. Her encouragement has extended beyond the academic realm, offering solace and understanding during the tough moments in my life. I am grateful for her generosity and compassion.

To all those who have been a part of this journey, whether in spirit or in person, your contributions have made this endeavor richer and more meaningful. Thank you for being an integral part of this chapter in my life.

**palavras-chave**

Extração líquido-líquido enantiosseletiva, Solventes eutéticos profundos, Estabilidade em água, Quiralidade, Seletor quiral, Ofloxacina, COSMO

**resumo**

Muitas moléculas biológicas importantes, como aminoácidos, açúcares e certos medicamentos, apresentam quiralidade (são enantiómeros). Embora os enantiómeros tenham propriedades físicas e químicas idênticas, podem ter efeitos fisiológicos diferentes. Portanto, métodos como a extração líquido-líquido enantiosseletiva (ELLE) são cruciais para obter o enantiómero desejado com a pureza necessária, de modo a alcançar medicamentos mais seguros e eficazes. Este estudo investiga o potencial dos solventes eutéticos profundos (DES) como uma alternativa sustentável e eficiente aos solventes orgânicos voláteis para a enantioseparação por ELLE, focando-se na separação dos enantiómeros da ofloxacina (OFX). O trabalho está dividido em três fases.

Primeiro, a estabilidade de diferentes DES hidrofílicos e hidrofóbicos em água foi investigada usando o Modelo de Screening Conductor-like (COSMO). Os resultados mostraram que os DES hidrofóbicos apresentavam maior estabilidade em água. Alterar as proporções molares e as concentrações dos componentes dos DES teve um efeito significativo na sua estabilidade. A validação experimental confirmou que, com o aumento da hidrofobicidade, a densidade e a solubilidade em água diminuíram, mas a viscosidade aumentou. Portanto, controlar a hidrofobicidade ou hidrofilicidade dos DES é crucial para o desenvolvimento de DES estáveis em água.

Em segundo lugar, foi investigada a capacidade de quatro grupos de DES hidrofóbicos - mentol: ácidos gordos, mentol: álcoois gordos, ácidos gordos: ácidos gordos e ácidos gordos: álcoois gordos - para extrair OFX de soluções aquosas. Numa triagem inicial com COSMO, os DES à base de ácidos gordos, especialmente aqueles com cadeias alquilas mais longas, provaram ser os mais eficazes. O DES, composto por ácido decanoico e ácido dodecanoico numa proporção molar de 2:1, foi validado por testes experimentais. Em condições ótimas - pH 5.2, proporção DES/água de 1.3 e concentração de OFX de 2.5 mg/ml - foi alcançada uma eficiência de extração de 98.8 ± 0.9%. Estes resultados sublinham a importância de selecionar solventes adequados e otimizar parâmetros de extração para aumentar a eficiência da extração.

Finalmente, a ELLE dos enantiómeros de OFX foi investigada usando DES hidrofóbicos e derivados de beta-ciclodextrina como seletivos quirais. A carboximetil-beta-ciclodextrina de sódio (CM-beta-CD) e o DES, composto por ácido decanoico e ácido dodecanoico numa razão molar de 2:1, surgem, respetivamente, como o seletor quiral e o solvente mais eficazes para a enantioseparação de OFX. Fatores como o valor do pH, a proporção de DES para água e a concentração do seletor quiral foram otimizados. Em condições ótimas - pH 3.6, proporção de DES para água de 1:2 e um excesso molar de 77 vezes do seletor quiral - uma seletividade de OFX (α) de 3.8 ± 0.3 foi alcançada numa única etapa.

Este trabalho destaca o potencial dos DES como solventes sustentáveis e eficientes para ELLE. Os DES oferecem uma alternativa ecológica aos solventes orgânicos voláteis e ajudam no desenvolvimento de processos farmacêuticos e químicos mais seguros e eficazes. São necessárias mais investigações para expandir o uso desses solventes, considerando fatores como segurança e biocompatibilidade. No entanto, os resultados sublinham a sua importância para o futuro dos processos de (enantio)separação.

**keywords**

Enantioselective liquid–liquid extraction, Deep eutectic solvents, Water stability, Chirality; Chiral selector, Ofloxacin, COSMO.

**abstract**

Many important biological molecules, such as amino acids, sugars, and certain drugs, exhibit chirality (they are enantiomers). Although enantiomers have identical physical and chemical properties, they can have different physiological effects. Therefore, methods such as enantioselective liquid-liquid extraction (ELLE) are crucial for obtaining the desired enantiomer with the required purity in order to achieve safer and more effective drugs. This study investigates the potential of deep eutectic solvents (DESs) as a sustainable and efficient alternative to volatile organic solvents for enantioseparation by ELLE, focusing on the separation of the enantiomers of ofloxacin (OFX). The research is divided into three phases.

First, the stability of different hydrophilic and hydrophobic DESs in water was investigated using the Conductor-like Screening Model (COSMO). The results showed that hydrophobic DESs had higher water stability. Morover, changing the molar ratios and concentrations of the DES components had a significant effect on their stability. Additinaly, experimental validation confirmed that with increasing hydrophobicity, the density and solubility in water decreased, but the viscosity increased. Therefore, controlling the hydrophobicity or hydrophilicity of DES is crucial for the development of stable DES in water.

Second, the ability of four groups of hydrophobic DESs - menthol: fatty acids, menthol: fatty alcohols, fatty acids: fatty acids and fatty acids: fatty alcohols - to extract OFX from aqueous solutions was investigated. In an initial screening with COSMO, DES based on fatty acids, especially those with longer alkyl chains, proved to be the most effective. The DES, composed of decanoic acid and dodecanoic acid in a molar ratio of 2:1, was validated by experimental tests. Under optimal conditions - pH 5.2, DES/water ratio of 1.3 and OFX concentration of 2.5 mg/ml - an extraction efficiency of 98.8 ± 0.9 % was achieved. These results underline the importance of selecting suitable solvents and optimizing extraction parameters to enhance extraction efficiency.

Finally, ELLE of OFX enantiomers was investigated using hydrophobic DES and beta-cyclodextrin derivatives as chiral selectors. Sodium carboxymethyl-beta-cyclodextrin (CM-beta-CD) and the DES, composed of decanoic acid and dodecanoic acid in a molar ratio of 2:1, respectively emerge as the most effective chiral selector and solvent for the enantioseparation of OFX. Morover, factors such as the pH value, the volume ratio of DES to water and the concentration of the chiral selector were optimized and under optimal conditions - pH 3.6, volume ratio of DES to water (1:2) and a 77-fold molar excess of the chiral selector - an OFX selectivity (α) of 3.8 ± 0.3 was achieved in a single step.

This work highlights the potential of DESs as sustainable and efficient solvents for ELLE. DESs offer a more environmentally friendly alternative to volatile organic solvents and contribute to the development of safer and more effective pharmaceutical and chemical processes. Although further research is still needed to expand the use of these solvents and systems, taking into account factors such as safety and biocompatibility, the results underline their importance for the further development of (enantio)separation processes.

**keywords** خراج مایع-مایع، حلال‌های اتکتیک عمیق، افلوکساسین، کایرال گزین، کازمو. ،

**abstract**

بسیاری از مولکول‌های مهم زیستی، مانند اسیدهای آمینه، قندها و داروهای خاص، کایرال (ترکیبی با دو انانتیومر) هستند. اگرچه انانتیومرها دارای خواص فیزیکی و شیمیایی یکسانی هستند، اما می توانند اثرات فیزیولوژیکی متفاوتی داشته باشند. بنابراین، روش‌هایی مانند استخراج مایع- مایع انانتیومرگزین (ELLE) برای به دست آوردن انانتیومر مورد نظر با خلوص مورد نیاز و به منظور دستیابی به داروهای ایمن تر و موثرتر بسیار مهم است. این مطالعه به بررسی پتانسیل حلال‌های اتکتیک عمیق (DESs) به عنوان یک جایگزین پایدار و کارآمد برای حلال‌های آلی فرار برای جداسازی انانتیومرهای افلوکساسین (OFX) توسط ELLE می‌پردازد. این کار به سه مرحله تقسیم می‌شود. ابتدا، پایداری DES های مختلف آب دوست و آبگریز در آب با استفاده از مدل غربالگری شبه هادی (COSMO) مورد بررسی قرار گرفت. نتایج نشان دادند که DES های آبگریز از پایداری آبی بالاتری برخوردار هستند. همچنین تغییر نسبت مولی و غلظت اجزای DES تأثیر معنی‌داری بر پایداری آن‌ها داشت. نتایج تجربی نیز تایید کردند که با افزایش آبگریزی، چگالی و حلالیت در آب کاهش می‌یابد، اما ویسکوزیته افزایش می‌یابد. بنابراین، کنترل آبگریزی یا آب دوستی DES برای توسعه DES های پایدار در آب بسیار مهم است. در مرحله دوم، توانایی چهار گروه از DES های آبگریز - منتول: اسیدهای چرب، منتول: الکل‌های چرب، اسیدهای چرب: اسیدهای چرب و اسیدهای چرب: الکل‌های چرب - برای استخراج OFX از محلول‌های آبی مورد بررسی قرار گرفت. در غربالگری اولیه با COSMO، DES های مبتنی بر اسیدهای چرب، به ویژه آن‌هایی که زنجیره‌های آلکیل طولانی‌تری دارند، مؤثرترین DES برای استخراج OFX بودند. توانایی DES، متشکل از اسید دکانوئیک و اسید دودکانوئیک در نسبت مولی 2: 1، در استخراج OFX با آزمایش‌های تجربی تایید شد. در شرایط بهینه – pH برابر با 5/2، نسبت حجمی DES-آب (v/v) برابر با 1/3، و غلظت افلوکساسین 2/5 میلی‌گرم بر میلی‌لیتر- راندمان استخراج 98/8±0/9 درصد به دست آمد. این نتایج بر اهمیت انتخاب حلال‌های مناسب و بهینه‌سازی پارامترهای استخراج برای افزایش کارایی استخراج تاکید می‌کند. در نهایت، انانتیومرهای OFX با استفاده از ELLE مبتنی بر DES آبگریز و مشتقات بتا سیکلودکسترین به عنوان انتخابگرهای کایرال مورد بررسی قرار گرفت. سدیم کربوکسی متیل بتا سیکلودکسترین (CM-beta-CD) به عنوان موثرترین انتخابگر کایرال و DES، متشکل از اسید دکانوئیک و اسید دودکانوئیک در نسبت مولی 2: 1، به عنوان مناسب‌ترین حلال برای جداسازی انانتیومرهای OFX انتخاب شدند. عواملی مانند مقدار pH، نسبت حجمی DES به آب و غلظت انتخابگر کایرال بهینه شدند. تحت شرایط بهینه - pH برابر با 3/6، نسبت حجمی DES-آب (v/v) برابر با 0/54 و نسبت مولی افلوکساسین-کایرال گزین (77:1)- حداکثر ضریب جداسازی افلوکساسین برابر با 3/0±8/3 در یک واحد استخراج به دست آمد. این کار پتانسیل حلال‌های DES را به عنوان حلال‌های پایدار و کارآمد در ELLE برجسته می‌کند. DES ها یک جایگزین زیست‌سازگار به جای حلال‌های آلی فرار هستند و به توسعه فرآیندهای دارویی و شیمیایی ایمن‌تر و موثرتر کمک می‌کنند. اگرچه هنوز تحقیقات بیشتری برای گسترش استفاده از این حلال‌ها و سیستم ها با در نظر گرفتن عواملی مانند ایمنی و زیست سازگاری مورد نیاز است اما با این وجود، نتایج به دست آمده بر اهمیت آن‌ها در توسعه بیشتر فرآیندهای جداسازی تاکید می‌کند.

**acknowledgement of use of AI tools**

I acknowledge the use of ChatGPT 3.5 (OpenAI, https://chat.openai.com) to summarize the initial notes and to proofread the final draft, the use of Office365 (Microsoft, https://www.office.com) for text writing and productivity, the use of COSMO-SAC and COSMO-RS (Software for Chemistry & Materials, https://www.scm.com/product/cosmo-rs/) for the calculations of activity coefficients and partition coefficients, the use of Material Studio (https://www.3ds.com/products/biovia/materials-studio) for the calculations of intractions between compounds and for Energy/Geometry optimization of the compounds, and Protimiza Experimental Design (https://experimental-design.protimiza.com.br/) for statistical analyses and representation of response surfaces.

## Contents

## List of tables

## List of figures

## List of symbols

| | | | |
|---|---|---|---|
| $[OFX]_{HDES}$ | Concentration of OFX in HDES phase | r | Distance between molecules |
| $[OFX]_{Water}$ | Concentration of OFX in water phase | T | Temperature |
| $a_i^{\alpha/\beta}$ | Activity of component *i* in phase α or β | $\frac{V_{HDES}}{V_{Water}}$ | Ratio of molar volume of HDES and water phases |
| $a_w$ | Water activity in (HBA+HBD+water) | $w_{OFX}^{HDES}$ | Weight of OFX in HDES phase |
| $a_{wA}^0$ | Water activity in (HBA+water) | $w_{OFX}^{water}$ | Weight of OFX in water phase |
| $a_{wB}^0$ | Water activity in (HBD+water) | wt% | Weight fraction percentage |
| $a_w$ | Water activity in (HBA+HBD+water) | $x_w$ | Mole fraction of water in (HBA+HBD+water) |
| $a_{wA}^0$ | Water activity in (HBA+water) | $x_{wA}$ | Mole fraction of water in (HBA+water) |
| $a_{wB}^0$ | Water activity in (HBD+water) | $x_{wB}$ | Mole fraction of water in (HBD+water) |
| $C_{0,O}$ | Total concentration in octanol-rich phase | $X_i$ | Independent variable i |
| $C_{0,W}$ | Total concentration in water-rich phase | $x_i^{\alpha/\beta}$ | mole fraction of component *i* in phase α or β |
| $C_{bot\ S/R-OFX}$ | Concentration of R-OFX or S-OFX in bottom phase | $\alpha_{R-OFX/S-OFX}$ | Selectivity of R-OFX or S-OFX |
| $C_{\mathrm{OFX}}$ | Concentration of OFX | $\gamma_i^{\alpha/\beta}$ | Activity coefficient of component *i* in phase α or β |
| $C_{top\ S/R-OFX}$ | Concentration of R-OFX or S-OFX in top phase | $\gamma_i^{O,\infty}$ | Activity coefficient of component *i* in oil phase at infinite dilution |
| $EE_{OFX}\,\%$ | Extraction efficiency of OFX | $\gamma_{i,s}$ | Activity coefficient of component (i) in solvent (S) |
| $K_i^{\alpha,\beta}$ | Partition coefficient of component *i* in phases α and β | $\gamma_{i,s}^C$ | Activity coefficient of component (i) in solvent (S) combinatorial part |
| $K_{\mathrm{OFX}}$ | Partition coefficient of OFX | $\gamma_{i,s}^R$ | Activity coefficient of component (i) in solvent (S) combinatorial part |
| $K_{\mathrm{OW}}$ | Octanol-water partition coefficient | $\gamma_i^{W,\infty}$ | Activity coefficient of component *i* in water phase at infinite dilution |
| $K_{S/R-OFX}$ | Partition coefficient of S-OFX or R-OFX | $\gamma_w$ | Water activity coefficient in (HBA+HBD+water) |
| $m_A$ | Molality of HBA in the mixtures | $\gamma_{wA}^0$ | Water activity coefficient in (HBA+water) |
| $m_B$ | Molality of HBD in the mixtures | $\gamma_{wB}^0$ | Water activity coefficient in (HBD+water) |
| Mw | Molecular Weight | $\mu_{OFX}^{DES}$ | Chemical potential of the OFX in DES phase |
| $\mathrm{p}K_a$ | Acidic dissociation constant | $\mu_{OFX}^{W}$ | Chemical potential of the OFX in water phase |
| R | Universal Gas Constant | σ | Polarized charge distribution |
| $R^2$ | Correlation coefficient | | |

## List of abbreviations

| | | | |
|---|---|---|---|
| ABS | Aqueous biphasic system | Ga | gallium |
| Al | Aluminium | GC | Gas chromatography |
| ANOVA | Analysis of variance | HBA | Hydrogen bond acceptors |
| APIs | Active Pharmaceutical Ingredients | HBD | Hydrogen bond donors |
| ATPE | Aqueous two-phase biphasic extraction | HDES | Hydrophobic deep eutectic solvent |
| β-CD | β-Cyclodextrin | H NMR | Proton nuclear magnetic resonance |
| BRCE | Biphasic recognition chiral extraction | HP-β-CD | Hydroxypropyl-β-cyclodextrin |
| CCRD | Central composite rotatable design | HPLC | High performance liquid chromatography |
| CE | Capillary electrophoresis | IL | Ionic liquid |
| [Ch]Cl | Choline chloride | In | Indium |
| CILs | Chiral ionic liquids | L-TA | L-tartaric acid |
| Cl | Chlorine | LEC | Ligand Exchange Chromatography |
| CM-β-CD | Carboxymethyl-β-cyclodextrin sodium salt | LECE | Ligand Exchange Capillary Electrophoresis |
| Co | Cobalt | LLE | liquid-liquid extraction |
| COSMO | Conductor-Like Screening Model | LLME | liquid-liquid microextraction |
| COSMO-RS | Conductor-like Screening Model for Real Solvent | LM-DTTA | (+)-Di-p-toluoyl-D-tartaric acid |
| COSMO-SAC | Conductor-like Screening Model-Segment Activity Coefficient | NaF | Sodium fluoride |
| Cr | Chromium | Ni | Nickel |
| CSP | Chiral stationary phases | OFX | Ofloxacin |
| Cu | Copper | PEG | Polyethylene glycol |
| DES | Deep eutectic solvent | PPCPs | Pharmaceuticals and personal care products |
| $D_2EHPA$ | Di-(2-ethylhexyl)-phosphoric acid | PsC | Preparative-scale chromatography |
| $D_2O$ | Deuterated water | QSARs | Quantitative structure-activity relationships |

| | | | |
|---|---|---|---|
| DBTA | (N,N'-dibenzoyl-L-tartaric acid) | RDF | Radial distribution function |
| DFT | Density functional theory | RMSD | Root mean square deviation |
| DIPT | (+)-Diisopropyl L tartrate | RSM | Response surface methodology |
| ELLE | Enantioselective liquid–liquid extraction | S-β-CD | Sulfated-β-cyclodextrin sodium salt |
| EMA | European Medicines Agency | SFC | Supercritical fluid chromatography |
| EPA | Environmental Protection Agency | Sn | Tin |
| ES | Eutectic solvent | SPE | Solid phase extraction |
| Fe | Iron | TLC | Thin-layer chromatography |
| FDA | Food and Drug Administration | VLE | Vapor−liquid equilibrium |
| F NMR | Fluorine-19 nuclear magnetic resonance | Zn | Zinc |
| FT-IR | Fourier transform infrared | | |

# 1. INTRODUCTION

## 1.1. General Introduction

Chirality is a geometric property exhibited by certain molecules, characterized by the presence of an asymmetric carbon, rendering them non-superposable onto their mirror images (Figure 1.1). Enantiomers, comprising a chiral compound and its mirror image, form an equimolar mixture known as a racemic mixture [1]. Enantiomers are commonly denoted as D (dextro) or L (levo), R (rectus) or S (sinister), (+) or (−), and P (plus) or M (minus) [2]. Despite enantiomers sharing similar physical and chemical properties, their stereoscopic and spatial arrangements result in divergent pharmacological and toxicological effects [3]. Consequently, one enantiomer may exhibit efficacy, while its counterpart may prove ineffective or even harmful [1, 3]. The enantiomer responsible for a biological activity is called the "eutomer," while its less active or inactive counterpart is known as the "distomer" [4].

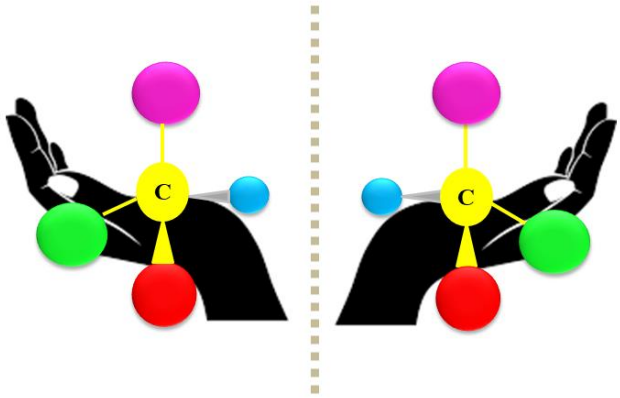


**Figure 1.1.** Generic representation of a chiral structure with two non-superimposable forms as an analogy to two hands.

Piutti pointed out the different biological effects of enantiomers as early as 1886 [5]. The pharmacodynamic differences of enantiomers can be categorized into four groups, as detailed in Table 1.1. However, it was only a century later, in the late 1950s and early 1960s, that the infamous "thalidomide scandal" came to light. It turned out that the (R)-isomer of thalidomide, which was originally marketed as a racemic mixture, had the desired effects, while the (S)-isomer proved to be teratogenic and caused severe birth defects. This tragic incident, administered widely to relieve nausea in pregnant women, affected over 10,000 embryos [6, 7]. The impact of this incident led to increased scrutiny of the stereochemistry of drugs and subsequently to the introduction of stricter regulations by regulatory authorities worldwide. In 1992, the Food and Drug

Administration (FDA) introduced comprehensive guidelines for the pharmaceutical development of both single enantiomers and racemates [4, 8]. As a result, pharmaceutical companies must submit detailed toxicological and pharmacological data for each enantiomer and the corresponding racemate in order to market a drug in its racemic form [4].

**Table 1.1.** Classification of the different biological effects of enantiomers [9, 10].

| Group | Pharmacology | Example |
|---|---|---|
| **Group A** | Racemic compound with one major bioactive enantiomer. | Ofloxacin (OFX): Antibacterial activity levofloxacin (S-OFX) is 8–128 times higher than R-OFX. |
| **Group B** | Racemic compound with independent therapeutic effects through action on different targets. | Methorphan: L-enantiomer is potent opioid analgestic while D-enantiomer is a cough suppressant. |
| **Group C** | Racemic compound where one enantiomer may induce undesirable side effects. | Ethambutol: S-enantiomer possesses anti-tuberculotic effect while R-enantiomer causes blindness. |
| **Group D** | Racemic compound where one enantiomer may attenuate the efficacy of the active enantiomer. | Citalopram: S-enantiomer is active while R-enantiomer is inactive. |

Therefore, recent trends in medicinal chemistry show an increasing tendency towards using pure enantiomers to reduce the toxicity or side effects associated with inactive enantiomers [3, 4] (Figure 1.2). As shown in Figure 1.2, most medications approved by the US Food and Drug Administration in recent years have been marketed in their enantiomerically pure form [6]. Consequently, exploring new methods to obtain pure chiral compounds is crucial for drug development [3].

There are currently three main methods for obtaining pure enantiomers: (i) extraction of natural chiral drugs, (ii) asymmetric synthesis and (iii) chiral separation (or also known as enantiomer separation). The extraction of natural chiral drugs has its limitations due to the limited number and type of natural chiral compounds available in combination with the complicated extraction procedures. Asymmetric synthesis, which involves both non-enzymatic and enzymatic approaches, requires highly enantiomerically pure raw materials and/or exceptionally stereospecific catalysts, making it a costly method limited by the number of reactions required to obtain highly enantiomerically pure

compounds. In contrast, chiral separation of racemic compounds proves to be an optimal approach to obtain pure enantiomers [3].

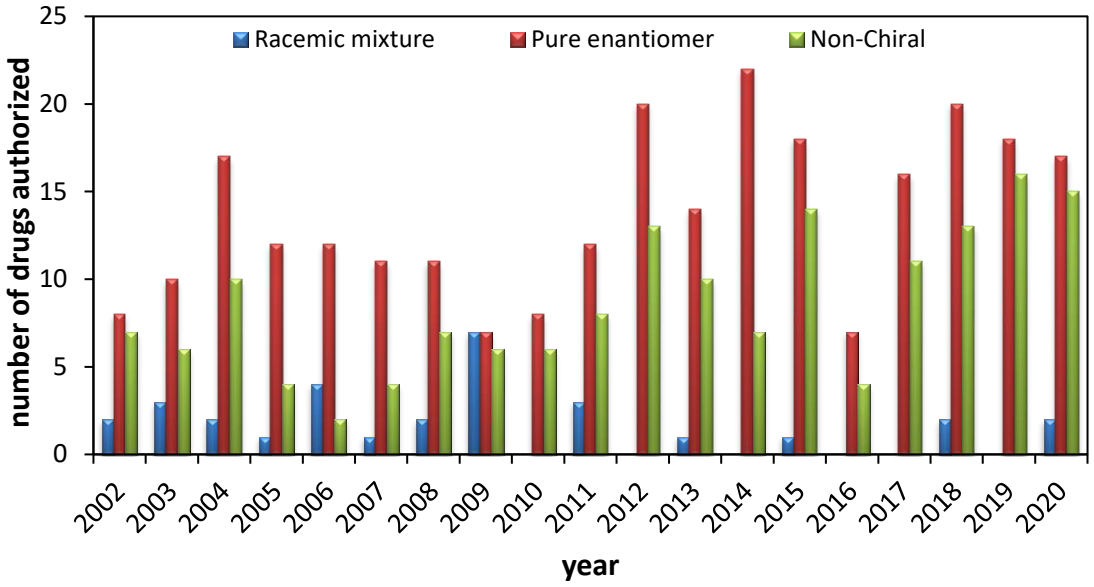


**Figure 1.2.** The annual number of drugs authorized by the FDA for the period 2002 to 2020 [11, 12].

Chiral separation is particularly attractive because it resolves racemic mixtures into individual enantiomers without requiring complex synthetic routes or relying on limited and costly natural chiral sources, making it a more cost-effective method applicable to a wide variety of compounds [13]. In this method, the introduction of a chiral selector is essential for improving separation efficiency and enantioselectivity. The chiral selector interacts at the intermolecular level and forms complexes with different stabilities for each enantiomer, facilitating selective enantiomer separation [14]. The various chiral separation methods include crystallization, capillary electrophoresis (CE), gas chromatography (GC), high-performance liquid chromatography (HPLC), supercritical fluid chromatography (SFC), and enantioselective liquid–liquid extraction (ELLE). The percentage use of these methods/techniques for the enantiomer separation of chiral compounds is shown in Figure 1.3. As shown, HPLC is the most commonly used technique for enantioseparation. In contrast, ELLE, a newer method, is used less frequently compared to other techniques. However, ELLE has recently gained attention due to its ability to efficiently separate enantiomers under mild conditions while preserving the integrity of sensitive molecules. It is also scalable, making it suitable for both laboratory and industrial applications [9]. Figure 1.4 shows a schematic representation of the most common techniques for obtaining enantiomerically pure

compounds. Each technique has its own advantages and limitations, which are described in more detail below.

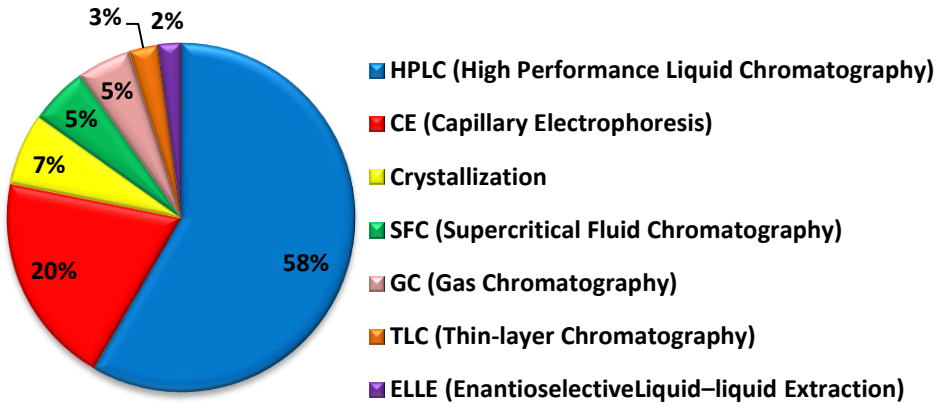


**Figure 1.3.** Percentage of published articles on enantioseparation of chiral compounds by different enantiomer separation techniques. Data obtained from SciFinder Scholar up to May 2024.

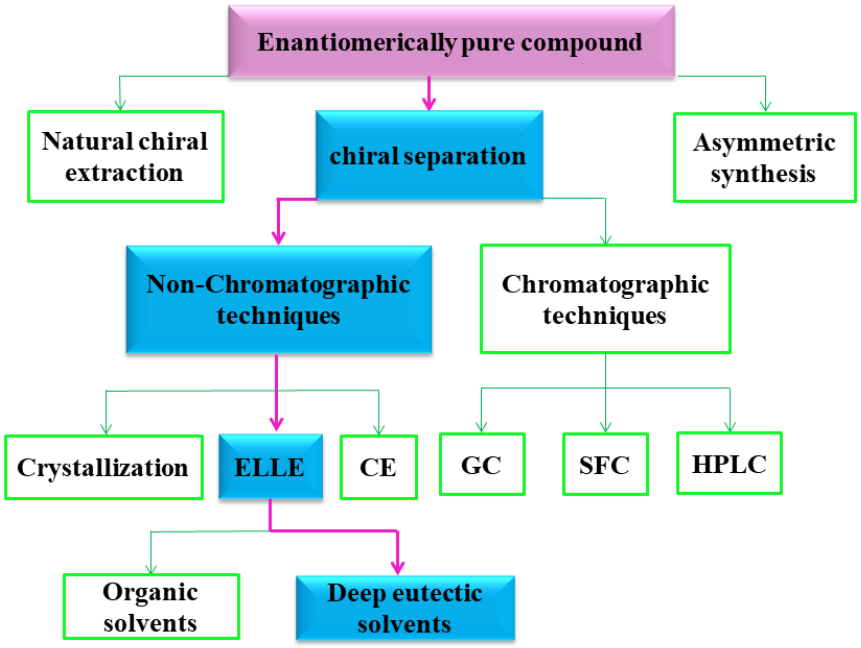


**Figure 1.4.** Summary of the (green lines) most used techniques to obtain enantiopure compounds, and (pink lines) alternative methods utilizing deep eutectic solvents (DESs)-based ELLE employed in this thesis.

**Gas Chromatography (GC).** It is a method employed to separate components in the gas phase, requiring that the compounds possess sufficient volatility and thermal stability for analysis. GC stands out for its elevated peak efficiency when compared to

other chromatographic methods. However, it does come with certain limitations: it is exclusively applicable to thermostable and volatile compounds, the options for stationary and mobile phases are restricted, and its utility for preparative purposes is not straightforward [9].

**High-Performance Liquid Chromatography (HPLC).** It is extensively used in both the analytical and preparative separation of enantiomers, playing a crucial role in both industrial and academic research settings. The fundamental principle of chiral chromatography lies in the chiral stationary phase's capability to interact differentially with each enantiomer, forming transient diastereomeric complexes with distinct free energy of formation [9]. While HPLC boasts advantages such as the separation of thermolabile and nonvolatile compounds, a diverse array of chiral stationary phases/chiral selectors, and high efficiency in chiral compound separation [9], the broader adoption of preparative-scale chromatography seems less prevalent than analytical methods. This discrepancy is related to the substantial solvent requirements and the limited availability of chiral stationary phases under high-pressure conditions [2, 15].

**Supercritical Fluid Chromatography (SFC).** It combines the attributes of both HPLC and GC, often employing low-viscosity, high-diffusion supercritical $CO_2$ or $N_2O$ as the mobile phase. This choice not only diminishes solvent consumption by 60–70% but also reduces operating costs by 70–80% [2, 9]. Demonstrating industrial capability in resolving at least 95% of racemates, SFC has emerged as a robust competitor to HPLC, renowned for its exceptional solvent compatibility, enantioselectivity, and minimal residence time [2]. However, SFC does have limitations, including a lower degree of flexibility in adjusting separation based on the mobile phase compared to HPLC. Additionally, the solubility of polar compounds in SFC mobile phases is constrained, necessitating the use of alcohols or other polar modifiers, and there is currently no alternative separation principle as versatile as HPLC [9].

**Crystallization.** It is known as a predominant technique for the industrial resolution of racemic compounds into their enantiomers. In this procedure, diastereomeric salts are formed through the interaction of bases and acids. The resolving agent, employed to distinguish between enantiomers, is designed to be easily removable and recyclable [9, 16]. Despite its operational simplicity, cost-effectiveness, and compatibility with other techniques, crystallization has significant drawbacks. Notably, it is time-consuming, labor-intensive, and not easily automatable. Sourcing the resolving agent can be

challenging, posing a potential risk of contamination in the final product. Furthermore, the maximum chemical yield of enantiomers in this process, without involving racemization, is limited to 50% [9].

**Capillary Electrophoresis (CE).** It is a separation technique renowned for its high efficiency, as well as its minimal consumption of reagents and samples [9]. For enantioseparation, the crucial principle lies in the stereoselective interaction between the chiral selector and the analyte enantiomers [17]. In CE, distinctions in complexation equilibria between analyte enantiomers and the selector, coupled with electroosmotic flow generated by the high electric field applied to the ends of the separation capillary, influence mobile phase and analyte transport within the background electrolyte [18]. Notably, CE eliminates the need for expensive chiral columns, as a small quantity of a chiral selector is introduced into the background electrolyte. Chiral CE excels in swiftly screening optimal conditions, given its generally faster enantiomeric separation and the absence of prolonged equilibration times when transitioning between different chiral background electrolytes. However, it is essential to note that CE is not suitable for gaseous molecules and is not applicable for preparative purposes [9].

**Enantioselective Liquid–Liquid Extraction (ELLE).** It emerges as a cost-effective, rapid, and versatile method that is easy to operate and scalable, offering low solvent consumption. ELLE provides an advantageous solution by avoiding the use of chiral stationary phases, although it may sacrifice some enantioselectivity compared to alternative methods [2, 19]. In ELLE, the complex that the chiral selector forms with one of the enantiomers preferably has a different partitioning behavior than the other enantiomer to ensure effective enantioseparation. In addition, the composition of ELLE also has a significant influence on enantiomer separation. Therefore, the careful selection of the phase composition and the chiral selector is crucial for the adaptability and versatility of the process. However, conventional ELLE systems often contain organic solvents, which can pose problems in terms of volatility, flammability and toxicity. In addition, polymer-based ELLE processes struggle with issues such as high viscosity and a limited polarity range, which affects extraction efficiency and selectivity. To overcome these problems, ELLE methods based on new alternative solvents such as ionic liquids (ILs) and deep eutectic solvents (DESs) have gained much attention [2, 20]. Figure 1.5 shows the number of published articles on ELLE using either conventional organic solvents or more environmentally friendly alternatives. As illustrated, most ELLE methods still rely on organic solvents for enantioseparation, while only a few

studies investigate DES-based ELLE for this purpose. Therefore, further research is needed to fill the gaps in the use of DES-based ELLE for the separation of chiral compounds and to promote more sustainable and efficient extraction methods.

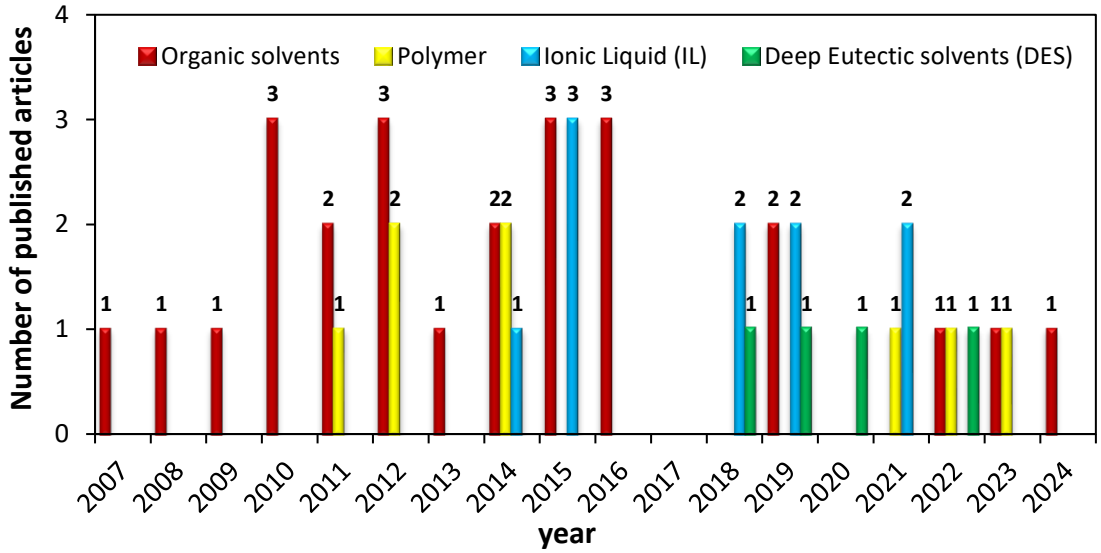


**Figure 1.5.** Number of published articles per year related to conventional ELLE (organic solvent) and ELLE based on alternative solvents (i.e., polymer, ionic liquid (IL), deep eutectic solvent (DES)). Data obtained from SciFinder Scholar up to May 2024.

## 1.2. Scopes and Objectives

The current work focuses on the development and design of cost-effective, sustainable, and integrated extraction/recovery platforms using deep eutectic solvents (DESs) based on liquid-liquid extraction (LLE). The core objective of this thesis is to explore and investigate the applicability of DES-based LLE for the efficient and biocompatible separation of racemic ofloxacin (S/R-OFX) through enantioselective liquid–liquid extraction (ELLE), which represents an innovative alternative to conventional techniques.

OFX was chosen as a model racemate due to the different effects of its enantiomers, in particular, S-OFX shows 8–128 times higher antibacterial activity than R-OFX [21]. In addition, OFX is the second most widely used drug in the fluoroquinolone category, which is also a significant environmental concern as an emerging pollutant [10, 21]. Since the body absorbs less than 10% of OFX and excretes the remaining 90% in urine and feces [10], significant amounts of OFX enter water sources both in its original chemical form and in the form of metabolites [22]. This phenomenon raises significant

environmental concerns, particularly with regard to bacterial resistance, which has received considerable scientific attention [10, 22].

DES-based LLE/ELLE were selected as a cost-effective and environmentally friendly extraction/separation technology. DESs were chosen as alternative solvents due to their remarkable biocompatibility, biodegradability, ease of synthesis, cost-effectiveness, and wide availability of raw materials, leading to more than a million possible combinations [23, 24]. DESs are characterized by their high solvation capacity for organic and inorganic compounds and serve as improved stabilization media for proteins, nucleic acids, and various other substances. Their unique design capabilities have led to extensive research in a variety of applications over the past decades [23, 24].

In order to determine the optimal DESs and conditions for the enantioseparation of OFX, this study was divided into three phases. First (**Chapter 2**), a comprehensive screening of different DESs, both hydrophilic and hydrophobic, was performed using the Conductor-like Screening Model-Segment Activity Coefficient (COSMO-SAC) to identify the most stable DESs in the presence of water while maintaining low viscosity. Secondly (**Chapter 3**), those DESs that exhibited both high water stability and low viscosity were selected for further evaluation of their performance in the separation of OFX by LLE. The systems were evaluated both computationally and experimentally. This study provided valuable insights to identify the most effective phase formers - DESs - for the optimal extraction of OFX. Finally, (**Chapter 4**), the efficiency of the most promising DES-based systems in the enantioseparation of S/R-OFX using β-cyclodextrin (β-CD) and its derivatives, such as hydroxypropyl-β-cyclodextrin (HP-β-CD), carboxymethyl-β-cyclodextrin sodium salt (CM-β-CD) and sulfated-β-cyclodextrin sodium salt (SBE-β-CD), as chiral selectors were evaluated. In addition, parameters such as pH, DES-water ratio, OFX concentration and excess chiral selector were optimized using response surface methodology (RSM) in Chapters 3 and 4 to refine the extraction conditions for OFX and improve its enantiomeric separation. An overview of the work performed in this thesis can be found in Figure 1.6.

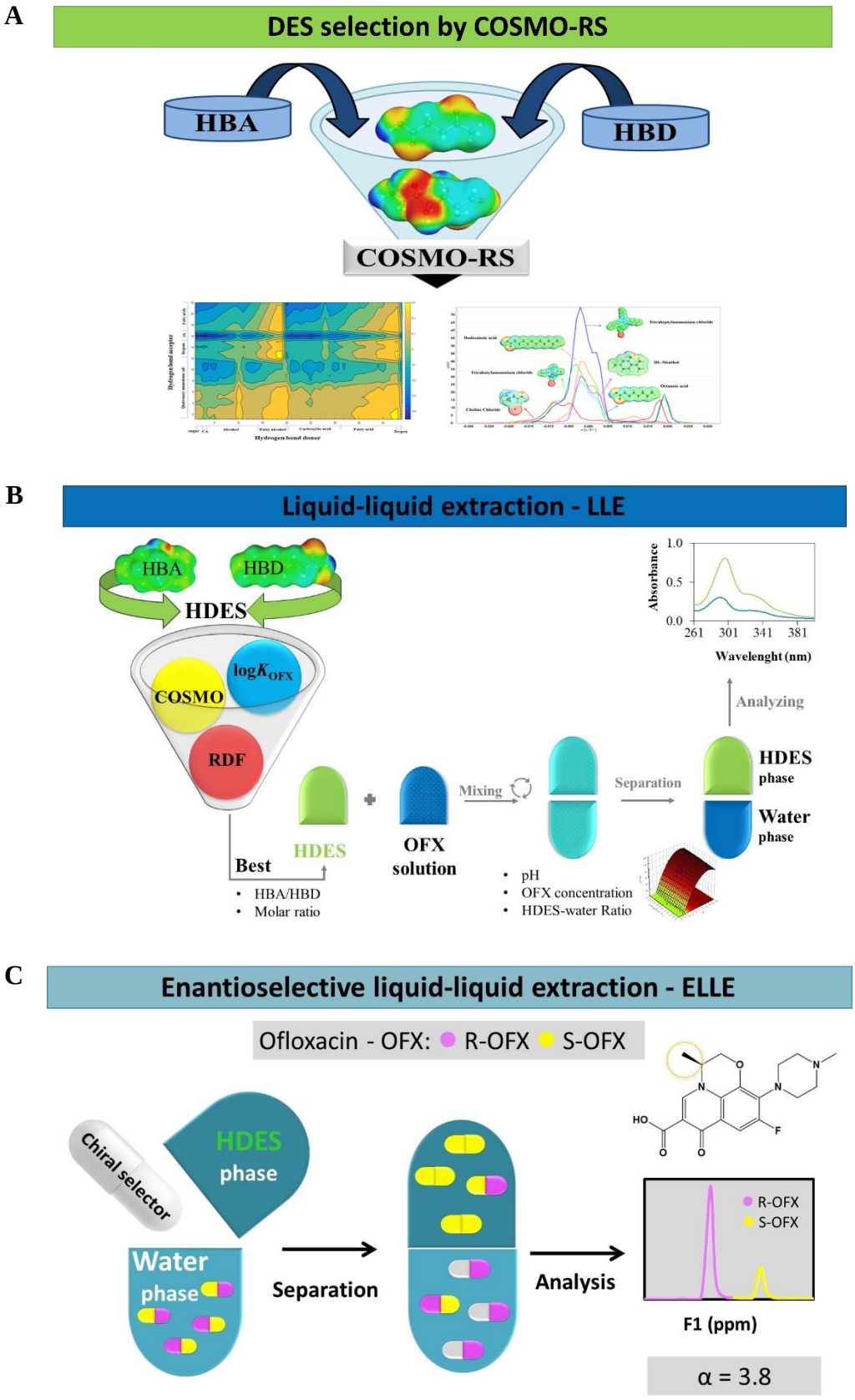


**Figure 1.6.** Layout of the current thesis: (**A**) Chapter 2, (**B**) Chapter 3, (**C**) Chapter 4.

## 1.3. Deep eutectic solvents (DESs)

Solvents play a crucial role in various applications ranging from drug delivery and discovery to the extraction of biologically important compounds. Despite the considerable potential that volatile organic solvents have in these applications, their disadvantages, such as high volatility, toxicity and environmental harmfulness, are becoming increasingly apparent [25]. Therefore, there is a growing interest in the chemical industry and research community to integrate "green and sustainable solvents" in line with the twelve key green principles. In the last two decades, ILs have emerged as the most important candidates among these green solvents, as described in the literature [25, 26]. Known for their non-volatility, non-flammability, thermal stability, and ease of handling, these liquids have garnered significant attention as environmentally friendly solvents. On the other hand, despite the remarkable success in the use of ILs in many applications, these substances have been criticized for their environmental impact, toxicity, high cost of starting materials, complicated synthesis procedures, difficult purification, and complex regeneration cycles [26]. In view of these problems, DESs have emerged as a promising alternative due to their biocompatibility, biodegradability and cost-effectiveness. As a result, the development and application of DESs have experienced a significant growth [26, 27]. However, the assessment of toxicity can be controversial and depends on the specific DESs rather than the class as a whole. The use of natural DESs consisting of components of natural origin, such as sugars, polyols, organic acids and amino acids, could further reduce toxicity while ensuring a low price [28, 29].

The definition of "deep eutectic solvents" (DESs) is somewhat unclear, as there is no generally accepted definition among authors. The term was first coined by Abbott et al. [30] to describe mixtures of cholinium chloride with urea whose melting points are significantly lower than those of the pure compounds. This lowering of the melting point is attributed to the formation of a hydrogen bond complex between a hydrogen bond donor (HBD) and a hydrogen bond acceptor (HBA) in a precisely defined stoichiometric ratio. However, the definition of a solvent as a DES requires more than the mere presence of a eutectic point or a hydrogen bond between the components. This distinction is crucial because all mixtures of immiscible solid compounds have a eutectic point and numerous compounds can form hydrogen bonds when combined [31]. Furthermore, determining the exact "depth" of eutectic solvents (ESs) can be difficult

and is not essential for many applications. Therefore, more recently, Martins et al. [32] suggest that the term "eutectic solvent" (ES) is more appropriate for mixtures that do not strictly fulfill the classical DES criteria. These mixtures are primarily characterized by the fact that the temperature of the eutectic point is lower than expected for an ideal mixture, indicating a negative deviation from ideality. In addition, their reduced temperature should ensure that they remain liquid at the operating temperature within their specific composition range [31, 32]. For simplicity, all eutectic mixtures are referred to as DES in this work, although some of them do not strictly fulfill the classical criteria.

The interactions among DES components namely, HBAs and HBDs, primarily involve hydrogen bonds. Nevertheless, van der Waals interactions and occasional electrostatic forces are also present. Notably, most of these interactions manifest as intermolecular bonds, typically forming between the halide anion, commonly employed as an HBA, and the HBD. It is worth noting that, depending on the specific components involved, hydrogen bonds between HBDs are also possible, contributing to the generation of even more complex structural networks [23].

There are different types of DESs in which an HBD is combined either with an inorganic halide or, more commonly, with an organic halide that serves as an HBA. DESs composed of organic halide salts can be characterized by the generic molecular formula $Cat^+ X^- zY$, where $Cat^+$ can be an ammonium, phosphonium, or sulfonium cation; $X^-$ is a Lewis base, typically a halide anion; and $Y$ is a Lewis acid (such as a metal salt) or an HBD (like a Brønsted acid), forming a complex anionic species with $X^-$ [27]. The classification of DESs into four types based on the composition of the binary mixture was described by Emma et al. [27] and Abbott et al. [30]. Table 1.2 provides an overview of these classifications. Type I DESs consists of a metal chloride in combination with a quaternary organic ammonium salt. Type II DESs are formed by a metal chloride hydrate in combination with an organic salt. Type III, the most extensively studied in the literature, is notable for its versatility as a solvent, effectively interacting with a broad spectrum of oxides and transition metal ions. This type involves an HBD, such as an organic acid, amides, amino acids, alcohols, or other natural compounds, mixed with a quaternary ammonium salt structurally resembling ILs [25, 27, 30], as HBA. The importance of Type III DESs lies in their ability to solubilize a diverse range of transition metal species [26]. Type IV comprises a combination of an HBD and a metal chloride, typically in hydrate form. A recent addition to this

classification is the emergence of Type V DESs, a non-ionic category displaying pronounced negative deviations from ideality and a significant depression of the melting point. This type employs non-ionic compounds to create mixtures with low freezing points, representing a novel class within the DESs spectrum [25].

**Table 1.2.** Classification of DESs [26].

| Type | General formula | Mixture composition | Example |
|---|---|---|---|
| **I** | $Cat^+ X^- zMCl_x$<br>M = Zn, Sn, Fe, Al, Ga, In | Metal salt ($MCl_x$) + organic halide salt ($Cat^+ X^-$) | $ZnCl_2$ + |
| **II** | $Cat^+ X^- zMCl_x \cdot yH_2O$<br>M = Cr, Co, Cu, Ni, Fe | Metal salt hydrate ($MCl_x \cdot yH_2O$) + organic halide salt ($Cat^+ X^-$) | $CoCl_2 \cdot 6H_2O$ + [Ch]Cl |
| **III** | $Cat^+ X^- zRZ$<br>Z = amide, carboxylic acid, or alcohol group | HBD (RZ) + organic halide salt ($Cat^+ X^-$) | Urea + [Ch]Cl |
| **IV** | $MCl_x + RZ = MCl_{x-1}^+ \cdot RZ + MCl_{x+1}^-$<br>M = Al, Zn Z = amide or alcohol group | HBD (RZ) + inorganic halide salt ($MCl_X$) | Urea + $ZnCl_2$ |
| **V** | Non-ionic DES | Composed only of molecular substances | Thymol + methanol |

Note: The abbreviated names of the compounds are listed in the Table of Abbreviations.

The predominant method for preparing DESs is to heat and stir their components in a specific molar ratio until a uniform liquid is formed. Alternative methods for producing DESs include vacuum evaporation, milling, and freeze-drying. In evaporation, the ingredients are dissolved in water, and most of the water is then evaporated at 50 ºC under vacuum conditions. The resulting combination is stored in a desiccator with silica gel until it reaches a stable weight. For grinding, the two solid components are mixed in a mortar, usually under nitrogen or in a glove box, until a clear, homogeneous liquid is produced. In the freeze-drying process, both the HBDs and HBAs are dissolved in about 5% water. These two solutions are combined, frozen, and freeze-dried to obtain a clear and homogeneous liquid. The most widely used method is still heating and stirring the DES components to ensure that a characteristic molar ratio is maintained during the process in an inert atmosphere, ultimately resulting in a homogeneous liquid [33].

### 1.3.1. Physicochemical properties of deep eutectic solvents (DESs)

DESs exhibit a distinctive array of physicochemical properties that make them valuable as potential solvents in various industries. These properties include density, freezing

temperature, viscosity, surface tension, miscibility, conductivity, and polarity, among others. The exceptional versatility of DESs arises from the numerous formulations possible through different combinations of HBAs and HBDs, earning them the title of "designer solvents." The specific pairing of HBA and HBD creates a wide range of DESs, each with its unique physicochemical profile. This diversity allows for the intentional manipulation of DES properties by employing various combinations of HBA and HBD in different molar ratios. Additionally, factors such as the molar ratio of HBA to HBD, purity, temperature, water content, and preparation method significantly influence the resulting physicochemical characteristics of DESs [23]. Evaluating the physicochemical properties of DESs is crucial for their use as solvents in chemical processes. Designing DESs for specific applications requires a thorough understanding of their physicochemical characteristics. Precise knowledge of key properties such as density, speed of sound, refractive index, and viscosity is essential for their effective industrial deployment as solvents across various operational unit processes [23, 27].

**Density.** The PVT (pressure-volume-temperature) data, specifically the densities of DESs, are pivotal parameters with broad implications for equipment and process design. These data play an important role in many aspects, such as liquid–liquid equilibria, mass transfer, the formulation of equations of state and predictive models, and the calculation of thermodynamic properties like viscosity, expansion coefficient, and isothermal compressibility [26]. The densities of DESs are intricately linked to several factors, including temperature, the nature of HBDs and HBAs, the molar ratio of HBA to HBD, and the method of preparation [25, 26]. Literature highlights that, in general, DES densities surpass those of water and are typically higher than the density of the HBD, except in the case of certain hydrophobic DESs (HDESs) [25, 26, 34]. An insightful perspective on the variation of DES density concerning different factors is provided by the Hole theory [35]. According to this theory, DESs can be conceptualized as compositions of holes, and the properties of DESs are intricately linked to the available holes' approximate dimensions and sizes, representing mobile species. As DESs form, the addition of HBD to HBA alters the average hole size, consequently influencing the density of the DES. Therefore, changes in DES density can be attributed to the dynamic molecular interactions and the availability of free volumes within the DES [26]. The density of DESs exhibits a linear decrease as temperature rises [25, 26, 34]. This decline in DES density with increasing is due to the increased free spaces between the HBA and HBD within the DES. In other words, elevating the temperature

increases the amount of free space in the DES, facilitating a swifter movement of molecules and consequently resulting in a reduction in the density of the DES [26, 34]. Significant differences in density were found depending on the chain length of the HBD. As the chain length of the HBD increases, the density decreases accordingly [25, 34]. This correlation indicates that the longer alkyl chain length contributes to an increase in free volume, which ultimately leads to a decrease in density [34]. Conversely, an increase in the number of hydroxyl (–OH) functional groups in the HBD results in a higher count of hydrogen bonds. This, in turn, reduces the available free spaces and consequently raises the density of DESs [26]. A similar pattern occurs when the number of aromatic groups or alkyl chains in organic acids increases, with the density changes reflecting the changes in the free volume of DESs [26]. In addition, the density decreases with increasing water content as the number of hydrogen bonds decreases. This decrease leads to an increase in the free volume of DESs [26].

**Viscosity.** It is a crucial physical property of DESs, closely related to their transport properties and resulting conductivities [26, 34]. Most DESs are known to be viscous liquids at room temperature. This viscosity is attributed to the presence of an intricate hydrogen bonding network, along with additional interactions such as van der Waals and electrostatic forces between the HBD and HBA components of DESs. These interactions collectively contribute to high viscosity and reduced ion mobility within the limited void volume of liquid DESs [35]. Given the aspiration to use DESs as green solvents, there is a recognized need for lower viscosity to enhance their viability in such applications. The viscosity of DESs is primarily influenced by the chemical nature of HBAs and HBDs. Certain compounds, such as carbohydrates like xylitol and sorbitol or carboxylic acids like malonic acid, exhibit increased viscosity when used as HBDs due to the formation of extensive intermolecular hydrogen bonds. Additionally, the introduction of an –OH or –COOH group contributes to an increase in DES viscosity, likely due to the strengthening of hydrogen bonding [26]. Several reports emphasize the importance of the molecular structure of HBAs and HBDs, including factors such as molecular weight and size, for the mobility of the overall system. In this context, the viscosities of DESs show an upward trend with increasing molecular weight of HBAs and HBDs [27]. Higher molar ratios of HBA to HBD generally increase viscosities in DESs due to a more compact structure and reduced free volume, which limits molecular motion [26]. However, an opposing trend is observed in cholinium chloride: phenol DES, where viscosity decreases with an increase in the molar ratio of phenol [26]. The

high hygroscopic nature of most DESs means that the presence of water significantly decreases viscosity, ranging from 10 to 30 times lower than in the anhydrous state [26]. Water molecules, even in small amounts (<5% weight fraction), form hydrogen bonds with ions and polar HBDs within the DES matrix. When the water content exceeds 50% mole fraction, both intermolecular and intramolecular interactions diminish, drastically changing their properties [25]. In general, the viscosity of DESs decreases with increasing temperature, allowing highly viscous DESs at ambient temperatures to be effectively utilized at higher temperatures. The temperature-dependent viscosity behavior of DESs is explained by the Hole theory, as explored by Abbott and co-workers [26, 36]. This theory posits that viscosity and electrical conductivity depend on the presence of "holes" in the liquid, which enhance the mobility of ionic compounds. Viscosity is influenced more by volumetric factors than by interactions between HBAs and HBDs. The theory also considers the steric effect on viscosity and notes that the distribution of hole sizes depends on the types of HBA and HBD. According to the Hole theory, ionic materials exhibit empty spaces upon melting, due to changes in liquid density with temperature. These dynamic holes vary in location and size. At lower temperatures, the hole sizes are relatively small, limiting the mobility of DES components and resulting in higher viscosities (100–1000 Pa.s). As temperature increases, the average hole size becomes comparable to DES components, allowing for enhanced mobility. The theory suggests that cavities within DES move in the opposite direction to the solvent molecules, so a component can only move if a cavity of similar size is available [26].

**Melting point.** DESs are characterized by their depression in melting point due to the strong interaction between the HBD and HBA, resulting in lower melting points compared to their individual components. Researchers often prioritize DESs with melting points below 50 ℃ because of their safety, cost-effectiveness, and industrial applicability. The melting point of eutectic mixtures is significantly influenced by the interaction between the salt anion and the HBDs, lattice energies, and the entropy change from the formation of the liquid phase [34]. Additionally, the molar ratio of organic salts, alkyl chain length, and HBD content play significant roles in determining the melting point of DESs [25].

**Conductivity.** At room temperature, DESs generally exhibit poor conductivity due to their high viscosity, highlighting the strong correlation between viscosity and conductivity. The conductivity of DESs is influenced by factors such as the molar ratio

of HBDs to HBAs, the alkyl chain length of the cation, and temperature. For example, the conductivity of cholinium chloride and glycerol-based DES increases significantly when cholinium chloride mole fraction of 33% is used. The alkyl chain length of the cation also affects conductivity, with ethylammonium bromide showing higher conductivity than propylammonium bromide, which in turn is higher than butylammonium bromide. Temperature increases enhance conductivity by disrupting the hydrogen bonding network, increasing ionic mobility [34].

**Surface tension.** The surface tension of DESs is a key physical property that offers insights into the influence of molecular structure on the interactions between the HBA and HBD within DES mixtures. This property helps unravel the dynamics of intermolecular interactions shaping DES compositions. Factors such as temperature, molar ratio, the nature of HBAs and HBDs, and the alkyl chain length of the cation significantly affect DES surface tension. An increase in the alkyl chain length correlates with a decrease in surface tension [25, 34]. Additionally, the organic salt content can disrupt the hydrogen bond network, reducing surface tension. Variations in temperature and the specific nature of hydrogen acceptors and donors also influence DES surface tension [25].

**Refractive index.** The refractive index is a significant physical property of DESs, providing insights into their composition. As temperature increases, hydrogen bond interactions within the DES mixture decrease, leading to lower density and a reduction in the refractive index [34]. Studies by Zhen et al. [37] underscore that refractive index values are contingent upon the size of molecules, with larger molecules exhibiting higher refractive indices. Additionally, the alkyl chain length of the cation plays a role in influencing the refractive index of DESs [34].

**pH.** The acidity and basicity of DESs are among their most important physical properties, making them versatile for various industrial applications. The pH of DESs containing Brønsted acids and bases is primarily determined by the acidity and basicity of the HBD and HBA components. Temperature has a significant influence on the pH of DESs, which decreases linearly with increasing temperature[34]. In a study by Skulcova et al. [38], the temperature-dependent change in the pH of DESs was found to be closely related to the type of HBDs. Alcohol-based DESs showed a gradual decrease in pH with increasing temperature, whereas carboxylic acid-based DESs exhibited a steeper decrease under similar conditions [34].

**Toxicity.** The toxicity of DESs is closely related to the chemical structure of their constituents (HBA and HBD) and their combinations. Recent studies have focused on assessing the toxicity and cytotoxicity of DESs, specifically those based on cholinium chloride/urea, ethylene glycol, triethylene glycol, and glycine, against both gram-positive and gram-negative bacteria. These DESs showed no toxicity against bacteria. However, when evaluated against brine shrimp, the DES components exhibited higher cytotoxicity compared to each individual organic salt and HBD [34]. Further distinctions in toxicity were observed among different types of HBDs. Organic acids, as HBDs, exhibited higher toxicity compared to sugars, amino acids, and alcohols. For instance, DESs based on citric acid, lactic acid, fructose, and xylose demonstrated lower toxicity than glycolic acid and acetic acid when investigated with a fish cell line. Moreover, the toxicity of type I, II, and IV DESs exceeded that of type III, primarily due to the presence of heavy metals. In particular, DESs based on zinc chloride exhibited pronounced toxic effects on both bacteria and fungi. In a study conducted by Juneidi and colleagues [29], the toxicity of ten DESs was investigated. These DESs were based on cholinium chloride, employing various HBAs such as alcohols, sugars, and acids, in combination with urea, zinc chloride, glycerol, ethylene glycol, diethylene glycol, triethylene glycol, fructose, glucose, para-toluene sulfonic acid, and malonic acid as HBDs. The results showed a toxicity hierarchy among these DESs: zinc chloride > malonic acid > para-toluene sulfonic acid [34]. Additionally, the toxicity of acid-based DESs was found to be primarily dependent on the length of the carbon chain and the pH of the acid component [25]. In another study, the antibacterial activity of fatty acid-based DESs was explored utilizing the broth microdilution technique [28]. The results showed that decanoic acid: dodecanoic acid DES displayed the highest overall antimicrobial activity, followed closely by decanoic acid: tetradecanoic acid, with decanoic acid: octadecanoic acid DES exhibiting the least toxicity against the studied bacteria [28]. Despite the general observation that DESs tend to be more toxic than their precursors, even when derived from natural metabolites such as fructose, glucose, or cholinium [25], fatty acid-based DESs were found to be generally less toxic than their individual components. Additionally, it was observed that medium and long-chain fatty acids exhibiting higher antibacterial activity towards Gram-positive bacteria [28]. In another study, the evaluation of cytotoxicity of various menthol and saturated fatty acid-based DESs, including octadecanoic acid, tetradecanoic acid, and dodecaoic acid was also performed toward bacteria and HaCaT cells [39]. The results showed that menthol:

dodecanoic acid exhibited the highest cytotoxicity, comparable to pure menthol, while menthol: tetradecanoic acid and menthol: octadecanoic acid demonstrated lower cytotoxicity than their individual components. These studies underscore the substantial impact of the selected chemical compositions of DESs on their toxicity. The observed toxicity hierarchy emphasizes the critical role of careful component selection in achieving environmentally friendly and greener solvent options. Optimal choices in DES composition are pivotal for realizing sustainable and eco-friendly outcomes.

**Hydrophobicity.** DESs can be further classified into hydrophilic or hydrophobic types based on their application and physicochemical properties [25]. Hydrophilic DESs have proven invaluable as preconcentration media, playing a crucial role in lowering the detection limits of advanced analytical techniques. This, in turn, facilitates the early detection of well-known micropollutants, including pharmaceuticals, personal care products, and metals. Beyond their direct application in the development of sophisticated microextraction techniques for detecting ultra-low concentrations of various micropollutants like aluminum ($Al^{3+}$) and dyes, hydrophilic DESs have demonstrated versatility in the creation of smart materials including magnetic gels and nanoparticles based on carbon nanotubes and graphene, which serve in the efficient removal of nitroaromatic explosives, aluminum, lead, arsenic, and mercury from water [40]. Despite the applications of hydrophilic DESs in the extraction and purification of various compounds, their limitations, such as poor stability in the presence of water and their polarity, which makes them unsuitable for non-polar applications, have prompted the development and utilization of HDESs [41].

HDESs re primarily used to remove micropollutants from water. Their main advantages for water applications result from their low viscosity, even when in contact with water, which improves efficient mass transfer between the phases. In addition, they can be customized to be immiscible with water so that the water phase is not contaminated while achieving high efficiency in the removal of micropollutants [35]. The hydrophobicity of DESs depends on the chemical nature of the eutectic mixture of HBAs and HBDs. The hydrophobic long alkyl chain of HBAs leads to the hydrophobicity of DESs due to steric hindrance, which prevents the core salt from being charged with water. HDESs are characterized by low density and moderate viscosity at room temperature. The physical properties of HDESs are influenced by the size of the anion, and a larger anion size leads to a higher viscosity as well as a longer alkyl chain of the HBAs. In addition, as the temperature increases, both the density and viscosity of

HDESs and other physical properties decrease [34]. Due to these properties, they are often used in the implementation of LLE technologies for the removal of alkali and transition metal ions from the aquatic environment [40].

**Water stability.** The hydrophobic nature of HDESs facilitates their use in extracting or removing components from aqueous media. Examining the stability of HDESs in water is crucial, particularly for those composed of both hydrophobic and hydrophilic elements. Ideally, HDESs should exhibit minimal cross-contamination with water [23].

In the first study on HDESs, van Osch et al. [35] highlighted the hydrophobic properties of DESs formed by decanoic acid (HBD) with quaternary ammonium salts (HBA). They confirmed the water-immiscible nature of these DESs by observing low leaching (~1.9 wt%) and low water content (~1.8 wt%). Increasing the carbon chain length further reduced both water content and leaching [35].

In ionic HDESs systems, the length of the alkyl chain of the quaternary ammonium salt had a significant effect on the saturated water content, with longer chains exhibiting higher hydrophobicity than shorter ones. Most nonionic HDESs exhibited a saturated water content of less than 2.41%, indicating stronger hydrophobicity than their ionic counterparts [23]. Therefore, nonionic HDESs might play a more beneficial role in the aqueous phase, as the hydrophilic component tends to leach into the water phase, which is confirmed by previous studies [23, 35, 42]. The water insolubility of HDESs follows the order: quaternary ammonium salts < thymol < menthol < fatty acids. The literature also suggests that the hydrogen bonds in HDESs are partially broken with water, and the components penetrate into the aqueous phase due to their individual water solubility. Only if both components of DESs are hydrophobic, the produced DES is water-stable [41].

### 1.3.2. Hydrophobic DESs (HDESs) as phase-forming components of liquid-liquid systems

LLE, commonly referred to as solvent extraction, stands as a separation technique where a solvent facilitates the isolation of a solute from a liquid phase without a chemical reaction. Typically, the solute undergoes transfer from the aqueous phase to an organic phase through a chemical potential mechanism. Upon completion of this transfer, the system reaches equilibrium where the concentrations of the solute in both phases achieve a constant ratio, reflecting the solute's partition properties and

solubilities in the two phases. Successful of the extraction processes hinges on the essential prerequisite that the solvent and the raffinate exhibit contrasting polarities.

LLE has several key advantages, including its remarkable flexibility, low energy consumption, scalability, cost-effectiveness, and the potential for recycling [25, 43]. In the context of LLE processes utilizing DESs, the selection of DESs is contingent upon the water solubility or insolubility of the solution matrix. Careful consideration of this factor is imperative to optimize the efficacy of the extraction process.

In contrast to hydrophilic DESs, HDESs are more attractive to researchers due to their insolubility in water, which makes them valuable both as extractants and as phase-forming solvents [42]. HDESs have proven their value as extraction phases in a variety of applications, including volatile fatty acids [35, 44-46], dyes [47-49], heavy metals [50, 51], phenolic compounds [52-62], pesticides [63], and lower alcohols [64], as summarized in Table 1.3. As shown in Table 1.3, most studies used LLE methods based on fatty acids and terpenes for the extraction of phenolic compounds, pesticides, lower alcohols, drugs and estrogens [52-62]. In contrast, LLE methods with quaternary ammonium salts and fatty acids proved to be particularly effective for the extraction of dyes and heavy metals.

**Table 1.3.** Applications of HDESs as extractant and phase forming solvents in LLE.

| Sample | Best HDES (mol:mol) | Recovery (%) | Methodology | Key findings | Ref. |
|---|---|---|---|---|---|
| ***Phenolic compounds*** | | | | | |
| Phenol<br>Guaiacol<br>Eugenol<br>Pyrocatechol | Octanoic acid: Menthol (2:1) | 85 | The screening of twenty-six solvents has been done by COSMO-RS model. | It was observed that the HDES based on Menthol and fatty acid show higher extraction efficiency. | [52] |
| Phenol<br>O-cresol<br>2-chlorophenol | Menthol: Decanoic acid (1:1) | >85 | Six HDESs based on organic acids, menthol or thymol, were studied as extraction solvents and their behavior in water, measurement of physical properties, and capability to remove a mixture of phenols also were investigated. | --- | [53] |
| Phenol | DL-menthol: Nonanoic acid (2:1) | 97 | Eight HDESs composed of DL-menthol and various fatty were synthesized. | Regeneration and reuse of HDESs after phenol extraction was achieved by activated carbon recovery. | [54] |
| Phenol<br>2-nitrophenol<br>2-chlorophenol | Menthol: Octanoic acid (1:1) | >90 | The extraction of the three phenols was studied using four terpenoids, three hydrophobic eutectic solvents, and three conventional organic solvents. | It was observed that the HDESs indicate higher extraction efficiency compered to organic solvents. | [55] |
| Phenol<br>Guaiacol<br>Syringol | DL-menthol: Dodecaonic acid (2:1) | 92.5-98.8 | --- | The density decreases while viscosity increases as the alkyl chain length of the carboxylic acid is longer.<br>It was observed that extraction efficiencies were linked to hydrophobicity of the solvents and the more hydrophobic HDES the higher extraction capacity. | [56] |
| 3-chlorophenol<br>2-chlorophenol<br>2,4-dichlorophenol | Menthol: Hexanoic acid (1:2) | >94 | Seven HDESs were prepared based on menthol, thymol and fatty acids. The study evaluated the effect of different conditions such as pH, initial concentration of aqueous solution, and the phase ratio on the extraction efficiency of the chlorophenols. | HDES based on Menthol and fatty acid showed higher extraction efficiency. | [57] |
| 2-nitrophenol<br>4-nitrophenol | Menthol:Decanoic acid (2:1) | >90 | The six HDESs based on menthol, thymol and decanoic acid were prepared. | HDES based on Menthol and fatty acid showed higher extraction efficiency. | [58] |

| | | | | | |
|---|---|---|---|---|---|
| Bisphenol A | Menthol: Formic acid<br>(1:1) | 98–99 | Nine HDESs based on menthol, carboxylic acid and fatty acids were prepared<br>The study evaluated the effect of different conditions including preparation of DES at different molar ratios, adjustment of DES volume, mixing time variation, and stirring speed adjustment for the extraction process. | The HDES based on Menthol and carboxylic acid showed higher extraction efficiency. | [59] |
| Bisphenol A (BPA) | Nonanoic acid: Decanoic acid: Dodecanoic acid<br>(3:1:1) | 92 | Eighteen binary and ternary fatty acid-based DESs were prepared.<br>The hydrophobic character of the studied DESs was confirmed by the very low water contents of their dried and water-saturated forms. | --- | [60] |
| Bisphenol-A (BPA) | Methyltrioctylammonium bromide: Decanoic acid<br>(1:2) | | --- | The increase in extraction efficiencies was observed with the increase of the alkyl chain in the quaternary ammonium salt, confirming that DES hydrophobicity played a major role in extraction of BPA | [61] |
| Bisphenol-A (BPA) | Menthol: Camphor<br>(3:2) | >99 | --- | Eucalyptol, geraniol, and (menthol + camphor) DES outperformed conventional solvents in BPA extraction and showed high stability and effectiveness in scaling-up and reuse, with no degradation. | [62] |
| ***Fatty acids*** | | | | | |
| Acetic acid<br>Propionic acid<br>Butyric acid | Decanoic acid: Tetraheptylammonium chloride<br>(2:1) | 25-91 | The study used the HDESs consisting of decanoic acid and various quaternary ammonium salts in different molar ratios. | The extraction efficiencies increase with increasing chain length, and the hydrophobicity of DES. | [35] |
| Levulinic acid | Butanol: Trioctylamine<br>(3:1) | 95.79 | Three HDESs based on tri-n-octylamine and alcohols were synthesized. The study also investigated the influence of factors such as solution pH, DES-water volume ratio, and extraction time on the extraction efficiency and distribution coefficients. | --- | [44] |
| Adipic<br>Levulinic<br>Succinic acids | trioctylphosphine oxide: Dodecanoic acid<br>(1:1) | 83.14 | Two hydrophobic trioctylphosphine oxide (TOPO)-based DESs along with decanoic or dodecanoic acids were studied. | Fatty acid with longer alkyl chain length showed higher extraction efficiencies. | [45] |

| | | | | | |
|---|---|---|---|---|---|
| Butyric acid | Menthol: Trioctylphosphine oxide<br>(2:1) | >90 | The study used HDESs based on menthol combined with trioctylphosphine oxide (TOPO), fatty acids to separate butyric acid from aqueous solutions. | Among the parameters affecting the extraction process, DES phase volume was found as the most important parameter affecting the extraction of butyric acid. | [46] |
| ***Drug*** | | | | | |
| Harmine | DL-menthol: Anise alcohol<br>(1:1) | >95 | The study used three kinds of new HDESs based on natural perfumes, DL-menthol, and anise alcohol. | The HDESs evaluated can be easily recycled by adjusting pH and reused at least five times. | [65] |
| Ciprofloxacin | Decanoic acid: Dodecanoic acid<br>(2:1) | 90 | Ten HDESs based on quaternary ammonium salts, menthol and fatty acids were prepared | It was observed that the HDES based on fatty acid show higher extraction efficiency. | [66] |
| Ciprofloxacin<br>Trimethoprim<br>Sulfamethoxazole | Thymol: Dodecanoic acid<br>(0.56:0.44) | 96.1-99.9 | --- | Reducing the alkyl chain length of the carboxylic acid led to increase of the partial solubility of the acid in water, decreasing the pH of the aqueous phase and favoring the presence of the charged form of these antibiotics | [67] |
| ***Dyes*** | | | | | |
| Tartrazine<br>Methylene blue<br>Sudan III, | Tetrabutylammonium bromide: Polypropylene glycol 400<br>(1:2)<br>Cholinium chloride: Glycerol<br>(1:5) | 92–106 | --- | The partitioning behaviors of dyes in the ABSs were influenced by factors such as the carbon chain length of HDES and the proportion of glycerol in cholinium chloride-G, demonstrating the tunable nature of DES/DES ABSs for the partitioning of dyes with different hydrophobicity. | [47] |
| Ethyl violet<br>Crystal violet<br>Methyl violet | L-menthol: dodecanoic acid<br>(1:1) | 98.8-99.9 | Six HDESs based on menthol, carboxylic acid and fatty acids were prepared | HDES based on menthol and fatty acid show higher extraction efficiency. | [48] |
| Methyl orange dye | Tetrapropylammonium bromide: 1-Nonanol<br>(1:8) | 91–96 | --- | The HDESs based on the n-dodecyl trimethyl ammonium bromide, benzilic acid, diphenylamine, dioxybenzone do not show such outcome. | [49] |

| | | | | | |
|---|---|---|---|---|---|
| ***Heavy metal*** | | | | | |
| Cr (VI) | Trioctylmethylammonium chloride: Butyl 4-hydroxybenzoate (1:3) | >90 | Five HDESs were prepared based on quaternary ammonium salt and parabens. The molar ratio of 1:1 (DES: Cr (VI)) was used. | --- | [50] |
| Cr (VI) | Tetrabutylammonium chloride: Decanoic acid (1:2) | 99 | --- | Small water content is having advantageous as it dramatically affects the electrical conductivity and viscosity of the solvent | [51] |
| ***Pesticides*** | | | | | |
| Neonicotinoids Imidacloprid Acetamiprid Nitenpyram Thiamethoxam | DL-Menthol: Dodecanoic acid (2:1) | 77.45 | Two different families of DES one based on natural ingredients (DL-Menthol and natural organic acids and the other based on quaternary ammonium salts and organic acids), that present two phase forming ability with aqueous solutions, were prepared and studied regarding their water stability. | It was observed that the HDES based on Menthol and fatty acid show higher extraction efficiency. | [63] |
| ***Lower alcohols*** | | | | | |
| Ethanol 1-propanol 1-butanol | DL-menthol: dodecanoic acid (2:1) | 50-90 | --- | The distribution coefficient and selectivity were found to be much higher for 1- butanol as compared to ethanol and 1-propanol and follow the order: 1-butanol (~90%) > 1-propanol (~80%) > ethanol (~50%). | [64] |
| ***Estrogens*** | | | | | |
| Estriol Estrone 17α-ethynylestradiol 17α-estradiol 17β-estradiol | Menthol: Octanoic acid (1:1) | | Six HDESs based on menthol and fatty acids were studied as extraction solvents. . | The HDES can be used to extract estrogens from wastewater several times in sequence without regeneration, but after about three to five cycles, the extraction capacity of the HDES is exhausted | [68] |
| ***Biofuels*** | | | | | |
| Furfural | Tetrahexylammonium bromide: Decanoic acid (1:3) | 85 | --- | Shorter alkyl chains on the ammonium salts generally reduced the ability to remove furfural form water. | [69] |

| | | | | | |
|---|---|---|---|---|---|
| | Tetrahexylammonium bromide: dodecaonic acid (1:3) | | | Both decanoic and dodecanoic acid-based HDES can remove furfural from water even at very low concentrations of 0.1 mol %. | |
| Furfural 5-hydroxymethylfurfural | Camphor: 1-decanol (1:2) | 79.2-87.9 | --- | The HDESs demonstrated high extraction efficiency for the removal of biofuels from both model and real hydrolysates, with comparable results to enzymatic hydrolysis. Camphor: 1-decanol was successfully regenerated and reused without loss of activity. | [70] |
| ***Another compounds*** | | | | | |
| Lithium | Thenoyltrifluoroacetone-tributyl phosphate (HTTA-TBP) (1:1) | 80 | Five HDESs containing β-diketone structure and neutral extractants were synthesized. | Lithium was driven into HDES phase due to its strong electrostatic interaction with deprotonated HTTA, while TBP interacted with lithium via the coordination effect. | [71] |
| Lithium | DL-Menthol: dodecanoic acid (2:1) | 80.69 | Nine HDESs based on menthol and long-chain fatty acids were synthesized. The study also evaluated the optimization of various parameters such as pH, extraction time, rotational speed, O/L ratio, co-extraction agent, and initial concentration of lithium. | It was observed that fatty acid with longer alkyl chain length showed higher extraction efficiencies. | [72] |
| Polyfluoroalkyl Substances | Menthol: Glacial acetic acid (1:1) | 80–90 | --- | The mechanism of interaction between the Polyfluoroalkyl and the HDES was unraveled using density functional theory calculations. | [73] |
| Riboavin | Decanoic acid: Lidocaine (2:1) | 81.1 | The ability of eight HDESs in the riboavin extraction was studied. | They all show higher removal of riboflavin in comparison to the HDES based on ammonium salt and fatty acid. | [74] |
| Boron | Thymol:2-methyl-2,4-pentanediol (MPD) (2:1) | 90.1 | Four new HDES based on natural materials and alcohols were prepared. | The main reason for the extraction was due to the complexation between MPD in the DES and boric acid. | [75] |

#### *1.3.2.1. Hydrophobic DESs (HDEs) as alternative solvents for the extraction of drugs*

Pharmaceuticals and personal care products have garnered increasing concern in recent years as emerging aquatic contaminants, posing potential threats to both human populations and aquatic ecosystems. This category encompasses a wide array of chemical classes, ranging from pharmaceuticals like antibiotics, anti-inflammatory drugs, β-blockers, lipid regulators, and antiepileptics, to personal care product ingredients, including antimicrobials, insect repellents, preservatives, and sunscreen UV filters, along with their respective metabolites or transformation products [76]. In general, the partial excretion of pharmaceutical compounds by humans, coupled with the release of drug residues from hospitals and the pharmaceutical industry, ultimately reaches wastewater treatment plants, posing a significant threat to ecosystems, as pharmaceuticals can induce increased mortality rates and impair the reproductive functions of aquatic life. Furthermore, the consumption of contaminated food and water exposes individuals to drug-resistant bacteria [76]. The detection of pharmaceuticals in the environment dates back to the 1970s when the US Environmental Protection Agency issued the inaugural report on their presence in the environment in 1976 [77].

Given the diverse array of pharmaceutical species present in the environment at trace levels, alongside their varied physicochemical properties, the imperative to develop techniques for more accurate quantification becomes evident. Conventional methods are include chromatography, capillary electrophoresis, spectrometry, adsorption, solid-phase extraction, and electrochemical methods [78], which due to their drawbacks, such as the use of toxic and volatile organic solvents, time-consuming procedures, and the necessity for expensive equipment, there is a growing emphasis on transitioning from conventional extraction techniques to more environmentally friendly alternatives, often referred to as "greener" extraction techniques [79]. These sustainable approaches aim to address the shortcomings of traditional methods by minimizing the use of hazardous solvents, reducing processing time, and promoting cost-effectiveness. Therefore, the use of environmentally friendly solvents such as HDESs as an alternative to conventional organic solvents to extract/quantify is imperative.

As shown in Table 1.4, HDESs have been shown to be useful in the extraction of various types of drugs such as tetracycline antibiotics [80-83], nonsteroidal anti-inflammatory drugs [84-86], sulfonamide antibacterial [87-91], antibiotics [66, 92-96], β-blockers [97, 98], antidepressants [99-101], and beta2-adrenergic agonist [102], from various sources such as food, water, and biological samples.

**Table 1.4.** Applications of HDESs in extraction of drugs from diverse sources.

| Analytes | Sample matrix | Best HDES (mol:mol) | Method | Recovery (%) | Methodology | Key findings | Ref. |
|---|---|---|---|---|---|---|---|
| ***Antibiotic*** | | | | | | | |
| Oxytetracycline Doxycycline Tetracycline | Water | Thymol: Octanoic acid (1:1) | Dispersive LLME | 74-113 | Cholinium chloride: ethylene glycol DES was used as disperser solvent. Thymol: Octanoic acid DES was used as extraction solvent. | The addition of beta-cyclodextrin (β-CD) to the extraction phase improved extraction efficiencies. | [80] |
| Oxytetracycline, Tetracycline, Doxycycline | Milk | Thymol: Octanoic acid (1:1) | Dispersive LLME | 70-113 | Acetonitrile was used as disperser solvent. Eleven HDESs were used as extraction solvent. | It was observed that HDES based on thymol and fatty acid show higher extraction efficiency. | [81] |
| Tetracycline Oxytetracycline Chlortetracycline | Water | Methyltrioctylammonium chloride: Nonanoic acid (1:2) | LLME | 77-87 | Ten HDESs based on quaternary ammonium salts, fatty acids and fatty alcohol as extraction solvents were prepared | HDES based on quaternary ammonium salt and fatty acid show higher extraction efficiency. | [82] |
| Tetracycline, Doxycycline Oxytetracycline | Water | Cholinium chloride: Thymol: Nonanoic acid (1:2:2) | Dispersive LLME | 74–95 | Four new thymol-based ternary DESs were prepared. The DES hydrophobicity and its effect on the pH of water samples were studied. | --- | [83] |
| levofloxacin (S-OFX) Ciprofloxacin | Spiked water | Thymol: Hexanoic acid (2:1) | LLME | 94-110 | Four HDESs were used as extraction solvents. The impact of the solution pH of the phase transition behavior of the DESs was studied | --- | [92] |
| OFX Norfloxacin Ciprofloxacin Enrofloxacin | Surface water | Thymol: Heptanoic acid (2:1) | LLME | 84-113 | The developed method based on in situ formation of twenty one HDESs (composed of thymol, menthol, and camphor and fatty acids) coupled with shaker-assisted LLME (in situ) was validated. | It was observed that HDES based on thymol and fatty acid show higher extraction efficiency. | [93] |

| | | | | | | | |
|---|---|---|---|---|---|---|---|
| PenicillinG<br>Dihydrostreptomy<br>Cienrofloxacin<br>Ciprofloxacin | Honey | Tetrabutylammonium chloride: p –cresol<br>(0.27 g, 0.21 g) | LLME | 70-92 | The procedure was carried based on In-situ formation/decomposition of DES. | In-solution formation of DES provided wide contact areas among the extractant and sample solution, and accelerated sample preparation. Also, its decomposition enabled collection of the final extraction phase without centrifugation. | [94] |
| levofloxacin (S-OFX)<br>Ciprofloxacin | Water | Tricaprylylmethylammonium chloride: 1-octanol<br>(1:1) | LLME | 94.8 | Sixteen HDESs based on quaternary ammonium salts; fatty acids and fatty alcohol were prepared. | The HDES based on quaternary ammonium salt and fatty alcohol showed higher extraction efficiency. | [95] |
| PenicillinG<br>Ampicillin<br>Amoxicillin | Egg, Chicken, Meat, and Honey | Benzyl triethylammonium chloride: Decanoic acid<br>(1:3) | Ultrasound Assisted Dispersive LLME | > 97 | HDES and acetonitrile were used as extraction and dispersive solvents, respectively. | The applied method showed high capability in extraction for application in complex matrices. | [96] |
| Ciprofloxacin | Water | Decanoic acid: Dodecanoic acid<br>(2:1) | LLE | 90 | Ten HDESs based on quaternary ammonium salts, menthol and fatty acids were prepared. | The HDES based on fatty acid showed higher extraction efficiency. | [66] |
| ***Nonsteroidal anti-inflammatory drug*** | | | | | | | |
| Diclofenac<br>Flurbiprofen<br>Ketoprofen<br>Mefenamic acid | Bovine milk | Menthol: Analytes | LLME | 81-91 | --- | The procedure was done using in situ DESs formation between menthol and NSAIDs, which resulted in increased enrichment factors and exclusion of matrix effects. | [84] |
| Salicylic acid<br>Oxaprozin<br>Diclofenac<br>Ibuprofen | Water and Milk | Thymol: 1,1,3,3-tetramethylguanidine chloride<br>(2:1) | ultrasound-assisted Dispersive LLME | 79-107 | Three HDESs composed of guanidinium chloride and thymol, methyltrioctylammonium chloride and thymol, and chloride and thymol were used as extraction solvent. | --- | [85] |
| Ketoprofen<br>Diclofenac | Urine | Menthol: Analytes | LLME | 93-97 | The procedure was applied based on in-situ DES formation and menthol used as extractant solvent. | The extraction was based on the formation of hydrogen bond between OH group of menthol and the oxygen atom of COOH group of non-steroidal anti-inflammatory drugs. | [86] |

| | | | | | | | |
|---|---|---|---|---|---|---|---|
| Ketoprofen<br>Diclofenac | Beef liver | Menthol: formic acid<br>(1:40) | Dispersive LLME | 92-108 | The extraction was done in two stages and based on DES decomposition. For separation of analytes from a liver sample, a sodium carbonate solution (pH 11) was used because in this case analytes ionization promoted mass-transfer from solid sample phase to alkaline aqueous phase. | --- | [103] |
| Diclofenac | Aqueous solution | DL-menthol: Acetic acid<br>(1:1) | Reactive LLE | 47-78 | Diethyl succinate and DES were used as diluent and extractant. | The designed DES enhanced the removal of diclofenac by more than 2.7 to 4.5 times compared to a conventional solvent. | [104] |
| ***Sulfonamide antibacterial*** | | | | | | | |
| Sulfamethazine<br>Sulfamethoxazole | Chicken | Tetrabutylammonium bromide: Malonic acid: Hexanoic acid<br>(1:1:1) | Dispersive LLME | 86-104 | The procedure involved the extraction of sulfanilamides into the solvent phase and their preconcentration through the injection of aqueous phase into the DES phase, leading to its decomposition and the formation of hexanoic acid dispersed in the aqueous phase. | --- | [87] |
| Sulfapyridine,<br>Sulfamethazine<br>Sulfamethoxine | Fruit juices | Trioctylmethylammonium chloride: 2-octanol<br>(1:2) | Ultrasonic assisted LLME | 88-97 | Five HDES based on ammonium salts and 2-octanol and fatty acid were synthesized. | It was observed that HDES based on ammonium salt and alcohol showed higher extraction efficiency. | [88] |
| SulfamethoxazoleSulfamethazine<br>Sulfapyridine | Urine | Vanillin: Menthol<br>(1:1)<br>Vanillin: Thymol<br>(1:1) | LLME | 91-93 | Thymol and Vanillin were used as both media for Schiff bases formation and the precursor of DES. | --- | [89] |
| Sulfamethazine<br>Sulfamethoxazole<br>Sulfaquinoxaline<br>Sulfadiazine | Milk | Thymol: Octanoic acid<br>(3.40 g: 1.65 g) | LLME | 94-100 | Five HDESs were used in situ DESs formation by pH adjusting based on Thymol and fatty acids. | --- | [90] |

| | | | | | | | |
|---|---|---|---|---|---|---|---|
| Sulfadiazine<br>Sulfamerazine<br>Sulfametoxydiazine<br>Sulfamethoxazole | Water | Cholinium chloride: o-cresol<br>Cholinium chloride: m-cresol<br>Cholinium chloride: p-cresol<br>(1:2) | Dispersive LLME | 80-93 | --- | The three prepared HDESs showed commendable performance for extraction of sulfonamides compared to hydrophilic DESs. | [91] |
| ***Beta blocker*** | | | | | | | |
| Atenolol<br>Propranolol<br>Metoprolol | Plasma | Tetramethylammonium chloride: Alpha terpineol<br>(1:2) | LLME | 72-86 | Four types of DESs were used as the extraction solvents in situ DESs formation-based LLME | DES based on ammonium salt and monoterpenoid showed higher extraction efficiency. | [97] |
| Metoprolol<br>Propranolol | Water | Thymol: Azelaic acid<br>(17:1) | Vortex assisted LLME | 90-100 | Five novel HDESs were used as the extraction solvents in situ DESs formation-based LLME. | --- | [98] |
| Propranolol<br>Carvedilol<br>Verapamil<br>Amlodipine | Plasma, urine, pharmaceutical waste water | Cholinium chloride: 1-phenylethanol<br>(1:4) | Hollow fiber liquid phase microextraction | 95- 104 | --- | The prepared DES showed good compatibility to pores of hollow-fiber and high ability in extraction of ionizable organic compounds. | [105] |
| ***Antidepressant*** | | | | | | | |
| Amitriptyline<br>Nortriptyline<br>Desipramine<br>Clomipramine | Urine | Menthol: Decanoic acid<br>(1:2) | Dispersive LLME | 74-89 | DES was used as an extractant solvent, deionized water and sodium sulfate were used as disperser and phase separation agent. | --- | [99] |
| Citalopram<br>Sertraline<br>Venlafaxine | Water, urine, plasma | Tetrabutylammonium bromide: 1-dodecanol<br>(2:1) | Dispersive LLME | 87-99 | Tetrabutylammonium bromide and 1-dodecanol were used as a dispersive agent and as the extraction solvent, respectively. | --- | [100] |
| Amitriptyline<br>Nortriptyline<br>Desipramine<br>Clomipramine<br>Imipramine | Water, urine, plasma | Cholinium chloride: 4–chlorophenol<br>(1.39 g: 2.58 g) | Dispersive solid phase extraction air–assisted LLME | 62-77 | --- | The combination of dispersive solid phase extraction sorbent (C18) with DES-based air-assisted LLME represented a novel approach for the extraction and preconcentration of tricyclic antidepressant drugs in biological samples. | [101] |
| ***Beta2-adrenergic agonist*** | | | | | | | |

| | | | | | | | |
|---|---|---|---|---|---|---|---|
| Terbutaline<br>Clorprenaline<br>Tulobuterol<br>Clenbuterol<br>Salbutamol | Water | Tetra butyl ammonium chloride: Decanoic acid (1:3) | Dispersive LLME | 56-91 | Nine HDES based on quaternary ammonium salts and fatty acids were prepared. | It was observed that the fatty acid with longer alkyl chain length show higher extraction efficiency. | [102] |
| ***Stimulant drugs*** | | | | | | | |
| Amphetamine<br>Methamphetamine | Plasma, pharmaceutical wastewater | Cholinium chloride: Phenylethanol (1:4) | Emulsification microextraction | 63-66 | --- | This study used a new extraction solvent (cholinium chloride: Phenylethanol) for efficient and safe air-assisted extraction of stimulant drugs. | [106] |
| ***Others*** | | | | | | | |
| Methadone | Water, urine | Cholinium chloride: 5,6,7,8-Tetrahydro5,5,8,8-tetramethylnaphthalen-2-ol (1:2) | Air–assisted emulsification LLME | 98-101 | Tetrahydrofuran was used as a demulsifier solvent into homogeneous solution for providing a turbid state. | --- | [107] |
| Warfarin | Urine, plasma | Borneol: Decanoic acid (1:3) | Air-assisted LLME | > 88.80 | Ten HDESs based on borneol were used as disperser solvent. | The droplets of DESs were dispersed into the sample solution to accelerate the cloudy emulsion system formation and increase the mass transfer of the analyte to the DES-rich phase. | [108] |
| Calcium dobesilate | Water, urine | methyl trioctyl ammonium chloride: Bromoacetic acid (1:1) | Vortex-assisted LLME | 93-108 | Fifteen acidic HDESs were prepared from methyl trioctyl ammonium chloride and a series of haloacetic acids. | The DESs could be recycled and regenerated through back extraction and after fifteen cycles, the extraction efficiency was still up to 99%. | [109] |
| Daclatasvir<br>Sofosbuvir | Urine | p-aminophenol: Tetrabutyl ammonium chloride (2:1) | Ultrasound-assisted LLME | 96-90 | --- | The amino group in DES structure made it as a switchable hydrophobicity solvent. | [110] |
| Carbamazepine | Aqueous solution | Menthol: acetic acid (1:1) | Reactive LLE | > 90 | The study used various carboxylic acid-based DES such as menthol: acetic acid / formic acid/ diethyl succinate were used as diluent and extractant. | DESs increased the extraction performance of the diluent from 11 to 36% comparing to the untreated one. | [111] |

| | | | | | | | |
|---|---|---|---|---|---|---|---|
| Lamotrigine | Plasma | Cholinium chloride: Phenylethanol (1:4) | Ultrasound-assisted emulsification-microextraction | 58.3 | --- | The DES hydrophobicity eliminates the need of the third solvent as an emulsifying agent. | [112] |
| Artemisinin | Artemisia annua Leaves | Methyl trioctyl ammonium chloride: 1-butanol (1:4) | ultrasound-assisted extraction | 85.65 | --- | The HDES was reused at least two times without a significant decrease in extraction yield. | [113] |
| Ergosterol | Mushroom | menthol: pyruvic acid (1:2) | Solid phase extraction | > 90 | Thirty nine HDES were studied. | HDES based on menthol and carboxylic acid showed higher extraction efficiency. | [114] |
| Artemisinin | Artemisia annua Leaves | Hexafluoroisopropanol: Cholinium chloride (1:1)<br>Menthol: Tricaprylylmethylammonium chloride (2:1) | Biphasic extraction | 85.7 | --- | Resin adsorption was used to recover the compounds and achieve a reasonably high yield of compounds with a range of polarities. | [115] |

Specifically, the extraction of drugs with HDESs from various sources such as food, water, and biological samples has been performed for antibiotics, non-steroidal anti-inflammatory drugs, and antibacterial sulfonamides. However, for beta-blockers, antidepressants, beta2-adrenergic agonists and stimulants, the extraction studies focused only on water and biological samples. Table 1.4 also shows that liquid-liquid microextraction (LLME) and its various categories are the predominant methods for extracting drugs using HDESs. The extraction of antibiotics has gained particular attention due to the alarming rise in bacterial resistance caused by consuming contaminated food and water, which has become a significant concern within the scientific community [10].

## 1.4. COSMO theory

Understanding phase equilibrium and the thermodynamic properties, such as solubility and partition coefficients, of chemical compounds, particularly in the pharmaceutical realm, holds broad significance in designing, developing, and optimizing manufacturing processes whether in laboratory or industrial settings. While experimental approaches provide valuable insights, they are often time-consuming and expensive. In contrast, mathematical modeling has gained attention for its cost-effectiveness and extensive applicability across substance types and ambient conditions. [116]. Thermodynamic modelling typically falls into three categories: (1) semi-empirical models, (2) semi-predictive models, and (3) predictive models. These models vary in accuracy and reliable ranges. The distinguishing factors between groups (2) and (3) lie in the incorporation of theoretical quantum chemistry and the reliance on experimental data. Predictive models require theoretical foundations, whereas semi-empirical models often rely on empirical correlations lacking theoretical significance, derived from specific experimental conditions for certain species [116].

The COSMO is known as a predictive dielectric continuum model, wherein the core concept involves situating the solute within a dielectric continuum that simulates the solvent. The charge distribution on the solute induces polarization in the surrounding solvent. In the COSMO model, the molecular surface is discretized into homogeneous segments and the screening charge density of each segment meticulously is calculated [117]. Leveraging Density Functional Theory (DFT) computations, COSMO facilitates

the determination of screening charge density, total solvation energy, as well as cavity volume and area [118].

COSMO-based models seamlessly incorporate principles from quantum theory, dielectric continuum models, and surface interactions The concept of the Conductor-Like Screening Model for Real Solvents (COSMO-RS) was initially introduced by Klamt [119]. In this model, molecules are assumed to be a collection of surface segments. The interaction energy between the segments is computed by COSMO. An expression was derived in COSMO-RS for the effect of the chemical potential of molecules on the interaction energies between the segments in the condensed phase. While COSMO-RS has demonstrated promising results, it faces challenges, including convergence issues under specific boundary conditions and a lack of satisfaction of thermodynamic consistency relations [118, 120]. Addressing these limitations, Lin and Sandler [120] successfully resolved the difficulties in the COSMO-RS model. They developed a modification within the COSMO-RS framework, naming it the COSMO-SAC model. This advancement not only rectifies the convergence concerns but also enhances thermodynamic consistency, further refining the applicability of COSMO-based models in predicting complex interactions in real solvents.

The primary strength of predictive models lies in their independence from experimental data for parameter fitting, requiring only the chemical structures of the molecules under investigation. This model depends on a small number of general or element specific parameters rather than specific for types of molecules or functional groups, and can be determined from known properties of a small set of molecules [121].

The application of COSMO-based models depends on determining the charge distribution of molecules by embedding them in a virtual conductor environment. The interaction energies between molecules are computed in terms of the screening charge density on the surface of a molecule (σ), utilizing DFT to generate σ-profiles and σ-potentials. Among the critical descriptors derived from COSMO-RS, the σ-profile illustrates the probability distribution of finding a surface segment with a specific screening charge density, while the σ-potential characterizes the affinity of a solvent for a molecular surface of polarity [118]. Subsequently, leveraging these descriptors and employing statistical thermodynamic principles, the model calculates chemical potentials, molecular energies arising from interactions (such as van der Waals, electrostatic, and hydrogen bond interactions), and an array of thermodynamic properties, including solubility and activity coefficients [121]. This comprehensive

approach allows for a nuanced understanding of molecular interactions, enabling the prediction of various thermodynamic behaviors and properties within a given solvent environment.

### 1.4.1. Application of COSMO to evaluate deep eutectic solvents (DESs) properties

Predictive thermodynamic modeling of ILs-based systems has shown success, particularly using quantum chemistry-based models like the COSMO-RS. These models are crucial for designing, screening, and analyzing the thermodynamics of innovative solvents such as DESs [121]. Given that DESs consist of multiple molecules, selecting an accurate modeling approach within the COSMO-RS framework is pivotal [122]. For example, in the modeling of ILs, which are among the most studied alternative solvents, three distinct approaches are commonly employed [123]:

(a) Meta-file approach: This involves treating ions independently in quantum chemical COSMO calculations. However, for COSMO-RS calculations, the IL is characterized by the aggregate of σ-profiles, areas, and volumes from its constituent ions. The outcomes of separate COSMO calculations for each ion are consolidated into a unified file, known as the meta-file.

(b) Ion-pair approach: Here, the COSMO-optimized structure of the ion pair is used. Since IL ions often exhibit weak coordination, this method may require a broad range of conformations for the ion pairs.

(c) Electroneutral mixture approach: This involves treating distinct ions, which were previously analyzed separately in COSMO calculations, as an electroneutral mixture in COSMO-RS calculations. The mole fraction ratio of ions must reflect the stoichiometry of the IL at any composition of the mixture. Consequently, the mole fraction employed in these calculations differs from the conventional mole fraction used in experiments, where the IL is treated as a singular compound. For example, in a mixture of a 1:1 IL like 1-butyl-3-methylimidazolium chloride ([C4mim][Cl]) and a solute, the mole fraction used in experiments is contingent on the binary system. Conversely, in COSMO-RS calculations, it hinges on the ternary system. This discrepancy implies that properties dependent on mole fraction definitions, such as activity coefficients and Henry's law constants, necessitate conversion when utilized in conjunction with the alternative mole fraction definition.

The meta-file approach and the electroneutral mixture method offer substantial advantages in utilizing distinct ions for modeling. By accessing a COSMO database that includes files for both anions and cations, researchers can explore a vast array of ILs without the need for additional quantum chemical calculations. This accessibility is especially valuable for screening ILs effectively. Moreover, the conformational space of ions is significantly more manageable compared to that of ion-pairs, making simulations less computationally demanding [123]. In the electroneutral mixture approach, cations and anions are treated as separate entities, facilitating the creation of ILs without extra quantum computations. This method has been traditionally viewed as an accurate representation of DESs in their liquid form. By treating cations, anions, and HBDs as distinct entities in their respective molar proportions, these components collectively establish the DES structure [122].

To date, numerous studies have employed COSMO-based models to predict a wide spectrum of physicochemical and thermodynamic properties of DESs, including viscosity [124-127], density [124, 126-128], Kamlet−Taft (K−T) parameters [129, 130], conductivity [131], Henry's law constant [132, 133], vapor pressure [126, 127, 134], excess properties [133, 135], activity coefficients [136-139], partition coefficients [139-144], selectivity, and distribution ratio [64, 140-143, 145-155]. Furthermore, these models have successfully predicted the solid–liquid phase diagrams of solvents, including eutectic temperatures [135-137, 156-161], and the solubility of various substances such as rutin [162], different gases [163], carnosic acid or carnosol [138], limonene [164], rosemary biomolecules [165], $CO_2$ [132, 133, 166], sulfanilamide, and sulfacetamide [167].

Furthermore, COSMO models play a pivotal role in predicting the liquid-liquid equilibria (LLE) behavior of DESs in the extraction and separation of diverse molecules such as BTEX aromatics [145], aromatic and aliphatic hydrocarbons [146], aromatics [147], azeotropic mixtures [148], tocopherols [140], thiophene [141, 149], polyaromatic nitrogen hydrocarbons [142], azeotrope mixtures [150], ethylbenzene/styrene mixtures [150], aromatic hydrocarbons [151], lower alcohols [64], terpenoids [143], and in denitrification of liquid fuels [152], desulfurization of fuel [153], and denitrogenation of diesel fuel [154]. Specific studies have focused on LLE and vapor–liquid equilibrium (VLE) calculations for binary and ternary DES-based systems [135, 139, 155, 168, 169]. Finally, molecular descriptors derived from COSMO-RS, such as σ-profile and σ-potential, are instrumental in understanding regions of association and intermolecular

interactions essential to DES formation. These descriptors provide insights into thermophysical properties, affinity, and interactions with other species, proving essential for effective solvent screening [126-128, 131, 134, 143, 145, 170, 171].

### 1.4.2. Application of COSMO to evaluate the partition of molecules in liquid-liquid systems based on hydrophobic deep eutectic solvents (HDEs)

The partition coefficient (*K*) of a solute is a key factor in selecting the optimal solvent for LLE. The partition coefficient ($K_i^{\alpha\beta}$) of a solute *i* is expressed as the ratio of the solute's mole fraction in each phase [139].

$$K_i^{\alpha\beta} = \frac{x_i^{\alpha}}{x_i^{\beta}} = \frac{\gamma_i^{\beta}}{\gamma_i^{\alpha}} \tag{1.1}$$

Where $x_i$ and $\gamma_i$ are the mole fraction and activity coefficient of compound *i*, and $\alpha$ and $\beta$ are the two phases of a biphasic liquid system. At lower concentrations, the distribution of the solute tends to be linear, allowing the partition coefficient to be considered constant. Knowledge of the compositions of the two phases, typically obtained from literature or calculated using COSMOtherm, is essential for determining this coefficient [139]. In the specific context of HDES-based knowing the exact compositions of both phases is less critical as each phase can be considered essentially pure. Recently, some studies have applied COSMO-based models to explore partitioning in HDES-based systems [57, 145-148, 152-155, 172, 173].

For instance, Hizaddin et al. [147] investigated the LLE of ethylbenzene from n-octane using five tetrabutylammonium bromide-based DESs, varying the addition of a third compound. The results showed that DESs containing only ethylene glycol had high selectivity but a low partition ratio, while those containing only pyridine had a high partition ratio but low selectivity. In contrast, when both pyridine and ethylene glycol were present in the tetrabutylammonium bromide-based DES, increasing the molar ratio of pyridine generally improved the partition ratio, while increasing the molar ratio of ethylene glycol improved the selectivity. Furthermore, COSMO-RS successfully predicted the ternary tie lines for all systems, showing good agreement with experimental data. However, it was noted that COSMO-RS tended to underestimate the distribution ratios. Notably, a DES composed of tetrabutylammonium bromide and

pyridine in a 1:4 ratio achieved the highest distribution ratio, ranging between 0.8 and 1 [147]. Moreover, Gouveia et al. [146] explored the performance of various DESs composed of different ammonium salts such as cholinium chloride, benzylcholinium chloride, and tetrabutylammonium chloride - acting HBAs - with levulinic acid - as the HBD - in a 1:2 molar ratio. The study aimed to evaluate their effectiveness in separating aromatic-aliphatic hydrocarbon azeotropic mixtures. Notably, incorporating an aromatic ring in the HBA led to higher distribution coefficients and selectivities. A more hydrophobic HBA, like the quaternary ammonium salt, further improved distribution coefficient values. COSMO-RS effectively described the observed trends in phase diagrams and tie-line slopes, with a root mean square deviation (RMSD) ranging from 0.5% to 3.9%, and accurately reflected the experimental trends in distribution ratios and selectivity [146]. In another work, the performance of six different DESs, combining quaternary ammonium chlorides (such as tetramethylammonium chloride and tetrahexylammonium chloride) with polyols (ethylene glycol and glycerol), was evaluated for extracting aromatic components from mixtures containing aliphatic and aromatic compounds. It was observed that DESs with longer alkyl chains as HBA and ethylene glycol as HBD yielded the highest solute partition coefficients. Specifically, ethylene glycol proved more effective than glycerol, leading to higher solubilities and improved aromatic distribution ratios within the same mole fraction-based HBD:HBA ratio across various DESs. Although COSMO-RS typically overestimated these distribution ratios for aromatic compounds, it aligned qualitatively with experimental trends, accurately reflecting the influence of alkyl chain length and the type of HBD [155].

Further research involved a screening of 49 different DES combinations based on various cations, anions, and HBDs to explore their potential in extractive desulfurization of fuel. This study utilized the COSMO-RS model to derive the distribution coefficient, selectivity, and performance index from the mass-based liquid–liquid equilibrium in DES-involved systems. Notably, the σ-profiles of tetramethylammonium- and tetrabutylphosphonium-based DESs displayed significant peaks in the negative nonpolar region, suggesting a greater likelihood of interacting with dibenzothiophene and thus achieving a higher distribution coefficient. Conversely, the σ-profile for cholinium-based DESs, which was predominantly in the polar region, indicated a lesser tendency for such interactions. Among the 49 DESs, tetrabutylphosphonium bromide combined with N,N-dimethylformamide in a 1:3 ratio was identified as the top-

performing extractive solvent [153]. In recent work, Chen et al. [173] applied COSMO-RS for prediction the extraction of antibiotics and dyes from aqueous media using terpenoid-based DESs. They screened twenty-six terpenoid-based DESs, maintaining a constant molar ratio of HBA and HBD (1:1), against fifteen target compounds, including antibiotics and dyes. The screening was based on selectivity, capacity, and performance index, evaluated using COSMO-RS. The results highlighted that the Thymol: Benzyl alcohol DES exhibited superior extraction efficiency for the pollutants under investigation compared to other DESs. The study found that DESs with higher polarity, smaller molecular volume, shorter alkyl chain lengths, and specific aromatic ring structures demonstrated more favorable extraction performance. Moreover, the predicted results closely matched the experimental outcomes, underscoring the method's applicability and reliability [173].

The outcomes from these studies demonstrate that despite some quantitative inaccuracies, the qualitative consistency of COSMO-RS predictions with experimental results underscores the model's utility in effectively screening solvents for specific applications.

## 1.5. Enantioselective liquid-liquid extraction (ELLE)

ELLE utilizes enantioselective recognition between chiral selectors and enantiomers in at least one of the liquid phases [2]. This technique can be categorized into three different types based on the mutual solubility of the liquid phases involved. The first type, LLE, consists of a hydrophilic phase, usually water, and an organic phase [174]. The second type, aqueous two-phase extraction (ATPE), uses two water-soluble substances that form two water-rich phases when a certain concentration is exceeded, thus facilitating separation [175]. Lastly, synergistic extraction incorporates additional extractants, often called adjuvants, often called adjuvants, are used to enhance the two-phase system and increase the overall efficiency of the separation process. Each of these categories is tailored to optimize the separation process based on the specific properties and interactions of the target enantiomers [176].

The principle of ELLE is closely interwoven with guest chemistry and includes elements of chiral recognition and solvent extraction. Chiral recognition is based on the premise that chiral extractants and enantiomers form diastereomers through various

intermolecular interactions. These interactions include ion pairing, hydrogen bonding, π-π interactions, dipole interactions and van der Waals forces [20].

The mechanism of enantiomer recognition is often explained with the help of the theory of three-point interactions. This theory is based on the assumption that an enantiomer can bind to three specific sites of a chiral host through the three-point binding model (Figure 1.7). According to this model, one enantiomer is bound to three specific binding sites, making it impossible for the other enantiomer to bind to these identical sites simultaneously [177]. The success of this interaction is influenced not only by the attractive forces at these binding sites, but also by other factors such as conformational changes, steric hindrance and repulsive interactions. As a result, the original three-point binding model has been refined into what is now known as the three-point interaction model [20].

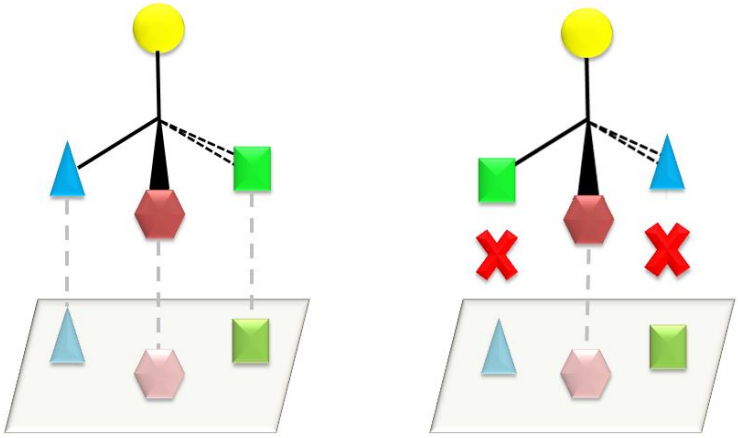

**Figure 1.7.** A schematic of three-point interaction theory.

The success of ELLE depends largely on the effective development and optimization of chiral selectors. Over the past decade, significant progress has been made in identifying chiral selectors that are not only highly enantioselective, but also environmentally friendly and cost effective. The literature documents a variety of chiral selectors used in ELLE, including metal complexes, cyclodextrins, chiral ionic liquids (CILs), tartaric acid derivatives, crown ethers, and others [20]. Each type of chiral selector is explained in more detail below.

**Metal complexes.** They have been extensively utilized as chiral extractants due to their notable stereoselectivity, especially in resolving various amino acids through the formation of diastereomers via coordination bonds. Copper (Cu) and palladium (Pd)

complexes, including the widely studied (S)-2,2′ -bis(diphenylphosphino)-1,1′ -binaphthyl-Cu (BINAP-Cu) and BINAP-Pd complexes, are prominent examples demonstrating high enantioseparation capacity [20]. Tang et al. [178] made a significant contribution with their study on the ELLE based on organic solvent (trichloromethane) and water for enantioseparation of phenylglycine using (S)-BINAP-metal complexes. They employed an interface ligand exchange mechanism, well-suited for the reactive extraction system due to the high hydrophobicity of phenylglycine. This method was pivotal in demonstrating the effectiveness of the extraction process. Schuur et al. [179] expanded on different chiral selectors for resolving DL-α-methyl phenylglycine amide using ELLE based on organic solvent (1- chloropentane) and water, demonstrating the versatility of this technique. Additionally, studies by other researchers involving PdCl2-(S)-BINAP highlighted its effectiveness as a chiral selector, successfully separating enantiomers of p-hydroxyphenylglycine, 4-nitro-phenylalanine, 4-chlorophenylglycine, and 2-fluoro-phenylalanine, achieving enantioseparation factors of 1.73, 3.37, 1.86, and 3.64, respectively [20]. The exploration of other chiral diphosphine ligands, traditionally used in asymmetric reactions, has also been a focus of recent research in ELLE, reflecting the ongoing innovation in this field [20]. Liu et al. [180] reported (*S*)-MeO-2,2′-bis(diphenylphosphino)- 1,1′-biphenyl (BIPHEP) metal complexes as chiral selectors for the enantioseparation of amino acids using ELLE based on organic solvent (1,2-dichloroethane) and water, marking their first application for this purpose. The (S)-MeO-BIPHEP-Cu complex proved to be an effective chiral extractant, demonstrating impressive selectivity in resolving several amino acids. Specifically, it achieved selectivity values of 1.81 for 3-chloro-phenylglycine, 4.22 for tyrosine, 2.24 for phenylglycine, and 2.56 for phenylalanine. In a another study, Liu et al. [181] explored the potential of spirodiphosphine, specifically (S)-(-)-7,7-bis(diphenylphosphino)-2,2,3,3-tetrahydro-1,1-spiirobiindane (SDP), as a chiral extractant for enantioseparation of 4-nitrophenylalanine using ELLE based on organic solvent (1,2-dichloroethane) and water. The (S)-SDP-Pd complex achieved a separation factor of up to 3.32 for L-4-nitrophenylalanine under optimal conditions. Furthermore, the investigation into other chiral diphosphine ligands, such as (S,S)-DIOP and (S)-SEGPHOS, revealed strong enantioseparation capabilities for racemic amino acids, underscoring the ongoing potential of these compounds in ELLE [20].

**Cyclodextrins.** They are cyclic oligosaccharides composed of six to twelve glucopyranose units linked by α-1,4-glycosidic bonds. Depending on the number of glucose units, they are categorized as α-cyclodextrin (hexamer), β-cyclodextrin (heptamer), and γ-cyclodextrin (octamer) [20]. Among these, β-cyclodextrin is most widely applied due to its unique structure. It features numerous primary and secondary hydroxyl groups on its exterior, alongside oxygen atoms, creating a high electron cloud density. This arrangement enables the formation of diastereomeric complexes with enantiomers through electrostatic forces, hydrogen bonds, van der Waals forces, and hydrophobic interactions. The hydrophobic cavity and hydrophilic exterior facilitate these interactions, allowing the β-cyclodextrin's cavity to either wholly or partially enclose a guest molecule, depending on the size and shape of the macrocyclic structure [20].

Recently, derivatives of β-cyclodextrin such as hydroxypropyl-β-cyclodextrin (HP-β-CD), carboxymethyl-β-cyclodextrin (CM-β-CD), hydroxyethyl-β-cyclodextrin (HE-β-CD), and methyl-β-cyclodextrin (Me-β-CD) have been developed for enhanced enantioselectivity in ELLE [182]. For example, Jiao et al. [183] utilized carboxymethyl-β-cyclodextrin in an innovative aqueous two-phase system based on organic solvent (1-propanol) for enantioseparation of racemic zopiclone, achieving an impressive enantioselectivity of 2.58 in a single extraction run. Further, hydrophilic β-CD derivatives were investigated for the enantioselective extraction of oxybutynin enantiomers using a reactive extraction approach, with dichloromethane identified as the optimal solvent. HP-β-CD proved to be the most effective chiral selector, achieving an enantioselectivity of 1.26 under optimal conditions [184]. Tang et al. [185] explored the use of β-CD derivatives in the liquid-liquid reactive extraction of α-cyclohexyl-mandelic acid enantiomers. HP-β-CD and 1,2-dichloroethane were identified as the effective chiral selector and reactive extractant, achieving a maximum separation factor of 2.02 and an enantiomeric excess of 26.37%. Additionally, the enantioseparation of mandelic acid using aqueous two-phase systems consisting of polyethylene glycol and ammonium sulfate, with β-cyclodextrin as a chiral selector, was investigated. The results indicated a preference for the L-enantiomer, with a separation factor of 2.46 and enantiomeric excesses of 42.13% in the top phase and 40.43% in the bottom phase [186]. In another study, the enantioseparation of phenylsuccinic acid enantiomers was explored through liquid-liquid reactive extraction using β-cyclodextrin derivatives including HP-β-CD, HE-β-CD, and Me-β-CD and n-octanol as solvent. HP-β-CD

exhibited the strongest separation ability among the three, achieving a maximum enantioselectivity (α) of 2.38 under optimal conditions of pH 2.5 and temperature 5°C [187].

**Chiral ionic liquids (CILs).** They are a subclass of ILs - chemical compounds composed of ions with a melting point below 100 °C [20]. CILs feature chiral structures in their cations, anions, or both, and their structural diversity allows for the customization of chiral selectors. This versatility makes them widely employed in enantioseparation studies. The exceptional characteristics of CILs have led to a growing focus on them in recent years, both as standalone chiral selectors and in combination with other synergistic chiral selectors for ELLE. Several types have been explored, including imidazolium-based, tropine, amino acid ILs, and those incorporating boric acid, with research primarily concentrating on various amino acids [188-191]. Wu et al. [188] developed aqueous two-phase systems using imidazolium-based ILs and inorganic salts for the chiral extraction of racemic amino acids, achieving a notable maximum enantiomeric excess of 53% for phenylalanine. Similarly, Wu et al. [189] designed an aqueous two-phase system based on tropine ILs, copper ions, and inorganic salts for the enantioseparation of phenylalanine, finding that chiral tropine ILs with longer alkyl chains enhanced enantioselectivity, attaining a maximum enantiomeric excess of 65%. Carreira et al. [190] introduced a groundbreaking approach in chiral resolution using a novel spirocyclic chiral ILs, 1-butyl-3-methylimidazolium (T-4)-bis[(αS)-α-(hydroxy O)benzeneacetato-κO] borate ([BMIm][BSMB]), for the first-time application in the chiral resolution of propranolol, achieving an enantioselectivity of 1.76 in a 1,2-dichloroethane-water system. Furthermore, Tang et al. [191] reported the chiral extraction of amino acids using functional amino acid ILs as both solvent and chiral selector. These ILs, featuring alkylimidazolium cations and L-proline anions, were synthesized and modified with copper ions to form copper-proline complexes. In the functional amino acid IL-ethylacetate system, the logarithm of the distribution coefficient for L-phenylalanine ranged from 3.4 to 3.6, resulting in an impressive enantiomeric excess value of 50.6% through a chiral ligand-exchange process. Despite challenges such as cost and recycling difficulties limiting their practical application, CILs remain a promising alternative as chiral selectors in ELLE. Their unique ability to function as both solvent and chiral selector simultaneously in aqueous two-phase systems offers a convenient solution to enhance their utility in various applications.

**Tartrate assisted extractants.** D/L-tartrate derivatives are commonly employed as chiral selectors in enantioselective ELLE, encompassing variants such as n-butyl ester, isobutyl ester, n-amyl ester, isoamyl ester, n-hexyl ester, cyclohexyl ester, and benzyl ester of L or D tartaric acid. Although the standalone enantioseparation capabilities of tartrate derivatives were initially found to be limited [20], their enantiorecognition potential significantly improved when used in conjunction with synergistic chiral selectors such as boric acids, cyclodextrins, and phosphoric acids [192]. A notable application is the combination of tartrates and cyclodextrins in two-phase systems, widely adopted to enhance enantioselectivity. For example, Chen et al. [193] introduced an innovative biphasic recognition chiral extraction system utilizing an aqueous two-phase system based on ethanol/ammonium sulfate that incorporated L-(+)-tartaric acid diisopropyl ester and HP-β-CD as chiral selectors. This system, consisting of ethanol and ammonium sulfate, demonstrated a substantial increase in enantioselectivity for phenylsuccinic acid, achieving an enhancement up to 4.06 through a single-step extraction. The synergistic interaction between the biphasic chiral selectors was crucial for this notable improvement. Similarly, Jiao et al. [194] developed a two-phase system for the chiral separation of OFX, using β-CD in the aqueous phase and a combination of N,N'-dibenzoyl-L-tartaric acid (DBTA) with di-2-ethylhexyl phosphoric acid (D2EHPA) in the organic phase (n-Octanol) as synergistic extractants. The collaborative effect between the hydrophilic β-CD and the hydrophobic complexes formed by DBTA and D2EHPA led to an improved enantioselectivity and distribution ratio, with an enantioselectivity of up to 2.48 achieved under optimal conditions. The effectiveness of this synergistic two-phase extraction approach highlights the critical role of combined chiral selectors in enhancing separation performance.

**Crown ethers.** Crown ethers, part of the polyether family, are characterized by their internal cavities and have been historically instrumental in the chiral separation of compounds such as amino acids, aminoalcohols, and amines through enantioselective ELLE [20]. Although recent reports on the use of chiral crown ethers as selectors in ELLE have been limited, these instances primarily involve the separation of small molecules featuring amino groups [182]. A notable example includes the development of an enantioselective dispersive LLE system by Hashemi et al. [195], which employed an azophenolic crown ether for the micro-separation of trans-cyclohexane-1,2-diamine. This system achieved a high operational selectivity of 10.2 under optimum condition (300 µL of diethyl ether as the extraction solvent 1 mL of methanol as the disperser

solvent, with 5 mmol $L^{-1}$ chiral selector concentration, pH of the sample equal to 4.5, 30 min extraction time and a temperature of 10 °C). However, the intricate synthesis process and low overall yields of the chiral azophenol crown ether pose challenges for its broader application in large-scale industrial ELLE. These challenges necessitate careful consideration of cost-related factors and scalability.

The exploration of various chiral selectors, including metal complexes, cyclodextrins, CILs, tartrate-assisted extractants, and crown ethers, highlights the innovative approaches and significant advancements made in ELLE. These developments underscore the critical role of chiral selectors in achieving high enantioselectivity and optimizing the efficiency of the ELLE process. As research continues to evolve, the identification and refinement of effective and environmentally friendly chiral selectors will remain paramount in enhancing the precision and applicability of enantioseparation technologies.

In addition to chiral recognition, a critical component of ELLE is the process of solvent extraction, which involves host-mediated phase transfer of R/S enantiomers following the introduction of a chiral host into a system with two immiscible phases - usually an organic and an aqueous phase - similar to traditional LLE. The chiral extractant and the substrate are dissolved in these phases. Due to the different binding affinities between the R/S enantiomers and the chiral host, the (R)-enantiomer and the (S)-enantiomer are selectively enriched in separate phases [20]. To address the environmental concerns associated with organic solvents and ILs, the use of DESs has become increasingly popular in LLE systems. These solvents offer a more environmentally friendly alternative, enhancing the sustainability of the extraction processes.

### 1.5.1. Enantioselective liquid-liquid extraction (ELLE) based on hydrophobic deep eutectic solvents (HDESs)

The first application of DESs in enantioseparation using ELLE was investigated by Wang et al. [196]. They conducted a comprehensive study evaluating nine hydrophobic and six hydrophilic DESs for the enantioseparation of threonine. The study meticulously explored various factors that influence chiral separation, including the types of DES, phase volume ratio, water content, chiral selector concentration, initial threonine concentration, pH, and extraction temperature. The optimal system was found to comprise a HDES made of L-menthol and L-lactic acid paired with a hydrophilic DES of cholinium chloride and urea, at a volume ratio of 2:1. Chiral selectors,

specifically (+)-Diisopropyl L-tartrate (DIPT) for the hydrophobic phase and Hydroxylpropyl-β-cyclodextrin (HP-β-CD) for the hydrophilic phase, were integrated into the system. Optimal enantioseparation was achieved at a pH of 6.0, corresponding to the isoelectric point of threonine, culminating in a maximum enantiomeric excess (e.e.) of 31.6% [196].

In another investigation, the enantioseparation of tryptophan was studied using five ELLE systems combining two hydrophilic and three HDESs [197]. This innovative approach utilized DESs both as phase-forming components and chiral selectors, with the optimal configuration being a hydrophobic/hydrophilic system of methyl trioctyl ammonium chloride and L-Diethyl L-tartrate (2:1) combined with HP-β-CD and L-Malic Acid (10:1). Further optimization of the molar ratios HBA and HBD within the DESs was conducted to improve enantioseparation. The research also systematically evaluated the impact of phase volume ratio, initial tryptophan concentration, pH, and extraction temperature on separation efficiency, culminating in an impressive maximum enantiomeric excess (e.e.) of 38.46% [197].

Chen et al. [198] investigated the potential of using chiral DESs (CDESs) in ELLE for the enantioseparation of valsartan. Of the hydrophobic and hydrophilic DESs investigated, the hydrophobic variant of L-menthol and (+)-Di-p-toluoyl-D-tartaric acid (LM-DTTA) exhibited higher extraction selectivity for the valsartan enantiomers. Of the hydrophilic DESs, only Lys-Gly and Pro-CN-Gly exhibited enantioselectivity. In the study, four key parameters affecting chiral extraction were comprehensively evaluated: phase volume ratio, initial rac-valsartan concentration, extraction temperature and pH of the system. The results emphasized the remarkable enantioselectivity of LM-DTTA, which was attributed to the formation of a stable LM-DTTA/S-valsartan complex. The optimized conditions enabled a one-step chiral extraction that yielded an impressive enantiomeric excess of 91% for S-valsartan. Furthermore, the study showed the significant influence of system pH on enantioseparation and recommended a lower pH, lower valsartan concentration and lower extraction temperature as conducive for the selective separation of the S-enantiomer of rac-valsartan [198]. Table 1.5 presents a summary of the studies that utilized ELLE based on HDESs for the enantioseparation.

**Table 1.5.** A summary of the studies regarding the enantioseparation of compounds using HDESs-based ELLE based.

| Compound | BEST DES (molar ratio) | Chiral selector | Methodology | Best Enantioseparation conditions | Enantiomeric excess (%) | Ref. |
|---|---|---|---|---|---|---|
| **Threonine** | L-Menthol: L(+)-Lactic acid (1:1) + Cholinium chloride: Urea (1:1) | (+)-Diisopropyl L-tartrate (DIPT) Hydroxylpropyl-β-cyclodextrin (HP-β-CD) | Nine HDESs with six hydrophilic DESs were studied. Hydrophobic (DIPT) and hydrophilic (HP-β-CD) chiral selectors were added to the hydrophobic phase and to the hydrophilic phase. | DESs-water ratio (v/v)= 2:1, [DIPT] = 0.108 mol/L, [HP-β-CD] = 0.1 mol/L, [threonine] = 13 mg/g, water content = 20 wt% in the hydrophilic phase, pH=6.0, T = 35 °C. | 31.6 | [196] |
| **Tryptophan** | Methyl trioctyl ammonium chloride: L(+)-Diethyl L-tartrate (1:2) + HP-β-CD:L-(−)-Malic Acid (1:10) | * | Three HDESs with two hydrophilic DESs composed of chiral selectors were studied for enantioseparation of tryptophan. | DESs-water ratio (v/v )= 2:1, [Tryptophan] =10 mg/g, pH = 3.0, | 38.46 | [197] |
| **Valsartan** | L-menthol: (+)-Di-p-toluoyl-D-tartaric Acid (8:1) | * | Four chiral HDESs with five chiral hydrophilic DESs were studied for enantioseparation of valsartan. | DESs-water ratio (v/v) = 1, [Valsartan] = 80 mg/L, pH = 3.0, T = 30 °C. | 91 | [198] |

*DESs used as phase forming and chiral selector.

As shown in Table 1.5, DESs can act as both phase formers and chiral selectors. The proper selection of DESs provides a more stable and safer solvent alternative that effectively addresses the significant drawbacks of conventional chiral selectors, such as high volatility, flammability, and biotoxicity. As a result, DESs are proving to be the preferred option for many applications as they overcome the limitations associated with widely used conventional chiral selectors.

## 1.6. Additional remarks

DESs hold significant potential as alternative solvents for the extraction and purification of various compounds from a wide range of sources. Their key advantage lies in their "designer" ability, which allows customization of their extraction and purification performance. This chapter outlines the structure of the current thesis and provides an overview of the potential and suitability of DES-based solvents for the extraction and separation of compounds, with a focus on LLE and ELLE.

Despite extensive research by various authors on the screening of different DESs and the evaluation of different process conditions, most studies focus on hydrophilic DESs. However, their high water solubility poses a challenge for applications such as wastewater treatment. For LLE based on hydrophilic DES, a third component is required to enable phase separation. In addition, the recovery and reusability of hydrophilic DESs are often not as straightforward and cost-effective as desired, which is a significant drawback for their wide industrial application. Furthermore, hydrophilic DESs are limited in their ability to extract highly hydrophobic molecules, such as drugs. Therefore, the use of HDES-based LLE is more practical. However, the toxicity of DESs is a crucial factor to be considered in extraction and separation processes. Although some studies have investigated the toxicity of certain groups of DESs, there is still a long way to explore the potential of more biocompatible DESs as extraction solvents and in separation processes. In this thesis particular emphasis is placed on the use of more benign HDESs, addressing both the drawbacks of using hydrophilic DESs and toxicity concerns.

The use of HDES-based LLE/ELLE for the extraction and separation of biomolecules, such as drugs, is particularly advantageous. By designing HDESs tailored to the target compound and taking into account key factors such as high water stability, low cost, viscosity and toxicity, the limitations of other extraction systems can be overcome and

high extraction efficiency can be achieved. Furthermore, if carefully and appropriately selected, DESs can be used together with the extracted target compounds, eliminating the need for an additional recovery step in the process. For the development and selection of the most promising DESs, the use of a thermodynamic model as a pre-screening tool can be very beneficial as it avoids the cost and time associated with experimental measurements. Similar to the present work, COSMO-RS has been used in some studies for the initial screening of solvents [64, 140-143, 145-155].

The studies discussed in this chapter show that the use of suitable HDESs leads to high extraction yields, recoveries and enantioseparation factors. However, in order to develop cost-effective and sustainable extraction and separation processes using HDESs, several requirements must be met. These include: (i) identifying efficient, cost-effective and biocompatible HDESs that can compete with commonly used solvents; (ii) developing effective strategies for compound recovery and recycling of HDESs; (iii) conducting scale-up studies for optimized processes; and (iv) performing economic and life cycle analyzes for the developed processes. Although significant progress is still needed, HDES-based separation processes offer remarkable advantages and hold the potential to become an industrial reality in the coming decades.

## 1.7. References

[1] P.Y. Quintas, E.F. Fiorentini, M. Llaver, R.E. González, R.G. Wuilloud, State-of-the-art extraction and separation of enantiomers through the application of alternative solvents, TrAC Trends in Analytical Chemistry, 157 (2022) 116733.

[2] J. Sui, N. Wang, J. Wang, X. Huang, T. Wang, L. Zhou, H. Hao, Strategies for chiral separation: from racemate to enantiomer, Chemical Science, 14 (2023) 11955-12003.

[3] Q. Cheng, Q. Ma, H. Pei, Z. Mo, Chiral membranes for enantiomer separation: A comprehensive review, Separation and Purification Technology, 292 (2022) 121034.

[4] J. Ceramella, D. Iacopetta, A. Franchini, M. De Luca, C. Saturnino, I. Andreu, M.S. Sinicropi, A. Catalano, A look at the importance of chirality in drug activity: Some significative examples, Applied Sciences, 12 (2022) 10909.

[5] A. Piutti, Sintesi e costituzione delle asparagine, Gazz Chim Ital, 18 (1888) 457-472.

[6] M.C. Nunez, M.E. Garcia-Rubino, A. Conejo-Garcia, O. Cruz-Lopez, M. Kimatrai, M.A. Gallo, A. Espinosa, J.M. Campos, Homochiral drugs: a demanding tendency of the pharmaceutical industry, Current medicinal chemistry, 16 (2009) 2064-2074.

[7] M.T. Miller, K. Strömland, The study of malformations" by the company they keep", Transactions of the American Ophthalmological Society, 90 (1992) 247.

[8] Food, D. Administration, FDA's policy statement for the development of new stereoisomeric drugs, 57 Fed. Reg. 22, 249 (1992).

[9] M. Gumustas, S.A. Ozkan, B. Chankvetadze, Analytical and preparative scale separation of enantiomers of chiral drugs by chromatography and related methods, Current medicinal chemistry, 25 (2018) 4152-4188.

[10] J. Georgin, D.S.P. Franco, C.G. Ramos, D.G. Piccilli, E.C. Lima, F. Sher, A review of the antibiotic ofloxacin: Current status of ecotoxicology and scientific advances in its removal from aqueous systems by adsorption technology, Chemical Engineering Research and Design, (2023).

[11] E. Sanganyado, Z. Lu, Q. Fu, D. Schlenk, J. Gan, Chiral pharmaceuticals: A review on their environmental occurrence and fate processes, Water research, 124 (2017) 527-542.

[12] S. Orlandini, G. Hancu, Z.-I. Szabó, A. Modroiu, L.-A. Papp, R. Gotti, S. Furlanetto, New trends in the quality control of enantiomeric drugs: quality by design-compliant development of chiral capillary electrophoresis methods, Molecules, 27 (2022) 7058.

[13] M. Kholany, F.A. e Silva, T.E. Sintra, P. Brandao, S.P. Ventura, J.A. Coutinho, Separation of mandelic acid enantiomers using solid-liquid biphasic systems with chiral ionic liquids, Separation and Purification Technology, 252 (2020) 117468.

[14] L. Nie, A. Yohannes, S. Yao, Recent advances in the enantioseparation promoted by ionic liquids and their resolution mechanisms, Journal of Chromatography A, 1626 (2020) 461384.

[15] D. Wu, F. Pan, W. Tan, L. Gao, Y. Tao, Y. Kong, Recent progress of enantioseparation under scale production (2014–2019), Journal of separation science, 43 (2020) 337-347.

[16] H. Lorenz, F. Czapla, D. Polenske, M. Elsner, A. Seidel-Morgenstern, Crystallization based separation of enantiomers, Journal of the University of Chemical Technology and Metallurgy, 42 (2007) 5-16.

[17] D. Mangelings, M. Maftouh, Y. Vander Heyden, Capillary electrochromatographic chiral separations with potential for pharmaceutical analysis, Journal of separation science, 28 (2005) 691-709.

[18] S. Krait, M.L. Konjaria, G.K. Scriba, Advances of capillary electrophoresis enantioseparations in pharmaceutical analysis (2017–2020), Electrophoresis, 42 (2021) 1709-1725.

[19] B. Schuur, B.J. Verkuijl, A.J. Minnaard, J.G. De Vries, H.J. Heeres, B.L. Feringa, Chiral separation by enantioselective liquid–liquid extraction, Organic & Biomolecular Chemistry, 9 (2011) 36-51.

[20] B. Zhu, H. Qiu, C. Ma, S. Chen, J. Zhu, S. Tong, Recent progress on chiral extractants for enantioselective liquid-liquid extraction, Journal of Chromatography A, (2023) 464389.

[21] M.H. Al-Jabari, S. Sulaiman, S. Ali, R. Barakat, A. Mubarak, S.A. Khan, Adsorption study of levofloxacin on reusable magnetic nanoparticles: Kinetics and antibacterial activity, Journal of Molecular liquids, 291 (2019) 111249.

[22] M. Feng, Z. Wang, D.D. Dionysiou, V.K. Sharma, Metal-mediated oxidation of fluoroquinolone antibiotics in water: a review on kinetics, transformation products, and toxicity assessment, Journal of hazardous materials, 344 (2018) 1136-1154.

[23] Á. Santana-Mayor, R. Rodríguez-Ramos, A.V. Herrera-Herrera, B. Socas-Rodríguez, M.Á. Rodríguez-Delgado, Deep eutectic solvents. The new generation of green solvents in analytical chemistry, TrAC Trends in Analytical Chemistry, 134 (2021) 116108.

[24] A. Paiva, R. Craveiro, I. Aroso, M. Martins, R.L. Reis, A.R.C. Duarte, Natural deep eutectic solvents–solvents for the 21st century, ACS Sustainable Chemistry & Engineering, 2 (2014) 1063-1071.

[25] C.M. Chabib, J.K. Ali, M. Abi Jaoude, E. Alhseinat, I.A. Adeyemi, I.M. Al Nashef, Application of deep eutectic solvents in water treatment processes: A review, Journal of Water Process Engineering, 47 (2022) 102663.

[26] S.P. Ijardar, V. Singh, R.L. Gardas, Revisiting the physicochemical properties and applications of deep eutectic solvents, Molecules, 27 (2022) 1368.

[27] E.L. Smith, A.P. Abbott, K.S. Ryder, Deep eutectic solvents (DESs) and their applications, Chemical reviews, 114 (2014) 11060-11082.

[28] J.M. Silva, E. Silva, R.L. Reis, A.R.C. Duarte, A closer look in the antimicrobial properties of deep eutectic solvents based on fatty acids, Sustainable chemistry and pharmacy, 14 (2019) 100192.

[29] I. Juneidi, M. Hayyan, O. Mohd Ali, Toxicity profile of choline chloride-based deep eutectic solvents for fungi and Cyprinus carpio fish, Environmental Science and Pollution Research, 23 (2016) 7648-7659.

[30] A.P. Abbott, G. Capper, D.L. Davies, R.K. Rasheed, V. Tambyrajah, Novel solvent properties of choline chloride/urea mixtures, Chemical communications, (2003) 70-71.

[31] T. El Achkar, H. Greige-Gerges, S. Fourmentin, Basics and properties of deep eutectic solvents: a review, Environmental chemistry letters, 19 (2021) 3397-3408.

[32] M.A. Martins, S.P. Pinho, J.A. Coutinho, Insights into the nature of eutectic and deep eutectic mixtures, Journal of Solution Chemistry, 48 (2019) 962-982.

[33] M.B.S. Mr, V.S.K. Mr, M. Chaudhary, P. Singh, A mini review on synthesis, properties and applications of deep eutectic solvents, Journal of the Indian Chemical Society, 98 (2021) 100210.

[34] K.A. Omar, R. Sadeghi, Physicochemical properties of deep eutectic solvents: A review, Journal of Molecular Liquids, 360 (2022) 119524.

[35] D.J. van Osch, L.F. Zubeir, A. van den Bruinhorst, M.A. Rocha, M.C. Kroon, Hydrophobic deep eutectic solvents as water-immiscible extractants, Green Chemistry, 17 (2015) 4518-4521.

[36] A.P. Abbott, G. Capper, S. Gray, Design of improved deep eutectic solvents using hole theory, Chemphyschem: a European journal of chemical physics and physical chemistry, 7 (2006) 803-806.

[37] H.-Z. SU, J.-M. YIN, Q.-S. LIU, C.-P. LI, Properties of four deep eutectic solvents: density, electrical conductivity, dynamic viscosity and refractive index, Acta Physico-Chimica Sinica, 31 (2015) 1468-1473.

[38] A. Skulcova, A. Russ, M. Jablonsky, J. Sima, The pH behavior of seventeen deep eutectic solvents, BioResources, 13 (2018) 5042-5051.

[39] J.M. Silva, C.V. Pereira, F. Mano, E. Silva, V.n.I. Castro, I. Sá-Nogueira, R.L. Reis, A. Paiva, A.A. Matias, A.R.C. Duarte, Therapeutic role of deep eutectic solvents based on menthol and saturated fatty acids on wound healing, ACS Applied Bio Materials, 2 (2019) 4346-4355.

[40] C. Florindo, F. Lima, B.D. Ribeiro, I.M. Marrucho, Deep eutectic solvents: overcoming 21st century challenges, Current Opinion in Green and Sustainable Chemistry, 18 (2019) 31-36.

[41] M. Moradi, G. Pazuki, S.Z. Mahmoudabadi, A comprehensive study of the water stability of eutectic solvents using COSMO-SAC, Journal of Molecular Liquids, 387 (2023) 122605.

[42] W. Tang, Y. An, K.H. Row, Emerging applications of (micro) extraction phase from hydrophilic to hydrophobic deep eutectic solvents: opportunities and trends, TrAC Trends in Analytical Chemistry, 136 (2021) 116187.

[43] M. Marchel, M.P. Rayaroth, C. Wang, L. Kong, J.A. Khan, G. Boczkaj, Hydrophobic (deep) eutectic solvents (HDESs) as extractants for removal of pollutants from water and wastewater–a review, Chemical Engineering Journal, (2023) 144971.

[44] Y. Mai, X. Xian, L. Hu, X. Zhang, X. Zheng, S. Tao, X. Lin, Liquid–liquid extraction of levulinic acid from aqueous solutions using hydrophobic tri-n-octylamine/alcohol-based deep eutectic solvent, Chinese Journal of Chemical Engineering, 54 (2023) 248-256.

[45] E. Riveiro, B. González, Á. Domínguez, Extraction of adipic, levulinic and succinic acids from water using TOPO-based deep eutectic solvents, Separation and Purification Technology, 241 (2020) 116692.

[46] M. Lalikoglu, Separation of butyric acid from aqueous media using menthol-based hydrophobic deep eutectic solvent and modeling by response surface methodology, Biomass Conversion and Biorefinery, 12 (2022) 1331-1341.

[47] K. Xu, P. Xu, Y. Wang, Aqueous biphasic systems formed by hydrophilic and hydrophobic deep eutectic solvents for the partitioning of dyes, Talanta, 213 (2020) 120839.

[48] T. Fan, Z. Yan, C. Yang, S. Qiu, X. Peng, J. Zhang, L. Hu, L. Chen, Preparation of menthol-based hydrophobic deep eutectic solvents for the extraction of triphenylmethane dyes: quantitative properties and extraction mechanism, Analyst, 146 (2021) 1996-2008.

[49] K.A. Omar, R. Sadeghi, Hydrophobic deep eutectic solvents: thermo-physical characteristics and their application in liquid–liquid extraction, Journal of the Iranian Chemical Society, 19 (2022) 3529-3537.

[50] Y. Shi, D. Xiong, Y. Zhao, T. Li, K. Zhang, J. Fan, Highly efficient extraction/separation of Cr (VI) by a new family of hydrophobic deep eutectic solvents, Chemosphere, 241 (2020) 125082.

[51] S. Ruggeri, F. Poletti, C. Zanardi, L. Pigani, B. Zanfrognini, E. Corsi, N. Dossi, M. Salomäki, H. Kivelä, J. Lukkari, Chemical and electrochemical properties of a hydrophobic deep eutectic solvent, Electrochimica Acta, 295 (2019) 124-129.

[52] P.-A. Cablé, Y. Le Brech, F. Mutelet, Liquid-liquid extraction of phenolic compounds from aqueous solution using hydrophobic deep eutectic solvents, Journal of Molecular Liquids, 366 (2022) 120266.

[53] O.G. Sas, M. Castro, Á. Domínguez, B. González, Removing phenolic pollutants using deep eutectic solvents, Separation and Purification Technology, 227 (2019) 115703.

[54] H. Cheng, Y. Huang, H. Lv, L. Li, Q. Meng, M. Yuan, Y. Liang, M. Jin, Insights into the liquid extraction mechanism of actual high-strength phenolic wastewater by hydrophobic deep eutectic solvents, Journal of Molecular Liquids, 368 (2022) 120609.

[55] D. Rodríguez-Llorente, A. Cañada-Barcala, C. Muñoz, G. Pascual-Muñoz, P. Navarro, R. Santiago, V.I. Águeda, S. Álvarez-Torrellas, J. García, M. Larriba, Separation of phenols from aqueous streams using terpenoids and hydrophobic eutectic solvents, Separation and Purification Technology, 251 (2020) 117379.

[56] E.J. González, M. González-Miquel, I. Díaz, M. Rodríguez, C. Fontela, R. Cañadas, J. Sánchez, Enhancing aqueous systems fermentability using hydrophobic eutectic solvents as extractans of inhibitory compounds, Separation and Purification Technology, 250 (2020) 117184.

[57] I. Adeyemi, R. Sulaiman, M. Almazroui, A. Al-Hammadi, I. AlNashef, Removal of chlorophenols from aqueous media with hydrophobic deep eutectic solvents: Experimental study and COSMO RS evaluation, Journal of Molecular Liquids, 311 (2020) 113180.

[58] O.G. Sas, L. Villar, Á. Domínguez, B. González, E.A. Macedo, Hydrophobic deep eutectic solvents as extraction agents of nitrophenolic pollutants from aqueous systems, Environmental Technology & Innovation, 25 (2022) 102170.

[59] Y. An, K.H. Row, Evaluation of menthol-based hydrophobic deep eutectic solvents for the extraction of bisphenol A from environment water, Analytical Letters, 54 (2021) 1533-1545.

[60] C. Florindo, L. Romero, I. Rintoul, L.C. Branco, I.M. Marrucho, From phase change materials to green solvents: Hydrophobic low viscous fatty acid–based deep eutectic solvents, ACS Sustainable Chemistry & Engineering, 6 (2018) 3888-3895.

[61] C. Florindo, N.V. Monteiro, B.D. Ribeiro, L. Branco, I. Marrucho, Hydrophobic deep eutectic solvents for purification of water contaminated with Bisphenol-A, Journal of Molecular Liquids, 297 (2020) 111841.

[62] D. Rodríguez-Llorente, P. Navarro, R. Santiago, V.I. Águeda, S. Álvarez-Torrellas, J. García, M. Larriba, Extractive removal and recovery of bisphenol A from aqueous solutions using terpenoids and hydrophobic eutectic solvents, Journal of Environmental Chemical Engineering, 9 (2021) 106128.

[63] C. Florindo, L. Branco, I. Marrucho, Development of hydrophobic deep eutectic solvents for extraction of pesticides from aqueous environments, Fluid Phase Equilibria, 448 (2017) 135-142.

[64] R. Verma, T. Banerjee, Liquid–liquid extraction of lower alcohols using menthol-based hydrophobic deep eutectic solvent: experiments and COSMO-SAC predictions, Industrial & Engineering Chemistry Research, 57 (2018) 3371-3381.

[65] Y. Fan, H. Wu, D. Cai, T. Yang, L. Yang, Effective extraction of harmine by menthol/anise alcohol-based natural deep eutectic solvents, Separation and Purification Technology, 250 (2020) 117211.

[66] C. Florindo, F. Lima, L.s.C. Branco, I.M. Marrucho, Hydrophobic deep eutectic solvents: a circular approach to purify water contaminated with ciprofloxacin, ACS sustainable chemistry & engineering, 7 (2019) 14739-14746.

[67] P. Gutiérrez-Sánchez, D. Rodríguez-Llorente, P. Navarro, V.I. Águeda, S. Álvarez-Torrellas, J. García, M. Larriba, Extraction of antibiotics identified in the EU Watch List 2020 from hospital wastewater using hydrophobic eutectic solvents and terpenoids, Separation and Purification Technology, 282 (2022) 120117.

[68] T. Hložek, T. Bosáková, Z. Bosáková, P. Tůma, Hydrophobic eutectic solvents for endocrine disruptors purification from water: Natural and synthetic estrogens study, Separation and Purification Technology, 303 (2022) 122310.

[69] K. McGaughy, M.T. Reza, Liquid–Liquid Extraction of Furfural from Water by Hydrophobic Deep Eutectic Solvents: Improvement of Density Function Theory Modeling with Experimental Validations, ACS omega, 5 (2020) 22305-22313.

[70] P. Makoś, E. Słupek, J. Gębicki, Extractive detoxification of feedstocks for the production of biofuels using new hydrophobic deep eutectic solvents–Experimental and theoretical studies, Journal of Molecular Liquids, 308 (2020) 113101.

[71] H. Luo, H. Yao, X. Wang, X. Liang, B. Li, H. Liu, Y. Li, Selective recovery of lithium from mother liquor of Li2CO3 by synergistic hydrophobic deep eutectic solvents: Performance and mechanistic insight, Separation and Purification Technology, 313 (2023) 123353.

[72] K. Xue, D. Fan, X. Wang, Z. Dong, Z. Zhu, P. Cui, F. Meng, Y. Wang, J. Qi, Lithium extraction from aqueous medium using hydrophobic deep eutectic solvents, Journal of Environmental Chemical Engineering, 11 (2023) 110490.

[73] L. Fortunato, L. Al Fuhaid, S. Murgolo, C. De Ceglie, G. Mascolo, L. Falivene, J.S. Vrouwenvelder, G.-J. Witkamp, A. Farinha, Removal of polyfluoroalkyl substances (PFAS) from water using hydrophobic natural deep eutectic solvents (NADES): A proof of concept study, Journal of Water Process Engineering, 56 (2023) 104401.

[74] D.J. Van Osch, C.H. Dietz, J. Van Spronsen, M.C. Kroon, F. Gallucci, M. van Sint Annaland, R. Tuinier, A search for natural hydrophobic deep eutectic solvents based on natural components, ACS Sustainable Chemistry & Engineering, 7 (2019) 2933-2942.

[75] G. Almustafa, R. Sulaiman, M. Kumar, I. Adeyemi, H.A. Arafat, I. AlNashef, Boron extraction from aqueous medium using novel hydrophobic deep eutectic solvents, Chemical Engineering Journal, 395 (2020) 125173.

[76] M.P. Kusturica, M. Jevtic, J.T. Ristovski, Minimizing the environmental impact of unused pharmaceuticals: review focused on prevention, (2022).

[77] A. Garrison, GC/MS analysis of organic compounds in domestic wastewaters, Identification and analysis of organic pollutants in water, (1976).

[78] M.R. Siddiqui, Z.A. AlOthman, N. Rahman, Analytical techniques in pharmaceutical analysis: A review, Arabian Journal of chemistry, 10 (2017) S1409-S1421.

[79] P. Makoś, E. Słupek, J. Gębicki, Hydrophobic deep eutectic solvents in microextraction techniques–A review, Microchemical journal, 152 (2020) 104384.

[80] H. Sereshti, F. Karami, N. Nouri, A green dispersive liquid-liquid microextraction based on deep eutectic solvents doped with β-cyclodextrin: Application for determination of tetracyclines in water samples, Microchemical Journal, 163 (2021) 105914.

[81] H. Sereshti, S.S. Jazani, N. Nouri, G. Shams, Dispersive liquid–liquid microextraction based on hydrophobic deep eutectic solvents: application for tetracyclines monitoring in milk, Microchemical Journal, 158 (2020) 105269.

[82] X. Di, X. Zhao, X. Guo, Hydrophobic deep eutectic solvent as a green extractant for high-performance liquid chromatographic determination of tetracyclines in water samples, Journal of Separation Science, 43 (2020) 3129-3135.

[83] H. Sereshti, G. Abdolhosseini, S. Soltani, F. Jamshidi, N. Nouri, Natural thymol-based ternary deep eutectic solvents: Application in air-bubble assisted-dispersive liquid-liquid microextraction for the analysis of tetracyclines in water, Journal of Separation Science, 44 (2021) 3626-3635.

[84] A. Shishov, D. Nechaeva, A. Bulatov, HPLC-MS/MS determination of non-steroidal anti-inflammatory drugs in bovine milk based on simultaneous deep eutectic solvents formation and its solidification, Microchemical Journal, 150 (2019) 104080.

[85] L. Qiao, R. Sun, C. Yu, Y. Tao, Y. Yan, Novel hydrophobic deep eutectic solvents for ultrasound-assisted dispersive liquid-liquid microextraction of trace non-steroidal anti-inflammatory drugs in water and milk samples, Microchemical Journal, 170 (2021) 106686.

[86] A.Y. Shishov, M.V. Chislov, D.V. Nechaeva, L.N. Moskvin, A.V. Bulatov, A new approach for microextraction of non-steroidal anti-inflammatory drugs from human urine samples based on in-situ deep eutectic mixture formation, Journal of Molecular Liquids, 272 (2018) 738-745.

[87] A. Shishov, A. Gorbunov, E. Baranovskii, A. Bulatov, Microextraction of sulfonamides from chicken meat samples in three-component deep eutectic solvent, Microchemical Journal, 158 (2020) 105274.

[88] Y. Ji, Z. Meng, J. Zhao, H. Zhao, L. Zhao, Eco-friendly ultrasonic assisted liquid–liquid microextraction method based on hydrophobic deep eutectic solvent for the determination of sulfonamides in fruit juices, Journal of Chromatography A, 1609 (2020) 460520.

[89] F. Shakirova, A. Shishov, A. Bulatov, Automated liquid-liquid microextraction and determination of sulfonamides in urine samples based on Schiff bases formation in natural deep eutectic solvent media, Talanta, 234 (2021) 122660.

[90] A. Pochivalov, K. Cherkashina, A. Shishov, A. Bulatov, Microextraction of sulfonamides from milk samples based on hydrophobic deep eutectic solvent formation by pH adjusting, Journal of Molecular Liquids, 339 (2021) 116827.

[91] Q. Qu, Y. Lv, L. Liu, K.H. Row, T. Zhu, Synthesis and characterization of deep eutectic solvents (five hydrophilic and three hydrophobic), and hydrophobic application

for microextraction of environmental water samples, Analytical and bioanalytical chemistry, 411 (2019) 7489-7498.

[92] W. Ma, K.H. Row, pH-induced deep eutectic solvents based homogeneous liquid-liquid microextraction for the extraction of two antibiotics from environmental water, Microchemical Journal, 160 (2021) 105642.

[93] K. Li, Y. Jin, D. Jung, K. Park, H. Kim, J. Lee, In situ formation of thymol-based hydrophobic deep eutectic solvents: Application to antibiotics analysis in surface water based on liquid-liquid microextraction followed by liquid chromatography, Journal of Chromatography A, 1614 (2020) 460730.

[94] M. Nemati, M.R.A. Mogaddam, M.A. Farazajdeh, M. Tuzen, J. Khandaghi, In-situ formation/decomposition of deep eutectic solvent during solidification of floating organic droplet-liquid-liquid microextraction method for the extraction of some antibiotics from honey prior to high performance liquid chromatography-tandem mass spectrometry, Journal of Chromatography a, 1660 (2021) 462653.

[95] W. Tang, Y. Dai, K.H. Row, Evaluation of fatty acid/alcohol-based hydrophobic deep eutectic solvents as media for extracting antibiotics from environmental water, Analytical and bioanalytical chemistry, 410 (2018) 7325-7336.

[96] M. Shirani, B. Akbari-Adergani, F. Shahdadi, M. Faraji, A. Akbari, A hydrophobic deep eutectic solvent-based ultrasound-assisted dispersive liquid–liquid microextraction for determination of β-lactam antibiotics residues in food samples, Food Analytical Methods, (2021) 1-10.

[97] A. Jouyban, M.A. Farajzadeh, M.R.A. Mogaddam, F. Khodadadeian, M. Nemati, M. Khoubnasabjafari, In-situ formation of a hydrophobic deep eutectic solvent based on alpha terpineol and its application in liquid-liquid microextraction of three β-blockers from plasma samples, Microchemical Journal, 170 (2021) 106687.

[98] S. Yıldırım, H.E. Sellitepe, Vortex assisted liquid-liquid microextraction based on in situ formation of a natural deep eutectic solvent by microwave irradiation for the determination of beta-blockers in water samples, Journal of Chromatography A, 1642 (2021) 462007.

[99] A. Mohebbi, M.A. Farajzadeh, M. Nemati, N. Sarhangi, M.R. Afshar Mogaddam, Development of green sodium sulfate-induced solidification of floating organic droplets–dispersive liquid phase microextraction method: Application to extraction of four antidepressants, Biomedical Chromatography, 33 (2019) e4642.

[100] M. Ghane, A. Mohadesi, M. Ezoddin, M. Ali Karimi, K. Abdi, Dispersive liquid–liquid microextraction with back extraction based on in situ deep eutectic solvent decomposition and air-assisted for determination of some antidepressant drugs in biological samples prior to HPLC-UV, International Journal of Environmental Analytical Chemistry, (2022) 1-15.

[101] A. Mohebbi, S. Yaripour, M.A. Farajzadeh, M.R.A. Mogaddam, Combination of dispersive solid phase extraction and deep eutectic solvent–based air–assisted liquid–liquid microextraction followed by gas chromatography–mass spectrometry as an efficient analytical method for the quantification of some tricyclic antidepressant drugs in biological fluids, Journal of Chromatography A, 1571 (2018) 84-93.

[102] Y. Liu, W. Xu, H. Zhang, W. Xu, Hydrophobic deep eutectic solvent-based dispersive liquid–liquid microextraction for the simultaneous enantiomeric analysis of five β-agonists in the environmental samples, Electrophoresis, 40 (2019) 2828-2836.

[103] A. Shishov, A. Gerasimov, D. Nechaeva, N. Volodina, E. Bessonova, A. Bulatov, An effervescence-assisted dispersive liquid–liquid microextraction based on deep eutectic solvent decomposition: Determination of ketoprofen and diclofenac in liver, Microchemical Journal, 156 (2020) 104837.

[104] E. Kurtulbaş, A.G. Pekel, İ. Toprakçı, G. Özçelik, M. Bilgin, S. Şahin, Hydrophobic carboxylic acid based deep eutectic solvent for the removal of diclofenac, Biomass Conversion and Biorefinery, (2020) 1-9.

[105] M. Rajabi, N. Ghassab, M. Hemmati, A. Asghari, Highly effective and safe intermediate based on deep eutectic medium for carrier less-three phase hollow fiber microextraction of antiarrhythmic agents in complex matrices, Journal of Chromatography B, 1104 (2019) 196-204.

[106] M. Rajabi, N. Ghassab, M. Hemmati, A. Asghari, Emulsification microextraction of amphetamine and methamphetamine in complex matrices using an up-to-date generation of eco-friendly and relatively hydrophobic deep eutectic solvent, Journal of Chromatography A, 1576 (2018) 1-9.

[107] N. Lamei, M. Ezoddin, K. Abdi, Air assisted emulsification liquid-liquid microextraction based on deep eutectic solvent for preconcentration of methadone in water and biological samples, Talanta, 165 (2017) 176-181.

[108] S.M. Majidi, M.R. Hadjmohammadi, Hydrophobic borneol-based natural deep eutectic solvents as a green extraction media for air-assisted liquid-liquid micro-

extraction of warfarin in biological samples, Journal of Chromatography A, 1621 (2020) 461030.

[109] W. Zhu, P. Jin, M. Cheng, H. Yang, M. Du, T. Li, G. Zhu, J. Fan, Novel recyclable acidic hydrophobic deep eutectic solvents for highly efficient extraction of calcium dobesilate in water and urine samples, Talanta, 233 (2021) 122523.

[110] A. Jouyban, M.A. Farajzadeh, F. Khodadadeian, M. Khoubnasabjafari, M.R.A. Mogaddam, Development of a deep eutectic solvent-based ultrasound-assisted homogenous liquid-liquid microextraction method for simultaneous extraction of daclatasvir and sofosbuvir from urine samples, Journal of Pharmaceutical and Biomedical Analysis, 204 (2021) 114254.

[111] A.G. Pekel, E. Kurtulbaş, İ. Toprakçı, S. Şahin, Menthol-based deep eutectic solvent for the separation of carbamazepine: reactive liquid-liquid extraction, Biomass Conversion and Biorefinery, (2020) 1-8.

[112] H. Heidari, C. Mammostafaei, Spectrophotometric determination of lamotrigine in plasma samples: Ultrasound-assisted emulsification-microextraction based on a hydrophobic deep eutectic solvent followed by back-extraction, Spectrochimica Acta Part A: Molecular and Biomolecular Spectroscopy, 247 (2021) 119098.

[113] J. Cao, M. Yang, F. Cao, J. Wang, E. Su, Well-designed hydrophobic deep eutectic solvents as green and efficient media for the extraction of artemisinin from Artemisia annua leaves, ACS Sustainable Chemistry & Engineering, 5 (2017) 3270-3278.

[114] L. Khare, T. Karve, R. Jain, P. Dandekar, Menthol based hydrophobic deep eutectic solvent for extraction and purification of ergosterol using response surface methodology, Food Chemistry, 340 (2021) 127979.

[115] W. Tang, K.H. Row, Design and evaluation of polarity controlled and recyclable deep eutectic solvent based biphasic system for the polarity driven extraction and separation of compounds, Journal of cleaner production, 268 (2020) 122306.

[116] S.Z. Mahmoudabadi, G. Pazuki, Investigation of COSMO-SAC model for solubility and cocrystal formation of pharmaceutical compounds, Scientific Reports, 10 (2020) 19879.

[117] J. Yang, Z. Hou, G. Wen, P. Cui, Y. Wang, J. Gao, A brief review of the prediction of liquid–liquid equilibrium of ternary systems containing ionic liquids by the COSMO-SAC model, Journal of Solution Chemistry, 48 (2019) 1547-1563.

[118] S.Z. Mahmoudabadi, G. Pazuki, Modeling of thermodynamics properties of amino acid solutions by COSMO-SAC model, Fluid Phase Equilibria, 541 (2021) 113078.

[119] A. Klamt, Conductor-like screening model for real solvents: a new approach to the quantitative calculation of solvation phenomena, The Journal of Physical Chemistry, 99 (1995) 2224-2235.

[120] S.-T. Lin, S.I. Sandler, A priori phase equilibrium prediction from a segment contribution solvation model, Industrial & engineering chemistry research, 41 (2002) 899-913.

[121] I.I. Alkhatib, D. Bahamon, F. Llovell, M.R. Abu-Zahra, L.F. Vega, Perspectives and guidelines on thermodynamic modelling of deep eutectic solvents, Journal of Molecular Liquids, 298 (2020) 112183.

[122] I. Bashir, A.H. Dar, K.K. Dash, V.K. Pandey, U. Fayaz, R. Shams, S. Srivastava, R. Singh, Deep eutectic solvents for extraction of functional components from plant-based products: A promising approach, Sustainable Chemistry and Pharmacy, 33 (2023) 101102.

[123] M. Diedenhofen, A. Klamt, COSMO-RS as a tool for property prediction of IL mixtures—A review, Fluid Phase Equilibria, 294 (2010) 31-38.

[124] T. Lemaoui, N.E.H. Hammoudi, I.M. Alnashef, M. Balsamo, A. Erto, B. Ernst, Y. Benguerba, Quantitative structure properties relationship for deep eutectic solvents using Sσ-profile as molecular descriptors, Journal of Molecular Liquids, 309 (2020) 113165.

[125] Y. Benguerba, I.M. Alnashef, A. Erto, M. Balsamo, B. Ernst, A quantitative prediction of the viscosity of amine based DESs using Sσ-profile molecular descriptors, Journal of Molecular Structure, 1184 (2019) 357-363.

[126] T. Aissaoui, Y. Benguerba, M.K. AlOmar, I.M. AlNashef, Computational investigation of the microstructural characteristics and physical properties of glycerol-based deep eutectic solvents, Journal of molecular modeling, 23 (2017) 1-11.

[127] S. Benabid, Y. Benguerba, I.M. AlNashef, N. Haddaoui, Theoretical study of physicochemical properties of selected ammonium salt-based deep eutectic solvents, Journal of Molecular Liquids, 285 (2019) 38-46.

[128] T. Aissaoui, Y. Benguerba, I.M. AlNashef, Theoretical investigation on the microstructure of triethylene glycol based deep eutectic solvents: COSMO-RS and TURBOMOLE prediction, Journal of Molecular Structure, 1141 (2017) 451-456.

[129] J.P. Wojeicchowski, D.O. Abranches, A.M. Ferreira, M.R. Mafra, J.o.A. Coutinho, Using COSMO-RS to predict solvatochromic parameters for deep eutectic solvents, ACS Sustainable Chemistry & Engineering, 9 (2021) 10240-10249.

[130] J. Sherwood, J. Granelli, C.R. McElroy, J.H. Clark, A method of calculating the Kamlet–Abboud–Taft solvatochromic parameters Using COSMO-RS, Molecules, 24 (2019) 2209.

[131] T. Lemaoui, A.S. Darwish, N.E.H. Hammoudi, F. Abu Hatab, A. Attoui, I.M. Alnashef, Y. Benguerba, Prediction of electrical conductivity of deep eutectic solvents using COSMO-RS sigma profiles as molecular descriptors: a quantitative structure–property relationship study, Industrial & Engineering Chemistry Research, 59 (2020) 13343-13354.

[132] Y. Liu, H. Yu, Y. Sun, S. Zeng, X. Zhang, Y. Nie, S. Zhang, X. Ji, Screening deep eutectic solvents for CO2 capture with COSMO-RS, Frontiers in Chemistry, 8 (2020) 82.

[133] H. Qin, Z. Song, H. Cheng, L. Deng, Z. Qi, Physical absorption of carbon dioxide in imidazole-PTSA based deep eutectic solvents, Journal of Molecular Liquids, 326 (2021) 115292.

[134] T. Aissaoui, I.M. AlNashef, Y. Benguerba, Dehydration of natural gas using choline chloride based deep eutectic solvents: COSMO-RS prediction, Journal of Natural Gas Science and Engineering, 30 (2016) 571-577.

[135] J.L. Trenzado, C. Benito, M. Atilhan, S. Aparicio, Hydrophobic Deep eutectic Solvents based on cineole and organic acids, Journal of Molecular Liquids, 377 (2023) 121322.

[136] L. Fernandez, L.P. Silva, M.A. Martins, O. Ferreira, J. Ortega, S.P. Pinho, J.A. Coutinho, Indirect assessment of the fusion properties of choline chloride from solid-liquid equilibria data, Fluid Phase Equilibria, 448 (2017) 9-14.

[137] D. Peng, A. Alhadid, M. Minceva, Assessment of COSMO-SAC predictions for solid–liquid equilibrium in binary eutectic systems, Industrial & Engineering Chemistry Research, 61 (2022) 13256-13264.

[138] J.P. Wojeicchowski, A.M. Ferreira, D.O. Abranches, M.R. Mafra, J.A. Coutinho, Using COSMO-RS in the design of deep eutectic solvents for the extraction of antioxidants from rosemary, ACS Sustainable Chemistry & Engineering, 8 (2020) 12132-12141.

[139] F. Bezold, M.E. Weinberger, M. Minceva, Assessing solute partitioning in deep eutectic solvent-based biphasic systems using the predictive thermodynamic model COSMO-RS, Fluid Phase Equilibria, 437 (2017) 23-33.

[140] F. Bezold, M.E. Weinberger, M. Minceva, Computational solvent system screening for the separation of tocopherols with centrifugal partition chromatography using deep eutectic solvent-based biphasic systems, Journal of Chromatography A, 1491 (2017) 153-158.

[141] S.E. Warrag, I. Adeyemi, N.R. Rodriguez, I.M. Nashef, M. van Sint Annaland, M.C. Kroon, C.J. Peters, Effect of the type of ammonium salt on the extractive desulfurization of fuels using deep eutectic solvents, Journal of Chemical & Engineering Data, 63 (2018) 1088-1095.

[142] P.K. Naik, S. Paul, T. Banerjee, Liquid Liquid Equilibria measurements for the extraction of poly aromatic nitrogen hydrocarbons with a low cost Deep Eutectic Solvent: Experimental and theoretical insights, Journal of Molecular Liquids, 243 (2017) 542-552.

[143] B. Ozturk, M. Gonzalez-Miquel, Alkanediol-based deep eutectic solvents for isolation of terpenoids from citrus essential oil: Experimental evaluation and COSMO-RS studies, Separation and Purification Technology, 227 (2019) 115707.

[144] J.-B. Chagnoleau, N. Papaiconomou, M. Jamali, D.O. Abranches, J.o.A. Coutinho, X. Fernandez, T. Michel, Toward a critical evaluation of DES-based organic biphasic systems: are deep eutectic solvents so critical?, ACS Sustainable Chemistry & Engineering, 9 (2021) 9707-9716.

[145] S. Mulyono, H.F. Hizaddin, I.M. Alnashef, M.A. Hashim, A.H. Fakeeha, M.K. Hadj-Kali, Separation of BTEX aromatics from n-octane using a (tetrabutylammonium bromide+ sulfolane) deep eutectic solvent–experiments and COSMO-RS prediction, Rsc Advances, 4 (2014) 17597-17606.

[146] A.S. Gouveia, F.S. Oliveira, K.A. Kurnia, I.M. Marrucho, Deep eutectic solvents as azeotrope breakers: liquid–liquid extraction and COSMO-RS prediction, ACS Sustainable Chemistry & Engineering, 4 (2016) 5640-5650.

[147] H.F. Hizaddin, M. Sarwono, M.A. Hashim, I.M. Alnashef, M.K. Hadj-Kali, Coupling the capabilities of different complexing agents into deep eutectic solvents to enhance the separation of aromatics from aliphatics, The Journal of Chemical Thermodynamics, 84 (2015) 67-75.

[148] M.K. Hadj-Kali, H.F. Hizaddin, I. Wazeer, S. Mulyono, M.A. Hashim, Liquid-liquid separation of azeotropic mixtures of ethanol/alkanes using deep eutectic solvents: COSMO-RS prediction and experimental validation, Fluid Phase Equilibria, 448 (2017) 105-115.

[149] M.K. Hadj-Kali, S. Mulyono, H.F. Hizaddin, I. Wazeer, L. El-Blidi, E. Ali, M.A. Hashim, I.M. AlNashef, Removal of thiophene from mixtures with n-heptane by selective extraction using deep eutectic solvents, Industrial & Engineering Chemistry Research, 55 (2016) 8415-8423.

[150] I. Wazeer, H.F. Hizaddin, L. El Blidi, E. Ali, M.A. Hashim, M.K. Hadj-Kali, Liquid–liquid equilibria for binary azeotrope mixtures of benzene and alcohols using choline chloride-based deep eutectic solvents, Journal of Chemical & Engineering Data, 63 (2018) 613-624.

[151] N. Delgado Mellado, M. Larriba, M. Ayuso, P. Navarro, M. Gonzalez-Miquel, J. García González, F. Rodríguez Somolinos, Choline Chloride-Based Deep Eutectic Solvents in the Dearomatization of Gasolines, (2017).

[152] H.F. Hizaddin, A. Ramalingam, M.A. Hashim, M.K. Hadj-Kali, Evaluating the performance of deep eutectic solvents for use in extractive denitrification of liquid fuels by the conductor-like screening model for real solvents, Journal of Chemical & Engineering Data, 59 (2014) 3470-3487.

[153] H. Cheng, C. Liu, J. Zhang, L. Chen, B. Zhang, Z. Qi, Screening deep eutectic solvents for extractive desulfurization of fuel based on COSMO-RS model, Chemical Engineering and Processing-Process Intensification, 125 (2018) 246-252.

[154] H.F. Hizaddin, M.K. Hadj-Kali, A. Ramalingam, M.A. Hashim, Extractive denitrogenation of diesel fuel using ammonium-and phosphonium-based deep eutectic solvents, The Journal of Chemical Thermodynamics, 95 (2016) 164-173.

[155] N.R. Rodriguez, T. Gerlach, D. Scheepers, M.C. Kroon, I. Smirnova, Experimental determination of the LLE data of systems consisting of {hexane+ benzene+ deep eutectic solvent} and prediction using the Conductor-like Screening Model for Real Solvents, The journal of chemical thermodynamics, 104 (2017) 128-137.

[156] D.O. Abranches, M.A. Martins, L.P. Silva, N. Schaeffer, S.P. Pinho, J.A. Coutinho, Phenolic hydrogen bond donors in the formation of non-ionic deep eutectic solvents: the quest for type V DES, Chemical communications, 55 (2019) 10253-10256.

[157] D.O. Abranches, M. Larriba, L.P. Silva, M. Melle-Franco, J.F. Palomar, S.P. Pinho, J.A. Coutinho, Using COSMO-RS to design choline chloride pharmaceutical eutectic solvents, Fluid Phase Equilibria, 497 (2019) 71-78.

[158] Z. Song, J. Wang, K. Sundmacher, Evaluation of COSMO-RS for solid–liquid equilibria prediction of binary eutectic solvent systems, Green Energy & Environment, 6 (2021) 371-379.

[159] A. Alhadid, C. Jandl, L. Mokrushina, M. Minceva, Cocrystal formation in l-menthol/phenol eutectic system: experimental study and thermodynamic modeling, Crystal Growth & Design, 22 (2022) 3973-3980.

[160] L.P. Silva, L. Fernandez, J.H. Conceição, M.A. Martins, A. Sosa, J. Ortega, S.P. Pinho, J.A. Coutinho, Design and characterization of sugar-based deep eutectic solvents using conductor-like screening model for real solvents, ACS sustainable chemistry & engineering, 6 (2018) 10724-10734.

[161] M.M. Abdallah, S. Müller, A. González de Castilla, P. Gurikov, A.A. Matias, M.d.R. Bronze, N. Fernández, Physicochemical characterization and simulation of the solid–liquid equilibrium phase diagram of terpene-based eutectic solvent systems, Molecules, 26 (2021) 1801.

[162] T. Jeliński, P. Cysewski, Application of a computational model of natural deep eutectic solvents utilizing the COSMO-RS approach for screening of solvents with high solubility of rutin, Journal of Molecular Modeling, 24 (2018) 1-17.

[163] A. Kamgar, S. Mohsenpour, F. Esmaeilzadeh, Solubility prediction of CO2, CH4, H2, CO and N2 in Choline Chloride/Urea as a eutectic solvent using NRTL and COSMO-RS models, Journal of Molecular Liquids, 247 (2017) 70-74.

[164] B. Ozturk, J. Winterburn, M. Gonzalez-Miquel, Orange peel waste valorisation through limonene extraction using bio-based solvents, Biochemical engineering journal, 151 (2019) 107298.

[165] J.P. Wojeicchowski, C. Marques, L. Igarashi-Mafra, J.A. Coutinho, M.R. Mafra, Extraction of phenolic compounds from rosemary using choline chloride–based deep eutectic solvents, Separation and Purification Technology, 258 (2021) 117975.

[166] O. Alioui, Y. Benguerba, I.M. Alnashef, Investigation of the CO2-solubility in deep eutectic solvents using COSMO-RS and molecular dynamics methods, Journal of Molecular Liquids, 307 (2020) 113005.

[167] T. Jeliński, M. Przybyłek, P. Cysewski, Solubility advantage of sulfanilamide and sulfacetamide in natural deep eutectic systems: experimental and theoretical investigations, Drug development and industrial pharmacy, 45 (2019) 1120-1129.

[168] H. Jiang, D. Xu, L. Zhang, Y. Ma, J. Gao, Y. Wang, Vapor–liquid phase equilibrium for separation of isopropanol from its aqueous solution by choline chloride-based deep eutectic solvent selected by COSMO-SAC model, Journal of Chemical & Engineering Data, 64 (2019) 1338-1348.

[169] X. Shang, S. Ma, Q. Pan, J. Li, Y. Sun, K. Ji, L. Sun, Process analysis of extractive distillation for the separation of ethanol–water using deep eutectic solvent as entrainer, Chemical Engineering Research and Design, 148 (2019) 298-311.

[170] E. Zurob, R. Cabezas, E. Villarroel, N. Rosas, G. Merlet, E. Quijada-Maldonado, J. Romero, A. Plaza, Design of natural deep eutectic solvents for the ultrasound-assisted extraction of hydroxytyrosol from olive leaves supported by COSMO-RS, Separation and Purification Technology, 248 (2020) 117054.

[171] H. Cheng, J. Li, J. Wang, L. Chen, Z. Qi, Enhanced vitamin E extraction selectivity from deodorizer distillate by a biphasic system: A COSMO-RS and experimental study, ACS sustainable chemistry & engineering, 6 (2018) 5547-5554.

[172] D. Rodríguez-Llorente, E. Hernández, P. Gutiérrez-Sánchez, P. Navarro, V.I. Águeda, S. Álvarez-Torrellas, J. García, M. Larriba, Extraction of pharmaceuticals from hospital wastewater with eutectic solvents and terpenoids: Computational, experimental, and simulation studies, Chemical Engineering Journal, 451 (2023) 138544.

[173] C. Chen, Y. Cao, A. Ali, S. Toufouki, S. Yao, How to apply terpenoid-based deep eutectic solvents for removal of antibiotics and dyes from water: Theoretical prediction, experimental validation and quantum chemical evaluation, Environmental Research, 231 (2023) 116180.

[174] K. Tang, L. Song, Y. Liu, J. Miao, Enantioselective partitioning of 2-phenylpropionic acid enantiomers in a biphasic recognition chiral extraction system, Chemical engineering journal, 180 (2012) 293-298.

[175] L. Liu, D. Sun, F. Li, S. Ma, Z. Tan, Enantioselective liquid-liquid extraction of valine enantiomers in the aqueous two-phase system formed by the cholinium amino acid ionic liquid copper complexes and salt, Journal of Molecular Liquids, 294 (2019) 111599.

[176] D. Kong, Z. Zhou, H. Zhu, Y. Mao, Z. Guo, W. Zhang, Z. Ren, Selective separation of salbutamol enantiomers with simultaneously synergistic extraction and stripping method, Journal of Membrane Science, 499 (2016) 343-351.

[177] R. Kafri, D. Lancet, Probability rule for chiral recognition, Chirality: The Pharmacological, Biological, and Chemical Consequences of Molecular Asymmetry, 16 (2004) 369-378.

[178] K. Tang, G. Wu, P. Zhang, C. Zhou, J. Liu, Experimental and model study on enantioselective extraction of phenylglycine enantiomers with BINAP–metal complexes, Industrial & engineering chemistry research, 51 (2012) 15233-15241.

[179] B. Schuur, M. Blahušiak, C.R. Vitasari, M. Gramblička, A.B. De Haan, T.J. Visser, Selector screening for enantioseparation of DL-α-methyl phenylglycine amide by liquid–liquid extraction, Chirality, 27 (2015) 123-130.

[180] X. Liu, Y. Ma, T. Cao, D. Tan, X. Wei, J. Yang, L. Yu, Enantioselective liquid-liquid extraction of amino acid enantiomers using (S)-MeO-BIPHEP-metal complexes as chiral extractants, Separation and Purification Technology, 211 (2019) 189-197.

[181] X. Liu, S. Chen, Y. Ma, W. Xiao, Enantioseparation of 4-Nitrophenylalanine using (S)-SDP-metal complex as chiral extractant, Separation and Purification Technology, 239 (2020) 116547.

[182] Y. Teng, C. Gu, Z. Chen, H. Jiang, Y. Xiong, D. Liu, D. Xiao, Advances and applications of chiral resolution in pharmaceutical field, Chirality, 34 (2022) 1094-1119.

[183] J. Wang, H. Yang, J. Yu, X. Chen, F. Jiao, Macrocyclic β-cyclodextrin derivative-based aqueous-two phase systems: phase behaviors and applications in enantioseparation, Chemical Engineering Science, 143 (2016) 1-11.

[184] K. Tang, P. Zhang, C. Pan, H. Li, Equilibrium studies on enantioselective extraction of oxybutynin enantiomers by hydrophilic β-cyclodextrin derivatives, AIChE journal, 57 (2011) 3027-3036.

[185] K. Tang, J. Miao, Y. Liu, T. Zhou, L. Song, Equilibrium Studies on Reactive Extraction of α-Cyclohexyl-mandelic Enantiomers Using Hydrophilic β-Cyclodextrin Derivatives Extractants, Chinese Journal of Chemistry, 28 (2010) 1444-1450.

[186] L. Tan, Y. Long, F. Jiao, X. Chen, Enantioselective extraction of mandelic acid enantiomers by aqueous two-phase systems of polyethylene glycol and ammonium sulfate containing β-cyclodextrin as chiral selector, Journal of the Iranian Chemical Society, 8 (2011) 889-896.

[187] T. Kewen, M. Jiabing, Z. Tao, L. Yongbing, Equilibrium Studies on Liquid-Liquid Reactive Extraction of Phenylsuccinic Acid Enantiomers Using Hydrophilic β-CD Derivatives Extractants, Chinese Journal of Chemical Engineering, 19 (2011) 397-403.

[188] D. Wu, Y. Zhou, P. Cai, S. Shen, Y. Pan, Specific cooperative effect for the enantiomeric separation of amino acids using aqueous two-phase systems with task-specific ionic liquids, Journal of Chromatography A, 1395 (2015) 65-72.

[189] H. Wu, S. Yao, G. Qian, T. Yao, H. Song, A resolution approach of racemic phenylalanine with aqueous two-phase systems of chiral tropine ionic liquids, Journal of Chromatography A, 1418 (2015) 150-157.

[190] A.R. Carreira, A.M. Ferreira, M.R. Almeida, J.A. Coutinho, T.E. Sintra, Propranolol resolution using enantioselective biphasic systems, Separation and Purification Technology, 254 (2021) 117682.

[191] F. Tang, Q. Zhang, D. Ren, Z. Nie, Q. Liu, S. Yao, Functional amino acid ionic liquids as solvent and selector in chiral extraction, Journal of Chromatography A, 1217 (2010) 4669-4674.

[192] X.Y. Huang, K.J. Quan, D. Pei, J.F. Liu, D.L. Di, The development of biphasic chiral recognition in chiral separation, Chirality, 30 (2018) 974-981.

[193] X. Chen, J. Wang, F. Jiao, Efficient enantioseparation of phenylsuccinic acid enantiomers by aqueous two-phase system-based biphasic recognition chiral extraction: Phase behaviors and distribution experiments, Process Biochemistry, 50 (2015) 1468-1478.

[194] F. Jiao, W. Yang, D. Huang, J. Yu, X. Jiang, X. Chen, Enantioseparation of ofloxacin enantiomers by mixed extractants in biphasic system, Separation Science and Technology, 47 (2012) 1971-1976.

[195] M. Hashemi, M.R. Hadjmohammadi, Using enantioselective dispersive liquid–liquid microextraction for the microseparation of trans-cyclohexane-1, 2-diamine enantiomers, Tetrahedron: Asymmetry, 28 (2017) 454-459.

[196] R. Wang, D. Sun, C. Wang, L. Liu, F. Li, Z. Tan, Biphasic recognition chiral extraction of threonine enantiomers in a two-phase system formed by hydrophobic and hydrophilic deep-eutectic solvents, Separation and Purification Technology, 215 (2019) 102-107.

[197] S. Ma, F. Li, L. Liu, L. Liao, L. Chang, Z. Tan, Deep-eutectic solvents simultaneously used as the phase-forming components and chiral selectors for

enantioselective liquid-liquid extraction of tryptophan enantiomers, Journal of Molecular Liquids, 319 (2020) 114106.

[198] L. Chen, L. Ge, Q. Liang, Z. Zhao, K. Yang, Eutectic solvents formed by (+)-DTTA and L-menthol as novel chiral recognition and separation media for enantioselective extraction of valsartan enantiomers, Journal of Molecular Liquids, 368 (2022) 120818.

# 2. A COMPREHENSIVE STUDY OF THE WATER STABILITY OF DEEP EUTECTIC SOLVENTS USING COSMO-SAC*

***Chapter based on the published manuscript:**

Mahtab Moradi, Gholamreza Pazuki, Samane Zarei Mahmoudabadi, "*A comprehensive study of the water stability of eutectic solvents using COSMO-SAC"*, Journal of Molecular Liquids, 387, 2023, 122605

## 2.1. Abstract

The water stability of DESs is an important factor because the preferential interaction with water of one or both DESs precursors may change the nature of the solvent and impact its performance. In this work, Conductor-like Screening Model-Segment Activity Coefficient (COSMO-SAC) was applied to investigate the stability of both hydrophilic and hydrophobic DESs in the presence of water. With this objective, an initial computational evaluation of all possible combinations of DES composed by twenty-two different hydrogen bond acceptors (HBAs) and forty-four hydrogen bond donors (HBDs) at three different molar ratios of HBA: HBD (2:1, 1:1, and 1:2) was carried out. The results revealed that the DESs based on tetraalkyl-ammonium salts, terpenes and fatty acids as HBA and fatty alcohols and fatty acids as HBD are the DESs with higher water stability. Therefore, four different groups of eutectic solvents, namely menthol: fatty alcohol, menthol: fatty acid, fatty acid: fatty acid and fatty acid: fatty alcohols were selected to evaluate the COSMO-SAC predictions using water activity measurements. It is shown that a good agreement was obtained between the calculated and the experimental results and that the hydrophobicity of the eutectic solvents controls its water stability. A thermophysical characterization of the DESs studied is also reported.

**Keywords:** Stability, Hydrophobic eutectic solvents, Hydrophilic eutectic solvents, COSMO, Water activity, Density, Viscosity.

## 2.2. Introduction

DESs besides a high solvation capacity, present unique advantages as low cost solvents of simple preparation, many with a renewable character, and good biodegradability [1]. DESs are the mixtures HBA and HBD of different acidity. By changing the DES components (HBAs and HBDs) and their molar ratio, the physicochemical properties of DESs, namely freezing point, density, viscosity, hydrophobicity or hydrophilicity, and stability of DESs can be tuned [2]. Since DESs have a wide application in many extraction and purification processes, designing DESs with the optimal physicochemical properties is critical because this may lead to syntheses more sustainable solvents and development of more eco-friendly processes.

The definition of DES is somewhat vague [3] and in general is not easy to establish its "deepness" nor is this characteristic essential for many applications. Marins et al., [4] demonstrated that "eutectic solvent", as a simpler term, can be used to describe mixtures which do not fulfill these criteria: first the mixture has a eutectic point temperature lower than that of an ideal mixture, which exhibits a negative deviation from ideality. Second the temperature depression should be such that the mixture remains liquid for a certain composition range at the operating temperature.

Water stability is one important factor in selecting the DES because the preferential interaction with water of one, or both, DESs precursors may change the nature of the solvent and negatively impacts its performance increasing the amount of solvent needed and making more difficult the recycling of the DESs [5]. The water stability of the DESs can be evaluated by exploring the interactions between the DES components and water. Zafarani-Moattar et al. [6] investigated the impact of water content on the existing hydrogen bonding interactions in the choline chloride-based DESs, by measuring the isopiestic equilibrium water mass fraction values in the aqueous mixtures. The obtained results suggest that adding water to these DESs weakens the H-bonding interactions between the DES components, and these bonds will mostly disappear when the water content exceeds 75 wt%. In another study, Paul et al. [7] used molecular dynamics simulation (MD) to examine the water stability of ten DESs based on menthol and tetrabutylammonium chloride ($N_{4444}Cl$) as HBA and organic acids as HBD through analysis of the intermolecular interaction between the DESs components and water. The results confirmed that the structure and the alkyl chain length of the HBAs and HBDs play a main role in the stability of the DES in water. Moreover, several works applied proton nuclear magnetic resonance ($^1$H NMR) to check the water stability of the DESs. Riveiro et al. [5] prepared the mixtures of water and trioctylphosphine oxide-based DESs and analyzed both phases by $^1$H NMR. The behavior of the DESs in aqueous solutions indicated that both DESs are stable in presence of water and can be considered as extracting agents of adipic, levulinic and succinic acids present in aqueous solutions. In other studies, $^1$H NMR was used to confirm the water stability of the DESs based on terpenes, fatty acids, and ammonium salts [8]. It was demonstrated that if one of the DES constituents is soluble in water, the partial disruption of the DES occurs after mixing with water. Moreover, it has been reported by some authors that the water stability of DESs depends on the nature of the DES precursors. Farias et al. showed that the nature of the HBD, the aqueous biphasic system (ABS) components and their

concentration has significant impact to manipulate the molar ratio of cholinium chloride (as HBA) and glucose (as HBD) in ABS phases [9]. In other studies, Florindo et al. confirmed that the DESs formed by hydrophobic compounds are stable in water. However, the hydrophilic HBA or HBD will leach to water because of their water solubility [10]. In addition, Tang et al. indicated that HBA is the main factor in the water stability of DESs based on ammonium salts and fatty acids and fatty alcohols [11]. Despite these investigations, a comprehensive study of the water stability of a wide range of DESs considering the impact of key factors such as the molar ratio of HBAs and HBDs and their concentration on water stability has not yet been performed. Since the experimental evaluation would be very costly and lengthy, thermodynamic models can be used as a valuable tool to evaluate the water stability of the DESs.

One of the most widely used predictive models to describe the DESs thermodynamic behavior is the COSMO-SAC, which is based on quantum chemistry and statistical thermodynamics. Lin and Sandler [12] proposed the COSMO-SAC model as an open access tool that could be used to overcome some limitations of the original COSMO-RS model [13]. COSMO-SAC is a useful method to estimate the thermodynamic properties of mixtures. Several studies used this method to predict the activity coefficient,[14] octanol/water partition coefficients of amino acids [15] and Henry's law constant [16]. This method also has been applied to estimate LLE [17], the solid-liquid phase diagram for predicting eutectic temperature [18], and the solubility of some drugs in various solvents [19]. To the best of our knowledge, COSMO-SAC to evaluate the interaction between the DES precursors and water has not yet been reported.

In this work, COSMO-SAC is used to evaluate the water stability of both hydrophilic and DESs by calculating the water activities in binary and ternary mixtures of the DES components and water. Then, the most stable DESs identified by the initial screening were selected to have their water activities measured and compared with the predicted COSMO-SAC results. Moreover, the stability of these DESs was investigated using a Fourier transform infrared spectrometer (FT-IR spectra). Finally, the physical properties of these DESs, namely density and viscosity, were measured.

## 2.3. Materials and methods

### 2.3.1. Materials

DL-menthol (≥98%), octanoic acid (≥98%), decanoic acid (≥98%), dodecanoic acid (≥98%), 1-Decanol (≥98%), and 1-Dodecanol (≥98%), were purchased from Merck and are detailed along with their properties in Table 2.1. In all experiments, double-distilled water was used to prepare the sample solutions.

**Table 2.1.** Chemical Species Name, CAS Number, Molecular Weight (Mw), Supplier Company Name, Purity in Mass Fraction, and Octanol-Water Partition Coefficient (log ($K_{OW}$)) [20].

| Name | CAS number | $M_w$ ($g.m^{-1}$) | supplier | purity (w/w) | log ($K_{OW}$) |
|---|---|---|---|---|---|
| DL-menthol | 1490-04-6 | 156.26 | Merck | ≥0.98 | 2.66 |
| Octanoic acid | 124-07-2 | 144.21 | Merck | ≥0.98 | 2.7 |
| Decanoic acid | 334-48-5 | 172.26 | Merck | ≥0.98 | 3.59 |
| Doecanoic acid | 143-07-7 | 200.32 | Merck | ≥0.98 | 4.48 |
| 1-Decanol | 112-30-1 | 158.28 | Merck | ≥0.98 | 3.47 |
| 1-Dodecanol | 112-53-8 | 186.33 | Merck | ≥0.98 | 4.36 |

### 2.3.2. DES's studied and their preparation

All the DESs selected, with the specified molar ratio of HBA and HBD, were prepared by heating the mixture at 80 °C for 4-5 h under continual stirring until a clear and homogenous liquid was obtained [8,21–23]. The list of the DESs prepared is presented in Table 2.2.

**Table 2.2.** List of DESs used in this work and their molar ratio

| HBA | HBD | DES | Abbreviation | Molar ratio |
|---|---|---|---|---|
| DL-menthol | Octanoic acid | DES 1 | Menthol: C8 acid | 1:1 |
| | Decanoic acid | DES 2 | Menthol: C10 acid | 2:1 |
| | Dodecanoic acid | DES 3 | Menthol: C12 acid | 2:1 |
| | 1-Decanol | DES 4 | Menthol: C10 alcohol | 1:2 |
| | 1-Dodecanol | DES 5 | Menthol: C12 alcohol | 1:2 |
| Octanoic acid | Decanoic acid | DES 6 | C8 acid: C10 acid | 2:1 |
| | Dodecanoic acid | DES 7 | C8 acid: C12 acid | 2:1 |
| | 1-Decanol | DES 8 | C8 acid: C10 alcohol | 1:2 |
| | 1-Dodecanol | DES 9 | C8 acid: C12 alcohol | 1:2 |
| | Dodecanoic acid | DES 10 | C8 acid: C12 acid | 2:1 |
| Decanoic acid | 1-Decanol | DES 11 | C10 acid: C10 alcohol | 1:2 |
| | 1-Dodecanol | DES 12 | C10 acid: C12 alcohol | 1:2 |

### 2.3.3. COSMO-SAC model

A set of DESs based on the hydrophilic and hydrophobic precursors commonly used in the literature was evaluated [2,10,11,23–28]. The database comprises twenty-two HBAs and forty-four HBDs, as detailed in Tables A.1 and A.2 in Appendix A.

The procedure to use COSMO-SAC has two steps: The first step is related to the calculation of the COSMO files. The geometry structure of all the HBDs, the HBAs, and water, was fully optimized using the dmol3 module in Material studios 2017 software, which is the most used software to perform the density functional theory (DFT) and COSMO calculations [12]. In this work, GGA (VWN-BP) was considered as the DFT to optimize the geometry structure of molecules [14]. Moreover, the quality fine was selected for the computation accuracy, and the multipolar expansion, in electronic options, was set on octupole. The computations were run on four parallel cores, and the default values of dMol3 were used for other options; In the second step, the COSMO files prepared were used in COSMOthermX 2.1 program to calculate the activity coefficient of water in binary and ternary mixtures including (HBA+water), (HBD+water), and (HBA+HBD+water).

The COSMO-SAC uses solvation energy at two steps to compute activity coefficients; first, a solute is dissolved in the conductor, second, the conductor converted to a real solvent. Then, the activity coefficient $\gamma_{i,s}$ of component (i) in solvent (S) is calculated by considering two contributions: combinatorial part $\gamma_{i,s}^{C}$ and residual part $\gamma_{i,s}^{R}$ as follows [19]:

$$ln\,\gamma_{i,s} = ln\,\gamma_{i,s}^{C} + ln\,\gamma_{i,s}^{R} \tag{2.1}$$

More details on the calculation procedure to predict the activity coefficients using COSMO-SAC are presented by Mahmoudabadi and Pazuki [19].
Finally, the water activity ($a_w$) in the binary and ternary mixtures is obtained from the water activities coefficients considering following equations:

$$a_{wA}^{0} = \gamma_{wA}^{0}.x_{wA} \tag{2.2}$$

$$a_{wB}^{0} = \gamma_{wB}^{0}.x_{wB} \tag{2.3}$$

$$a_w = \gamma_w.x_w \tag{2.4}$$

where $a_{wA}^{0}$, $a_{wB}^{0}$, and $a_w$ are the activities of water and $\gamma_{wA}^{0}$, $\gamma_{wB}^{0}$ and $\gamma_w$ are the water activities coefficients in (HBA+water), (HBD+water), and (HBA+ HBD+water) mixtures, respectively. Moreover, $x_{wA}$, $x_{wB}$, and $x_w$ denote the mole fraction of water in the binary and ternary mixtures, which are calculated according to the following equations [19]:

$$x_{wA} = 1 - \frac{m_A}{\frac{1000}{M_w} + m_A} \tag{2.5}$$

$$x_{wB} = 1 - \frac{m_B}{\frac{1000}{M_w} + m_B} \tag{2.6}$$

herein $m_A$ and $m_B$ represent the molalities of HBA and HBD in the mixtures and $M_w$ is the molecular weight of water.

### 2.3.4. Octanol/water partition coefficient

The distribution of component *i* between two immiscible liquid phases is related to its activity coefficients at infinite dilution $\gamma_i^{\infty}$ in both phases, which is obtain from the equality of activities as follows [19]:

$$a_i^{\alpha} = a_i^{\beta} \implies (x_i\gamma_i)^{\alpha} = (x_i\gamma_i)^{\beta} \Rightarrow K_i^{\alpha,\beta} = \frac{x_i^{\alpha}}{x_i^{\beta}} = \frac{\gamma_i^{\beta}}{\gamma_i^{\alpha}} \tag{2.7}$$

And at infinite dilution [19]:

$$K_i^{\alpha,\beta} = \frac{x_i^{\alpha}}{x_i^{\beta}} = \frac{\gamma_i^{\beta,\infty}}{\gamma_i^{\alpha,\infty}} \;;\; x_i \to 0 \tag{2.8}$$

Where $x_i^{\alpha}$ and $x_i^{\beta}$ denote the mole fractions of component *i* in phases α and β; and $\gamma_i^{\alpha,\infty}$ and $\gamma_i^{\beta,\infty}$ are their activity coefficients, respectively. Thus, the octanol/water partition coefficient of component *i* can be defined as follows [19]:

$$\log K_{OW,i} = log\left(\frac{C_{0,W}\,\gamma_i^{W,\infty}}{C_{0,O}\,\gamma_i^{O,\infty}}\right) \tag{2.9}$$

where $C_{0,O}$ and $C_{0,W}$ represent the total concentrations in octanol-rich and water-rich phases, which the default values for $\frac{C_{0,W}}{C_{0,O}}$ is 0.151. The $\gamma_i^{W,\infty}$ and $\gamma_i^{O,\infty}$ are the activity coefficients of component *i* in both octanol and water phases at infinite dilution.

### 2.3.5. Measurement of water activities

A Novasina hygrometer LabMaster (Lucerne, Switzerland, $\pm\, 0.001\ a_w$) was used to measure the water activities in the binary and ternary mixtures of water and the ES components. The measuring principle of the water activity meter is based on the resistive electrolytic method [29]. To calibrate the instrument, six saturated pure salts with a defined water activity range (from 0.113 to 0.973), which were included in the instrument, were used as the standard solutions. Moreover, the temperature was kept constant at $25 \pm 0.1$ ℃ by the temperature control chamber in the instrument. For binary mixtures, the samples of (HBA+water) and (HBD+water) were prepared in the

specific molar ratio of HBA and HBD and at three different molalities of HBA and three different molalities of HBD as presented in Table A.3, Appendix A. In addition, the ternary mixtures (HBA+HBD+water) were prepared at the same molalities of HBA and HBD in binary mixtures. These molalities were same with those selected for COSMO-SAC calculation.

To measure the water activity, 5 ml of each sample was prepared and placed in the air-tight equilibrium chamber. Then, the water activity is recorded when the partial pressure of water vapor reaches the equilibrium and the variation of water activity with time remains unchanged.

### 2.3.6. Density and viscosity measurements

Density and speed of sound were measured using a vibrating tube densitometer (Anton Paar, DSA5000) and with the uncertainty of 0.3 kg/m$^3$ and 0.5 m/s for density and speed of sound, respectively. Moreover, water and dry air were employed to calibrate the instruments at atmospheric pressure.

The viscosity of the synthesized DESs was measured by applying a digital viscometer (Lovis 2000M, Anton Paar). The uncertainty of the viscosity was 0.001 mPa s, in each measurement. In addition, for all measurements, the temperature was kept constant at 25 ± 1.0 °C using the Peltier device built in both densitometer and viscometer.

## 2.4. Results and discussion

### 2.4.1. COSMO-SAC model results

The polarity of the DESs components and their action as HBAs or HBDs can be understood using screening charge density distributions, known as σ-profiles. For non-polar compounds, the σ-profiles distribution will locate essentially in the non-polar region, while mildly polar compounds have also peaks in the polar regions. HBAs have σ-profiles with peaks predominantly on the positive side while HBDs have peaks predominantly on the negative side. The DES components will consider as the best HBA or HBD when there are no peaks on the opposite side, which means they act as pure acceptors or pure donors [30].

The σ-profiles of the different groups of HBAs and HBDs, including tetraalkyl - ammonium salts, terpenoids, carboxylic acids, alcohols, carbamide, sugars, fatty acids, and fatty alcohols are presented in Figures 2.1 and 2.2. It can be observed from the

Figures that, increasing the alkyl chain length in tetraalkyl-ammonium salts, fatty acids, and fatty alcohols leads to stronger peaks in the non-polar region. Therefore, it is expected that i) the DESs composed of both hydrophobic HBA and HBD are more stable in the presence of water, and ii) the length of alkyl chain has a significant impact on the water stability of DES.

COSMO-SAC was used to evaluate the water stability of 968 mixtures consisting of twenty-two HBAs and forty-four HBDs at three molar ratios of HBA: HBD (2:1, 1:1, 1:2). To this purpose, the activity coefficients of water in the binary and ternary mixtures including (HBA+water), (HBD+water), and (HBA+ HBD+water) with the specified molar ratio of HBA and HBD were predicted. The following equation was applied to investigate the stability of the DESs in water [31,32]. A description of measured and calculated $\Delta a_w$, as well as an explanation of driving the equation 10 is presented in supporting information (Table A.4, Appendix A).

$$\Delta a_w = 1 + a_w - (a_{wA}^0 + a_{wB}^0) \tag{2.10}$$

Where $a_w$ is the activity of water in (HBA+ HBD+water) mixture, and $a_{wA}^0$ and $a_{wB}^0$ are the activity of water in (HBA+water), (HBD+water) mixtures, respectively.

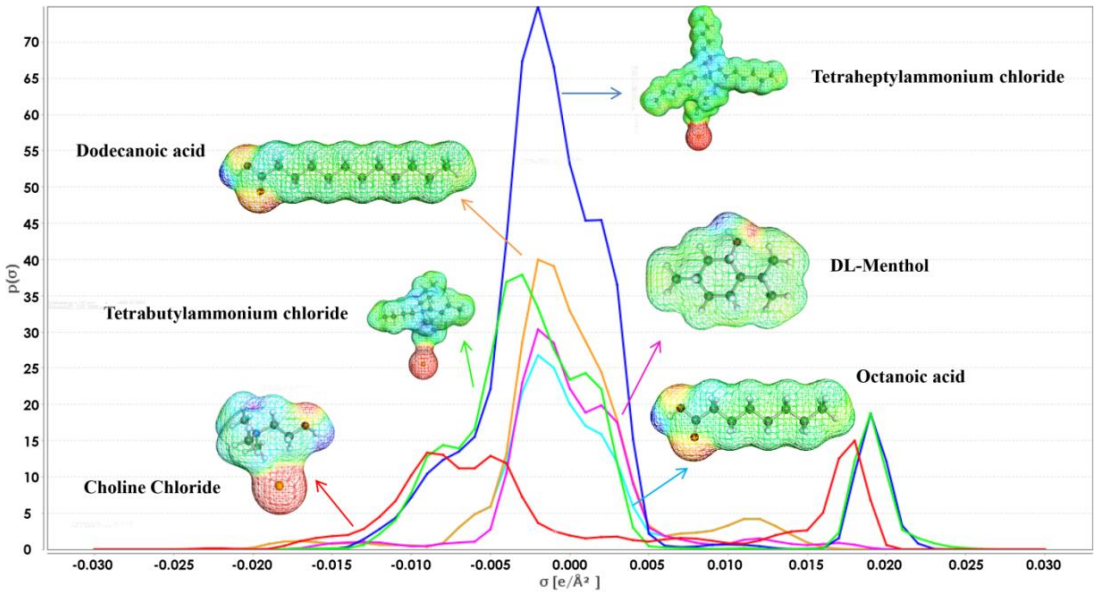


**Figure 2.1.** Examples of σ-profile of the HBA families of compounds studied.

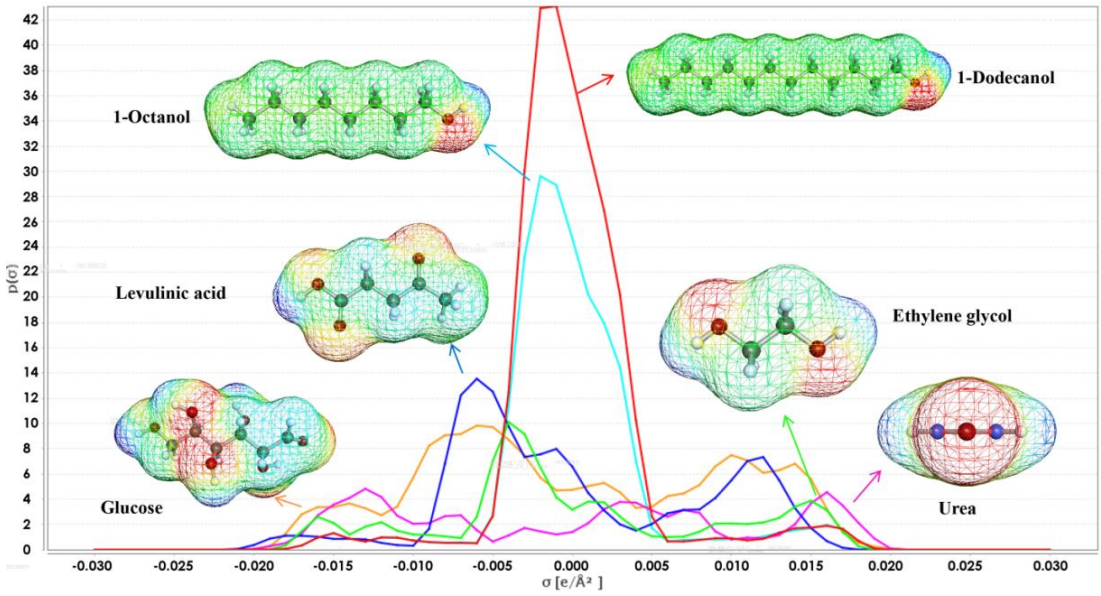


**Figure 2.2.** Examples of σ-profile of the HBD families of compounds studied.

Equation 10 indicates whether the interactions between DES components are favorable, or not, in the presence of water, because the negative or positive deviations of $\Delta a_w$ depend on the strength of the interactions between the species in the solution. Because of these interactions, the vapor pressures/water activities of water in the presence of the DES may increase, or decrease, compared to the vapor pressures/water activities of water in the presence of the HBD or HBA alone [33]. No or negative deviations of $\Delta a_w$ means that the interactions between HBA and HBD are less favorable than the interactions of these compounds with water. Therefore, the molecules of each DES precursor are hydrated with several molecules of water, which result in fewer free water molecules being available in solution and a reduction in the values of $a_w$. On the other hand, positive deviation from Equation 10 is obtained when the interactions between HBA and HBD are stronger than the interactions between the HBA or HBD and the water molecules [31]. Thus, in these systems, the intermolecular hydrogen bonds between the DES precursors are, at least partly, maintained in the presence of water.

The water stability of the DESs in each molar ratio of HBA: HBD and at three different modalities was explored and the results presented in Figures 2.3-2.5 and A.1-A.6, Appendix A. Figures 2.3-2.5 describe the stability of the DESs in water at concentrations of HBA and HBD 5 mol/kg: 2.5 mol/kg, 2.5 mol/kg: 2.5 mol/kg, 1.25 mol/kg: 2.5 mol/kg. Other concentrations are reported in Figures A.1-A.6, Appendix A

showing similar results. These concentrations were chosen to cover significant differences in water concentration in the mixtures.

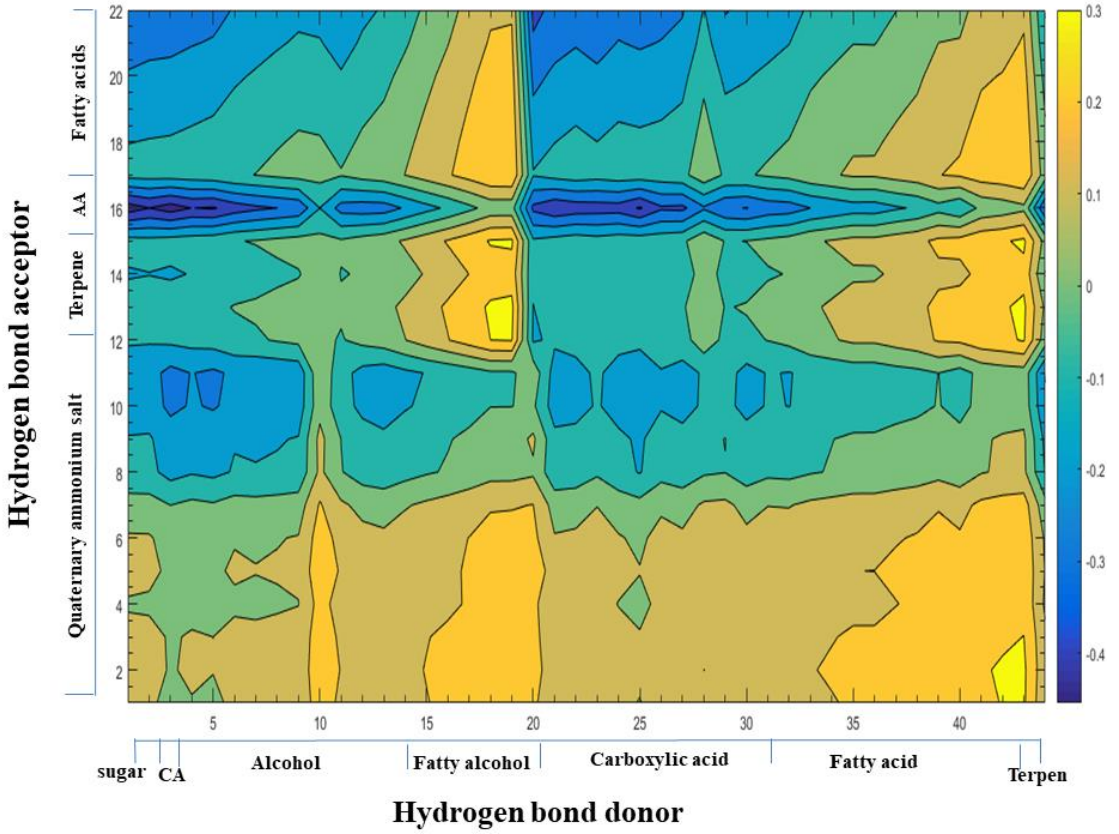


**Figure 2.3.** Predicted $\Delta a_w$ in the molar ratio (2:1) and at molalities 5 mol/kg: 2.5 mol/kg of the HBA: HBD, at 25 °C using COSMO-SAC.

It can be seen from the Figures that hydrophobicity or hydrophilicity plays a crucial role in the stability of the DESs in water. The results obtained indicate that increasing the molar ratio as well as the concentrations of the components with more hydrophobicity lead to an increase in their water stability. For the same reason, the molar ratio 2:1 and 1:2 show the highest and lowest values of $\Delta a_w$, respectively, because of higher hydrophobicity in the HABs than the HBDs. Even though increasing the concentration of the DESs components along with molar ratio increases the stability of DES in presence of water (Figures A.1-A.4, Appendix A), but in molar ratio 1:2 increasing the concentration results in a decrease in the values of $\Delta a_w$ (Figures A.5-A.6, Appendix A). This can be explained by the fact that, since the hydrophobicity seems to be the driving factor in the stability of DESs, increasing the concentration or molar ratio of the most hydrophilic compound increases the hydrophilicity of the DESs, which reduces their water stability, significantly.

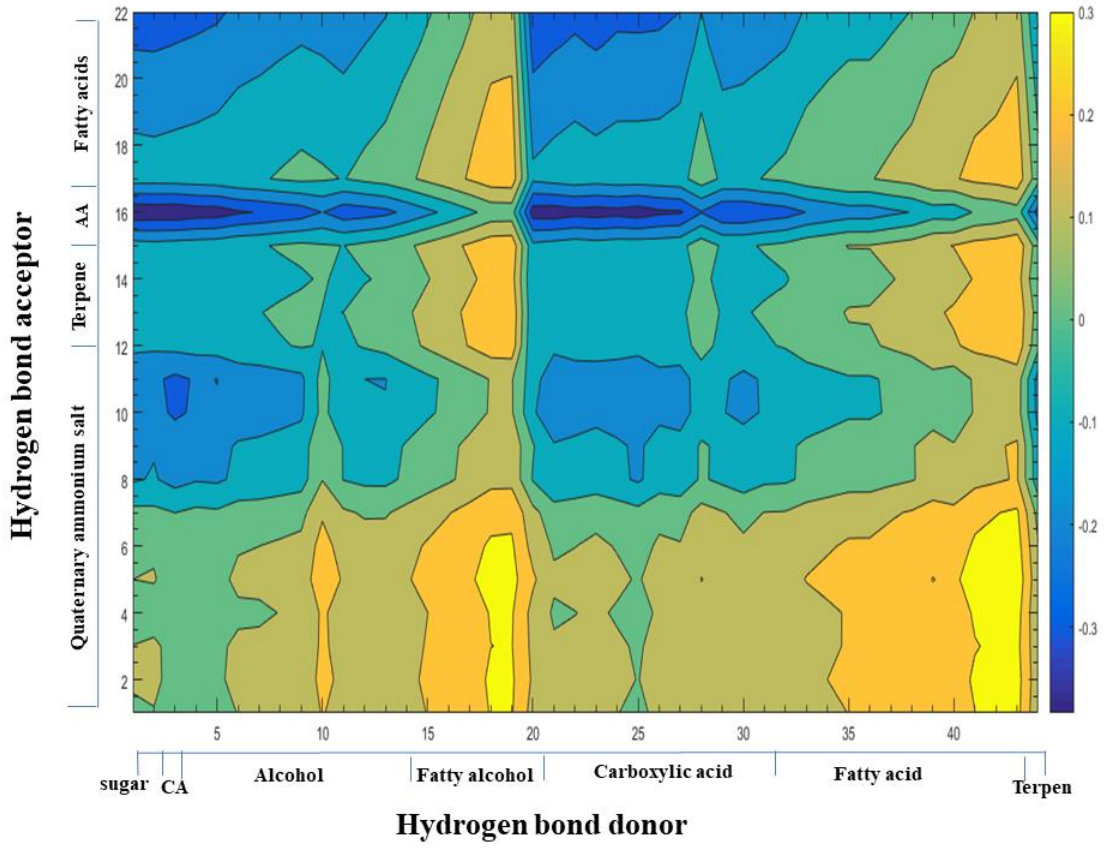


**Figure 2.4.** Predicted $\Delta a_w$ in the molar ratio (1:1) and at molalities 2.5 mol/kg: 2.5 mol/kg of the HBA: HBD, at 25 °C using COSMO-SAC.

The initial screening by COSMO-SAC suggests that the DESs composed of tetraalkyl-ammonium salt, terpenes, and fatty acids as HBA and fatty alcohols and fatty acids as HBD are the most stable DESs in water. In addition, it is found out that, changing the counterion in quaternary-ammonium salts, namely $Cl^-$ by $Br^-$ has only a minor effect on the water stability of DESs.

Although an increase in the alkyl chain length leads to a higher stability of the DESs in water, it also increases the viscosity of the DESs [7,8]. Since it has been shown that the DESs based on the quaternary-ammonium salts have the highest viscosity among DESs [10,34], four other groups of the DESs, which were also stable in the presence of water, namely menthol: fatty acid, menthol: fatty alcohol, fatty acid: fatty acid and fatty acid: fatty alcohol were selected for the further evaluation.

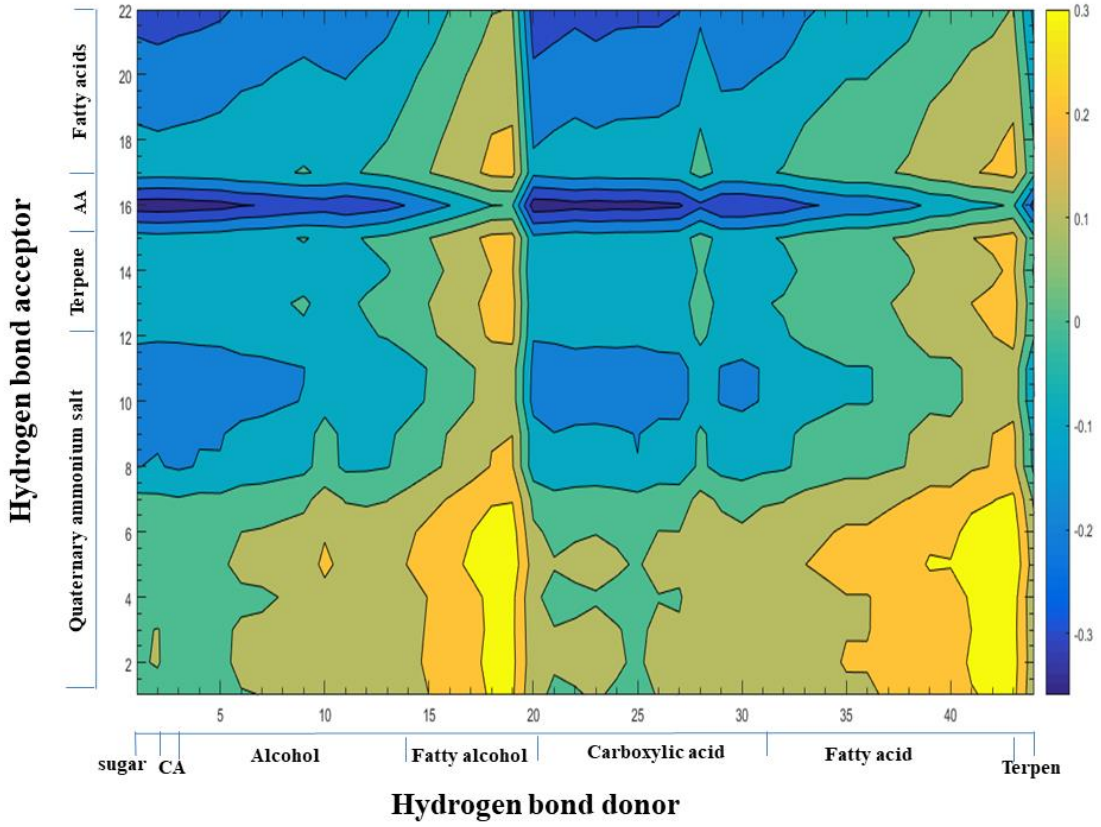


**Figure 2.5.** Predicted $\Delta a_w$ in the molar ratio (1:2) and at molalities 1.25 mol/kg: 2.5 mol/kg of the HBA: HBD, at 25 °C using COSMO-SAC.

### 2.4.2. Experimental validation

These DESs with low viscosity and predicted high stability in presence of water were selected to experimentally validate the COSMO-SAC results. Moreover, in order to evaluate the impact of the length of the alkyl chain on the water stability of the DESs, two DESs in each category were investigated. The values of $\Delta a_w$ for the selected DESs were calculated using equation 10, and the results are listed in Table A.3, Appendix A.

As Figure 2.6 describes, although the values of experimental $\Delta a_w$ exceed the calculated $\Delta a_w$, a consistent pattern of variation is observed in both measured and predicted $\Delta a_w$. Moreover, the experimental results corroborate the fact that a longer alkyl chain in ES components enhances their hydrophobicity, which in turn promotes the stability of DESs in water. In addition, comparing the $\Delta a_w$ of selected DESs show the following trend: menthol: C8 acid < menthol: C10 acid < C8 acid: C10 acid < menthol: C10 alcohol $\leq$ C8 acid: C10 alcohol $<$ C8 acid: C12 acid $<$ C10 acid: C10 alcohol < C8 acid: C12 alcohol $<$ menthol: C12 alcohol < C10 acid: C10 alcohol.

Since the water stability of DES seems to be strongly affected by the structure of HBA and HBD [35], it was decided to use the octanol/water partition coefficients ($K_{OW}$) of the compounds as descriptors for their hydrophobicity.

The octanol/water partition coefficient is a reliable indicator to evaluate the solute hydrophobicity. In general, a hydrophobic compound tends to partition into the octanol-rich phase, which results in a high value of $K_{OW}$. Conversely, a hydrophilic compound preferentially partitions into the water-rich phase and has low value of $K_{OW}$ [36]. This parameter provides valuable information of the hydrophobic interactions in quantitative structure-activity relationships (QSARs), which is widely used for the overall understanding of the solute behavior in the solution [37]. Although experimental methods are preferred for obtaining the physicochemical properties, the measurements of octanol−water partition coefficient for hydrophobic solutes are usually expensive and time-consuming.

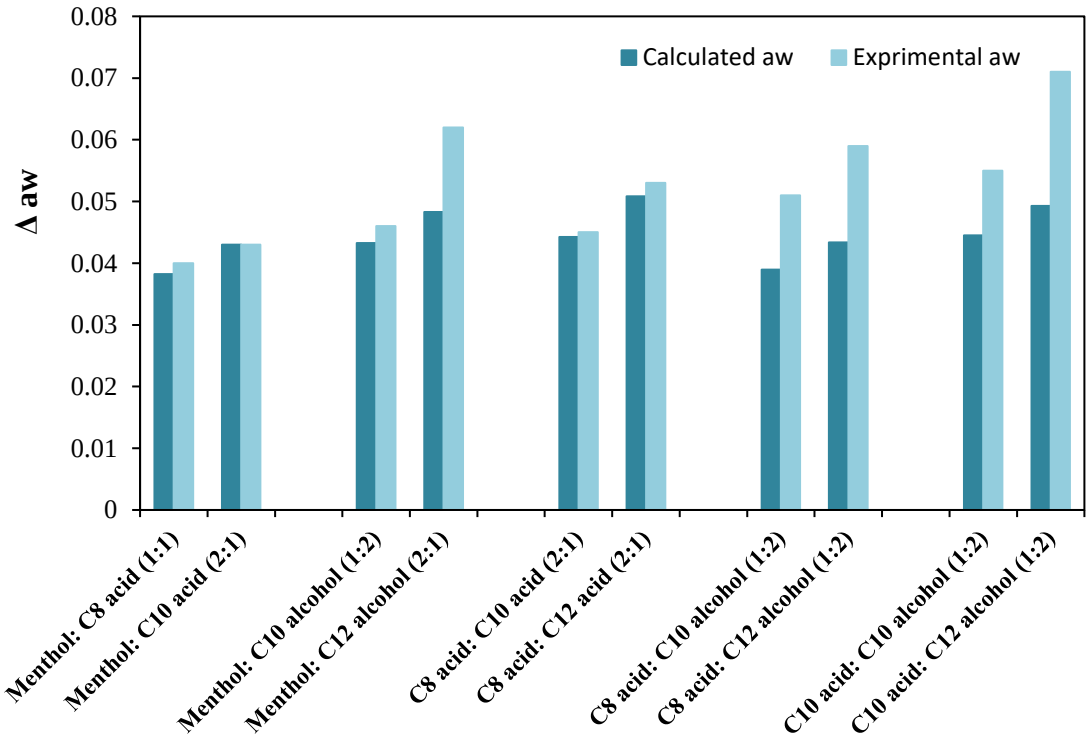


**Figure 2.6.** The experimental and calculated values of $\Delta a_w$ for the selected DESs.

To predict the octanol−water partition coefficients for selected DESs, the geometry structure of each DES with specific molar ratio was optimized in Material studios 2017 software, and then the COSMO files prepared were used in COSMOthermX 2.1 program to calculate the $K_{OW}$ as described in section 2.4.

The values of octanol/water partition coefficient of DESs (Figure2.7), which indicate their hydrophobicity, confirm that DESs containing more hydrophobic components are less likely to interact with water molecules, which can result in stronger interactions and increased water stability. For this reason, the DESs based on C12 alcohol have the highest stability in water among other selected DESs. Moreover, an increasing in the alkyl chain length of fatty acids-based DES increases the values of $K_{OW}$ and $\Delta a_w$, as demonstrated in Figures 2.6 and 2.7.

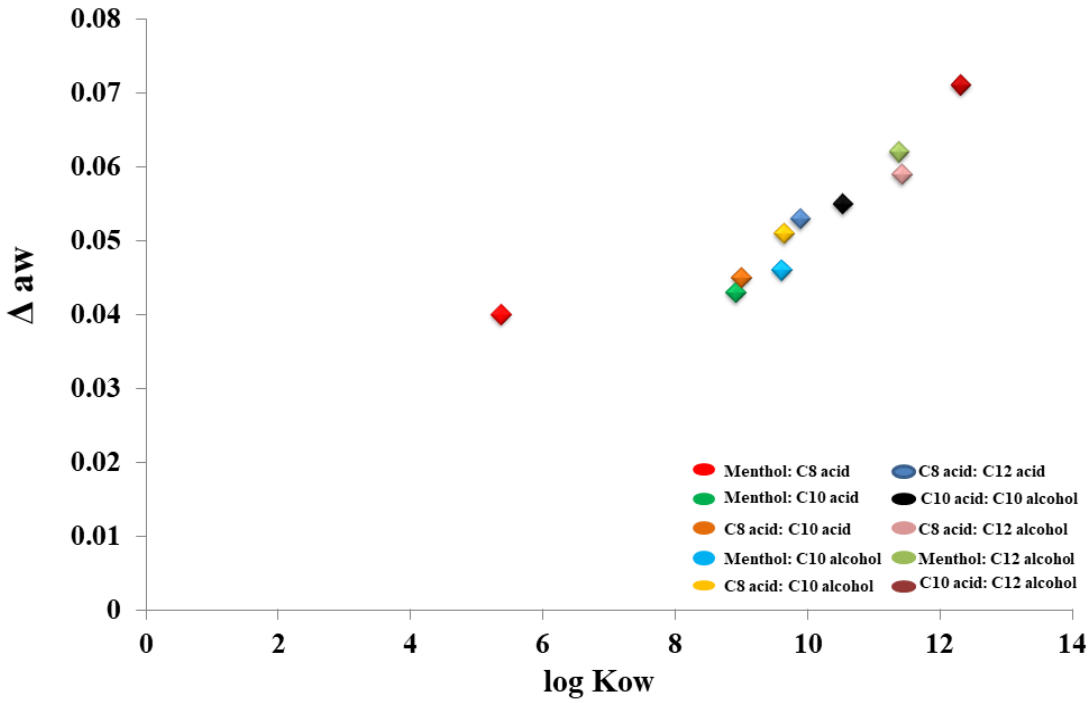


**Figure 2.7.** The stability of the DES studied as function of the log *K*ow of selected DESs.

### 2.4.3. FT-IR measurements

FT-IR spectra were applied to observe the formation of the hydrogen bonds in the synthesized DESs. The FT-IR spectra of four different families of DESs based on menthol, fatty acids and fatty alcohols were carried out and presented in Figure 2.8 and Figures A.7-A.14, Appendix A. The existence of hydrogen bonding in prepared DESs can be confirmed by the shifts of representative peaks in the FT-IR spectra of the pure compounds [38], which highlighted in gray in Figure 2.8. For example, as Figure 2.8A shows, the peak at 3282.4 $cm^{-1}$ for DL-menthol related to the O-H vibration are shifted to 3361.93 $cm^{-1}$, and 3442.9 in DL-menthol: decanoic acid and DL-menthol: octanoic acid DESs. Moreover, the vibration peaks of the carboxylic group in fatty acids are shifted to a higher wave number, from 1705.66 $cm^{-1}$to 1719.39 $cm^{-1}$ for octanoic acid

and from 1692.28 $cm^{-1}$ to 1710.10 $cm^{-1}$ for decanoic acid [39]. In the DESs based on DL-menthol and fatty alcohols (Figure 2.8B), the O-H vibration peaks for DL-menthol (at 3282.4 $cm^{-1}$), 1-decanol (at 3324.94 $cm^{-1}$) and 1-dodecanol (at 3325.33 $cm^{-1}$) are shifted to 3311.1 $cm^{-1}$, which indicate the formation of hydrogen bonding among the DES components [22]. Additionally, the FT-IR spectra of fatty acid-based DESs are presented in Figure 2.8C. The Peaks found at 1700 $cm^{-1}$ and 3000 $cm^{-1}$ belonged to the stretching vibration of hydroxyl and carboxylic groups in fatty acids, which the hydroxyl group shifted to a higher wave number (1713.15 $cm^{-1}$) for three fatty acid-based DESs. However, there are no significant changes in the absorbance peaks of the DESs and their components, which are in agreement with the literature reports and confirm the fact that, the shift of vibration peaks is heavily influenced by the nature of compounds [40]. As Figure 2.8D describes, the stretching vibration peak of O-H in fatty acid: fatty alcohols DESs shifted to 1710 $cm^{-1}$ and 3301.1 $cm^{-1}$ for fatty acids and fatty alcohols, respectively, which proves the formation of hydrogen bonding in the long-chain alkanol–alkyl carboxylic acid DESs [21].

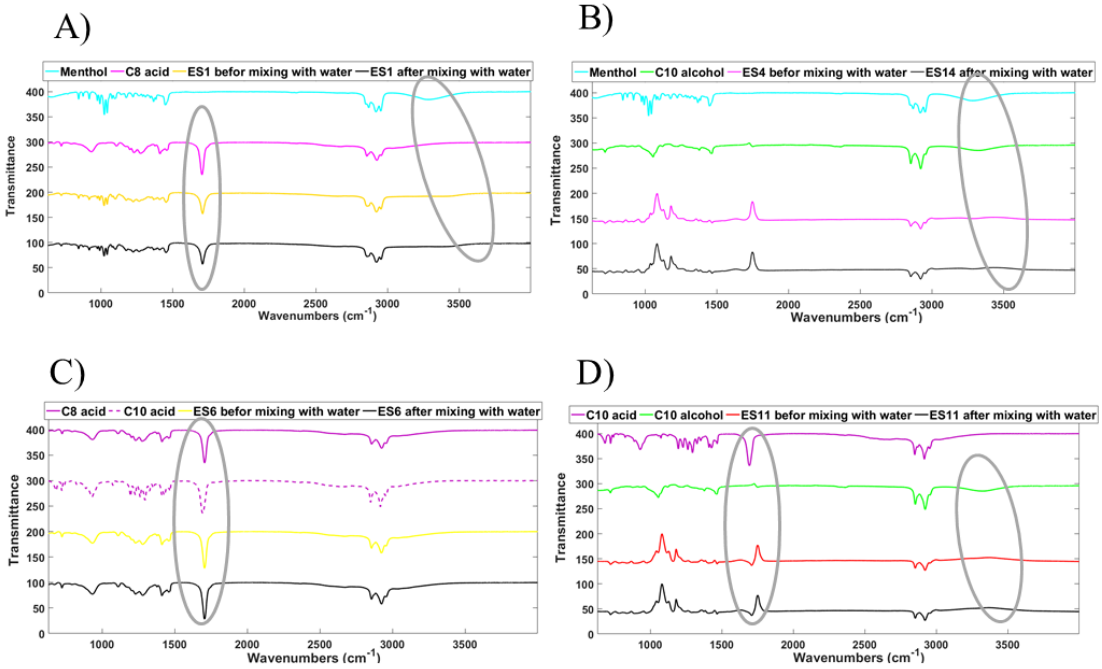


**Figure 2.8.** The FT-IR spectra of four different families of hydrophobic DESs: (**A**) Menthol: fatty acid, (**B**) Menthol: fatty alcohol, (**C**) fatty acid: fatty acid, (**D**) fatty acid: fatty alcohol.

The FT-IR spectra show that there are no shifts of the vibration peaks of the functional groups and chemical bonds in the DESs after mixing with water. These results prove that the hydrogen bonding formed between the DESs components can be maintained in

presence of water because of the high hydrophobicity of HBAs and HBDs, which reduces their ability to interact with water.

### 2.4.4. Thermophysical properties

Density and viscosity are the solvents' main physical properties because they significantly impact dissolution, reaction, mass transport phenomena, and the extraction efficiency of compounds. It has been found out that most of the DESs exhibit high viscosities at room temperature, which is related to the network of hydrogen bonds taking place among DES components [41]. However, the reports showed that, the water solubility of solvents has a great effect on reducing the viscosity of the DES [27]. In other words, the amount of water present in the DESs plays a significant role in decreasing their viscosity, and this is highly dependent on the hydrophobicity of the DES components. Therefore, it can be anticipated that DESs with higher hydrophobicity would have higher viscosities. Since high viscosity reduces the recovery yield of the target compounds from DESs, the design of DESs with the lowest viscosity is essential. As previously mentioned, the thermophysical properties of DESs strongly dependents on the type of the HBAs and HBDs and their molar ratio. Therefore, the viscosity and density of the DESs in a certain molar ratio, which remained stable in water and at room temperature, were measured and are presented in Table A.4, Appendix A and Figures 2.9 and 2.10.

It can be seen from Figure 2.9 that, by increasing the alkyl chain length in the HBA and HBD, the viscosity of the DESs increases [2]. This can be explained by the fact that an increase in the alkyl chain length of the ES components leads to a higher hydrophobicity, which reduces the water solubility of the DES. Thus, the DES becomes more viscous, as shown in the figure. Moreover, as Figure 2.9 describes, fatty acids-based DESs have the lowest viscosity among the four studied categories, which can be interpreted as the absence of coulombic interactions in this group of DESs [27]. These results highlight the importance of compound nature and molecular interactions on physical properties. However, the coulombic charge interactions are responsible for high viscosity of tetraalkylammonium salts-based DESs [42], in the DESs based on fatty acids and terpenes either, the lack of these interactions or weak hydrogen-bonding interactions between the components of DESs will result in lower viscosity compared to the other groups of DESs.

Generally, the following trend in viscosity is observed: fatty acid: fatty acid < fatty acid: fatty alcohols < menthol: fatty acids < menthol: fatty alcohols, which are in agreement with previous reports [2,10,38,40].

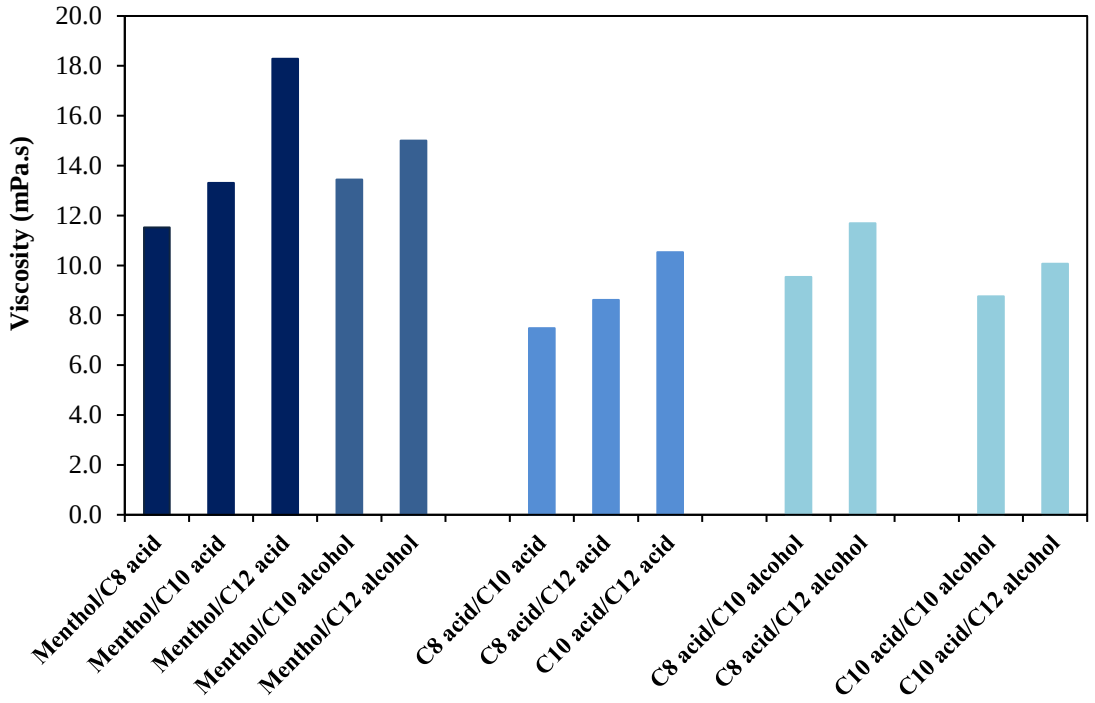


**Figure 2.9.** Viscosity of four different families of DESs at 25 °C.

Density is another important property because the phase separation in liquid-liquid systems depends on the density of the solvents. In other words, an easier phase separation in DES-based systems is obtained when the density difference between DES and water is as large as possible, leading to lower energy demands and higher efficiency [43]. The density of selected DESs were between 0.84 and 0.90 g/cm$^3$ (Figure 2.10), which are lower than the well-known hydrophilic DESs [44]. Moreover the long alkyl chains in DESs, also lead to a decrease in the density of the DESs with increasing alkyl chain length of the DES precursors [2]. As previously described, the hydrophobic nature of the selected DESs reduces the presence of water, and the weak hydrogen-bonding interactions between the ES components lead to the lower density in these DESs.

As Figure 2.10 indicates, the density data in four different families of DESs are very close to each other. However, the DESs based on fatty alcohols, namely menthol: fatty alcohols and fatty acid: fatty alcohols, show the lowest density [21,45]. In contrast, the speed of sound increases with an increase in the alkyl chain length of the HBA and HBD, and the fatty acids-based DESs have the lowest speed of sound (Figure 2.11).

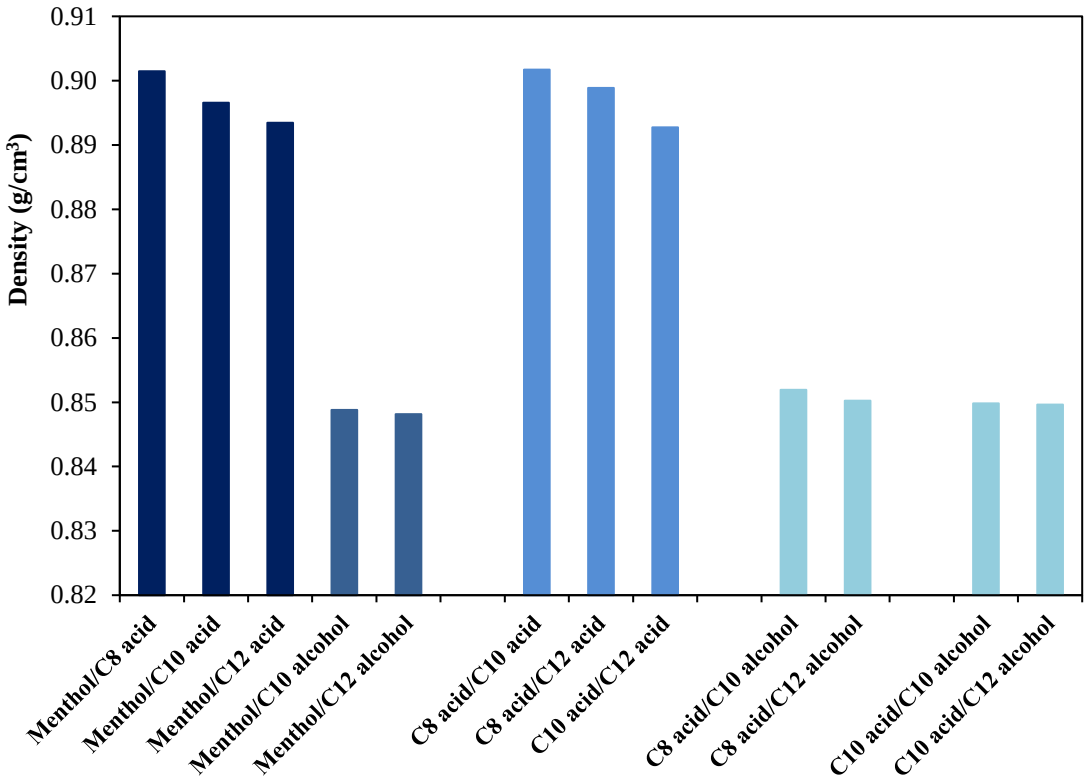


**Figure 2.10.** Densities of four different families of DESs at 25 °C.

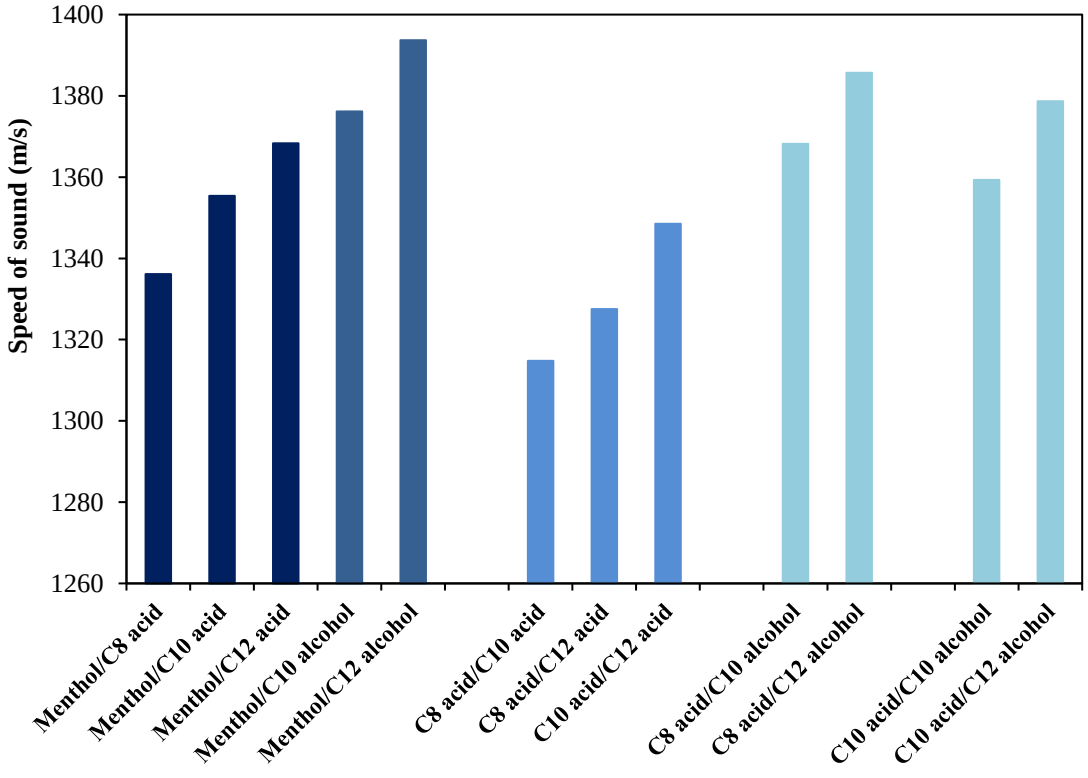


**Figure 2.11.** Speed of sound values of four different families of DESs at 25 °C.

## 2.5. Conclusions

Choosing the DESs, which are stable in the presence of water, reduces the cost and energy and increases the efficiency of separation processes. As a quick screening tool, COSMO-SAC was applied to investigate the water stability of hydrophilic and hydrophobic DESs in three different molar ratios and three concentrations of HBA and HBD. The computational results indicated that the DESs composed of HBA and HBD with higher hydrophobicity are more stable in water. Moreover, it has been found out that changing the molar ratios as well as the concentrations of the components make significant differences in the water stability of the DESs because these factors increase the hydrophobicity or hydrophilicity of the DESs, which lead to a great change in their stability. This was experimentally confirmed for a selected group of DES composed of menthol: fatty acid, menthol: fatty alcohol, fatty acid: fatty acid and fatty acid: fatty alcohol. In addition, a good correlation between the octanol/water partition coefficients of the selected DESs and the obtained results confirm that DESs containing more hydrophobic components show reduced affinity towards water molecules, which result in stronger interactions between DES components and improved their water stability. Since the results revealed that the thermophysical characterization of the studied DES are significantly affected by their hydrophobicity, increasing the hydrophobicity through modifications in the DES components or the length of alkyl chain led to a reduction in the solubility DES in water, which increases the viscosity and decreases the density. Therefore, this work supports the notion that controlling the hydrophobicity or hydrophilicity of DESs is crucial factor for designing the stable DESs in water.

## 2.6. References

[1] M. Moradi, M. Mohammadian, G. Pazuki, S. Shahriari, Partitioning of Crocin in a Novel Aqueous Two-Phase System Composed of a Deep Eutectic Solvent and Acetonitrile, J. Chem. Eng. Data. (2022)

[2] P. Makoś, E. Słupek, J. Gębicki, Hydrophobic deep eutectic solvents in microextraction techniques–A review, Microchem. J. 152 (2020).

[3] E.L. Smith, A.P. Abbott, K.S. Ryder, Deep Eutectic Solvents (DESs) and Their Applications, Chem. Rev. 114 (2014) 11060–11082.

[4] M.A.R. Martins, S.P. Pinho, J.A.P. Coutinho, Insights into the Nature of Eutectic and Deep Eutectic Mixtures, J. Solution Chem. 48 (2019) 962–982..

[5] E. Riveiro, B. González, Á. Domínguez, Extraction of adipic, levulinic and succinic acids from water using TOPO-based deep eutectic solvents, Sep. Purif. Technol. 241 (2020) 116692.

[6] M.T. Zafarani-Moattar, H. Shekaari, F. Ghaffari, The study of extent of interactions between components of natural deep eutectic solvents in the presence of water through isopiestic investigations, J. Mol. Liq. 311 (2020).

[7] T. Banerjee, N. Paul, P.K. Naik, B.D. Ribeiro, P.S.G. Pattader, I.M. Marrucho, Molecular dynamics insights and water stability of hydrophobic deep eutectic solvents aided extraction of nitenpyram from an aqueous environment, J. Phys. Chem. B. 124 (2020) 7405–7420.

[8] C. Florindo, L.C. Branco, I.M. Marrucho, Development of hydrophobic deep eutectic solvents for extraction of pesticides from aqueous environments, Fluid Phase Equilib. 448 (2017) 135–142.

[9] F.O. Farias, H. Passos, Á.S. Lima, M.R. Mafra, J.A.P. Coutinho, Is It Possible to Create Ternary-like Aqueous Biphasic Systems with Deep Eutectic Solvents?, ACS Sustain. Chem. Eng. 5 (2017) 9402–9411.

[10] C. Florindo, L.C. Branco, I.M. Marrucho, Quest for Green-Solvent Design: From Hydrophilic to Hydrophobic (Deep) Eutectic Solvents, ChemSusChem. 12 (2019) 1549–1559.

[11] W. Tang, Y. Dai, K.H. Row, Evaluation of fatty acid/alcohol-based hydrophobic deep eutectic solvents as media for extracting antibiotics from environmental water, Anal. Bioanal. Chem. 410 (2018) 7325–7336.

[12] S.T. Lin, S.I. Sandler, Erratum: A Priori Phase Equilibrium Prediction from a Segment Contribution Solvation Model (Industrial and Engineering Chemistry Research 41, 5 (903)), Ind. Eng. Chem. Res. 43 (2004) 1322.

[13] A. Klamt, Conductor-like screening model for real solvents: A new approach to the quantitative calculation of solvation phenomena, J. Phys. Chem. 99 (1995) 2224–2235.

[14] S.Z. Mahmoudabadi, G. Pazuki, Modeling of thermodynamics properties of amino acid solutions by COSMO-SAC model, Fluid Phase Equilib. 541 (2021).

[15] C.M. Hsieh, S. Wang, S.T. Lin, S.I. Sandler, A predictive model for the solubility and octanol-water partition coefficient of pharmaceuticals, J. Chem. Eng. Data. 56 (2011) 936–945.

[16] M. Jaschik, D. Piech, K. Warmuzinski, J. Jaschik, Prediction of gas solubility in ionic liquids using the COSMO-SAC model, Chem. Process Eng. - Inz. Chem. i Proces. 38 (2017) 19–30.

[17] R. Verma, T. Banerjee, Liquid-Liquid Extraction of Lower Alcohols Using Menthol-Based Hydrophobic Deep Eutectic Solvent: Experiments and COSMO-SAC Predictions, Ind. Eng. Chem. Res. 57 (2018) 3371–3381.

[18] D. Peng, A. Alhadid, M. Minceva, Assessment of COSMO-SAC Predictions for Solid-Liquid Equilibrium in Binary Eutectic Systems, Ind. Eng. Chem. Res. 61 (2022) 13256–13264.

[19] S.Z. Mahmoudabadi, G. Pazuki, Investigation of COSMO-SAC model for solubility and cocrystal formation of pharmaceutical compounds, Sci. Rep. 10 (2020).

[20] Royal Society of Chemistry, ChemSpider. Search and Share Chemistry, R. Soc. Chem. (2015).

[21] A. Huang, W. Deng, X. Li, Q. Zheng, X. Wang, Y. Xiao, Long-chain alkanol–alkyl carboxylic acid-based low-viscosity hydrophobic deep eutectic solvents for one-pot extraction of anthraquinones from Rhei Radix et Rhizoma, J. Pharm. Anal. 12 (2022) 87–95.

[22] Y. Wu, M. Chen, X. Wang, Y. Zhou, M. Xu, Z. Zhang, Development and validation of vortex-assisted dispersive liquid–liquid microextraction method based on solidification of floating hydrophobic deep eutectic solvent for the determination of endocrine disrupting chemicals in sewage, Microchem. J. 163 (2021).

[23] D.P. Arcon, F.C. Franco, All-fatty acid hydrophobic deep eutectic solvents towards a simple and efficient microextraction method of toxic industrial dyes, J. Mol. Liq. 318 (2020).

[24] Y. Dai, J. van Spronsen, G.J. Witkamp, R. Verpoorte, Y.H. Choi, Natural deep eutectic solvents as new potential media for green technology, Anal. Chim. Acta. 766 (2013) 61–68.

[25] Q. Zhang, K. De Oliveira Vigier, S. Royer, F. Jérôme, Deep eutectic solvents: Syntheses, properties and applications, Chem. Soc. Rev. 41 (2012) 7108–7146.

[26] A.K. Dwamena, Recent advances in hydrophobic deep eutectic solvents for extraction, Separations. 6 (2019).

[27] J. Lee, D. Jung, K. Park, Hydrophobic deep eutectic solvents for the extraction of organic and inorganic analytes from aqueous environments, TrAC - Trends Anal. Chem. 118 (2019) 853–868.

[28] S.M. Majidi, M.R. Hadjmohammadi, Hydrophobic borneol-based natural deep eutectic solvents as a green extraction media for air-assisted liquid-liquid micro-extraction of warfarin in biological samples, J. Chromatogr. A. 1621 (2020).

[29] I. Khan, K.A. Kurnia, T.E. Sintra, J.A. Saraiva, S.P. Pinho, J.A.P. Coutinho, Assessing the activity coefficients of water in cholinium-based ionic liquids: Experimental measurements and COSMO-RS modeling, Fluid Phase Equilib. 361 (2014) 16–22.

[30] D.O. Abranches, J.A.P. Coutinho, Type V deep eutectic solvents: Design and applications, Curr. Opin. Green Sustain. Chem. 35 (2022) 100612.

[31] B. Jamehbozorg, R. Sadeghi, Vapor Pressure Osmometry Studies of Aqueous Ionic Liquid-Carbohydrate Systems, J. Chem. Eng. Data. 63 (2018) 331–340.

[32] N. Ebrahimi, R. Sadeghi, Salting-out effect in polypropylene glycol-amino acid aqueous solutions revealed by vapor pressure osmometry, Fluid Phase Equilib. 425 (2016) 237–243.

[33] M. Maali, R. Sadeghi, Vapour pressure osmometry determination of water activity of binary and ternary aqueous (polymer + polymer) solutions, J. Chem. Thermodyn. 84 (2015) 41–49.

[34] T. El Achkar, S. Fourmentin, H. Greige-Gerges, Deep eutectic solvents: An overview on their interactions with water and biochemical compounds, J. Mol. Liq. 288 (2019).

[35] F.O. Farias, J.F.B. Pereira, J.A.P. Coutinho, L. Igarashi-Mafra, M.R. Mafra, Understanding the role of the hydrogen bond donor of the deep eutectic solvents in the formation of the aqueous biphasic systems, Fluid Phase Equilib. 503 (2020).

[36] S. T. Lin, &, S. I. Sandler, Prediction of octanol− water partition coefficients using a group contribution solvation model, Industrial & engineering chemistry research, 38 (1999) 4081-4091.

[37] J. Marrero & R. Gani, Group-contribution-based estimation of octanol/water partition coefficient and aqueous solubility, Industrial & Engineering Chemistry Research, 41 (2002) 6623-6633.

[38] K. Zhang, C. Liu, S. Li, J. Fan, A hydrophobic deep eutectic solvent based vortex-assisted liquid-liquid microextraction for the determination of formaldehyde from biological and indoor air samples by high performance liquid chromatography, J. Chromatogr. A. 1589 (2019) 39–46.

[39] I. Adeyemi, R. Sulaiman, M. Almazroui, A. Al-Hammadi, I.M. AlNashef, Removal of chlorophenols from aqueous media with hydrophobic deep eutectic solvents: Experimental study and COSMO RS evaluation, J. Mol. Liq. 311 (2020).

[40] C. Florindo, L. Romero, I. Rintoul, L.C. Branco, I.M. Marrucho, From Phase Change Materials to Green Solvents: Hydrophobic Low Viscous Fatty Acid-Based Deep Eutectic Solvents, ACS Sustain. Chem. Eng. 6 (2018) 3888–3895.

[41] M.B. Haider, M. Dwivedi, D. Jha, R. Kumar, B. Marriyappan Sivagnanam, Azeotropic separation of isopropanol-water using natural hydrophobic deep eutectic solvents, J. Environ. Chem. Eng. 9 (2021).

[42] D. J. van Osch, L. F. Zubeir, A. van den Bruinhorst, M. A. Rocha, M. C. Kroon, Hydrophobic deep eutectic solvents as water-immiscible extractants, Green Chemistry, 17 (2015) 4518-4521.

[43] J. Cao, E. Su, Hydrophobic deep eutectic solvents: the new generation of green solvents for diversified and colorful applications in green chemistry, J. Clean. Prod. 314 (2021).

[44] D.J.G.P. Van Osch, C.H.J.T. Dietz, J. Van Spronsen, M.C. Kroon, F. Gallucci, M. Van Sint Annaland, R. Tuinier, A Search for Natural Hydrophobic Deep Eutectic Solvents Based on Natural Components, ACS Sustain. Chem. Eng. 7 (2019) 2933–2942.

[45] X.H. Fan, L.T. Wang, Y.H. Chang, J.Y. An, Y.W. Zhu, Q. Yang, D. Meng, Y. jie Fu, Application of green and recyclable menthol-based hydrophobic deep eutectic solvents aqueous for the extraction of main taxanes from Taxus chinensis needles, J. Mol. Liq. 326 (2021).

# 3. EXTRACTION OF OFLOXACIN FROM WATER USING HYDROPHOBIC DEEP EUTECTIC SOLVENTS *

***Chapter based on the published manuscript:**

Mahtab Moradi, Ana M. Ferreira, Catarina M. S. S. Neves, Samane Zarei Mahmoudabadi, Gholamreza Pazuki and João A.P. Coutinho, "Extraction of ofloxacin from water using hydrophobic eutectic solvents". Journal of Environmental Chemical Engineering, 2024, 12, 113075.

## 3.1. Abstract

Wastewater treatment plants do not cope well with emerging micropollutants, such as pharmaceuticals, because they are not effective to remove them. Therefore, this work aims to develop a process for the extraction of ofloxacin (OFX) based on a liquid-liquid extraction (LLE) using hydrophobic DESs (HDES), coupled with the Conductor-like Screening Model for Real Solvent (COSMO-RS) for solvent screening. First, COSMO-RS was used to predict the partition coefficient of OFX for four HDES families: L-menthol: fatty acid, L-menthol: fatty alcohol, fatty acid: fatty acid and fatty acid: fatty alcohols, at three different molar ratios (2:1, 1:1, and 1:2). These results showed that HDES formed by fatty acids, especially those with a longer alkyl chain and a higher fatty acid molar ratio, were the most suitable solvents for OFX extraction. Then, the most promising HDES to extract OFX was evaluated experimentally. The HDES decanoic acid: dodecanoic acid (C10 acid: C12 acid) in a molar ratio of 2:1 being the system with best extraction results of OFX was selected to optimize the extraction conditions of OFX, namely pH, HDES: water ratio (v/v), and OFX concentration, using a response surface methodology (RSM). The results obtained showed that at a pH of 5.2, HDES-water ratio (v/v) of 1.3, and 2.5 mg/ml of OFX that an extraction efficiency of OFX of (98.8 ± 0.9)% could be achieved. The results show that one-step OFX extraction is possible, but is significantly influenced by both the extraction parameters and the hydrophobic properties of the HDES.

**Keywords:** Deep eutectic solvents; Liquid-liquid extraction; COSMO-RS; Water treatment; Response surface methodology.

## 3.2. Introduction

The widespread use of pharmaceuticals has led to them entering wastewater through various routes, such as excretion, improper disposal and residues from medical facilities and the pharmaceutical sector [1]. However, many wastewater treatment plants are not able to effectively remove pharmaceutical compounds, which leads to contamination of the water and consequently the environment. Studies have shown that these substances can damage ecosystems by increasing mortality rates and disrupting the reproductive functions of aquatic organisms [2]. In addition, antibiotic residues in water sources promote the development of resistant bacteria, making it difficult to treat infections and

posing a risk to public health [3]. Voogt et al. [4] emphasized the need to improve pharmaceutical removal from wastewater systems, focusing on fluoroquinolones such as OFX. OFX, the second most widely used drug in the fluoroquinolone category, is used in human and veterinary medicine due to its broad spectrum of activity against various bacteria [5]. However, its low absorption rate is a problem for the environment as about 90% is excreted unchanged or as metabolites, contributing significantly to environmental pollution. This contributes to the persistence of OFX in wastewater systems [6,7], making it an emerging pollutant with remarkable resistance to biodegradation.

Conventional wastewater treatment processes, including adsorption and activated sludge treatment, are not specifically designed to efficiently remove pharmaceutical compounds such as OFX [8]. This leads to suboptimal treatment, as the effectiveness of these processes varies widely and is influenced by the unique properties of the compounds. [9]. Reports from different WWTPs reflect this inconsistency, with some achieving high OFX removal efficiencies of up to 86%, while others report much lower efficiencies of around 56% [10]. These differences highlight the limitations of conventional treatment methods, particularly due to the resistance of these compounds to microbial and chemical degradation, which makes them difficult to remove from wastewater systems [11]. Therefore, there is an urgent need for the development of cost-effective, environmentally sustainable technologies specifically tailored to the extraction of persistent pharmaceuticals, including fluoroquinolones such as OFX, from wastewater streams.

Solid phase extraction (SPE) [12] and LLE [13] have been established as alternative methods for the removal of pharmaceuticals. Although these methods are very efficient, they also have disadvantages such as high costs or considerable consumption of organic solvents, respectively [5,14]. Recently, environmentally friendly solvent-based LLE has emerged as a promising option for the removal of fluoroquinolones, using alternative solvents such as ionic liquids (ILs) and deep eutectic solvents (DESs) [15]. DES, a mixture of HBA and HBD, offers simple preparation and cost advantages over ILs, although conventional organic solvents such as methanol are less expensive. On the other hand, DES is preferable to organic solvents due to their lower toxicity. However, the assessment of toxicity can be controversial and depends on the DES rather than the whole class [16]. The use of natural DES, i.e. components from natural sources such as sugars, polyols, organic acids, amino acids, can reduce the price. In addition, by

selecting the components of the DES mixture, their physicochemical properties such as hydrophobicity and hydrophilicity can be tuned. Hydrophilic DESs are often used for the extraction and purification of various compounds [17]. However, their high water solubility poses a challenge in applications such as wastewater treatment. In LLE a third component must be added to enable phase separation. Additionally, their recovery and reusability are usually not as straightforward and cost-effective as desired, which is one of the major drawbacks of DES for wide industrial application. Furthermore, hydrophilic DESs are limited in their ability to extract highly hydrophobic molecules, such as pharmaceuticals.

To overcome these issues, hydrophobic DES, also known as hydrophobic deep eutectic solvents (HDES), have been employed [18]. Numerous studies have demonstrated the efficacy of hydrophobic deep eutectic solvents (HDES)-based LLE for various compounds, including pharmaceuticals (see Table B.1 in Appendix B for more details) such as fluoroquinolones [19–21]. Although there have been some studies on the extraction of OFX using HDES-based LLE, the extraction of OFX using these systems has not yet been deeply studied [20,21]. Li et al. [20] investigated seventeen HDES based on monoterpenes, fatty acids and a benzoate ester for the quantification of fluoroquinolones in surface water using liquid-liquid microextraction (LLME). Thymol and heptanoic acid in a 2:1 ratio at a pH of 4-7 showed the highest extraction efficiency for OFX, with relative recoveries between 85% and 104%. Pochivalov et al. [21] investigated HDES composed of thymol-fatty acids for extraction of fluoroquinolones using LLME followed by magnetic phase separation for concentration. Thymol-nonanoic acid-based HDES with a molar ratio of 1:1 and at pH 6 showed high extraction yield for fluoroquinolones, especially for OFX. While LLME is very efficient, it requires specialized equipment and is generally used for low volume samples. In addition, the limited flexibility in solvent choice due to viscosity constraints may limit its attractiveness for certain applications. Considering these factors, LLE is a preferred platform for broader applications due to its robustness, scalability, simplicity and higher flexibility in solvent choice [22].

Although the potential of HDES as viable eco-friendly has been demonstrated in numerous applications, researchers still face the challenge of quickly identifying the most effective HDES in LLE in a fast way. The partition coefficient of a solute is a key factor in selecting the optimal solvent for LLE. However, since experimental measurements are costly and lengthy, the use of a thermodynamic model as a pre-

screening tool can be very helpful. The COSMO-RS is an advanced computational method that applies the principles from quantum chemistry and statistical thermodynamics to predict the physicochemical and thermodynamic properties of mixed and pure compounds [23,24]. The COSMO-RS model has been successful in predicting the octanol-water partition coefficient of some compounds, such as small drug-like molecules [25] and numerous compounds from different pollutant categories [24], yet it has been used to estimate the partition coefficient for screening solvents in LLE in only a few studies [26–29]. Spieß *et al.* [26] used the model COSMO-RS, to screen the best hydrophobic organic solvents for the maximum conversion of alcohol dehydrogenase-catalyzed oxide reductions of prochiral ketones using LLE. Burghoff *et al.* [27] also applied the COSMO-RS model to the screening of nitrogen- and phosphorus-based solvents in phenol extraction by LLE. Ferreira and co-workers [28] compared the use of COSMO-RS and non-random activity coefficients for two liquid segments (NRTL-SAC) to predict the partition coefficients of four phenolic compounds - vanillin, ferulic acid, (S)-hesperetin and quercetin - in different LLE. Chagnoleau et al. [29] showed that COSMO-RS is able to predict partition coefficients for natural compounds (quercetin, apigenin, coumarin, β-ionone, and α-tocopherol) in organic biphasic systems with very different chemical structures. These systems were based on heptane, ethanol, and a selection of six different third components, including glycerol, ethylene glycol, levulinic acid, and the corresponding choline chloride-based DES.

In this work, the potential of four different families of HDES based on menthol, fatty acids and fatty alcohols as alternative solvents for the extraction of OFX from water by LLE was investigated. In order to minimize the experimental effort and identify the best possible solvent, COSMO-RS was used as a screening tool to determine the most effective HDES for the extraction of OFX from water. The best solvents selected from the screening were evaluated experimentally and for the best solvent a response surface methodology (RSM) was used to optimize the partition coefficient of OFX ($K_{OFX}$) and the extraction efficiency of OFX ($EE_{OFX}$ %) by changing the operating conditions, namely pH, OFX concentration, and HDES-water ratio (v/v). To the best of our knowledge, this is the first time that computational and experimental methods have been integrated to minimize the number of experiments required to develop a process for OFX extraction using HDES-based LLE.

## 3.3. Materials and methods

### 3.3.1. Materials

The chemical compounds used in this study are listed in Table B.2 in Appendix B. All experiments used ultrapure water subjected to a double distillation process, passed through a reverse osmosis system, and treated with a Milli-Q plus 185 water purifier.
The HDES from four different families (L-menthol: fatty acid, L-menthol: fatty alcohol, fatty acid: fatty acid, and fatty acid: fatty alcohols), which here studied here are listed in Table 3.1. Those were evaluated at three different molar ratios of HBA:HBD (2:1, 1:1, 1:2), totaling 36 different HDES used in the screening by COSMO-RS for the most effective solvents to extract OFX.

**Table 3.1.** List of HDES studied in this work.

| HBA | HBD | Abbreviation |
|---|---|---|
| L-menthol | Octanoic acid | L-menthol: C8 acid |
| | Decanoic acid | L-menthol: C10 acid |
| | Dodecanoic acid | L-menthol: C12 acid |
| | 1-Decanol | L-menthol: C10 alcohol |
| | 1-Dodecanol | L-menthol: C12 alcohol |
| Octanoic acid | Decanoic acid | C8 acid: C10 acid |
| | Dodecanoic acid | C8 acid: C12 acid |
| | 1-Decanol | C8 acid: C10 alcohol |
| | 1-Dodecanol | C8 acid: C12 alcohol |
| | Dodecanoic acid | C8 acid: C12 acid |
| Decanoic acid | 1-Decanol | C10 acid: C10 alcohol |
| | 1-Dodecanol | C10 acid: C12 alcohol |

Finally, the selected HDES were prepared by heating the mixture to 80 °C for 4-5 h in the desired molar ratio with constant stirring, and a clear and homogeneous liquid was obtained, as previously documented [30]. These HDES did not undergo any visual changes after cooling, remaining stable at 25 ºC (clear and homogeneous liquid). The only exception was L-menthol: C12 acid in a 1:2 ratio, which solidified at 25 ºC and, therefore, was not evaluated experimentally. The melting point of the selected HDES and their individual compounds is presented in Table B.3 in Appendix B. In addition,

the water solubility of the individual HDES compounds is listed in Table B.4 in Appendix B.

### 3.3.2. COSMO-RS model

COSMO-RS is a predictive model that relies on the principles of quantum chemistry and statistical thermodynamics. The procedure for the application of COSMO-RS to select HDES involved two steps. First, the COSMO files are calculated by optimizing the geometric structure of the water and each HDES at specific molar ratios of HBA and HBD using the DMol$^3$ module in Material Studios 2017 software, the most widely used software for performing density functional theory (DFT) and COSMO calculations [31]. In the present work, the optimization of the structures of the compounds was performed using GGA (VWN-BP) as DFT. Also, the multipolar expansion in the electronic options was set to octupole and the quality fine was chosen for all calculations. The calculations were performed on four parallel cores, and the default values of DMol$^3$ were used for other options [32]. Then, the generated COSMO files were used in the COSMOthermX 2.1 program to calculate the partition coefficients of OFX in the systems of HDES and water at 25 °C.

In the present work, the calculation of the logarithm partition coefficient of OFX (log$K_{OFX}$) between HDES and water was determined through the computation of the chemical potentials of the OFX (in HDES ($\mu_{OFX}^{HDES}$) and in water ($\mu_{OFX}^{W}$)) in infinite dilution and in the pure solvents as follows [33]:

$$log(K_{OFX}) = log\left[\exp\left(\frac{\mu_{OFX}^{HDES} - \mu_{OFX}^{Water}}{RT}\right).\frac{V_{HDES}}{V_{Water}}\right] \quad (3.1)$$

In addition, the ratio of molar volume of two phases ($\frac{V_{HDES}}{V_{Water}}$) was estimated by COSMO-RS according to the volumes of molecules and the temperature ($T$) was set at 25 °C.

### 3.3.3. Liquid-Liquid Extraction (LLE)

For the extraction of OFX from water, the twelve most promising HDES identified in the screening with COSMO-RS were evaluated. Briefly, extractions were conducted for 12 hours at 25 °C and 150 rpm. Afterwards, phases were separated by centrifugation at

10000 rpm for 10 minutes, and OFX in both phases was quantified using UV-spectrophotometry. Figure 3.1 provides a summary of the experimental procedure. Further details on the OFX extraction using HDES-based LLE are outlined in Appendix B.

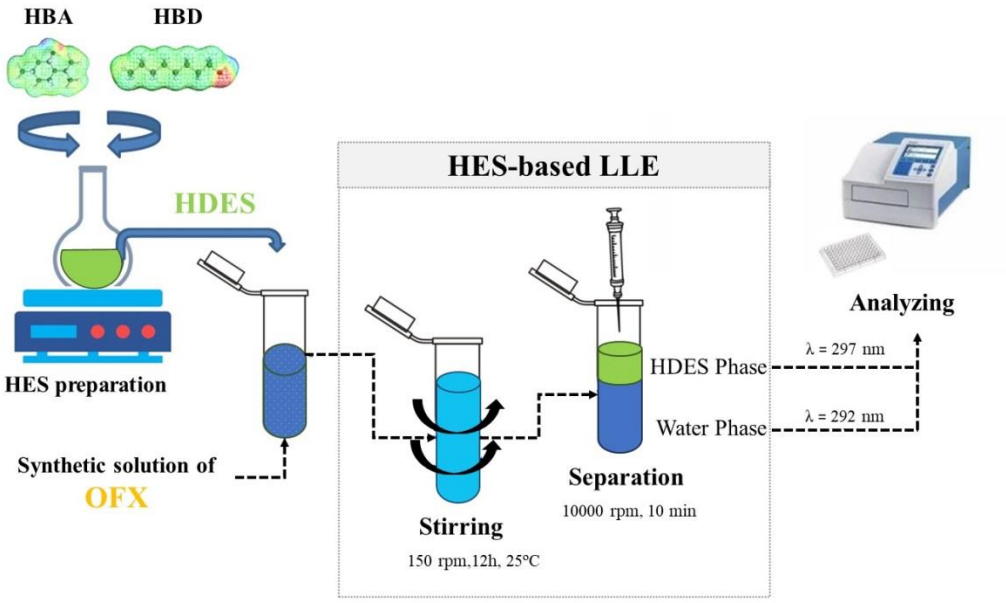


**Figure 3.1.** Schematic representation of the HDES-based LLE procedure for the extraction of OFX.

The partition coefficient of the OFX ($K_{OFX}$) was determined according to the following equation:

$$K_{OFX} = \frac{[OFX]_{HDES}}{[OFX]_{Water}} \tag{3.2}$$

Where $[OFX]_{HDES}$ and $[OFX]_{Water}$ are the concentrations of OFX in the HDES and water phases, respectively.

The percentage extraction efficiency of OFX ($EE_{\mathrm{OFX}}$ %) is the percentage ratio between the total weight of OFX in the HDES-rich phase to that in the total mixture, which was determined according to the following equation:

$$EE_{OFX}\ \% = \left(\frac{w_{OFX}^{HDES}}{w_{OFX}^{DES} + w_{OFX}^{water}}\right) \times 100 \tag{3.3}$$

Where $w_{OFX}^{HDES}$ and $w_{OFX}^{water}$ are the weight of OFX in the HDES and aqueous phases, respectively.

### 3.3.4. Optimization of the operating extractions conditions

To study the synergistic or antagonistic effects on the extraction of the operating conditions, the use of an experimental design is helpful. The response surface methodology (RSM) is a robust experimental design tool that uses mathematical and statistical methods to correlate and optimize the unknown function. In a $2^k$ factorial planning, *k* represents the number of factors (independent variables) that can contribute to a response *y* through a polynomial equation as follows:

$$y = \beta_0 + \sum \beta_i X_i + \sum \beta_i \beta_i X_i^2 + \sum_{i<j} \beta_i \beta_j X_i X_j \quad (3.4)$$

In this equation, $\beta_0$, $\beta_i$, $\beta_{ii}$, and $\beta_{ij}$ correspond to the adjusted coefficients for the intercept, linear, quadratic, and interaction terms, respectively, while $X_i$ and $X_j$ refer to the operational variables.

A central composite rotatable design (CCRD, $2^3$ plus axial) with six replicates at the central point was employed for factorial planning to optimize OFX extraction efficiency. Three key operating variables were evaluated: pH (ranging from 2.0 to 6.0), OFX concentration (ranging from 0.5 to 2.5 mg/ml), and the HDES-water ratio (v/v, ranging from 6:10 to 21:10). A total of twenty experiments were conducted, including the central point (at zero level), factorial points (at level one, denoted as 1 and -1) and axial points (at level α). Further information on the RSM, such as the actual and coded levels of the parameters considered, can be found in Tables B.5 and B.6 in Appendix B.

The data was subjected to statistical analysis with a 95% confidence level. The model's suitability was assessed based on the lack of fit, regression coefficient ($R^2$), and the F-value derived from the analysis of variance (ANOVA). Using these analytical approaches, the interactions between the variables and their effects on OFX extraction efficiency were investigated to determine the most favorable operating conditions. These conditions were then validated experimentally. All statistical analyses and representation of response surfaces were performed using Protimiza Experimental Design software.

## 3.4. Results and discussion

### 3.4.1. Simulation results

The first step of this work was the selection of HDES for the extraction of OFX from water by LLE, using COSMO-RS. For this purpose, the σ-profiles (Figure 3.2) were first determined to obtain information about the chemical nature of the compounds, such as polarity and hydrogen bonding ability, which contribute to the understanding of the potential interactions between the solute and the solvents during extraction [34]. Figure 3.2A shows the polarized charge distribution (σ) of OFX and water, where three regions can be identified. The region between -0.01e/Å$^2$ and +0.01e/Å$^2$ is considered non-polar, while the polar regions extend below -0.01e/Å$^2$ and above +0.01e/Å$^2$ and have the potential to form HBD and HBA, respectively [32]. It is noteworthy that for non-polar compounds, the distribution of the σ-profile is predominantly in the non-polar region, whereas moderately polar compounds have peaks in both the non-polar and polar regions. The σ-profile of OFX, characterized by a significant segment in the non-polar region and a smaller peak in the polar region (see Figure 3.2A), suggests that HDES reflecting this pattern are likely to be more effective extractants [35]. In addition, our results suggest that the HDES investigated in this study act primarily as pure HBAs, as evidenced by a single peak in the positive region (see Figure 3.2B). This observation emphasizes a strong interaction potential between OFX and HDES, especially since DES act most effectively as either HBA or HBD when their σ profiles do not show peaks in the opposite range, confirming their role as pure acceptors or donors [36]. In particular, fatty acid-based HDES are identified as excellent candidates for enhancing the extraction of OFX due to their pronounced peak in the polar region.

Notice that the structures of the HDES were modelled as pseudo-compound; thus, the σ-profile of the HDES can be described as the sum of the σ-profiles of its individual compounds weighted by their molar ratio (model HBAHBD). The HDES σ-profiles are in agreement with the σ-profiles of their individual compounds (L-menthol, C12 acid, and C10 alcohol), since all of them exhibit favorable characteristics, with C10 acid showing a more pronounced peak in the polar region (Figure B.1 in Appendix B).

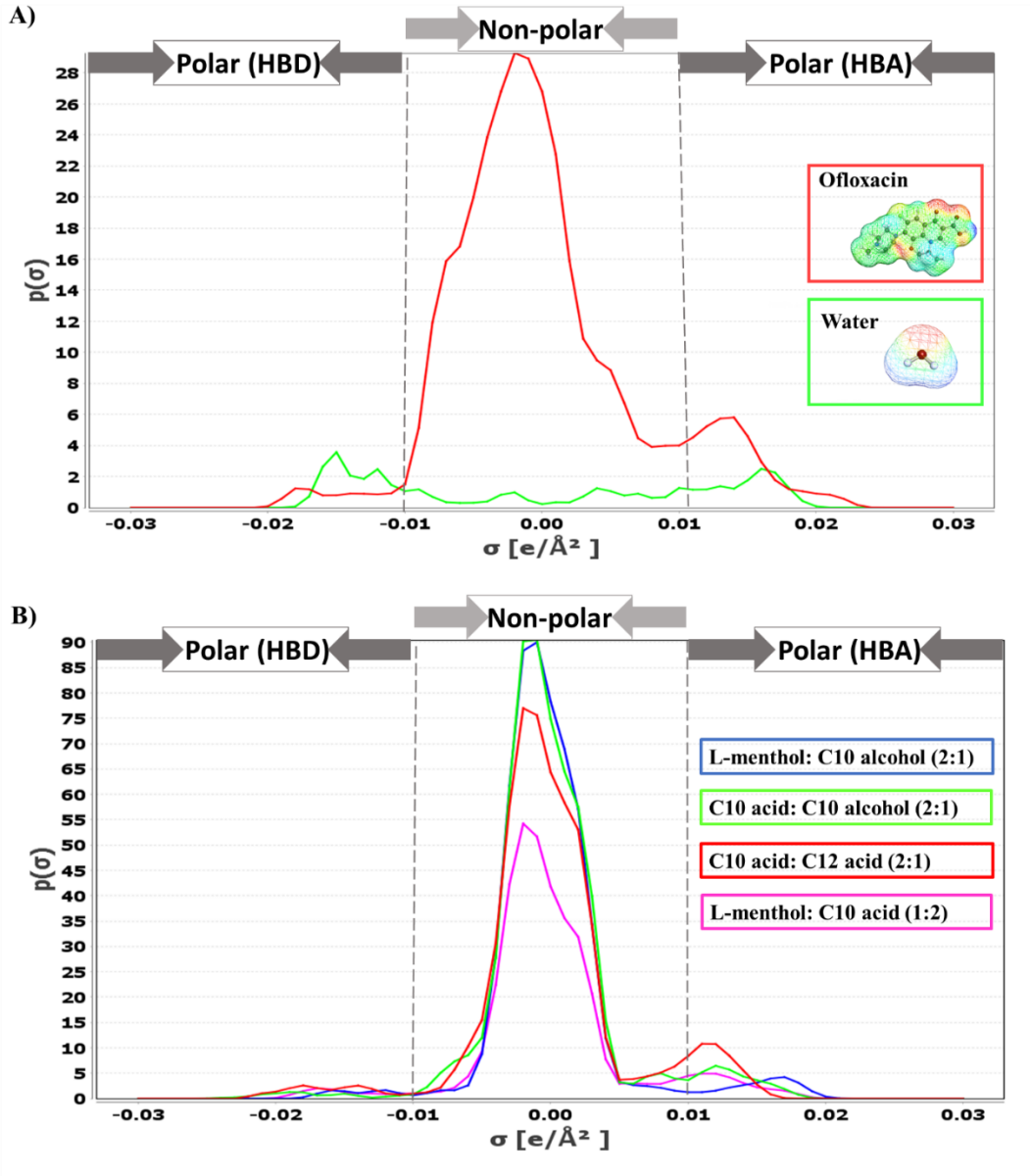


**Figure 3.2.** (**A**) The σ-profiles of water and OFX; (**B**) The σ-profiles of an HDES representative of each in each family.

By evaluating the logarithm of partition coefficient of OFX (log($K_{OFX}$)) it is possible to compare the partition of a given solute in several different LLE under the same conditions. In this case, COSMO-RS was used to predict log ($K_{OFX}$) between water and twelve HDES at three different molar ratios of HBA and HBD (1:2, 1:1, and 2:1) at 25 °C. The results are shown in Figure 3.3 (for more details, see in Appendix B, Table B.7).

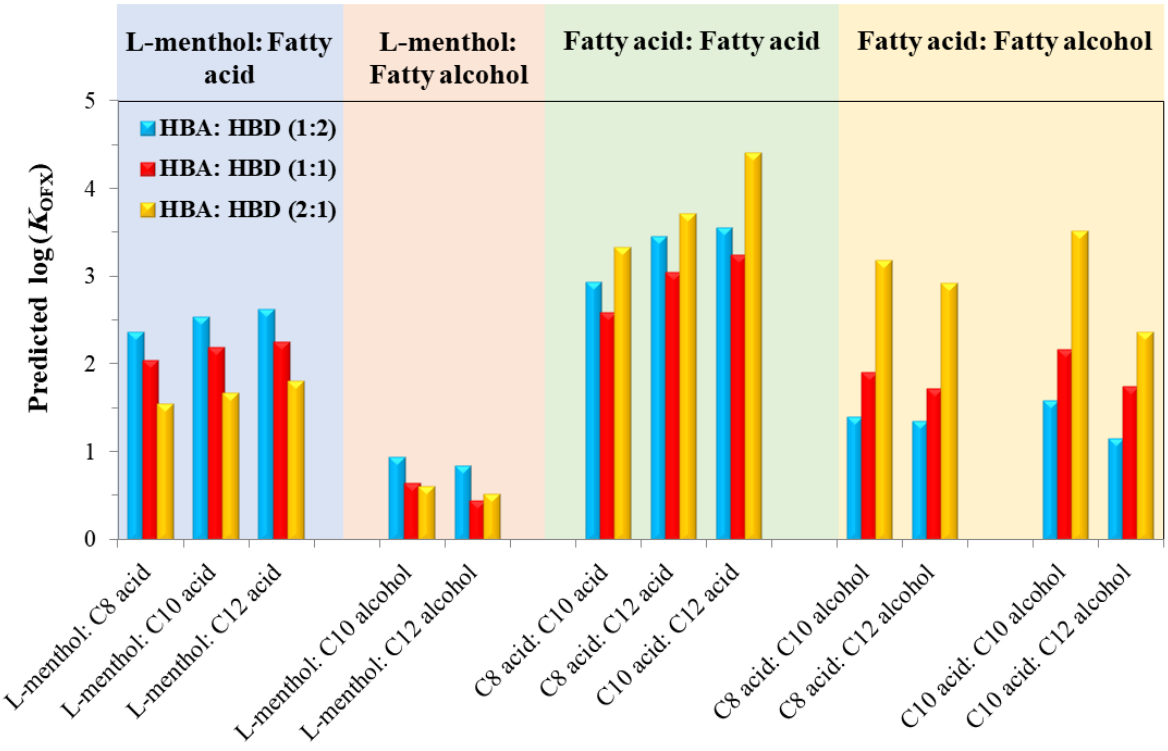


**Figure 3.3.** Predicted log($K_{OFX}$) for the HDES in different molar ratios (1:1, 1:2 and 2:1), at 25 °C using COSMO-RS.

As shown in Figure 3, fatty acids HDES seem to be indeed the best option to obtain the highest partition coefficients for OFX. The use of the fatty acid: fatty acid-based HDES resulted in the highest partition coefficients for OFX among all the studied HDES.

This is in line with the studies of Li et al. [20], which highlights the higher efficiency of fatty acid-based solvents compared to menthol-based solvents. Another study [37] reinforces the efficacy of fatty acid-based HDES over other HDES families in the extraction of ciprofloxacin, another fluoroquinolone. In particular, this study emphasizes that HDES formulated with non-ionic components such as fatty acids exhibit better extraction efficiency than HDES derived from ionic components such as quaternary ammonium salts. These results emphasize the central role of solvent properties in enhancing intermolecular interactions with the target analyte (OFX/ ciprofloxacin). As Chen et al. [38] stated, the structure and chemical composition of HDES play a crucial role in the efficiency of extraction. Building on these findings, our study goes further and investigates the effects of HDES composition on extraction efficiency of OFX.

Figure 3.3 shows a correlation between log ($K_{OFX}$) and alkyl chain length and the molar ratio of the components of HDES. In general, an increase in the alkyl chain length of the

fatty acids and their molar ratio leads to higher log ($K_{OFX}$) values. For example, the log ($K_{OFX}$) value in the L-menthol: fatty acid HDES changed from 2.36 to 2.61 when the alkyl chain length of the fatty acids increased from C8 to C12 at a constant molar ratio (1:2). These results agree with the observations of Pochivalov et al. [21], and Rodríguez-Llorente et al. [39] who also reported a positive effect on the extraction of antibiotics, such as OFX, with HDES based on thymol and fatty acids with longer hydrocarbon chains (from hexanoic acid to nonanoic acid). However, the trend is different for fatty alcohol-based HDES. As shown in Figure 3.3, an extension in the alkyl chain length of the fatty alcohol results in a decrease in the log ($K_{OFX}$) in L-menthol: fatty alcohol and fatty acid: fatty alcohol HDES. For instance, in C10 acid: fatty alcohol HDES, increasing the alkyl chain length of the fatty alcohols from C10 to C12 at a constant molar ratio (2:1) leads to a notable reduction in the log ($K_{OFX}$) values from 3.51 to 2.36.

Regarding the influence of the molar ratio in L-menthol: C8 acid and C8 acid: C10 alcohol HDES, increasing the ratio of C8 acid from (1:1) to (1:2) and from (1:1) to (2:1) resulted in higher log ($K_{OFX}$) values, specifically an increase from 2.04 to 2.36 for L-menthol: C8 acid and from 1.73 to 2.91 for C8 acid: C10 alcohol. In the case of fatty acid: fatty acid-HDES, an increase in the ratio of fatty acid ether in HBA or HBD, in particular (1:2) or (2:1), resulted in higher log ($K_{OFX}$) values compared to the molar ratio (1:1). This observation can be explained by the fact that an increase in the molar ratio of the fatty acid promotes the formation of hydrogen bonds between the hydroxyl groups of OFX and the carboxyl group of the fatty acid [21]. These results show that the intermolecular interactions are strongly influenced by both the length of the alkyl chain and the molar ratio of the HDES components.

In addition to the COSMO-RS, radial distribution function (RDF) also was applied to gain some more insights into the separation of OFX using HDES-based LLE. This tool uses a graphical representation to establish a correlation between the distance 'r' and g (r), where 'r' stands for the distance between molecules and neighboring atoms, while g (r) indicates the tendency of different atoms to interact. Strong intermolecular interactions are indicated by higher 'g (r)' values at smaller distances ('r'), which can improve extraction [40,41]. RDF analysis was performed for five HDES using Material Studios 2017 software. Specifically, one HDES (and the respective composition) within each promising family, L-menthol:C10 acid (1:2), C10 acid:C12 acid (2:1) and C10 acid:C10 alcohol (2:1), were evaluated to assess the effect of specific components. L-

menthol:C10 acid (2:1) and C8 acid:C10 acid (2:1) were also investigated to determine the influence of the molar ratio and alkyl chain length, respectively. The results in Table 3.2 and Figures A.2 to A.6 in Appendix B show the peak values and the corresponding distances for each HDES. Further details on the methodology can be found in Appendix B.

**Table 3.2.** Radial distribution function (RDF) between HDES and OFX.

| ***HDES*** | ***Molar ratio (HBA:HBD)*** | ***g (r)*** | ***r (Å)*** |
|---|---|---|---|
| L-menthol:C10 acid | (1:2) | 0.016024 | 1.09 |
| L-menthol:C10 acid | (2:1) | 0.013223 | 1.09 |
| C8 acid:C10 acid | (2:1) | 0.01587 | 1.09 |
| C10 acid:C12 acid | (2:1) | 0.01926 | 1.09 |
| C10 acid:C10 alcohol | (2:1) | 0.016178 | 1.09 |

The results show an 'r' distance of 1.09 Å for all HDES, indicating a uniform spatial distribution of OFX molecules relative to the HDES. This small value of 'r' suggests a strong interaction between HDES and OFX, likely due to hydrogen bonding between functional groups [21]. Different g (r) values for each HDES indicate different affinities for OFX due to different chemical properties. For example, increasing C10 acid molar ratio in L-menthol:C10 acid resulted in increased interaction with OFX, as indicated by higher g (r) values. A similar trend was observed with increasing alkyl chain length in fatty acids (from C8 to C12 in C8 acid: C10 acid and C10 acid: C12 acid). Furthermore, HDES compositions such as L-menthol:C10 acid (1:2), C10 acid:C12 acid (2:1) and C10 acid:C10 alcohol (2:1) exhibited higher g (r) values, indicating improved extraction potential, with slightly better interaction observed with C10 acid:C12 acid HDES. These findings are consistent with the COSMO results.

In summary, the COSMO-RS predictions indicate that the most promising HDES for the extraction of OFX are those composed of fatty acids with a higher molar ratio of fatty acids and longer alkyl chains, although a balance between the molar ratio and the size of the alkyl chain is required. These results were supported also by RDF. As result, the most effective HDES for the experimental extraction of OFX from water were selected from three families: L-menthol: fatty acid (L-menthol: C8 acid (1:2), L-menthol: C10 acid (1:2), L-menthol: C12 acid (1:2)), fatty acid: fatty acid (C8 acid: C10

acid (2:1), C8 acid: C12 acid (2:1), C10 acid: C12 acid (2:1)) and fatty acid: fatty alcohol (C8 acid: C10 alcohol (2:1), C10 acid: C10 alcohol (2:1)).

### 3.4.2. Liquid-Liquid Extraction (LLE)

To further evaluate the suitability of the selected HDES for the extraction of OFX, the partition coefficient and extraction efficiency of OFX were determined experimentally. Although L-menthol: C12 acid (1:2) HDES in the L-menthol: fatty acid families showed promising results in the extraction of OFX in COSMO-RS, this HDES was not selected for further investigation because it is solid at room temperature. In addition, in order to explore a little more the impact of higher molar ratios of fatty acids, novel molar ratios were studied for the most promising HDES within each family, *i.e.*, L-menthol: C10 acid (1:3), C10 acid: C12 acid (3:1), and C10 acid: C10 alcohol (3:1).

The chemical and physical properties of the HDES used in this study have been previously investigated [32]. Fourier transform infrared spectroscopy (FTIR) confirmed the presence of hydrogen bonding in the HDES, even in the presence of water. In addition, the evaluation of water activity showed that HDES with longer alkyl chains have higher water stability. The evaluation of thermophysical properties showed that the hydrophobic nature significantly affects the viscosity and density, with HDES with longer alkyl chains having higher values. These results emphasize the water stability of HDES, which is crucial for the development of efficient, environmentally friendly water-based separation processes. In addition, the melting points of these HDES, as indicated in Table B.3 in Appendix B, are well below our operating temperature of 25 ºC, which is important to ensure that the solvents remain in a liquid state under the experimental conditions.

All experiments were performed at constant OFX concentration (1 mg/ml), at 25 °C and HDES-water ratio (1:1, v/v) as described in section 3.3.3, and without adjusting the pH of the systems. The results of the partition coefficient and extraction efficiency of OFX, along with the initial pH of each system are shown in Figure 3.4, and Table B.8 in Appendix B.

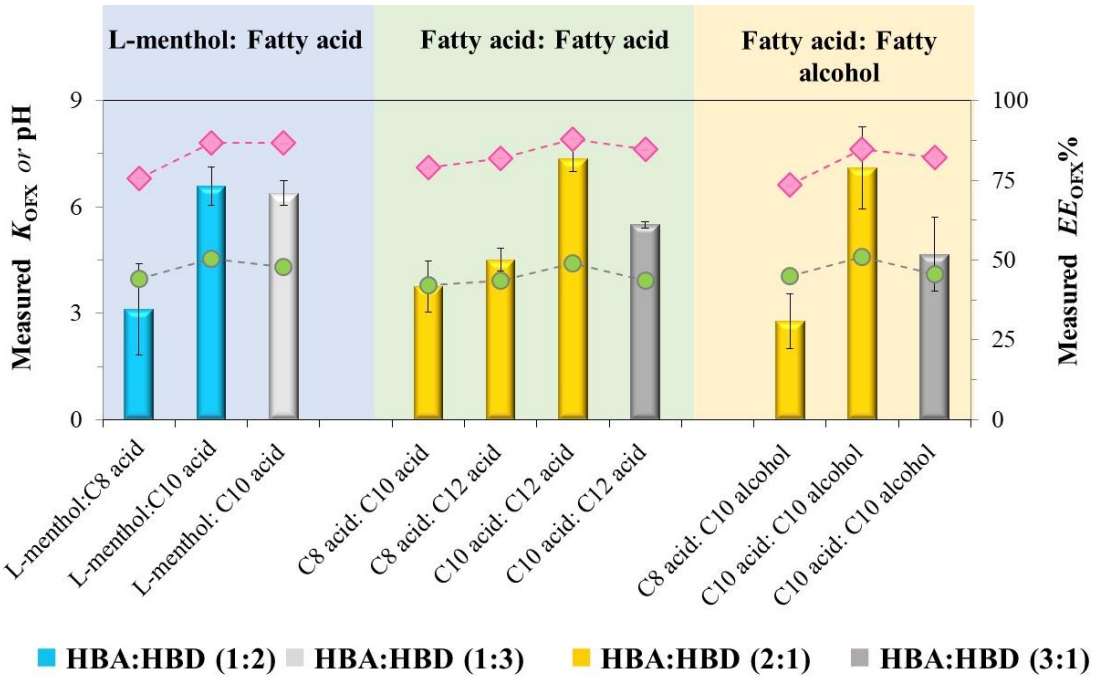


**Figure 3.4.** The measured partition coefficient (bars), extraction efficiency (diamonds) of OFX and pH (circles) for the selected HDES at 25 °C.

As expected, the experimental results presented in Figure 4 show a significant influence of the alkyl chain length on the partition coefficient of OFX, which varies between (2.8 ± 0.1) and (7.4 ± 0.2). The same is true for the extraction efficiency of OFX, although this effect is not so impressive (ranging between (73.5 ± 0.8)% and (88. 02 ± 0.4)%). These effects are particularly pronounced for the HDES based on C10 acid. The increase in chain length from C8 to C10, for example for C8 acid: C12 acid to C10 acid: C12 acid, increases the $K_{OFX}$ by over 63% and the $EE_{OFX}$ by 11%. This trend applies to all HDES that change from C8 to C10. The changes become less pronounced as the chain length increases further from C10 to C12 (e.g. C8 acid: C10 acid to C8 acid: C12 acid), with an increase of about 20% for $K_{OFX}$ and 4% for $EE_{OFX}$. This could be related to the pH effect, as the pH increases more with increasing alkyl chain length from C8 to C10 (e.g. fatty acid: fatty acid from 3.92 to 4.40) compared to C10 to C12 (e.g. from 3.80 to 3.92), with higher pH values leading to higher efficiency in the extraction of OFX. These results emphasize the influence of structure and pH on OFX extraction, with the alkyl chain length having the greatest impact. However, they also highlight the role of pH in extraction processes. A more detailed study on the pH effect is carried out in the following section.

Additionally, Figure 3.4 shows a decrease in the partition coefficient and in the extraction efficiency of OFX within the three different HDES families when the molar ratio of C10 acid increases from 2 to 3, especially for C10 acid: C12 acid (3:1) and C10 acid: C10 alcohol (3:1). This trend can be attributed to the increase in the molar ratio of C10 acid, which likely increases the intermolecular interactions, including hydrogen bonds, van der Waals forces, and electrostatic forces between the HDES constituents, thereby decreasing the interactions between the HDES and the analytes and affecting the overall extraction efficiency [42]. These results emphasize that while the length of the alkyl chain is a critical factor for the interaction between the compounds, the molar ratio of HBA to HBD is equally important.

The evaluation of both the predicted and measured results show how important it is to consider key factors such as the nature of the compounds and their molar ratio when developing solvents for the extraction of compounds. Another important point to emphasize is that the COSMO-RS simulations reproduce the experimental results at certain pH values corresponding to the neutral form of the drugs. Thus, pH is another critical factor to consider. Our experiments were conducted without pH control, with the pH levels of our systems falling within the range of 3.3 to 4.6 (see Figure 3.4 and Table B.8 in Appendix B). Given that the p$K_{a1}$ and p$K_{a2}$ values for OFX are 5.2 and 8.4, respectively (see Figure B.7 in Appendix B for further details), the extractions predominantly occurred with 98% to 70% of the molecule in its positive form, with only a small fraction remaining in the zwitterionic (neutral) form. Thus, these differences between computational and experimental results may be attributed, in part, to this pH-related phenomenon.

In summary, L-menthol:C10 acid (1:2), C10 acid:C10 alcohol (2:1), and C10 acid:C12 acid (2:1) were similar in terms of their efficiency in extracting OFX, with the latter performing slightly better. When selecting the best HDES to optimize OFX extraction conditions, it is important to consider not only efficiency but also solvent stability and cost. When comparing L-menthol:C10 acid (1:2) with the HDES C10 acid:C10 alcohol and C10 acid:C12 acid (2:1), L-menthol:C10 acid is more expensive due to the higher cost of L-menthol, while C10 acid:C12 acid is slightly cheaper than C10 acid:C10 alcohol. Further details on the prices of the compounds can be found in Table B.9 in Appendix B. Additionally, C10 acid:C12 acid (2:1) exhibited greater stability in water [32] and lower solubility in water [37,43] - crucial factors to consider in a water extraction process. Furthermore, it was known that the hydroxyl group (–OH) can

undergo esterification reactions with carboxylic acids (–COOH) to form ester bonds [17,44]. This degradation process does not take place when only carboxylic acids are present. Therefore, the C10 acid:C12 acid (2:1) was selected as the HDES for the optimization of operating variables in OFX extraction.

### 3.4.3. Optimization of the operating extractions conditions

A RSM was applied to optimize the operating conditions to maximize the extraction of OFX. This method establishes a statistical correlation between the independent variables (pH, OFX concentration ($C_{OFX}$) and HDES-water ratio (v/v)), and the response, i.e., the extraction efficiency of OFX ($EE_{OFX}$ %). In addition, previous evaluations of different molar ratios of the selected HDES, namely C10 acid to C12 acid (1:2, 1:1, 2:1, 3:1), showed that the 2:1 ratio was the most effective for OFX extraction. Therefore, this ratio was chosen for the RSM experiments. Details of the extraction efficiency measurements for OFX and statistical analyzes can be found in Appendix B (Tables B.10-B.12, Figures B.8-B.10) and the respective data are depicted in Figure 3.5. The statistical significance of the variables and their interactions was assessed using an analysis of variance (ANOVA). The results were subjected to a statistical analysis with a confidence level 95%. The value of $R^2_{adj}$ obtained for the model was 0.89, indicating a strong correlation between the experimental and calculated responses. This supports the effectiveness of the developed statistical models in providing a reliable and accurate description of the experimental results.

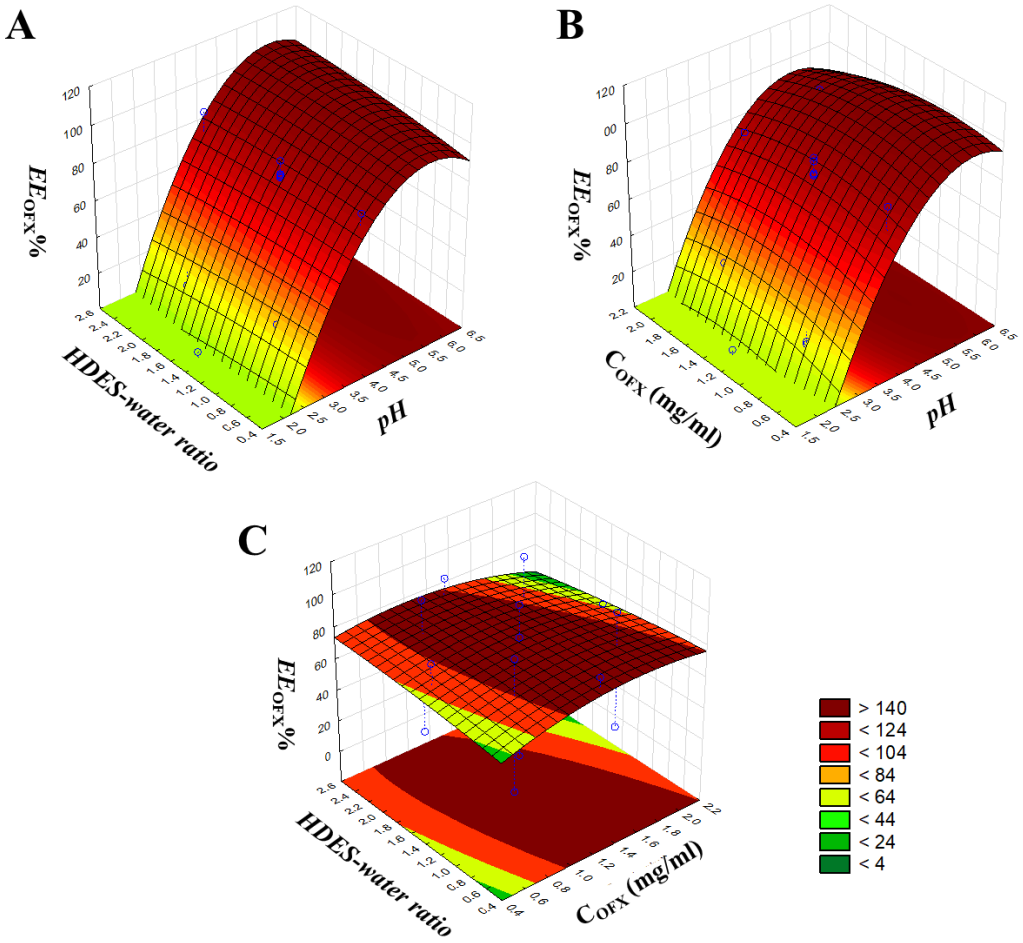


**Figure 3.5.** Surface plots of the extraction efficiency of OFX using C10 acid: C12 acid (2:1) with the combined effects: (**A**) HDES-water ratio (V/V) and pH, (**B**) pH and OFX concentration (mg/ml), and (**C**) HDES-water ratio (V/V) and OFX concentration.

All three variables (pH, OFX concentration, and HDES-water ratio) were found to be significant, and their statistically significant effects follow this order: pH >> $pH^2$ > HDES-water $ratio^2 \geq$ pH x $C_{OFX}$, ≈ $C_{OFX}$ x HDES-water ratio ≈ pH x HDES-water ratio ≈ HDES-water ratio≈ $C_{OFX}$, (Figure B.8 in Appendix B).

Regarding the influence of pH, the ANOVA results and the Pareto chart (Table B.11 and Figure B.8 in Appendix B) show that it has a significant influence on the response and outperforms the other variables. The crucial role of pH in OFX extraction is mainly due to the fact that OFX is amphiprotic and has pH-dependent factors such as ionization, polarity and water solubility [45]. Keeping the pH of the solution below the p$K_a$ of the analyte improves its distribution in the organic phase [46], which justifies the choice of a pH range from 2.0 to 6.0 for this study. Since the quadratic effect of pH is the most

significant variable and has a negative influence on the response, this means that there is a maximum pH value that leads to optimal extraction efficiency. Our results show that the optimal extraction efficiency for OFX is at a pH of 5-6. This is in agreement with the results of Pochivalov et al. [21], who observed a lower extraction efficiency for fluoroquinolones below pH 5, and Horstkotte and co-workers [45], who found a slight improvement in fluoroquinolone extraction at pH 5-7. Mohammad et al. [47] also reported that OFX extraction is highest at pH 6 and decreases at higher pH values. This improvement in extraction efficiency is attributed to the fact that the molecule changes from a monocharged form to a zwitterionic form in this pH range (OFX p$K_{a1}$ = 5.2 and p$K_{a2}$ = 8.4, see Figure B.7 in Appendix B). The low water solubility of the zwitterionic form (pH 5 to 6) facilitates efficient mass transfer into the HDES phase [45], resulting in improved extraction efficiency.

Regarding the HDES-water ratio variable, while it is statistically significant, its influence on the response is minimal (see Figure B.8 in Appendix B). The quadratic effect, which is the most significant factor, has a negative influence, suggesting that the efficiency of OFX extraction increases with an increase in the HDES-water ratio (i.e., an increase in HDES volume) and optimal performance is achieved at a threshold of 1.3 (corresponding to a ratio of 13:10), as shown in Figure B.10 in Appendix B. Beyond this threshold, an excess of extraction solvent – corresponding to a higher solid-liquid ratio – can have a negative effect on the overall extraction efficiency, which is consistent with the results of previous studies [46,48].

Although the OFX concentration was statistically significant, its effect on the response was minimal, similar to that of the HDES-water ratio, as shown by the analysis of variance (ANOVA). Figure 3.5C shows that a decrease in the initial concentration of OFX is accompanied by a slight decrease in extraction yield. This tendency could be due to the lower driving force and distribution of the drug at lower concentrations, resulting in a lower extraction of OFX [39].

Analyzing the surface plots reported Figure 3.5, the optimal operating conditions using HDES C10 acid and C12 acid (2:1) for the extraction efficiency of OFX were as follows: an OFX concentration of 2.5 mg/ml, an HDES-water ratio of 1.3, and a pH of 6 (Figure B.10 in Appendix B). However, it should be noted that a pH of 5.2 was used to prevent the formation of a precipitate at the interface between the two phases. Under these optimized extraction conditions, an average extraction efficiency of (98.8 ± 0.9)% was achieved for OFX, compared to the predicted value of 103% obtained from

multiple regression using RSM analysis, resulting in a relative error of 4%. It should be noted that, under these conditions, a partition coefficient of (65 ± 1) was obtained. The close agreement between the experimental and predicted results confirms the validation of the model with a confidence interval of 95%. Furthermore, Figure B.10 in Appendix B alongside with Figure 3.5 shows that a reduction in the HES-water ratio has no significant effect on extraction efficiency, which emphasizes the minor role of this variable in the extraction process. In particular, when the HDES-water ratio is reduced from 1.3 (13:10) to 0.54 (6:10, the lowest evaluated ratio), the predicted extraction efficiency remains constant at 103 % (see Figure B.10 in Appendix B). Therefore, optimal OFX extraction can be achieved even with a lower amount of HDES, bringing significant economic and industrial benefits by minimizing material costs and waste without compromising efficiency. This aspect is particularly important from an economic and industrial perspective, as it offers a more sustainable and cost-effective approach to OFX extraction.

A comparison of the OFX extraction method developed in this work with previous approaches can be found in Table 3.3 Both solid-phase SPE and IL-based aqueous biphasic system (IL-ABS, a type of LLE) showed lower OFX extraction efficiency compared to HDES-based LLE. On the other hand, adsorption and advanced oxidation methods show remarkable efficiency in the extraction of OFX, however, it is difficult to transfer these methods from laboratory scale to large scale and reduce the operating costs. Furthermore, these processes require the use of compounds such as bases and acids, leading to concerns about the environmental impact of these technologies [5]. Although LLME, based on the traditional organic solvents or HDES, has high extraction efficiency for OFX extraction (see Table 3.3), it is not the best technique for processing larger sample volumes, as is the case for wastewater. In addition, equipment designed for lab-scale LLME may not scale seamlessly for industrial use and requires customized solutions to ensure efficiency and consistency [22].

Another important point to consider with solvent-based processes such as LLE, LLME and ABS is the cost of the solvent. Solvents used in our approach and in the literature include ILs (e.g. 1-ethyl-3-methylimidazolium trifluoromethanesulfonate), HDES (consisting of thymol: heptanoic acid, thymol: nonanoic acid, and C10 acid:C12 acid), and an organic solvent (tetrachloroethane) used in ABS, LLME, and LLE, as presented in this study. An estimate of the prices of these solvents and components for laboratory and industrial use can be found in Table B.9 in Appendix B.

**Table 3.3.** Comparison of the present method with previous approaches for extraction of OFX from water samples.

| Extraction method | Absorbent/ catalyst/ solvent | Extraction conditions | Water source | $EE_{OFX}$ (%) | Ref. |
|---|---|---|---|---|---|
| Adsorption | N-doped activated carbon | Adsorbent content = 0.2 g/l, [OFX] = 0.2 mg/ml, pH = 8, T = 40 ºC | Medical wastewater. | 98.3 | [49] |
| | Hydroxyapatite/activated carbon | Adsorbent content = 0.5 g/l, [OFX] = 0.02 mg/ml, pH= 7, T = 50 ºC | Synthetic solution | 99.2 | [50] |
| Solid-phase extraction (SPE) | Oasis HLB cartridges | Oasis HLB cartridge (6 ml, 200 mg), [OFX] = $3.1\times10^{-6}$ mg/ml, room temperature | Sewage treatment plant | 85 | [51] |
| | Oasis HLB cartridges | Oasis HLB cartridges (6 ml, 500 mg), [OFX] = $41\times10^{-11}$ mg/ml, pH=3, room temperature | Piggery wastewater | 90.7 | [52] |
| Advanced oxidation process | Neutral photo-fenton | $[Fe^{2+}]$ = 5 mg/l, $[H_2O_2]$ = 50 mg/l, $UV_{254}$, [OFX] = $4.1\times10^{-8}$ mg /ml, pH=7.4, T = 17 ºC | Domestic wastewater effluent | 100 | [53] |
| | Heterogeneous photo-Fenton | Fe-Mn oxides ratio of 8:3 (wt) = 5 mg/l, $[H_2O_2]$ = 0.14 mg/l, $UV_{288}$, [OFX] = 0.03 mg/ml, pH=6.8, T = 20 ºC | Synthetic solution | 98.1 | [54] |
| Liquid-liquid microextraction (LLME) | Thymol: Heptanoic acid (2:1) | HDES volume = 150 µL; sample solution volume = 10 mL, [OFX] = $6\times10^{-7}$ mg/ml, pH = 6 | Reservoir water<br>Pond water<br>Tap water recovery | 90-93<br>86-102<br>85-104 | [20] |
| | Thymol: Nonanoic acid (1:1) | HDES volume = 100 µL, sample solution volume = 2 ml, [OFX] = $0.1\times10^{-1}$ mg/ml, pH = 6 | River water<br>Lake water | 96-99<br>92-99 | [21] |
| | Tetrachloroethane | Tetrachloroethane volume =110 µl sample solution volume = 8.0 ml; methanol volume = 0.5 ml, [OFX] = 0.2 mg/ml, pH = 8.0 | Pharmaceutical wastewater | 83-102 | [54] |
| Liquid-liquid extraction (LLE) | C10 acid:C12 acid (2:1) | HDES-water ratio = 1.3, [OFX] = 2.5 mg/ml, pH = 5.2, T = 25 ºC | Synthetic solution | 98.8 ± 0.9 | This work |
| Aqueous biphasic system (ABS) | 1-ethyl-3-methylimidazolium trifluoromethanesulfonate | ABS composition: aluminum sulfate =15 wt.%, IL= 42 wt.%, [OFX] = 0.05 mg/ml, pH = 7.2, T = 25 ºC | Synthetic solution | 91.4 | [55] |

The IL is significantly more expensive than the other solvents. The organic solvent (tetrachloroethane) is less expensive than the HDES components, but its toxicity is

higher. However, the low toxicity of HDES should not be generalized and is discussed in more detail in the next section. Considering only the HDES, the thymol-based HDES are significantly more expensive than the fatty acid-based HDES, which is due to the cost of thymol.

Considering all these factors, LLE based on fatty acid-based HDES emerges as the most interesting approach due to its efficiency, simplicity, scalability and the economic advantage of using a more environmentally friendly solvent [15,56].

#### *3.4.3.1. Discussion*

For the development of an efficient and sustainable extraction process it is crucial to consider the saturation of the solvent, its recyclability (including regeneration and reuse) and its stability throughout the process. While these aspects were not directly investigated in our study, valuable insights can be gained from Florindo et al. [37]. They investigated the performance of the same HDES composition (C10 acid: C12 acid in a 1:2 molar ratio) over several cycles in the extraction of ciprofloxacin, a fluoroquinolone like OFX, by LLE and evaluated its recyclability. The results showed that HDES remained effective for up to four cycles before extraction efficiency decreased from the fifth cycle onwards, indicating saturation of HDES. Florindo et al. [37] used activated carbon to recover HDES in their approach and showed that it can be reused without loss of extraction efficiency. Crucially, they confirmed the properties of HDES after the recovery process with activated carbon and before reuse by $^{1}$H NMR analysis and found that its properties remained unchanged. These results highlight the potential of C10 acid: C12 acid (1:2) HDES for use in multiple extraction cycles prior to saturation, while emphasizing its reusability and stability during extraction and recovery processes. These results are of particular importance for our extraction process, as they demonstrate the stability of our solvent and the possibility of reusing HDES within our framework, thus making an important contribution to the efficiency and sustainability of our process.

Despite the advantages of HDES in extraction, another important is its toxicity. Only one study evaluated the effects of fatty acid-based HDES, including C10 acid: C8 acid, C10 acid: C12 acid, and C10 acid: tetradecanoic acid. Silva et al. [57] showed that fatty acid-based HDES inhibited the growth of the yeast *C. albicans*. However, the results varied depending on the toxicity test used, including minimum inhibitory concentration/minimum inhibitory fungal (MIC/MFC) and diffusion disk. Given the

limited research available, analyzing the C10 and C12 acids in HDES could offer a viable option for gaining insight into the toxicity of HDES, as these acids belong to the same family and have comparable alkyl chain lengths. In this line, an analysis of its individual components, shows that despite their cytotoxicity at high doses, these medium-chain fatty acids are generally considered to have low toxicity at suitable levels [58,59]. In addition, both acids are considered to have low toxicity at appropriate concentrations and are deemed safe by regulatory agencies such as the Food and Drug Administration (FDA) [60]. They are widely used in various industries, from perfumes to food additives. However, caution is advised due to potential skin, eye irritation, and gastrointestinal issues at high doses. While compliance with FDA regulations on C10 and C12 acids may mitigate the problem of HDES contamination of drugs, ideally, the active pharmaceutical ingredients should be free of any contamination.

Another crucial aspect to consider is the toxicity of HDES in the environment, known as ecotoxicity, particularly concerning aquatic ecosystems, considering the extraction process here developed. Unfortunately, no ecotoxicity tests were carried out for our HDES. However, employing the same rationale as previously mentioned, analyzing its individual components suggests that both acids may present a potential risk to aquatic life because they degrade slowly in water [61,62]. It is crucial to handle and dispose of C10 and C12 acids properly to minimize their adverse effects on the environment. Nevertheless, it is worth mentioning that Florindo et al. [37] highlighted that among the studied HDES variants, this one resulted in lower water contamination due to its lower water solubility (2 wt%), which is positive from an environmental sustainability point of view.

In summary, our results highlight the critical importance of optimizing operating conditions, including pH, solvent choice and concentration, to improve the efficiency of extraction processes. Achieving an extraction efficiency of 98.8% ± 0.9 for OFX using HDES-based LLE represents a remarkable advance in wastewater treatment, as it significantly mitigates pharmaceutical contamination of wastewater and thus contributes to address the issue of antibiotic resistance in aquatic ecosystems. Among the tested HDES, C10 acid: C12 ratio (1:2) emerged as the optimal choice for one-step OFX extraction due to its efficacy, water stability, cost-effectiveness and environmental friendliness. However, to fully realize the potential of HDES in industrial applications such as wastewater treatment, comprehensive assessments of their cost-effectiveness, environmental benefits and impact on human and animal health are required.

## 3.5. Conclusions

The development of LLE processes based on HDES has been shown to be effective in improving the efficiency of separation. For that reason, HDES were here used for the removal of OFX from water. To the best of our knowledge, this is the first work on the use of HDES-based LLE for the extraction of OFX, coupled with the application of COSMO-RS for an initial rapid and qualitative screening to identify promising HDES for OFX extraction from twelve HDES at three different molar ratios. Both computational experiments and subsequent experimental tests confirmed that a high molar ratio of fatty acids combined with an increase in their alkyl chain length significantly improved the partition coefficient of OFX, with decanoic acid: dodecanoic acid (2:1), L-menthol: decanoic acid (1:2), and decanoic acid: decanoic alcohol (2:1), being the most favorable extraction solvents. An experimental design was also applied to study keys factors in the extraction process, using decanoic acid: dodecanoic acid (2:1) as solvent. It was found that pH played a crucial role in the efficiency of OFX extraction, while the ratio OFX concentration had a minor influence. The optimal conditions determined were: an OFX concentration of 2.5 mg/ml, a pH of 5.2 and a HDES-water ratio of 1.3, resulting in OFX an OFX extraction efficiency of (98.8 ± 0.9)%. These results highlight the importance of carefully selecting appropriate solvents and establishing critical parameters of extraction to significantly improve the efficiency of the extraction processes. This work not only addresses the removal of OFX as a micropollutant in water streams, but may also be of interest to the pharmaceutical industry, which needs to treat its wastewater prior to discharge.

## 3.6. References

[1] T. Rasheed, M. Bilal, F. Nabeel, M. Adeel, H.M.N. Iqbal, Environmentally-related contaminants of high concern: Potential sources and analytical modalities for detection, quantification, and treatment, Environ Int 122 (2019) 52–66.

[2] M. Paut Kusturica, M. Jevtic, J.T. Ristovski, Minimizing the environmental impact of unused pharmaceuticals: Review focused on prevention, Front Environ Sci 10 (2022).

[3] S. Bhatt, S. Chatterjee, Fluoroquinolone antibiotics: Occurrence, mode of action, resistance, environmental detection, and remediation – A comprehensive review, Environmental Pollution 315 (2022) 120440.

[4] P. de Voogt, M.-L. Janex-Habibi, F. Sacher, L. Puijker, M. Mons, Development of a common priority list of pharmaceuticals relevant for the water cycle, Water Science and Technology 59 (2009) 39–46.

[5] J. Georgin, D.S.P. Franco, C.G. Ramos, D.G.A. Piccilli, E.C. Lima, F. Sher, A review of the antibiotic ofloxacin: Current status of ecotoxicology and scientific advances in its removal from aqueous systems by adsorption technology, Chemical Engineering Research and Design 193 (2023) 99–120.

[6] Y.-Z. Ouyang, H.-L. Wu, H. Fang, T. Wang, X.-D. Sun, Y.-Y. Chang, Y.-J. Ding, R.-Q. Yu, Rapid and simultaneous determination of three fluoroquinolones in animal-derived foods using excitation-emission matrix fluorescence coupled with second-order calibration method, Spectrochim Acta A Mol Biomol Spectrosc 224 (2020) 117458.

[7] M. Feng, Z. Wang, D.D. Dionysiou, V.K. Sharma, Metal-mediated oxidation of fluoroquinolone antibiotics in water: A review on kinetics, transformation products, and toxicity assessment, J Hazard Mater 344 (2018) 1136–1154.

[8] H. Abd El-Fattah, A. Maged, R. Kamel, S. Kharbish, Recent Technologies for The Elimination of Pharmaceutical Compounds from aqueous solutions: A review, Frontiers in Scientific Research and Technology 5 (2023) 0–0.

[9] OECD (Organisation for Economic Co-operation and Development), Pharmaceutical Residues in Freshwater Hazards and Policy Responses Pharmaceutical Residues in Freshwater Hazards and Policy Responses Contents, 2019.

[10] I. Michael, L. Rizzo, C.S. McArdell, C.M. Manaia, C. Merlin, T. Schwartz, C. Dagot, D. Fatta-Kassinos, Urban wastewater treatment plants as hotspots for the release of antibiotics in the environment: A review, Water Res 47 (2013) 957–995.

[11] J. Georgin, D.S.P. Franco, C.G. Ramos, D.G.A. Piccilli, E.C. Lima, F. Sher, A review of the antibiotic ofloxacin: Current status of ecotoxicology and scientific advances in its removal from aqueous systems by adsorption technology, Chemical Engineering Research and Design 193 (2023) 99–120.

[12] C. Kim, H.-D. Ryu, E.G. Chung, Y. Kim, J. Lee, A review of analytical procedures for the simultaneous determination of medically important veterinary antibiotics in environmental water: Sample preparation, liquid chromatography, and mass spectrometry, J Environ Manage 217 (2018) 629–645.

[13] V. Andruch, A. Kalyniukova, J. Płotka-Wasylka, N. Jatkowska, D. Snigur, S. Zaruba, J. Płatkiewicz, A. Zgoła-Grześkowiak, J. Werner, Application of deep eutectic solvents in

analytical sample pretreatment (update 2017–2022). Part A: Liquid phase microextraction, Microchemical Journal 189 (2023) 108509.

[14] M.S. de Ilurdoz, J.J. Sadhwani, J.V. Reboso, Antibiotic removal processes from water & wastewater for the protection of the aquatic environment - a review, Journal of Water Process Engineering 45 (2022) 102474.

[15] M.M. Khataei, S.B.H. Epi, R. Lood, P. Spégel, Y. Yamini, C. Turner, A review of green solvent extraction techniques and their use in antibiotic residue analysis, J Pharm Biomed Anal 209 (2022) 114487.

[16] W. Tang, Y. An, K.H. Row, Emerging applications of (micro) extraction phase from hydrophilic to hydrophobic deep eutectic solvents: opportunities and trends, TrAC Trends in Analytical Chemistry 136 (2021) 116187.

[17] D.O. Abranches, J.A.P. Coutinho, Everything You Wanted to Know about Deep Eutectic Solvents but Were Afraid to Be Told, Annu Rev Chem Biomol Eng 14 (2023) 141–163.

[18] M. Marchel, M.P. Rayaroth, C. Wang, L. Kong, J.A. Khan, G. Boczkaj, Hydrophobic (deep) eutectic solvents (HDESs) as extractants for removal of pollutants from water and wastewater – A review, Chemical Engineering Journal 475 (2023) 144971.

[19] P.-A. Cablé, Y. Le Brech, F. Mutelet, Liquid-liquid extraction of phenolic compounds from aqueous solution using hydrophobic deep eutectic solvents, J Mol Liq 366 (2022) 120266.

[20] K. Li, Y. Jin, D. Jung, K. Park, H. Kim, J. Lee, In situ formation of thymol-based hydrophobic deep eutectic solvents: Application to antibiotics analysis in surface water based on liquid-liquid microextraction followed by liquid chromatography, J Chromatogr A 1614 (2020) 460730.

[21] A. Pochivalov, K. Cherkashina, A. Sudarkin, M. Osmolowsky, O. Osmolovskaya, F. Krekhova, L. Nugbienyo, A. Bulatov, Liquid-liquid microextraction with hydrophobic deep eutectic solvent followed by magnetic phase separation for preconcentration of antibiotics, Talanta 252 (2023) 123868.

[22] G. Li, K.H. Row, Utilization of deep eutectic solvents in dispersive liquid-liquid micro-extraction, TrAC Trends in Analytical Chemistry 120 (2019) 115651.

[23] A. Klamt, F. Eckert, W. Arlt, COSMO-RS: An Alternative to Simulation for Calculating Thermodynamic Properties of Liquid Mixtures, Annu Rev Chem Biomol Eng 1 (2010) 101–122.

[24] D. van der Spoel, S. Manzetti, H. Zhang, A. Klamt, Prediction of Partition Coefficients of Environmental Toxins Using Computational Chemistry Methods, ACS Omega 4 (2019) 13772–13781.

[25] C. Loschen, J. Reinisch, A. Klamt, COSMO-RS based predictions for the SAMPL6 logP challenge, J Comput Aided Mol Des 34 (2020) 385–392.

[26] A.C. Spieß, W. Eberhard, M. Peters, M.F. Eckstein, L. Greiner, J. Büchs, Prediction of partition coefficients using COSMO-RS: Solvent screening for maximum conversion in biocatalytic two-phase reaction systems, Chemical Engineering and Processing: Process Intensification 47 (2008) 1034–1041.

[27] B. Burghoff, E.L. V Goetheer, A.B. de Haan, COSMO-RS-Based Extractant Screening for Phenol Extraction As Model System, Ind Eng Chem Res 47 (2008) 4263–4269.

[28] S.M. Vilas-Boas, I.W. Cordova, K.A. Kurnia, H.H.S. Almeida, P.S. Gaschi, J.A.P. Coutinho, S.P. Pinho, O. Ferreira, Comparison of two computational methods for solvent screening in countercurrent and centrifugal partition chromatography, J Chromatogr A 1666 (2022) 462859.

[29] J.-B. Chagnoleau, N. Papaiconomou, M. Jamali, D.O. Abranches, J.A.P. Coutinho, X. Fernandez, T. Michel, Toward a Critical Evaluation of DES-Based Organic Biphasic Systems: Are Deep Eutectic Solvents so Critical?, ACS Sustain Chem Eng 9 (2021) 9707–9716.

[30] M. Moradi, M. Mohammadian, G. Pazuki, S. Shahriari, Partitioning of Crocin in a Novel Aqueous Two-Phase System Composed of a Deep Eutectic Solvent and Acetonitrile, J Chem Eng Data 67 (2022) 1205–1213.

[31] S.-T. Lin, S.I. Sandler, A Priori Phase Equilibrium Prediction from a Segment Contribution Solvation Model, Ind Eng Chem Res 41 (2002) 899–913.

[32] M. Moradi, G. Pazuki, S. Zarei Mahmoudabadi, A comprehensive study of the water stability of eutectic solvents using COSMO-SAC, J Mol Liq 387 (2023) 122605.

[33] C. Loschen, A. Klamt, Prediction of Solubilities and Partition Coefficients in Polymers Using COSMO-RS, Ind Eng Chem Res 53 (2014) 11478–11487.

[34] I. Adeyemi, R. Sulaiman, M. Almazroui, A. Al-Hammadi, I.M. AlNashef, Removal of chlorophenols from aqueous media with hydrophobic deep eutectic solvents: Experimental study and COSMO RS evaluation, J Mol Liq 311 (2020) 113180.

[35] I. Timofeeva, K. Stepanova, A. Shishov, L. Nugbienyo, L. Moskvin, A. Bulatov, Fluoroquinolones extraction from meat samples based on deep eutectic solvent formation, Journal of Food Composition and Analysis 93 (2020) 103589.

[36] D.O. Abranches, J.A.P. Coutinho, Type V deep eutectic solvents: Design and applications, Curr Opin Green Sustain Chem 35 (2022) 100612.

[37] C. Florindo, F. Lima, L.C. Branco, I.M. Marrucho, Hydrophobic Deep Eutectic Solvents: A Circular Approach to Purify Water Contaminated with Ciprofloxacin, ACS Sustain Chem Eng 7 (2019) 14739–14746.

[38] C. Chen, Y. Cao, A. Ali, S. Toufouki, S. Yao, How to apply terpenoid-based deep eutectic solvents for removal of antibiotics and dyes from water: Theoretical prediction, experimental validation and quantum chemical evaluation, Environ Res 231 (2023) 116180.

[39] D. Rodríguez-Llorente, E. Hernández, P. Gutiérrez-Sánchez, P. Navarro, V. Ismael Águeda, S. Álvarez-Torrellas, J. García, M. Larriba, Extraction of pharmaceuticals from hospital wastewater with eutectic solvents and terpenoids: Computational, experimental, and simulation studies, Chemical Engineering Journal 451 (2023) 138544.

[40] M. Sharif, X. Wu, Y. Yu, T. Zhang, Z. Zhang, Estimation of diffusivity and intermolecular interaction strength of secondary and tertiary amine for CO2 absorption process by molecular dynamic simulation, Mol Simul 48 (2022) 484–494.

[41] Z. Su, Y. Zhang, D. Fan, P. Cui, Z. Zhu, Y. Wang, Liquid-liquid equilibrium experiment and mechanism analysis of menthol-based deep eutectic solvents extraction for separation of fuel additive tert-butanol, Environ Res 218 (2023) 115043.

[42] W. Ma, K.H. Row, pH-induced deep eutectic solvents based homogeneous liquid-liquid microextraction for the extraction of two antibiotics from environmental water, Microchemical Journal 160 (2021) 105642.

[43] C. Florindo, L. Romero, I. Rintoul, L.C. Branco, I.M. Marrucho, From Phase Change Materials to Green Solvents: Hydrophobic Low Viscous Fatty Acid-Based Deep Eutectic Solvents, ACS Sustain Chem Eng 6 (2018) 3888–3895.

[44] N. Rodriguez Rodriguez, A. van den Bruinhorst, L.J.B.M. Kollau, M.C. Kroon, K. Binnemans, Degradation of Deep-Eutectic Solvents Based on Choline Chloride and Carboxylic Acids, ACS Sustain Chem Eng 7 (2019) 11521–11528.

[45] S. Yıldırım, D.J. Cocovi-Solberg, B. Uslu, P. Solich, B. Horstkotte, Lab-In-Syringe automation of deep eutectic solvent-based direct immersion single drop microextraction coupled online to high-performance liquid chromatography for the determination of fluoroquinolones, Talanta 246 (2022) 123476.

[46] T. Gezahegn, B. Tegegne, F. Zewge, B.S. Chandravanshi, Salting-out assisted liquid–liquid extraction for the determination of ciprofloxacin residues in water samples by high performance liquid chromatography–diode array detector, BMC Chem 13 (2019) 28.

[47] R.E.A. Mohammad, A.A. Elbashir, J. Karim, N. Yahaya, N.Y. Rahim, M. Miskam, Development of deep eutectic solvents based ferrofluid for liquid phase microextraction of ofloxacin and sparfloxacin in water samples, Microchemical Journal 181 (2022) 107806.

[48] K. Yu, M.-E. Yue, J. Xu, T.-F. Jiang, Determination of fluoroquinolones in milk, honey and water samples by salting out-assisted dispersive liquid-liquid microextraction based on deep eutectic solvent combined with MECC, Food Chem 332 (2020) 127371.

[49] S. He, Q. Chen, G. Chen, G. Shi, C. Ruan, M. Feng, Y. Ma, X. Jin, X. Liu, C. Du, C. He, H. Dai, C. Cao, N-doped activated carbon for high-efficiency ofloxacin adsorption, Microporous and Mesoporous Materials 335 (2022) 111848.

[50] N. Rueangchai, P. Noisong, S. Sansuk, A facile synthesis of hydroxyapatite and hydroxyapatite/activated carbon composite for paracetamol and ofloxacin removal, Mater Today Commun 34 (2023) 105326.

[51] L. Gao, Y. Shi, W. Li, H. Niu, J. Liu, Y. Cai, Occurrence of antibiotics in eight sewage treatment plants in Beijing, China, Chemosphere 86 (2012) 665–671.

[52] J. Chen, Y.-S. Liu, J.-N. Zhang, Y.-Q. Yang, L.-X. Hu, Y.-Y. Yang, J.-L. Zhao, F.-R. Chen, G.-G. Ying, Removal of antibiotics from piggery wastewater by biological aerated filter system: Treatment efficiency and biodegradation kinetics, Bioresour Technol 238 (2017) 70–77.

[53] N. De la Cruz, J. Giménez, S. Esplugas, D. Grandjean, L.F. de Alencastro, C. Pulgarín, Degradation of 32 emergent contaminants by UV and neutral photo-fenton in domestic wastewater effluent previously treated by activated sludge, Water Res 46 (2012) 1947–1957.

[54] H. Yan, H. Wang, X. Qin, B. Liu, J. Du, Ultrasound-assisted dispersive liquid–liquid microextraction for determination of fluoroquinolones in pharmaceutical wastewater, J Pharm Biomed Anal 54 (2011) 53–57.

[55] H.F.D. Almeida, M.G. Freire, I.M. Marrucho, Improved extraction of fluoroquinolones with recyclable ionic-liquid-based aqueous biphasic systems, Green Chemistry 18 (2016) 2717–2725.

[56] C.M. Chabib, J.K. Ali, M.A. Jaoude, E. Alhseinat, I.A. Adeyemi, I.M. Al Nashef, Application of deep eutectic solvents in water treatment processes: A review, Journal of Water Process Engineering 47 (2022) 102663.

[57] J.M. Silva, E. Silva, R.L. Reis, A.R.C. Duarte, A closer look in the antimicrobial properties of deep eutectic solvents based on fatty acids, Sustain Chem Pharm 14 (2019) 100192.

[58] T. Plötz, A.S. von Hanstein, B. Krümmel, A. Laporte, I. Mehmeti, S. Lenzen, Structure-toxicity relationships of saturated and unsaturated free fatty acids for elucidating the lipotoxic effects in human EndoC-βH1 beta-cells, Biochimica et Biophysica Acta (BBA) - Molecular Basis of Disease 1865 (2019) 165525.

[59] T.M. Lima, C.C. Kanunfre, C. Pompéia, R. Verlengia, R. Curi, Ranking the toxicity of fatty acids on Jurkat and Raji cells by flow cytometric analysis, Toxicology in Vitro 16 (2002) 741–747.

[60] U.S. Food and Drug Administration, Food Additives Permitted for Direct Addition to Food for Human Consumption, Subpart I — Multipurpose Additives, (2023).

[61] European Food Safety Authority, Conclusion on the peer review of the pesticide risk assessment of the active substance Fatty acids C7 to C18 (approved under Regulation (EC) No 1107/2009 as Fatty acids C7 to C20), EFSA Journal 11 (2013) 3023.

[62] K. Boyle, K. Leifer, IIFG Decision documents on reassessment of exemptions from the requirement of a tolerance for fatty acids, Washington, (2002).

# 4. Enantioseparation of ofloxacin using a liquid-liquid extraction system based on hydrophobic deep eutectic solvents*

***Chapter based on the manuscript Accepted:**

Mahtab Moradi, Ana M. Ferreira, Catarina M.S.S. Neves, Filipe H.B. Sosa, Gholamreza Pazuki, João A.P. Coutinho, "Enantioseparation of ofloxacin using liquid-liquid system based on hydrophobic eutectic solvents". Separation and Purification Technology.

## 4.1. Abstract

The enantioseparation of chiral drugs is a major challenge for the pharmaceutical industry as the pharmacological activities of the enantiomers may differ, which can lead to severe secondary effects in the treatment of diseases. The aim of this study is to develop an enantioseparation platform for the resolution of ofloxacin (OFX) using enantioselective liquid-liquid extraction (ELLE) based on a hydrophobic deep eutectic solvent (HDES) in conjunction with one chiral selector. β-Cyclodextrin (β-CD) derivatives, including β-CD, hydroxypropyl-β-cyclodextrin (HP-β-CD), carboxymethyl-β-cyclodextrin sodium salt (CM-β-CD), and sulfated-β-cyclodextrin sodium salt (S-β-CD), were investigated as potential chiral selector for the separation of (R/S-OFX), with CM-β-CD proving to be the most promising. The efficiency of the HDES-based ELLE system was then studied, and a total of fourteen systems were evaluated using HDES from four groups: L-menthol: fatty acid, L-menthol: fatty alcohol, fatty acid: fatty acid, and fatty acid: fatty alcohols. Decanoic acid: dodecanoic acid (C10 acid: C12 acid) in a molar ratio of 2:1 was identified as the optimal HDES-based ELLE system for the enantioseparation of R/S-OFX. This selected system was further used to optimize enantioseparation conditions, including pH, HDES-water ratio (v/v), and excess of chiral selector (CM-β-CD), using response surface methodology (RSM). Under optimal conditions, i.e., pH 3.6, HDES-water ratio (v/v) of 1:2 and a 77-fold molar excess of chiral selector, an OFX selectivity (α) of 3.8 ± 0.3 was achieved in a single-step.

**Keywords:** Enantiomers; chirality; liquid-liquid extraction; deep eutectic solvents; cyclodextrin; response surface methodology; fluoroquinolones.

## 4.2. Introduction

Chirality is a significant factor in drug development, with approximately 50% of marketed drugs being chiral [1]. While the approval of racemates (mixtures of enantiomers) is declining, many chiral drugs are still used as racemates [1,2]. Regulatory concerns, such as those from the Food and Drug Administration of the United States (FDA) and the European Medicines Agency (EMA), arise due to the differing biological activities of enantiomers [3,4]. Typically, only one enantiomer (the eutomer) exhibits desired effects, while the other (the distomer) may cause adverse effects. Although certain racemic drugs are considered safe, regulatory authorities impose stringent requirements on pharmaceutical companies for the provision of comprehensive pharmacological, pharmacokinetic, and toxicological data on individual enantiomers and their racemates [5]. Therefore, the need for enantiopure compounds over racemic mixtures is growing, aiming to improve drug safety and efficacy.

OFX, a widely used quinolone antibiotic, is marketed both as levofloxacin (S-OFX) and in racemic form (S-OFX/R-OFX) for treating bacterial infections. Its antibacterial activity is highly dependent on its stereostructure, with S-OFX exhibiting significantly greater biological activity than R-OFX [6]. Due to R-OFX's lower activity and S-OFX's reduced toxicity, OFX has been exclusively marketed in its S-isomer form since 1998 [7]. Given the pivotal role of S-OFX in therapeutic effect, the enantioseparation of OFX holds significant importance.

The resolution of racemates to isolate individual enantiomers remains the primary approach in chiral separation. Various techniques, such as capillary electrophoresis (CE) [8], cocrystallization [9], high performance liquid chromatography (HPLC) [10], thin-layer chromatography (TLC) [11], and ligand exchange chromatography/capillary electrophoresis (LEC/LECE) [12,13], have been used to separate enantiomers, like the OFX. While these methods are effective, they have some drawbacks, including the need for expensive equipment, high operational costs, and environmental hazards [14,15], which complicate the scaling-up of enantioseparation processes. This highlights the need for more cost-effective and environmentally friendly techniques.

ELLE has recently emerged as a versatile technology for recovering single enantiomers from racemic mixtures, suitable for continuous operation [16]. ELLE is known for its scalability, tunability, and integration of enantiomer recognition and solvent extraction in a single-step [17]. In ELLE, there is a chiral selector that preferentially interacts with

one of the enantiomers and forming a complex through various intermolecular interactions (e.g. hydrogen bonding, π-π interactions, dipole and van der Waals interactions) [18]. This complex shows a different partitioning behavior from the other enantiomer and ensures effective enantioseparation [19]. The composition of ELLE also strongly influences enantiomer separation. Therefore, thoughtful selection of phase composition along with the chiral selector makes ELLE adaptable and versatile for enantiomer separation.

Jiao et al. [20] investigated the enantioseparation of OFX using a traditional ELLE based on n-octanol-water. Using a combination of hydrophilic (β-cyclodextrin) and hydrophobic (complex formed by O'O-dibenzoyl-(2R,3R)-tartaric acid (L-DBTA) and di(2-ethylhexyl)-phosphoric acid ($D_2$EHPA)) chiral selectors, they optimized conditions to enhance enantioselectivity, achieving a selectivity of 2.48. In another study in which different organic solvents for ELLE were investigated, octanol-water was found to be the most effective ELLE for OFX enantioseparation [21]. Tartaric acid derivatives and β-cyclodextrin (β-CD) were used as chiral selectors, achieving an enantioselectivity of 2.4 with di-p-toluoyl-l-tartaric acid (L-DTTA) and β-CD. Molecular simulations clarified the selectivity, highlighting the significant roles of interaction sites and steric effects in chiral recognition. In addition, Jiao et al. [22] utilized an aqueous biphasic system (ABS) - a specific type of ELLE - composed of polyethylene glycol (PEG) and ammonium sulfate for OFX enantioseparation. By adjusting the concentrations of L-tartaric acid (L-TA) and hydroxypropyl-β-cyclodextrin (HP-β-CD) and maintaining a pH of 4, they achieved a selectivity of 1.32.

However, conventional ELLE systems face issues like the volatility, flammability, and toxicity of some organic solvents, while polymer-based ELLE (ABS) struggles with high viscosity and limited polarity range, affecting extraction efficiency and selectivity, which hinders the achievement of high extraction efficiency [23]. Therefore, ELLE based on emerging alternative solvents, such as DES, has gained attention.

Typically, DES consist of a mixture of two (or more) compounds known as the hydrogen HBA and HBD [24]. These solvents are highly customizable and allow fine-tuning of physicochemical properties, such as hydrophobicity and hydrophilicity, by selecting the appropriate components [25]. Given the hydrophobic nature of OFX and the advantages offered by HDES, such as higher water stability [25], the development of a HDES-based ELLE emerges as a viable alternative.

The aim of this study was to investigate the potential of HDES as an alternative solvent for the enantioseparation of OFX by ELLE. First, four different β-CD derivatives were investigated as chiral selectors for OFX enantioseparation. Then, fourteen HDES-based ELLE systems were investigated, with HDES based on compounds such as L-menthol, fatty acids and fatty alcohols. Finally, optimization of the most effective system and the chiral selector was performed using a response surface method (RSM). The operating parameters, including pH, excess of chiral selector and HDES-water ratio (v/v), were optimized to achieve high selectivity for R/S-OFX.

## 4.3. Material and methods

### 4.3.1. Materials

All the chemical reagents used in the present work are reported in Table 4.1. Moreover, in all experiments ultrapure water was used, which underwent a rigorous double distillation procedure and meticulously treated through a reverse osmosis system and further refined using a Milli-Q plus 185 water purifier.

**Table 4.1.** List of compounds used in this work, including the abbreviation, CAS number, supplier and purity.

| Compound | Abbreviation | CAS number | Supplier | Purity (wt%) |
|---|---|---|---|---|
| ***HDES compounds*** | | | | |
| 1-Decanol | C10 alcohol | 112-30-1 | TCI | 98.0 |
| 1-Dodecanol | C12 alcohol | 112-53-8 | Alfa Aesar | 98.0 |
| Decanoic acid | C10 acid | 334-48-5 | Thermo Scientific | 99.0 |
| Dodecanoic acid | C12 alcohol | 143-07-7 | Acros Organics | 99.0 |
| L-menthol | --- | 1490-04-6 | Acros Organics | 99.5 |
| Octanoic acid | C8 acid | 124-07-2 | Thermo Scientific | 98.0 |
| ***Chiral selectors*** | | | | |
| Carboxymethyl-β-cyclodextrin sodium salt, DS* ~3 | CM-β-CD | 2828447-14-7 | BLD Pharmatech | 99 |
| Hydroxypropyl-β-cyclodextrin, DS* ~ 5-6 | HP-β-CD | 128446-35-5 | Sigma | --- |
| Sulfated-β-Cyclodextrin sodium salt, DS* ~12-15 | S-β-CD | 37191-69-8 | Sigma | --- |
| β-Cyclodextrin | β-CD | 7585-39-9 | Sigma | ≥ 97 |

| *Standards and compounds for NMR quantification* | | | | |
|---|---|---|---|---|
| 1-Butyl-3-methylimidazolium trifluoromethanesulfonate | $[C_4mim][CF_3SO_3]$ | 174899-66-2 | Iolitec | 99 |
| Deuterium oxide-D | $D_2O$ | 7789-20-0 | Aldrich | 99.9 |
| Dimethyl sulfoxide-D6 | DMSO | 2206-27-1 | Euriso-top | 99.80 |
| Levofloxacin | S-OFX | 100986-85-4 | TCI | 98 |
| Ofloxacin | R/S-OFX | 82419-36-1 | TCI | 98 |
| Sodium fluoride | NaF | 7681-49-4 | Thermo scientific | 99 |

*DS - degree of substitution.

### 4.3.2. HDES preparation

This work focused on the use of HDES for ELLE (Table 4.2), from which four groups were evaluated: (i) L-menthol: fatty acid; (ii) L-menthol: fatty alcohol; (iii) fatty acid: fatty acid and (iv) fatty acid: fatty alcohol. The selection of these HDES was based on our previous study [26]. In particular, the COSMO-RS predictions showed that the most promising HDES for OFX extraction are fatty acids with a higher fatty acid molar ratio and longer alkyl chains. The selected HDES were prepared with the indicated molar ratio of HBA and HBD (Table 4.2) by heating the mixture at 80 °C for 4-5 hours with constant stirring until a clear and homogeneous liquid was obtained. These HDES remained stable (clear and homogeneous liquid), with no detectable changes when cooled to 25 °C. In addition, their stability in water was previously studied confirming it [25].

**Table 4.2.** List of HDES studied in this work.

| HBA | HBD | Abbreviation | Molar ratio |
|---|---|---|---|
| L-menthol | Octanoic acid | L-menthol: C8 acid | 1:2 |
| | Decanoic acid | L-menthol: C10 acid | 1:2; 1:3 |
| | 1-Decanol | L-menthol: C10 alcohol | 2:1 |
| | 1-Dodecanol | L-menthol: C12 alcohol | 2:1 |
| Octanoic acid | Decanoic acid | C8 acid: C10 acid | 2:1 |
| | Dodecanoic acid | C8 acid: C12 acid | 2:1 |
| | 1-Decanol | C8 acid: C10 alcohol | 2:1 |
| | 1-Dodecanol | C8 acid: C12 alcohol | 2:1 |
| Decanoic acid | Dodecanoic acid | C10 acid: C12 acid | 2:1; 3:1 |
| | 1-Decanol | C10 acid: C10 alcohol | 2:1 |
| | 1-Dodecanol | C10 acid: C12 alcohol | 2:1; 3:1 |

### 4.3.3. Selection of the best chiral selector

First, the efficacy of β-cyclodextrin derivatives were investigated - namely β-cyclodextrin (β-CD), hydroxypropyl-β-cyclodextrin (HP-β-CD), carboxymethyl-β-cyclodextrin sodium salt (CM-β-CD) and sulfated-β-cyclodextrin sodium salt (S-β-CD) - as chiral selectors for the enantioseparation of OFX. To evaluate the suitability of these selectors and determine the initial appropriate molar excess for evaluated HDES-based ELLE, a solution containing racemic OFX (1 mg/ml) was mixed with different molar excesses of the chiral selector (20x, 40x, 80x, 120x, and 160x) in relation to OFX. For β-CD, the evaluation was limited to a 20-fold excess of the chiral selector, whereas HP-β-CD was evaluated in a range of 20 to 80-fold due to solubility issues. The mixtures were then stirred at 50 rpm and room temperature (25 ± 1 °C) for at least 12 hours to ensure optimal contact between the chiral selector and R/S-OFX. Afterwards, $^{19}F$ NMR spectroscopy was used to determine whether the R/S-OFX enantiomers were separated or not, as explained below.

### 4.3.4. HDES-based Enantioselective Liquid-Liquid Extraction (ELLE)

The HDES-based ELLE was chosen as the platform for the enantioseparation of R/S-OFX. A total of fourteen systems (see Table 4.2) with an equal volume ratio of HDES and water (HDES-water ratio, v/v) were analyzed for enantioseparation. The water phase contained the racemic mixture of OFX (2 mg/ml) and the previously identified

and optimized chiral selector. The mixture was stirred at 50 rpm for at least 12 hours at room temperature (25 ± 1 °C) to ensure the contact between the phases. Then, the system was centrifuged at 10,000 rpm for 10 minutes. Subsequent separation of the HDES phase (top) from the aqueous phase (bottom) was performed and analyzed by $^{19}F$ NMR spectroscopy to quantify the OFX enantiomers in each phase as described below. This entire procedure was repeated three times in order to determine the average of the partition coefficients and selectivity, as well as the respective standard deviations. Figure 4.1 gives an overview of the experimental process of OFX enantioseparation using HDES-based ELLE.

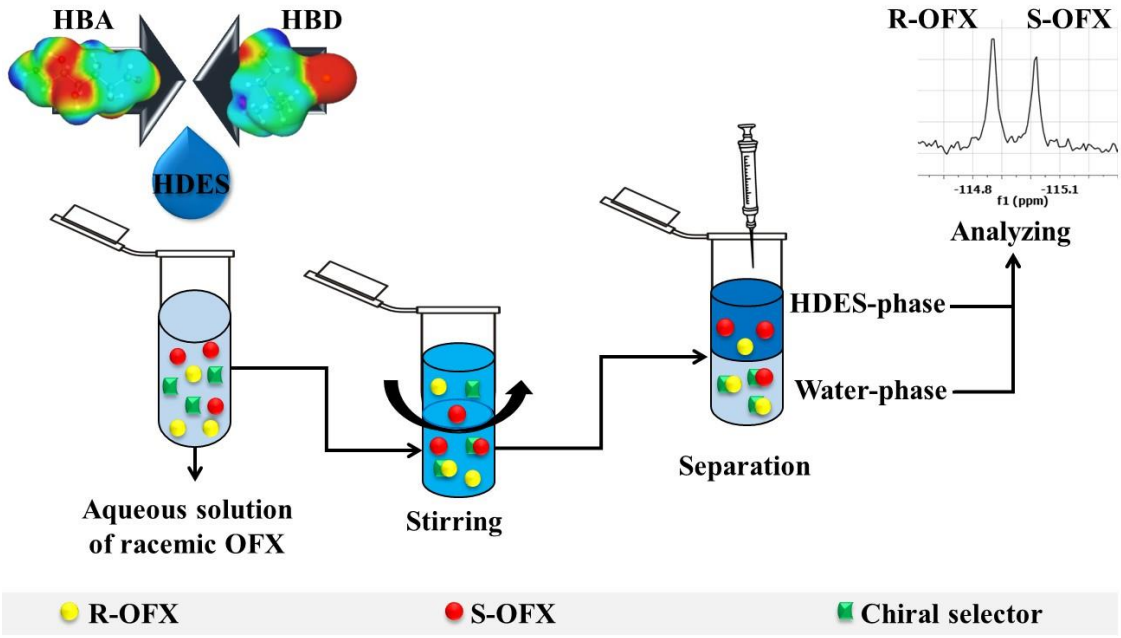


**Figure 4.1.** Schematic diagram of the enantioseparation of OFX using HDES-based ELLE.

### 4.3.5. Identification and quantification of OFX enantiomers by $^{19}F$ NMR

The NMR technique can be used to identify and quantify enantiomers, especially for fluorine-containing compounds such as OFX, as shown in Figure 4.2. The identification and quantification of OFX enantiomers were performed using the $^{19}F$ NMR spectroscopic method, following the established approach by Rofouei *et al*. [7]. This method is characterized by the observation of a doublet signal in the $^{1}H$-decoupled $^{19}F$ NMR spectrum of OFX, which is crucial for accurate enantiomeric analysis.

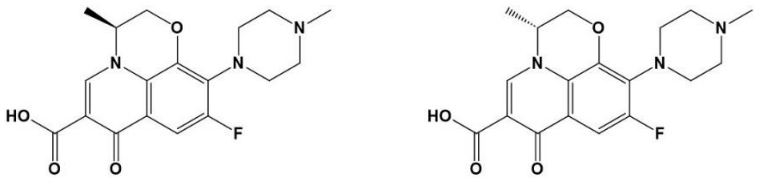


**Figure 4.2.** The structure of the OFX enantiomers.

All samples were analyzed by $^{1}$H-decoupled $^{19}$F recorded on a Bruker Avance 300 at 282 MHz to obtain their spectrum, and the depending on the chiral selector and its concentration different signals of R/S-OFX (ppm) were observed.

To quantify OFX enantiomers using $^{19}$F NMR, sodium fluoride (NaF) was employed as an internal standard, as it presents a distinct signal (-118.8 ppm) compared to OFX (-115.7 ppm) in the $^{1}$H-decoupled $^{19}$F NMR spectrum (Figure C.1 in Appendix C). A solution of NaF at a concentration of 2 mg/ml in deuterated water ($D_2O$) was prepared and distributed into separate capillaries to avoid interactions with the OFX enantiomers and to ensure accurate quantification. Each capillary was standardized using a reference solution of 1-butyl-3-methylimidazolium trifluoromethanesulfonate ($[C_4mim][CF_3SO_3]$). Then, these calibrated capillaries were used as an internal standard for the quantification of OFX enantiomers in each phase. For OFX quantification, 400 µl of each phase was weighed individually ($\pm 10^{-4}$ g) in a NMR tube with a NaF standardized capillary. Then, the samples were analyzed by $^{1}$H-decoupled $^{19}$F recorded and their spectrum recorded. The gathered spectra were analyzed in order to calculate the amount of R/S-OFX enantiomers present in the phases, aiming to determine the partition coefficient and the selectivity.

The partition coefficients ($K$) for each enantiomer were calculated separately through Equation 1:

$$K_{S/R-OFX} = \frac{C_{bot\ S/R-OFX}}{C_{top\ S/R-OFX}} \quad (1)$$

Where $C_{bot\ S/R-OFX}$ and $C_{top\ S/R-OFX}$ refer to the concentration of R-OFX or S-OFX in the bottom phase (aqueous phase) and in the top phase (HDES phase), respectively. Moreover, the selectivity ($\alpha$) of each system was calculated as described in Equation 2:

$$\alpha_{R-OFX/S-OFX} = \frac{K_{R-OFX}}{K_{S-OFX}} \quad (2)$$

Where $K_{R-OFX}$ and $K_{S-OFX}$ represent the partition coefficient of R-OFX and S-OFX, respectively.

### 4.3.6. Computational details

Initially, the geometry optimization of the β-CD trimer, CM-β-CD trimer, S-β-CD trimer, and OFX (in both zwitterionic and positive forms) was conducted using Turbomole v4.5.2 (TmoleX19 software package) at the BP86/TZVP level. In this step, a separate *.cosmo file was generated for each molecule, which was then used in the COSMOthermX software. To confirm the stability of the most stable conformer, a final single-point calculation was conducted to eliminate any oscillation frequencies [27].

The intermolecular interactions energies - specifically, hydrogen bonding (H-bond), electrostatic misfit (misfit) and van der Waals forces (vdW) - between the chiral selectors and OFX were then calculated. These calculations used the COSMO-RS approach [28], a thermodynamic model that combines quantum chemistry and statistical thermodynamics. All COSMO-RS calculations were performed utilizing the COSMOthermX software package (Version 21.0, COSMOlogic GmbH) at the BP86/TZVP level with the BP_TZVP_21.ctd parameterization [28,29].

### 4.3.7. Optimization of the operating extractions conditions.

In order to investigate synergies or antagonisms in the extraction process under different conditions, we employed the response surface methodology (RSM). RSM uses mathematical and statistical methods to determine correlations and optimize response(s) [30]. In a $2^k$ RSM, k variables contribute to different response (y), and the data are treated according to the following second-order polynomial equation:

$$y = \beta_0 + \sum \beta_i X_i + \sum \beta_{ii} X_i^2 + \sum_{i<j} \beta_{ij} X_i X_j \quad (3)$$

Where, $\beta_0$, $\beta_i$, $\beta_{ii}$, and $\beta_{ij}$ refer to the adjusted coefficients for the intercept, linear, quadratic, and interaction terms, respectively, while $X_i$ and $X_j$ represent the operational variables.

A $2^3$ RSM was used to optimize the selectivity of OFX by evaluating three operating variables, namely pH (between 3 and 5), excess of chiral selector (ranging from 20 to 121 times the amount of OFX) and HDES-water ratio (between 1:2 and 2:1 v/v). A total of twenty experiments were performed. Detailed information on the RSM can be found in Tables C.1 and C.2 in Appendix C.

Statistical analysis of the results was performed using Protimiza Experimental Design software with a 95% confidence level. This analysis included various methods, including analysis of variance (ANOVA), regression analysis and contour plots. These analysis techniques were used to determine and define the optimal operating conditions in this study.

## 4.4. Results and discussion

### 4.4.1. Selection of the best chiral selector

In enantioseparation, the interactions of the chiral selectors with the enantiomers are crucial for effective separation of the enantiomers [31]. Cyclodextrins (CD) are preferred as chiral selectors due to their cost efficiency, stability and water solubility [32]. Recently, β-CD derivatives with neutral or charged groups have proven to increase the solubility and enantioseparation efficiency. In this context, we investigated the efficiency of four β-CD derivatives (neutral β-CD: β-CD and HP-β-CD and anionic β-CD: S-β-CD, CM-β-CD) at different molar excesses of chiral selector (20x, 40x, 80x, 120x and 160x), at 25 ºC for the enantiomeric separation of OFX. The $^{19}$F NMR results obtained are shown in Figure 4.3. Please note that the results for the excess of β-CD from 40x to 160x and HP-β-CD from 120x to 160x are not shown in the figure, as it was not possible to dissolve these chiral selectors in water at these concentrations.

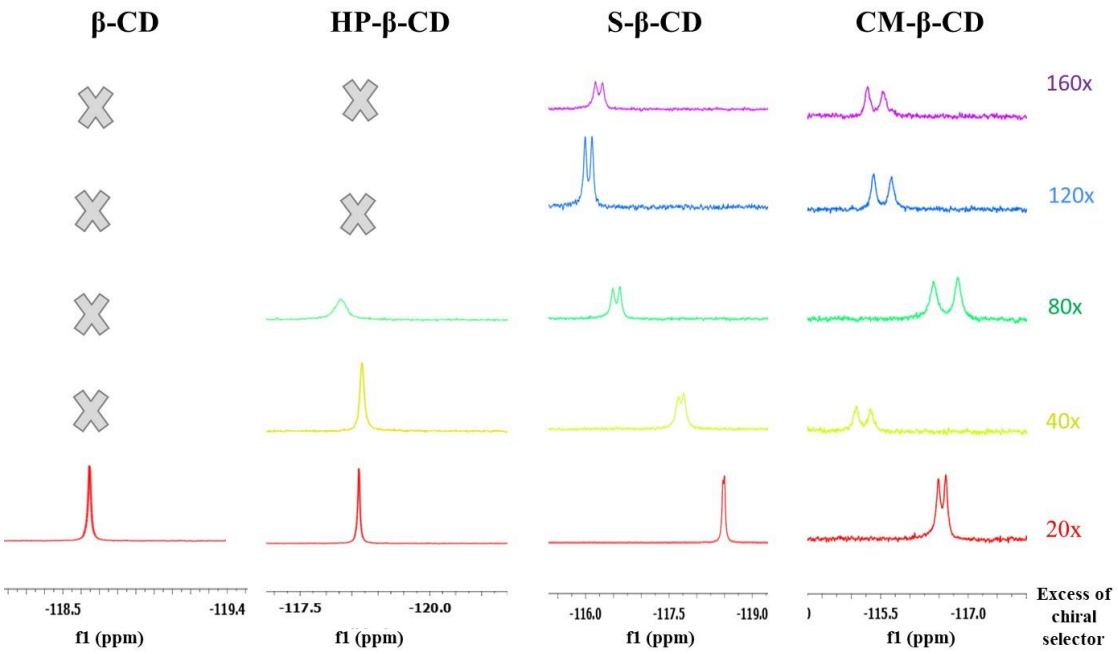


**Figure 4.3.** The $^{1}$H-decoupled $^{19}$F NMR spectrum of R/S-OFX in the presence of different chiral selectors and molar excess, at 25 ºC.

As shown in Figure 4.3, among the studied chiral selectors, the neutral β-CDs, namely β-CD and HP-β-CD, exhibit a negligible effect on the enantioseparation of OFX. This is evident from their $^{19}$F NMR spectra, which lack two distinct peaks even with a high excess of the chiral selector. These findings align with previous studies [7,33,34]. In contrast, anionic β-CD namely, CM-β-CD and S-β-CD showed considerable potential for the enantioseparation of OFX, since two peaks were observed in the NMR spectra, confirming the separation of OFX enantiomers. These results show that, while in neutral β-CD hydrophobic interactions are usually responsible for the formation of host-guest complexes by entrapping the aromatic part of the analytes into the CD cavity, in anionic β-CD electrostatic interactions and hydrogen bindings are the main driving forces for chiral recognition, in addition to the well-known hydrophobic interactions [35]. This allows the formation of a shallow external complex rather than an inclusion complex between anionic β-CD and analytes, which may explain the good enantiomeric results observed for anionic β-CD. However, note that the structure of the analytes also significantly influences the enantioseparation. Furthermore, two distinct peaks were observed with increasing excess of the anionic chiral selector, especially at 120-fold excess of the chiral selector. This improved separation can be associated with the formation of additional complexes when the concentration of the chiral selector was

increased [36]. However, a further increase in the excess of the anionic chiral selector to 160-fold leads to a decrease in the separation efficiency for the R/S-OFX peaks.

It is worth noting that despite some studies indicating successful OFX enantiomer separation with HP-β-CD [33,34,37], our observations are not consistent with this, suggesting that its efficacy may be limited to certain experimental conditions. On the other hand, only when CM-β-CD was used as a chiral selector, especially at 120-fold excess, two clearly separated peaks were observed, highlighting its superiority in the enantioseparation of OFX. These results are consistent with previous studies showing that anionic derivatives of β-CD, particularly CM-β-CD, produce the most stable complexes and the highest resolution in enantioseparation [33,38].

To gain insights into why the chiral selector CM-β-CD performs better than S-β-CD in the enantiomer separation of OFX, we calculated the intermolecular interaction energies, including hydrogen bonding (H-bond), electrostatic misfit (misfit), and van der Waals forces (vdW). These calculations were performed using COSMO-RS for water mixtures with β-CD, S-β-CD or CM-β-CD and OFX at 20- or 120-fold excess of the chiral selector. The results are shown in Figure 4.4 and Table C.3 in Appendix C. β-CD was not included at 120-fold excess because it is not water soluble at this concentration. In addition, the mixture of S-β-CD and OFX at 120-fold excess had a pH of 5.7, meaning that OFX was present in both its zwitterionic and positive forms (OFX p$K_{a1}$ = 5.2 and p$K_{a2}$ = 8.4 [39]), so calculations were performed for both OFX forms. For the other mixtures, the interaction energies were only calculated for this form, as they had a pH of about 6.1 and OFX was predominantly present in its zwitterionic form.

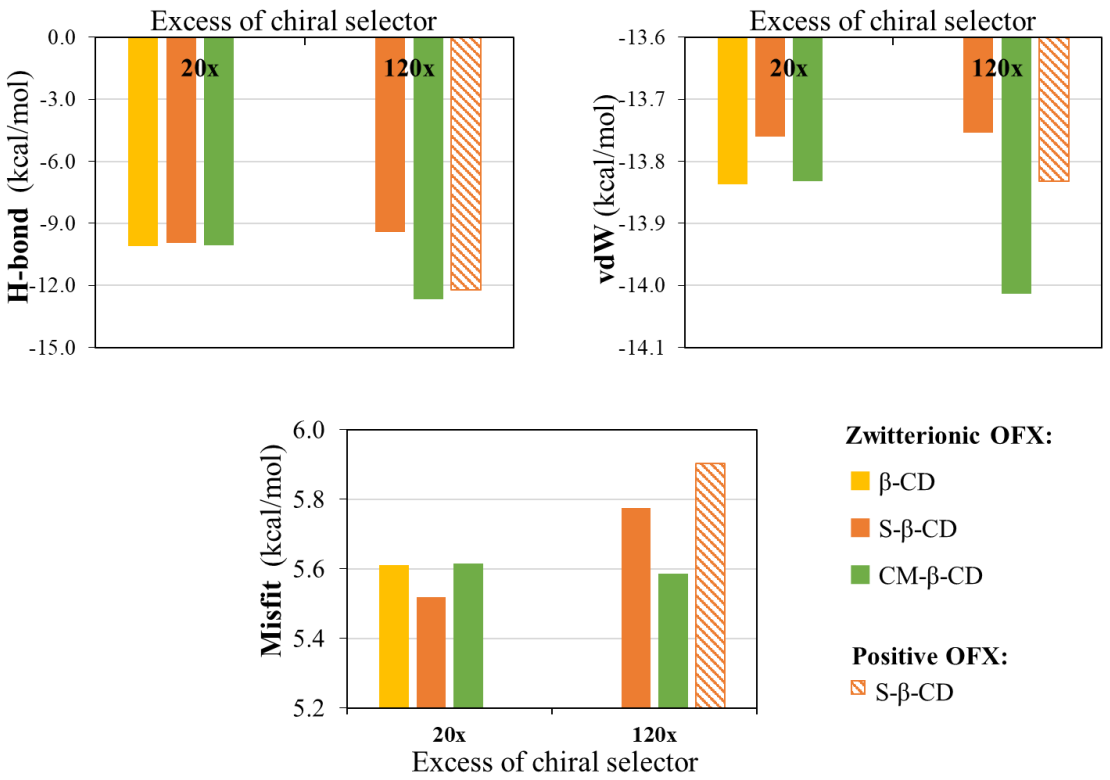


**Figure 4.4.** Interaction energies, including hydrogen bonding (H-bond), electrostatic misfit (misfit), and van der Waals forces (vdW), calculated using COSMO-RS for aqueous mixtures of β-CD (yellow), S-β-CD (orange), or CM-β-CD (green) with OFX in its zwitterionic (solid line) or positive (dashed line) form, at 20-fold and 120-fold excess of the chiral selector.

Figure 4.4 shows that both H-bond and vdW interactions are slightly more negative (with greater intensity) for the chiral selector CM-β-CD at an excess of 120x. Conversely, under these same conditions, the misfit energy interactions have less intensity. Negative values for H-bond and vdW interactions indicate stronger interactions between the chiral selector and OFX, while positive misfit interactions are generally disadvantageous - the lower the better [40]. These results show that CM-β-CD at 120x has the strongest interactions with OFX, as observed experimentally (Figure 4.3). When comparing different chiral selectors at 20x excess, especially in terms of H-bond energy, they show similar values, indicating a comparable affinity for OFX; consequently, no significant differences were expected under these conditions, as observed experimentally (Figure 4.3). In addition, for S-β-CD at 120x, it should be noted that half of the OFX is in its positive form and the other half in the zwitterionic form, which could explain why S-β-CD was less effective than CM-β-CD in enantiomer separation at this concentration (Figure 4.3). In this context, it is understandable that

CM-β-CD at 120x shows the highest efficiency in enantiomer separation, as it has the most negative values for both H-bond and vdW energies and the lowest misfit energy among the chiral selectors studied.

Since CM-β-CD with a 120-fold excess showed the most promising results in OFX enantiomer separation, this chiral selector and molar excess were chosen for subsequent studies.

### 4.4.2. Selection of the optimal Enantioselective Liquid-Liquid Extraction (ELLE)

To identify the optimal HDES-based ELLE for OFX enantioseparation, fourteen systems were explored, assessing four different HDES families (L-menthol: fatty acid, L-menthol: fatty alcohol, fatty acid: fatty acid, and fatty acid: fatty alcohol) with various molar ratios of HDES (Figure 5). The experiments were conducted under the following conditions: 1:1 (v/v) HDES-water ratio, 120-fold excess of CM-β-CD, stirring at 50 rpm for at least 12 hours at (25 ± 1 °C). Figure 4.5 shows the results obtained regarding the selectivity of the systems for the enantioseparation of OFX and initial pH of each system (for more details see Table C.4 in Appendix C). The pH was not adjusted during these experiments. Furthermore, CM-β-CD prefers the aqueous phase due to its high hydrophilicity, and since the partition coefficient of R-OFX exceeds the partition coefficient of S-OFX in the aqueous phase, this indicates that R-OFX is predominantly in this phase (water). As a result, the chiral cavities of CM-β-CD exhibit a specific affinity for the R-enantiomer of OFX due to its high hydrophilicity [38]. This selective recognition is consistent with the three-point interaction model, in which optimal chiral discrimination occurs through at least three simultaneous interaction points (hydrogen bonds, hydrophobic effects and van der Waals forces) [38]. These results support the complex formation with the preferred enantiomer and promote its separation from the racemic mixture.

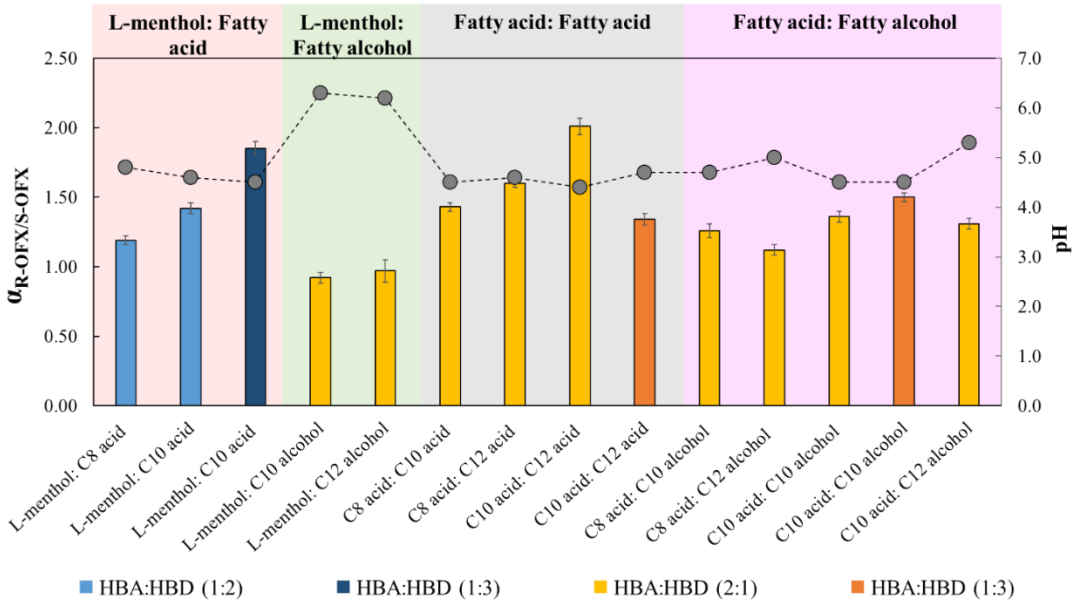


**Figure 4.5.** Selectivity of OFX ($\alpha_{R\text{-}OFX/S\text{-}OFX}$) for each system (bars) and pH (circles), using the chiral selector CM-β-CD at a 120-fold excess. Experiments were conducted at 25°C.

As shown in Figure 4.5, HDES-based ELLE are in general promising for OFX enantioseparation, which is consistent with the hypothesis that highly hydrophobic solvents are advantageous to achieve robust enantiorecognition when β-CD derivatives are used as chiral selectors [18]. The only exception is the HDES group based on L-menthol: fatty alcohol, which has a significantly lower selectivity, suggesting that this group may not be suitable for enantioseparations. These systems are characterized by being those with higher pH values (around 6.3), which could explain these results as the OFX molecule is in its zwitterionic form at this pH (OFX p$K_{a1}$ = 5.2 and p$K_{a2}$ = 8.4) [39], which could lead to weaker interactions with the chiral selector [41]. The impact of pH on enantioseparation will be further discussed in more detail ahead. On the other hand, fatty acid-based HDES proves to be a good option for OFX enantioseparation and shows the most promising results. It is noteworthy that these systems have pH values between 4.5 and 5.3, where the molecules are positively monocharged, and therefore have a higher affinity to interact with the anionic chiral selector. It is also observed that increasing the alkyl chain length of the fatty acids (e.g., L-menthol: C8 acid (1:2) with α of 1.19 ± 0.03 *vs.* L-menthol: C10 acid (1:2) with α of 1.42 ± 0.04) and their molar ratio (e.g., L-menthol: C10 acid (1:2) with an α of 1.42 ± 0.04 *vs.* L-menthol: C10 acid (1:3) with an α of 1.85 ± 0.05) contribute to a better separation of the OFX enantiomers. An exception was observed with HDES from fatty acid: fatty acid, where a higher molar

ratio of fatty acids led to a decrease in the selectivity of OFX enantiomer separation (i.e., C10 acid:C12 acid (2:1) with an α-value of 2.01 ± 0.06 versus C10 acid:C12 acid (3:1) with an α-value of 1.34 ± 0.04).

In summary, among the HDES-based ELLE systems, the one utilizing a C10 acid: C12 acid (in a 2:1 ratio) demonstrated the highest effectiveness, boasting a selectivity of up to 2.01 ± 0.06. Consequently, this system was chosen for further evaluation in subsequent steps.

### 4.4.3. Optimization of the operating extractions conditions

A RSM was used to optimize the operating conditions for OFX enantiomer separation in order to analyze different variables simultaneously and to identify the most significant parameters and their interaction. The independent variables considered were pH, excess of chiral selector and HDES-water ratio (v/v), and the dependent variable was the selectivity of OFX ($\alpha_{R\text{-}OFX/S\text{-}OFX}$). Details about the results, the statistical analyses and fitted model can be found in Appendix C (Tables C.5-C.7, Figures C.2 and C.3). The fitted model was obtained using the analysis of variance (ANOVA) to estimate the statistical significance of the variables and their interactions. It shows satisfying predictability at a confidence level of 95% with $R^2 = 0.92$ and F-calculated > F-tabulated, demonstrating the model reliability in describing experimental findings. The impact of these three variables on the selectivity of OFX is illustrated in Figure 4.6. In addition, the Pareto chart (Figure C.2 in Appendix C) highlights the significant effects of operating variables, including pH, excess of chiral selector, and HDES-water ratio, along with some of their interactions. The order of variables with statistical significance is HDES-water ratio ≥ pH > excess of chiral selector$^2$ > pH$^2$ > excess of chiral selector. The effects of each variable will be discussed in more detail below.

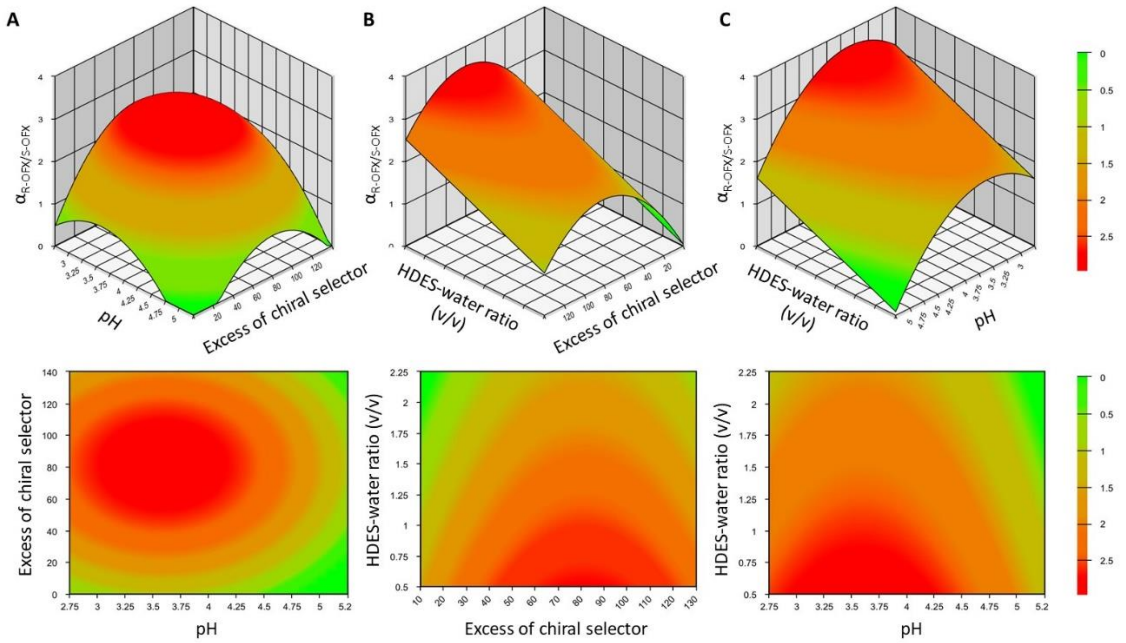


**Figure 4.6.** Responsive surface and contour plots of the selectivity of OFX ($\alpha_{R\text{-}OFX/S\text{-}OFX}$) with the combined effects: (**A**) pH and excess of chiral selector, (**B**) HDES-water ratio (v/v) and excess of chiral selector and (**C**) HDES-water ratio (v/v) and pH.

#### *4.4.3.1. Effect of HDES-water ratio (v/v) on the enantioseparation of OFX*

The volume ratio of the phases typically plays an important role in the enantioseparation in ELLE [20,31]. In our case, the HDES-water ratio (v/v) was the most important parameter, together with pH, as mentioned above. The results show a higher selectivity at a lower HDES-water ratio (v/v), highlighting the significant influence of a higher ratio of the aqueous phase on the enantiomer distribution [20]. This can be explained by the lower volume of HDES, which allows more OFX to enter the hydrophilic phase. Consequently, CM-β-CD can interact more effectively with the enantiomers enhancing enantioseparation [31].

#### *4.4.3.2. Effect of pH on enantioseparation of OFX*

The significance of pH in enantioseparation has been extensively investigated in previous studies [20,22], and the OFX enantiomers can usually be separated in a wide pH range, except when the molecule is in its neutral zwitterionic form (OFX has two p$K_a$ values: p$K_{a1}$ = 5.2 and p$K_{a2}$ = 8.4, with the neutral zwitterionic form prevailing between these p$K_a$ values) [39]. Therefore, a pH range of 3.0 to 5.0 was chosen for enantioseparation in this study.

As expected, the pH plays a crucial role in the separation of OFX enantiomers emerging as the second most significant variable. The results show that the quadratic effect of pH has a negative influence on the enantioseparation of OFX (Table C.6 in Appendix C). Thus, maximum selectivity is observed at intermediate pH values, where an increase from 3.0 to 3.5 enhances selectivity, but further increases above 3.5 lead to decreased selectivity.

This behavior can be attributed to the chemical structure of OFX, characterized by the presence of a carboxyl group ($pK_{a1}$ = 5.2) and a piperazine group ($pK_{a2}$ = 8.4) [39]. The charge of these functional groups varies with pH, becoming positively charged in an acidic medium [39]. Additionally, CM-β-CD is negatively charged at acid medium ($pK_a$ = 4) [41]. As a result, there is a strong ionic interaction between R-OFX and CM-β-CD, enhancing the selectivity. These results are consistent with previous research [33,38] showing that the complexes formed between R-OFX and CM-β-CD remain stable at acidic pH. Jiao et al. [22] also demonstrated the favorable influence of acidic conditions, specifically at pH 4, on the enantioseparation of OFX using an ABS based on PEG and ammonium sulfate, with two chiral selectors, L-TA and HP-β-CD.

On the other hand, a reduction in selectivity can be observed when the pH value increases. This is attributed to the increased deprotonation of the carboxyl groups of OFX, which leads to an increase in the zwitterionic form. Simultaneously, the electrostatic attraction between OFX and CM-β-CD decreases, contributing to a less efficient enantioseparation. In summary, the most efficient enantioseparation is achieved at a pH around 3.5, where CM-β-CD is negatively charged while OFX is positively charged.

#### *4.4.3.3. Effect of excess of chiral selector on enantioseparation of OFX*

The excess of the chiral selector is considered a critical factor in enantioseparation. Chiral selectors not only improve the selectivity of enantiomers in ELLE, but also influence the partitioning of enantiomers between phases [22]. The data from Figure 4.6 and Table C.6 in Appendix C show a positive correlation between CM-β-CD excess and the selectivity of R/S-OFX. This can be explained by the fact that an increase in CM-β-CD excess enhances interactions such as hydrogen bonding and dipole–dipole interactions between the enantiomers and the chiral selector, which facilitates the formation of more complexes and improves chiral recognition [20,33]. However, Figure 6 shows that exceeding a 100-fold excess of CM-β-CD leads to a decrease in the

selectivity of OFX enantioseparation. This decrease is consistent with the negative effects of the quadratic effect of excess CM-β-CD. The excess concentration of CM-β-CD likely leads to saturation of the binding sites for the OFX enantiomers, disrupting the chiral recognition process. This saturation could affect the separation efficiency and even lead to non-selective interactions between the enantiomers and the chiral selector. These findings are consistent with the results of previous studies [20,42]. Jiao et al. [20] demonstrated that in an ELLE system composed of n-octanol and water, increasing the concentration of the hydrophobic chiral selector (a complex of $D_2$EHPA and L-DBTA) improved the distribution, enantiomeric excess, and separation factor of OFX enantiomers up to a maximum. Beyond this optimal concentration, however, further increases led to a decrease in enantioseparation efficiency.

#### *4.4.3.4. Discussion*

After analyzing the surface plots shown in Figure 4.6, the optimal operating conditions for the enantioseparation of OFX with ELLE based on HDES-C10 acid:C12 acid (2:1) and CM-β-CD as chiral selector are an excess of chiral selector of 77, an HDES-water ratio of 1:2, and a pH of 3.5. Under these optimized conditions, a selectivity of R/S-OFX of 3.81 ± 0.33 was achieved. Remarkably, this experimental result aligns with the value predicted by multiple regressions using RSM analysis, which estimated a selectivity of R/S-OFX at 3.75, resulting in a relative error of only 1.6%. This validated the model with a confidence interval of 95%, underlining the robustness of the fitted model.

Table 4.3 shows a comparison of the developed method for the enantioseparation of OFX with previous ELLE approaches. Jiao et al. [22] used an ABS consisting of PEG 2000 and ammonium sulfate using L-TA in the PEG-rich phase and HP-β-CD in the salt-rich phase as chiral selectors and achieved a maximum selectivity of 1.32 for OFX under optimal conditions. In contrast, in another study [20], a higher separation factor of 2.48 was obtained for R/S-OFX using conventional ELLE with n-octanol, using both hydrophilic and hydrophobic chiral selectors; however, the hydrophobic component was a complex of L-DBTA and $D_2$EHPA. In addition, Li et al. [21] investigated different organic solvents and chiral selectors in ELLE for OFX extraction. Their most effective system, which used n-octanol and water with L-DTTA as the hydrophobic chiral selector and β-CD as the hydrophilic selector, achieved an enantioselectivity of 2.4 under optimized conditions. This demonstrates that complex chiral selectors are not

always necessary, depending on the specific conditions of enantioseparation. Overall, research on OFX enantioseparation in two-phase systems, as described both in the literature and in this study, highlights the importance of careful solvent and chiral selector selection, as well as optimized operating factors such as pH control. These elements are crucial for increasing the efficiency of OFX enantioseparation. Notably, the HDES-based ELLE system using a C10 acid:C12 acid (2:1) HDES with CM-B-CD as chiral selector at pH 3.5 proves to be the most promising approach.

**Figure 4.7.** A summary of extraction conditions for some enantioselective liquid-liquid systems in OFX enantioseparation from the literature.

| Enantioseparation method | Chiral selector | Extraction conditions | Selectivity (α) | Ref. |
|---|---|---|---|---|
| Enantioselective liquid-liquid extraction (ELLE), including aqueous biphasic system (ABS) | L-TA; HP-β-CD | [OFX] = 0.04 mg/ml, pH = 4, [HP-β-CD] = 0.02 mol/l, [L-TA] = 0.05 mol/l, 40 wt % of PEG 2000, 25 wt% of ammonium sulfate. (ABS - a specific type of ELLE) | 1.32 | [22] |
| | β–CD; | [OFX] = 0.002 g/ml, pH = 6.5, [β–CD] = 0.011 g/ml, [L-DBTA] = 0.055 g/ml and [$D_2$EHPA] = 0.3 g/ml, organic phase volume (n-octanol) = 14 ml, aqueous phase volume = 20 ml, temperature = 25 ºC. | 2.48 | [20] |
| | L-DTTA; β-CD | [OFX] = 1 mg/ml, [L-DTTA] = 0.012 g/ml and [β-CD] = 0.006 g/mL, organic phase volume (n-octanol) = 3 ml, aqueous phase volume = 3 ml, temperature = 25 ºC. | 2.4 | [21] |
| | CM-β-CD | [OFX] = 2 mg/ml, pH = 3.5, molar excess of chiral selector = 77-fold, HDES-water volume ratio = 1:2 (V/V), temperature = 25 ºC. | 3.8 ± 0.3 | This work |

Expanding the discussion to include process development, it is crucial to develop effective method for recovering the active pharmaceutical ingredient and to understand the toxicity (both eco- and cyto-toxicity) of HDES.

Regarding the recovery of the target enantiomer, we did not directly study the extraction of S-OFX from the HDES phase in this study. However, Li et al. [21] investigated this aspect using an acetic acid solution to recover S-OFX from octanol, a highly hydrophobic solvent, and showed effective recovery. This suggests that this approach could be effective for the extraction of S-OFX from the HDES phase, as it is also a highly hydrophobic solvent. Moreover, this method not only facilitates the recovery of

the enantiomer, but also enables the reuse of HDES in subsequent extractions, which is crucial for the development of a sustainable process. Nevertheless, further studies are needed to evaluate the stability of HDES after the recovery process.

Regarding the ecotoxicity of our HDES, although no specific tests have yet been carried out, the analysis of only the C10 and C12 acids can provide information on their hazard potential. Their slow degradation in water poses a risk to aquatic ecosystems and requires proper disposal to minimize the impact on the environment [43,44]. On the other hand, the low solubility of HDES (2 wt%) helps to reduce water pollution and improve environmental sustainability [45]. The challenge of complete separation of HDES from compounds also requires an evaluation of the cytotoxicity of HDES. Studies suggest different cytotoxic effects of fatty acid-based HDES on yeasts (*C. albicans*) [46], bacteria and HaCaT [47], so further targeted research is needed. Although the Food and Drug Administration (FDA) classifies the HDES components themselves as safe [48], and they are therefore widely used in the industry, high doses can cause irritation, so further research is needed.

Taking into account all the aforementioned points, the development of advanced recycling methods and the provision of comprehensive toxicity data are essential for a more effective integration of HDES into industrial applications.

## 4.5. Conclusions

Aiming at the enantioseparation of OFX, this study developed an ELLE method based on HDES, utilizing both neutral and anionic derivatives of β-CD as chiral selectors. An initial screening was conducted to identify the most promising chiral selector for the enantioseparation of OFX. The results highlighted the potential efficacy of anionic β-CD derivatives, particularly CM-β-CD, in the effective separation of R/S-OFX. After that, a screening of fourteen HDES-based ELLE systems revealed that an increased molar ratio of fatty acids, coupled with an extension of their alkyl chain length, significantly improved the efficiency of enantioseparation of OFX. Among these combinations, C10 acid: C12 acid at a ratio of 2:1 was found to be the most favorable extraction solvent. Finally, an experimental design was carried out to investigate the most important factors in enantioseparation with C10 acid: C12 acid (2:1) HDES and CM-β-CD as a chiral selector. The results showed that the three variables evaluated, i.e. pH, excess of chiral selector and HDES-water ratio (v/v), had an effect on improving

the selectivity of R/S-OFX separation. Under the optimal conditions, i.e. 77-fold excess of chiral selector, pH of 3.5 and HDES-water ratio (v/v) of 0.54, the highest selectivity (α) of 3.8 ± 0.3 was achieved in a single-step.

These results emphasize the critical significance of carefully selecting appropriate solvents and chiral selectors while evaluating key factors for the separation. This approach has the potential to significantly improve the efficiency of enantioseparation of chiral compounds. This research not only addresses the separation of OFX enantiomers, one of the most common quinolone antibiotics, but may also be of interest to the pharmaceutical industry at large, which needs to commercialize chiral drugs as single enantiomers.

## 4.6. References


[1] S. Orlandini, G. Hancu, Z.I. Szabó, A. Modroiu, L.A. Papp, R. Gotti, S. Furlanetto, New Trends in the Quality Control of Enantiomeric Drugs: Quality by Design-Compliant Development of Chiral Capillary Electrophoresis Methods, Molecules 27 (2022) 7058.

[2] R.U. McVicker, N.M. O'Boyle, Chirality of New Drug Approvals (2013-2022): Trends and Perspectives, J Med Chem 67 (2024) 2305–2320.

[3] A. Calcaterra, I. D'Acquarica, The market of chiral drugs: Chiral switches versus de novo enantiomerically pure compounds, J Pharm Biomed Anal 147 (2018) 323–340.

[4] S.W. Smith, Chiral Toxicology: It's the Same Thing…Only Different, Toxicological Sci 110 (2009) 4–30.

[5] FDA'S policy statement for the development of new stereoisomeric drugs, Chirality 4 (1992) 338–340.

[6] C. Zhao, W. Lu, X. Meng, Using chiral magnetic surface molecularly imprinted polymers for chiral separation of Ofloxacin, J Polym Res 28 (2021) 1–8.

[7] M.K. Rofouei, N. Sohrabi, S. Haghgoo, Application of 19 F NMR Spectroscopic Method to the Enantioresolution and Quantitative Determination of Ofloxacin in Pharmaceutical Formulations, Recent Researches in Modern Medicine (2011) 385–394.

[8] S. Deng, J. Pan, M. Wang, Y. Huang, Z. Xia, Study on improvement of chiral separation of capillary electrophoresis based on cyclodextrin by deep eutectic solvents, Talanta 220 (2020) 121419.

[9] L. He, X. Chen, X. Li, Z. Zhou, Z. Ren, Chiral co-selector induced chirality switching in the enantioseparation of ofloxacin by forming a co-crystal, New J Chem 43 (2019) 15048–15051.

[10] I. Ali, K. Sekkoum, N. Belboukhari, M.N. Rebizi, M.E.A. Zaid, K. Yusuf, A.A. Alothman, B.A. AlJumah, M. Ouladsmane, Determination of enantio-separation, absolute configuration and chiral recognition mechanism of ofloxacin and flumequine by HPLC and modeling studies, J Chem Technol Biotechnol 96 (2021) 2901–2908.

[11] N. Salama, H. Zaazaa, L. Abd El Halim, M. Salem, L. Abd El Fattah, Thin-layer chromatographic enantioseparation of ofloxacin and zopiclone using hydroxy-propyl-beta-cyclodextrin as chiral selector and thermodynamic studies of complexation, Journal of Planar Chromatography - Modern TLC 27 (2014) 166–173.

[12] C. Aydoğan, V. Karakoc, F. Yılmaz, H. Shaikh, A. Denizli, Enantioseparation of Ofloxacin by Ligand Exchange Capillary Electrophoresis Using L-Histidine Modified Nanoparticles as Chiral Ligand, J Biol & Chem 41 (2013) 29–36.

[13] N. Dat, N.Q. Vượng, T.H. Hanh, Enantioselective separation of ofloxacin by ligand exchange chromatography, Vietnam J Chem 53 (2015) 65–68.

[14] M. Gumustas, S.A. Ozkan, B. Chankvetadze, Analytical and Preparative Scale Separation of Enantiomers of Chiral Drugs by Chromatography and Related Methods, Curr Med Chem 25 (2018) 4152–4188.

[15] A.R.F. Carreira, A.M. Ferreira, M.R. Almeida, J.A.P. Coutinho, T.E. Sintra, Propranolol resolution using enantioselective biphasic systems, Sep Purif Technol 254 (2021) 117682.

[16] B. Schuur, B.J.V. Verkuijl, A.J. Minnaard, J.G. De Vries, H.J. Heeres, B.L. Feringa, Chiral separation by enantioselective liquid–liquid extraction, Org Biomol Chem 9 (2010) 36–51.

[17] Susanti, T.G. Meinds, E.B. Pinxterhuis, B. Schuur, J.G. De Vries, B.L. Feringa, J.G.M. Winkelman, J. Yue, H.J. Heeres, Proof of concept for continuous enantioselective liquid–liquid extraction in capillary microreactors using 1-octanol as a sustainable solvent, Green Chem. 19 (2017) 4334–4343.

[18] B. Zhu, H. Qiu, C. Ma, S. Chen, J. Zhu, S. Tong, Recent progress on chiral extractants for enantioselective liquid-liquid extraction, J Chromatogr A 1709 (2023) 464389.

[19] M. Steensma, N.J.M. Kuipers, A.B. de Haan, G. Kwant, Modelling and experimental evaluation of reaction kinetics in reactive extraction for chiral separation of amines, amino acids and amino-alcohols, Chem Eng Sci 62 (2007) 1395–1407.

[20] F. Jiao, W. Yang, D. Huang, J. Yu, X. Jiang, X. Chen, Enantioseparation of Ofloxacin Enantiomers by Mixed Extractants in Biphasic System, Sep Sci Technol 47 (2012) 1971–1976.

[21] J. Li, H. Cheng, Z. Qi, Enhancement of separation performance for ofloxacin enantiomers by a biphasic recognition chiral extraction system, AIChE Journal (2024) e18367.

[22] F. Jiao, J. Wang, X. Jiang, H. Yang, S. Shi, X. Chen, J. Yu, Biphasic recognition enantioseparation of ofloxacin enantiomers by an aqueous two-phase system, J Chem Technol Biotechnol 90 (2015) 2234–2239.

[23] D. Sun, R. Wang, F. Li, L. Liu, Z. Tan, Enantioselective Extraction of Phenylalanine Enantiomers Using Environmentally Friendly Aqueous Two-Phase Systems, Processes 6 (2018) 212.

[24] M. Moradi, M. Mohammadian, G. Pazuki, S. Shahriari, Partitioning of Crocin in a Novel Aqueous Two-Phase System Composed of a Deep Eutectic Solvent and Acetonitrile, J Chem Eng Data 67 (2022) 1205–1213.

[25] M. Moradi, G. Pazuki, S. Zarei Mahmoudabadi, A comprehensive study of the water stability of eutectic solvents using COSMO-SAC, J Mol Liq 387 (2023) 122605.

[26] M. Moradi, A.M. Ferreira, C.M.S.S. Neves, S.Z. Mahmoudabadi, G. Pazuki, J.A.P. Coutinho, Extraction of ofloxacin from water using hydrophobic eutectic solvents, Data Not Published yet, Article under Revision (2024).

[27] R. Santiago, F.H.B. Sosa, I. Díaz, M. González-Miquel, J.A.P. Coutinho, Predicting Partition Coefficients in Organic Biphasic Systems Using COSMO-RS, Ind Eng Chem Res 62 (2023) 17905–17913.

[28] F. Eckert, A. Klamt, Fast solvent screening via quantum chemistry: COSMO-RS approach, AIChE Journal 48 (2002) 369–385. https://doi.org/10.1002/AIC.690480220.

[29] BIOVIACOSMOtherm, DassaultSystèmes, (2021). https://www. 3ds.com/products/biovia/cosmo-rs/cosmotherm (accessed June 12, 2023).

[30] M. Moradi, S.N. Ashrafizadeh, Nitrate removal from tapwater by means of electrocoagulation-flotation process, Sep Sci Technol 55 (2020) 1577–1587.

[31] S. Ma, F. Li, L. Liu, L. Liao, L. Chang, Z. Tan, Deep-eutectic solvents simultaneously used as the phase-forming components and chiral selectors for enantioselective liquid-liquid extraction of tryptophan enantiomers, J Mol Liq 319 (2020) 114106.

[32] J.M. Saz, M.L. Marina, Recent advances on the use of cyclodextrins in the chiral analysis of drugs by capillary electrophoresis, J Chromatogr A 1467 (2016) 79–94.

[33] B. Zhu, S. Xu, X. Guo, L. Wei, J. Yu, T. Wang, Use of various β-cyclodextrin derivatives as chiral selectors for the enantiomeric separation of ofloxacin and its five related substances by capillary electrophoresis, J Sep Sci 40 (2017) 1784–1795.

[34] T. De Boer, R. Mol, R.A. De Zeeuw, G.J. De Jong, K. Ensing, Enantioseparation of ofloxacin in urine by capillary electrokinetic chromatography using charged cyclodextrins as chiral selectors and assessment of enantioconversion, Electrophoresis (2001).

[35] D. Boczar, K. Michalska, Cyclodextrin Inclusion Complexes with Antibiotics and Antibacterial Agents as Drug-Delivery Systems—A Pharmaceutical Perspective, Pharmaceutics 14 (2022).

[36] Q. Ma, W. Cong, Y. Liu, Z. Geng, Y. Lin, Z. Wang, Experimental and computational study on the enantioseparation of four chiral fluoroquinolones by capillary electrophoresis with sulfated-β-cyclodextrin as chiral selector, Chirality 33 (2021) 549–557.

[37] F.E.O. Suliman, A.A. Elbashir, O.J. Schmitz, Study on the separation of ofloxacin enantiomers by hydroxyl-propyl-β-cyclodextrin as a chiral selector in capillary electrophoresis: A computational approach, J Incl Phenom Macrocycl Chem 83 (2015) 119–129.

[38] G. Tóth, R. Mohácsi, Á. Rácz, A. Rusu, P. Horváth, L. Szente, S. Béni, B. Noszál, Equilibrium and structural characterization of ofloxacin-cyclodextrin complexation, J Incl Phenom Macrocycl Chem 77 (2013) 291–300.

[39] X. Liang, L. Zhao, M. Deng, L. Liu, Y. Ma, X. Guo, Separation of Ofloxacin and Its Six Related Substances Enantiomers by Chiral Ligand-Exchange Chromatography, Chirality 27 (2015) 843–849.

[40] I. Khan, K.A. Kurnia, T.E. Sintra, J.A. Saraiva, S.P. Pinho, J.A.P. Coutinho, Assessing the activity coefficients of water in cholinium-based ionic liquids: Experimental measurements and COSMO-RS modeling, Fluid Phase Equilib 361 (2014) 16–22.

[41] M. Fillet, I. Bechet, P. Hubert, J. Crommen, Resolution improvement by use of carboxymethyl-β-cyclodextrin as chiral additive for the enantiomeric separation of basic drugs by capillary electrophoresis, J Pharm Biomed Anal 14 (1996) 1107–1114.

[42] B. Chankvetadze, W. Linder, G.K.E. Schriba, Enantiomer separations in capillary electrophoresis in the case of equal binding constants of the enantiomers with a chiral selector: Commentary on the feasibility of the concept, Anal Chem 76 (2004) 4256–4260.

[43] European Food Safety Authority, Conclusion on the peer review of the pesticide risk assessment of the active substance Fatty acids C7 to C18 (approved under Regulation (EC) No 1107/2009 as Fatty acids C7 to C20), EFSA Journal 11 (2013) 3023.

[44] K. Boyle, K. Leifer, IIFG Decision documents on reassessment of exemptions from the requirement of a tolerance for fatty acids, Washington, 2002. https://www3.epa.gov/pesticides/chem_search/cleared_reviews/csr_PC-079029_31-Jul-02_a.pdf (accessed March 20, 2024).

[45] C. Florindo, F. Lima, L.C. Branco, I.M. Marrucho, Hydrophobic Deep Eutectic Solvents: A Circular Approach to Purify Water Contaminated with Ciprofloxacin, ACS Sustain Chem Eng 7 (2019) 14739–14746.

[46] J.M. Silva, E. Silva, R.L. Reis, A.R.C. Duarte, A closer look in the antimicrobial properties of deep eutectic solvents based on fatty acids, Sustain Chem Pharm 14 (2019) 100192.

[47] J.M. Silva, C. V Pereira, F. Mano, E. Silva, V.I.B. Castro, I. Sá-Nogueira, R.L. Reis, A. Paiva, A.A. Matias, A.R.C. Duarte, Therapeutic Role of Deep Eutectic Solvents Based on Menthol and Saturated Fatty Acids on Wound Healing, ACS Appl Bio Mater 2 (2019) 4346–4355.

[48] U.S. Food and Drug Administration, Food Additives Permitted for Direct Addition to Food for Human Consumption, Subpart I — Multipurpose Additives, (2023). https://www.ecfr.gov/current/title-21/chapter-I/subchapter-B/part-172/subpart-I/section-172.860 (accessed March 20, 2024).

# 5. CONCLUSIONS & FUTURE WORK

## 5.1. Conclusions

Liquid-liquid extraction (LLE) is a highly effective and versatile method for the separation of various compounds, including chiral compounds, referred to in this case as enantioselective liquid-liquid extraction (ELLE). LLE offers several advantages, including low energy consumption, continuous operation and easy scale-up. In this study, LLE based on deep eutectic solvents (DESs) was used to develop more cost-effective and sustainable methods for the extraction of ofloxacin (OFX) and the separation of its enantiomers.

In the first step (**Chapter 2**), the stability of a wide range of hydrophilic and hydrophobic DESs was investigated using the Conductor-like Screening Model-Segment Activity Coefficient (COSMO-SAC). In this study, three molar ratios and three different concentrations of hydrogen bond acceptors (HBAs) and hydrogen bond donors (HBDs) were investigated in the presence of water. The COSMO-SAC predictions showed that DESs with more hydrophobic components are more stable in water. In addition, changing the molar ratios and concentrations of the DES components significantly affected their water stability by changing their hydrophobicity or hydrophilicity. To validate the COSMO-SAC predictions, we experimentally investigated the water activities in two- and three-component mixtures of DES components from four selected groups: Menthol: fatty acid, menthol: fatty alcohol, fatty acid: fatty acid and fatty acid: fatty alcohol The experimental results confirmed the predictions of COSMO-SAC and showed that the properties of DESs, such as viscosity and density, are significantly influenced by the hydrophobicity of their components. Increasing the hydrophobicity of DESs by modifying their components or increasing the alkyl chain length decreased their density and solubility in water, but increased their viscosity. Therefore, controlling the hydrophobicity or hydrophilicity of DESs is crucial for the development of stable DESs in water.

In the second step (**Chapter 3**), the ability of four different groups of hydrophobic DESs - especially those with high water stability and low viscosity, such as L-menthol: fatty acid, L-menthol: fatty alcohol, fatty acid: fatty acid and fatty acid: fatty alcohol - to extract ofloxacin (OFX) from water by LLE was investigated. First, the Conductor-like Screening Model for Real Solvent (COSMO-RS) was used for a preliminary screening of twelve selected DESs in three different molar ratios by evaluating the logarithm of partition coefficient of OFX. The most suitable hydrophobic DESs for the extraction of

OFX as predicted by COSMO-RS were then validated by experimental tests. The experimental results confirmed the predictions, indicating that high molar ratios of fatty acids with longer alkyl chains significantly increase the partition coefficient of OFX. The hydrophobic DES composed of decanoic acid (C10 acid) and dodecanoic acid (C12 acid) in a molar ratio of 2:1, proved to be the most effective solvent for OFX extraction. Using the response surface methodology (RSM) model and under optimal conditions - an OFX concentration of 2.5 mg/ml, a volume ratio of HDES to water of 13:10 and a pH of 5.2 - the average values for the partition coefficient and extraction efficiency of OFX were (65 ± 1) and (98.8 ± 0.9)%, respectively. These results highlight the importance of selecting suitable solvents and optimizing extraction parameters to significantly enhance the efficiency of extraction processes.

In the final step (**Chapter 4**), the separation of OFX enantiomers was investigated using three different groups of hydrophobic DESs that had shown the highest efficiency in the extraction of OFX. In addition, the potential of neutral and anionic derivatives of beta-cyclodextrin (β-CD), including β-CD, hydroxypropyl-β-CD, sodium carboxymethyl-β-CD (CM-β-CD), and sodium sulfate-β-CD, in the enantioseparation of OFX was evaluated by 19F NMR spectroscopy. Preliminary screening identified CM-β-CD as the most effective chiral selector for the separation of OFX enantiomers. Subsequently, the efficiency of the HDES-based ELLE system was investigated, revealing that higher molar ratios of fatty acids in combination with longer alkyl chains significantly improved the separation of OFX enantiomers. As a result, the hydrophobic DES composed of decanoic acid (C10 acid) and dodecanoic acid (C12 acid) in a molar ratio of 1:2 was selected as the most suitable solvent for enantioseparation among those investigated. After, the variables affecting the enantioseparation process, including pH, excess chiral selector, and the volume ratio between hydrophobic DES and water, were investigated and optimized using RSM. The results showed that pH and chiral selector concentration significantly affected the separation coefficient of OFX, while the volume ratio between hydrophobic DES and water had a negligible effect. Under optimal conditions - a pH of 3.6, a volume ratio between hydrophobic DES and water of 0.54 and a 77-fold molar excess of the chiral selector - the maximum separation factor ($\alpha$ = 3.8 ± 0.3) for OFX was achieved in a single extraction step. These results underline the importance of selecting suitable solvents and chiral selectors as well as optimizing the extraction parameters to significantly enhance the efficiency of ELLE for the separation of chiral compounds.

The work presented in this thesis demonstrates that COSMO is a powerful tool capable of rapidly contributing to the rational development of DESs with specific properties tailored for industrial and environmental applications. Additionally, this study highlights the potential of DES-based ELLE methods for the separation of OFX enantiomers, a widely used quinolone antibiotic. This finding has significant implications for the pharmaceutical industry, as the ability to commercialize chiral drugs in their single-enantiomer form can greatly enhance drug efficacy and safety.

## 5.2. Future work

As future work and taking advantage of the results achieved and discussed above, it would be interesting to:

- Utilize the high efficiency of hydrophobic DES-based LLE for the extraction and separation of various hydrophobic compounds from water sources. This would extend the application of hydrophobic DES beyond OFX to a broader range of hydrophobic substances.
- Explore a wider range of DES components to develop even more effective solvents for the LLE of chiral compounds. This research could optimize solvent properties for specific extraction needs.
- Investigate the applicability of hydrophobic DES-based ELLE to separate other chiral compounds beyond OFX. This exploration could reveal the versatility of hydrophobic DES in chiral separation. Additionally, assess the potential of using DES not only as phase-forming agents but also as chiral selectors simultaneously. This dual functionality could significantly enhance the efficiency and selectivity of chiral separations.
- Explore the use of hydrophobic DES-based ELLE combined with $^{19}F$ NMR spectroscopy to separate other chiral compounds containing fluorine, such as citalopram and fluoxetine. This method offers a more straightforward and cost-effective alternative to other analytical techniques.
- Utilize molecular simulations for a detailed examination of hydrophobic DES-based extraction systems for the separation of chiral compounds. This approach can provide valuable insights into the effective interactions between chiral drugs, chiral agents, and solvents, enhancing the design and optimization of these systems.

- Develop and optimize processes for the recovery and reuse of DESs after extraction. This includes investigating the efficiency and feasibility of DES regeneration techniques to reduce waste and enhance the overall sustainability of DES-based extraction systems.
- Conduct detailed toxicological and biocompatibility assessments of DESs to ensure their safe use in pharmaceutical and industrial processes. Understanding the potential health effects of DES components is crucial for their application in sensitive areas.
- Investigate the biodegradability and environmental safety of DES solvents. Perform comprehensive environmental impact assessments of DESs compared to conventional volatile organic solvents, including a lifecycle analysis to evaluate the overall sustainability and potential environmental benefits of DESs.

# 6. SCIENTIFIC CONTRIBUTION

## 6.1. Scientific contributions related to this thesis

### 6.1.1. Peer-reviewed Journals

- **Mahtab Moradi**, Ana M. Ferreira, Catarina M.S.S. Neves, Filipe H.B. Sosa, Gholamreza Pazuki, João A.P. Coutinho, "Enantioseparation of ofloxacin using liquid-liquid system based on hydrophobic eutectic solvents". *Separation and Purification Technology*. (Accepted).

- **Mahtab Moradi**, Ana M. Ferreira, Catarina M.S.S. Neves, Samane Zarei Mahmoudabadi, Gholamreza Pazuki, João A.P. Coutinho, "Extraction of ofloxacin from water using hydrophobic eutectic solvents". *Journal of Environmental Chemical Engineering*. 2024, 12, (3), 113075. https://doi.org/10.1016/j.jece.2024.113075

- **Mahtab Moradi**, Samane Zarei Mahmoudabadi, Gholamreza Pazuki, "A comprehensive study of the water stability of eutectic solvents using COSMO-SAC". *Journal of Molecular Liquids*. 2023, 387, 122605. https://doi.org/10.1016/j.molliq.2023.122605

### 6.1.2. Manuscript under preparation

- **Mahtab Moradi**, Ana M. Ferreira, Gholamreza Pazuki, João A.P. Coutinho, "Separation of chiral compounds using liquid-liquid system: A review".

### 6.1.3. Conference Presentations

- **Mahtab Moradi,** Ana M. Ferreira, Catarina M.S.S. Neves, Filipe H.B. Sosa, Gholamreza Pazuki, João A.P. Coutinho, "Enantioselective liquid-liquid extraction of ofloxacin using hydrophobic eutectic solvents and β-cyclodextrin derivatives", 7th Edition of the Iberoamerican Meeting on Ionic Liquids (IMIL2024), Coimbra (Portugal), November 20-22, 2024. (Poster, Submitted)

- **Mahtab Moradi**, Ana M. Ferreira, Catarina M.S.S. Neves, Filipe H.B. Sosa, Gholamreza Pazuki, João A.P. Coutinho, "Enhanced enantioselective liquid-liquid extraction of ofloxacin using hydrophobic eutectic solvents and β-cyclodextrin derivatives", XIII Iberoamerican Conference on Phase Equilibria

and Fluid Properties for Process Design (EQUIFASE 2024), Évora (Portugal), September 9-12, 2024. (Poster, Accepted)

- **Mahtab Moradi,** Samane Zarei Mahmoudabadi, Ana M. Ferreira, Catarina M.S.S. Neves, João A.P. Coutinho, Gholamreza Pazuki, "Designing deep eutectic solvents for enantioseparation of ofloxacin using COSMO-SAC", Biopartitioning and Purification Conference (BBP 2022), Aveiro (Portugal), September 25-28, 2022. (Poster)
- **Mahtab Moradi,** Samane Zarei Mahmoudabadi, Ana M. Ferreira, Catarina M.S.S. Neves, João A.P. Coutinho, Gholamreza Pazuki, "Using COSMO-SAC to design eutectic solvents for separation of ofloxacin enantiomers by liquid-liquid extraction", Jornadas CICECO 2022, Aveiro (Portugal), October 12, 2022. (Poster)

## 6.2. Others scientific contributions

### 6.2.1. Peer-reviewed Journals

- **Moradi, Mahtab**, Mona Mohammadian, Gholamreza Pazuki, Shahla Shahriari. "Partitioning of Crocin in a Novel Aqueous Two-Phase System Composed of a Deep Eutectic Solvent and Acetonitrile." *Journal of Chemical & Engineering Data*. 2022, 67, (5), 1205–1213. https://doi.org/10.1021/acs.jced.2c00027
- **Mahtab Moradi**, Seyed Nezameddin Ashrafizadeh, "Nitrate removal from tapwater by means of electrocoagulation-flotation process," *Separation Science and Technology*. 2019, 55, (2), 1577-1587. https://doi.org/10.1080/01496395.2019.1602143

### 6.2.2. Manuscript under preparation

- Sara Yazdani, **Mahtab Moradi,** Augusto Q. Pedro, Gholamreza Pazuki, Ana M. Ferreira, João A.P. Coutinho, "Bioprocessing Strategies for Massive Production of Recombinant Protein".

### 6.2.3. Conference Presentations

**Mahtab Moradi** & Gholamreaza Pazuki, “The Modeling of Peng–Robinson, Soave-Redlich-Kwong and Pazuki equations of state to predict the solubility of Amiodarone Hydrochloride, Ketotifen fumarate and Celecoxib in supercritical carbon dioxide.” The 11 th International Chemical Engineering Congress & Exhibition (IChEC 2020) Fouman, Iran, April, 2020. (Oral)

# APPENDICES

# Appendix A

## Tables

**Table A.1.** The list of HBAs used in COSMO-SAC.

| Number | Categorization | Name | Abbreviation |
|---|---|---|---|
| 1 | Quaternary ammonium salt | Tetraoctylammonium Bromide | $[N_{8888}]$ Br |
| 2 | Quaternary ammonium salt | Tetraoctylammonium Chloride | $[N_{8888}]$ Cl |
| 3 | Quaternary ammonium salt | Tetraheptylammonium Bromide | $[N_{7777}]$ Br |
| 4 | Quaternary ammonium salt | Tetraheptylammonium Chloride | $[N_{7777}]$ Cl |
| 5 | Quaternary ammonium salt | Tetrabutylammonium Bromide | $[N_{4444}]$ Br |
| 6 | Quaternary ammonium salt | Tetrabutylammonium Chloride | $[N_{4444}]$ Cl |
| 7 | Quaternary ammonium salt | Tetrapropylammonium Bromide | $[N_{3333}]$ Br |
| 8 | Quaternary ammonium salt | Tetrapropylammonium Chloride | $[N_{3333}]$ Cl |
| 9 | Quaternary ammonium salt | Tetramethylammonium Bromide | $[N_{1111}]$ Br |
| 10 | Quaternary ammonium salt | Tetramethylammonium Chloride | $[N_{1111}]$ Cl |
| 11 | Quaternary ammonium salt | Choline Chloride | [Ch]Cl |
| 12 | Terpene | Thymol | Thy |
| 13 | Terpene | Menthol | ML |
| 14 | Terpene | Borneol | BN |
| 15 | Amino acid (AA) | Phenylalanine | Phe |
| 16 | Amino acid (AA) | Betaine | Bet |
| 17 | Fatty acid | Octadecanoic acid | OctadecA |
| 18 | Fatty acid | Hexadecanoic acid | HexadecA |
| 19 | Fatty acid | Tetradecanoic acid | TetradecA |
| 20 | Fatty acid | Dodecanoic acid | DodecA |
| 21 | Fatty acid | Decanoic acid | DecA |
| 22 | Fatty acid | Octanoic acid | OctaA |

**Table A.2.** The list of HBDs used in COSMO-SAC.

| Number | Categorization | Name | Abbreviation |
|---|---|---|---|
| 1 | Suger | Glucose | Glu |
| 2 | Carbamide (CA) | Urea | U |
| 3 | Alcohol | Glycerol | Gly |
| 4 | Alcohol | Ethyleneglycol | EtGly |
| 5 | Alcohol | 1,3-propanediol | 1.3-prop |
| 6 | Alcohol | 1,2-Butanediol | 1,2-but |
| 7 | Alcohol | Propyl alcohol | PrOH |
| 8 | Alcohol | Butyl alcohol | BuOH |
| 9 | Alcohol | Cyclohexanol | CH-ol |
| 10 | Alcohol | Hexafluoroisopropanol | HFIP |
| 11 | Alcohol | 4-Cyanophenol | 4-CP |
| 12 | Alcohol | 1-Phenylethanol | PhE |
| 13 | Alcohol | 1-Hexanol | 1hol |
| 14 | Fatty alcohol | 1-Octanol | 1ol |
| 15 | Fatty alcohol | 1-Decanol | 1dol |
| 16 | Fatty alcohol | 1-Dodecanol | 1dodol |
| 17 | Fatty alcohol | 1-Tetradecanol | Tetradol |
| 18 | Fatty alcohol | Hexadecanol | Hexadol |
| 19 | Fatty alcohol | Oleyl alcohol | OA |
| 20 | Carboxylic acid | Tartaric acid | TA |
| 21 | Carboxylic acid | Glycolic acid | GA |
| 22 | Carboxylic acid | Lactic acid | LA |
| 23 | Carboxylic acid | Malonic acid | MLA |
| 24 | Carboxylic acid | Acetic acid | AC |
| 25 | Carboxylic acid | Levulinic acid | LvA |
| 26 | Carboxylic acid | Pyruvic acid | Pyr |
| 27 | Carboxylic acid | Propionic acid | PA |
| 28 | Carboxylic acid | Phenyl salicylate | PS |
| 29 | Carboxylic acid | Mandelic acid | MdA |
| 30 | Carboxylic acid | Butyric acid | BTA |

| | | | |
|---|---|---|---|
| 31 | Carboxylic acid | Phenylacetic acid | PlA |
| 32 | Carboxylic acid | Hexanoic acid | HA |
| 33 | Fatty acid | Octanoic acid | OA |
| 34 | Fatty acid | Nonanoic acid | NAA |
| 35 | Fatty acid | Decanoic acid | DecA |
| 36 | Fatty acid | 10-undecylenic acid | UD |
| 37 | Fatty acid | undecanoic acid | UDA |
| 38 | Fatty acid | Dodecanoic acid | DodeA |
| 39 | Fatty acid | Tetradecanoic acid | TetA |
| 40 | Fatty acid | Ricinoleic acid | RA |
| 41 | Fatty acid | Hexadecanoic acid | HexaA |
| 42 | Fatty acid | Oleic acid | OleA |
| 43 | Fatty acid | Stearic acid | SA |
| 44 | Terpene | Camphor | CM |

**Table A.3.** The experimental values of water activities in binary and ternary mixtures for the selected DESs.

| DES (HBA: HBD) | Molar ratio (HBA: HBD) | Molalities (HBA:HBD, mol/kg) | $a_{wA}^{0}$ (water+HBA) | $a_{wB}^{0}$ (water+HBD) | $a_w$ (water+HBA+HBD) | $\Delta a_w$ |
|---|---|---|---|---|---|---|
| Menthol: Octanoic | (1:1) | 1.25:1.25 | 0.955 ± 0.001 | 0.967 ± 0.003 | 0.96 ± 0.001 | 0.038 |
| | | 2.5:2.5 | 0.949 ± 0.004 | 0.967 ± 0.003 | 0.956 ± 0.003 | 0.04 |
| | | 3.75:3.75 | 0.944 ± 0.003 | 0.963 ± 0.001 | 0.951 ± 0.001 | 0.044 |
| Menthol: Decanoic | (2:1) | 2.5: 1.25 | 0.96 ± 0 | 0.961 ± 0.003 | 0.963 ± 0.001 | 0.042 |
| | | 5: 2.5 | 0.96 ± 0.003 | 0.957 ± 0.001 | 0.960 ± 0.001 | 0.043 |
| | | 7.5: 3.75 | 0.946 ± 0.004 | 0.957 ± 0.003 | 0.95 ± 0.003 | 0.047 |
| Menthol: 1-Decanol | (1:2) | 0.625:1.25 | 0.955 ± 0.003 | 0.965 ± 0.003 | 0.966 ± 0.001 | 0.046 |
| | | 1.25:2.5 | 0.955 ± 0.001 | 0.965 ± 0.001 | 0.966 ± 0.003 | 0.046 |
| | | 1.875:3.75 | 0.944 ± 0.003 | 0.961 ± 0.002 | 0.957 ± 0.001 | 0.052 |
| Menthol: 1-Dodecanol | (1:2) | 0.625:1.25 | 0.955 ± 0.003 | 0.962 ± 0.001 | 0.977 ± 0.003 | 0.06 |
| | | 1.25:2.5 | 0.955 ± 0.001 | 0.947 ± 0.003 | 0.964 ± 0.001 | 0.062 |
| | | 1.875:3.75 | 0.944 ± 0.003 | 0.947 ± 0.001 | 0.96 ± 0.001 | 0.069 |
| Octanoic; Decanoic | (2:1) | 2.5:1.25 | 0.968 ± 0.001 | 0.961 ± 0.003 | 0.972 ± 0.003 | 0.043 |
| | | 5:2.5 | 0.965 ± 0.001 | 0.957 ± 0.001 | 0.967 ± 0.001 | 0.045 |
| | | 7.5:3.75 | 0.955 ± 0.002 | 0.957 ± 0.003 | 0.962 ± 0.004 | 0.050 |
| Octanoic: Dodecanoic acid | (2:1) | 2.5:1.25 | 0.968 ± 0.001 | 0.953 ± 0.003 | 0.97 ± 0.001 | 0.049 |
| | | 5:2.5 | 0.965 ± 0.001 | 0.944 ± 0.001 | 0.962 ± 0 | 0.053 |
| | | 7.5:3.75 | 0.955 ± 0.002 | 0.929 ± 0.003 | 0.948 ± 0.001 | 0.064 |
| Octanoic: 1-Decanol | (1:2) | 0.625:1.25 | 0.967 ± 0.001 | 0.965 ± 0.003 | 0.981 ± 0.003 | 0.049 |
| | | 1.25:2.5 | 0.967 ± 0.003 | 0.965 ± 0.001 | 0.983 ± 0.003 | 0.051 |
| | | 1.875:3.75 | 0.963 ± 0.003 | 0.961 ± 0.002 | 0.981 ± 0.003 | 0.057 |
| Octanoic:1-Dodecanol | (1:2) | 0.625:1.25 | 0.967 ± 0.001 | 0.962 ± 0.001 | 0.989 ± 0.003 | 0.06 |
| | | 1.25:2.5 | 0.967 ± 0.003 | 0.947 ± 0.003 | 0.973 ± 0.001 | 0.059 |
| | | 1.875:3.75 | 0.963 ± 0.003 | 0.947 ± 0.001 | 0.974 ± 0.001 | 0.064 |
| Decanoic: 1-Decanol | (1:2) | 0.625:1.25 | 0.961 ± 0.001 | 0.965 ± 0.003 | 0.981 ± 0.004 | 0.055 |
| | | 1.25:2.5 | 0.961± 0.003 | 0.965 ± 0.001 | 0.981± 0.003 | 0.055 |
| | | 1.875:3.75 | 0.93 ± 0.001 | 0.961 ± 0.002 | 0.96 ± 0.003 | 0.069 |
| Decanoic:1-Dodecanol | (1:2) | 0.625:1.25 | 0.961 ± 0.001 | 0.962 ± 0.001 | 0.982 ± 0.003 | 0.059 |
| | | 1.25:2.5 | 0.961 ± 0.03 | 0.947 ± 0.003 | 0.979 ± 0.001 | 0.071 |
| | | 1.875:3.75 | 0.93 ± 0.001 | 0.947 ± 0.001 | 0.948 ± 0.001 | 0.071 |

**Table A.4.** A description of measured and calculated $\Delta a_w$.

| | | | |
|---|---|---|---|
| $\Delta P_A^0 = (a_{WA}^0 - 1).P^*$ | $\Delta P_B^0 = (a_{WB}^0 - 1).P^*$ | $\Delta P = (a_w - 1).P^*$ | |
| $P_A^0 = a_{WA}^0 . P^0$ | + $P_B^0 = a_{WB}^0 . P^0$ | $P = a_w . P^*$ | + $P^*$ |
| $m_A$ in 1 kg water | $m_B$ in 1 kg water | $m_A$ and $m_B$ in 1 kg water | 1 kg water |
| $\Delta P_A^0 + \Delta P_B^0 = \Delta P$ | | $a_{WA}^0 + a_{WB}^0 = a_w + 1$ | |
| $\Delta a_w = 1 + a_w - (a_{wA}^0 + a_{wB}^0)$ | | | |
| Calculated $\Delta a_w$ | | Measured $\Delta a_w$ | |
| $a_{wA}^0 = \gamma_{wA}^0 . x_{wA}$ | | $P_A^0 = a_{WA}^0 . P^0$ | |
| $a_{wB}^0 = \gamma_{wB}^0 . x_{wB}$ | | $P_B^0 = a_{WB}^0 . P^0$ | |
| $a_w = \gamma_w . x_w$ | | $P = a_w . P^*$ | |

$P^*$, $\Delta P = P - P^*$, and $\Delta P_i^0 = P_i^0 - P^*$ respectively represent the vapor pressure of pure water, the vapor pressure depressions for ternary (A+B+water) and binary (A+water or B+water) solutions under the same solute molality condition.

**Table A.5.** The experimental values of densities, viscosities and speed of sound

| **DES (HBA: HBD)** | **Molar ratio (HBA: HBD)** | **Viscosity (mPa.s)** | **Density ($g/cm^3$)** | **Speed of sound (m/s)** |
|---|---|---|---|---|
| Menthol: Octanoic | (1:1) | 11.521 | 0.901464 | 1336.13 |
| Menthol: Decanoic | (2:1) | 13.3065 | 0.896569 | 1355.39 |
| Menthol: Dodecanoic acid | (2:1) | 18.2845 | 0.893454 | 1368.32 |
| Menthol: 1-Decanol | (1:2) | 13.4412 | 0.848806 | 1376.16 |
| Menthol: 1-Dodecanol | (1:2) | 15.0032 | 0.848146 | 1393.69 |
| Octanoic: Decanoic acid | (2:1) | 7.4823 | 0.901716 | 1314.78 |
| Octanoic: Dodecanoic acid | (2:1) | 8.6152 | 0.898871 | 1327.52 |
| Decanoic: Dodecanoic acid | (2:1) | 10.5285 | 0.89274 | 1348.51 |
| Octanoic: 1-Decanol | (1:2) | 9.536 | 0.851932 | 1368.19 |
| Octanoic: 1-Dodecanol | (1:2) | 11.6887 | 0.850241 | 1385.68 |
| Decanoic: 1-Decanol | (1:2) | 8.7589 | 0.849824 | 1359.31 |
| Decanoic:1- Dodecanol | (1:2) | 10.0661 | 0.849636 | 1378.68 |

## Figures

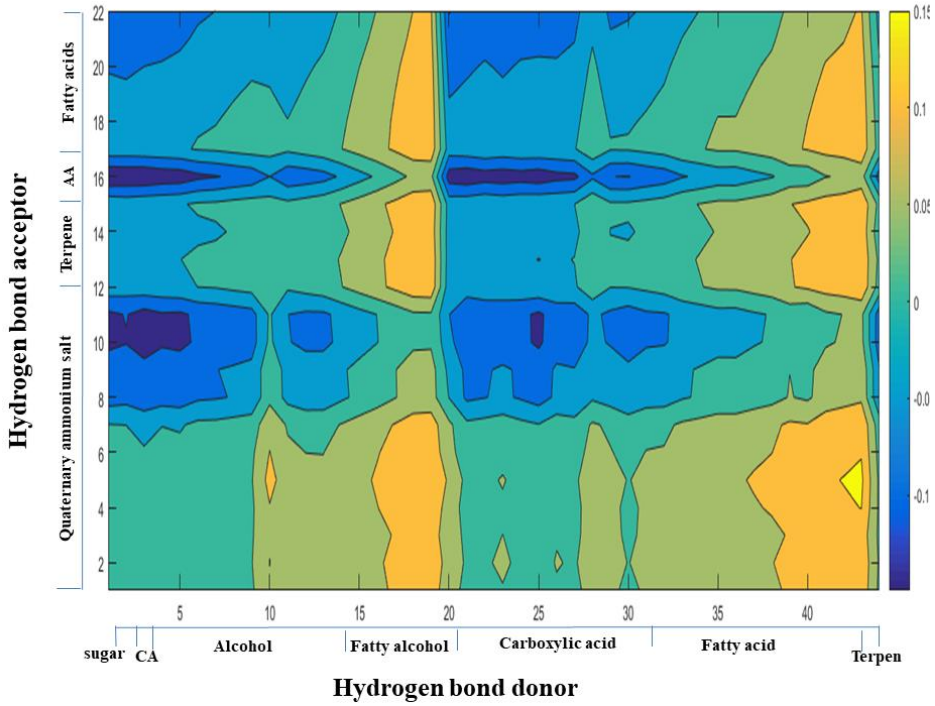


**Figure A.1.** Predicted $\Delta a_w$ in the molar ratio (2:1) and at molalities 2.5 mol/kg: 1.25 mol/kg of the HBA: HBD, at 25 °C using COSMO-SAC.

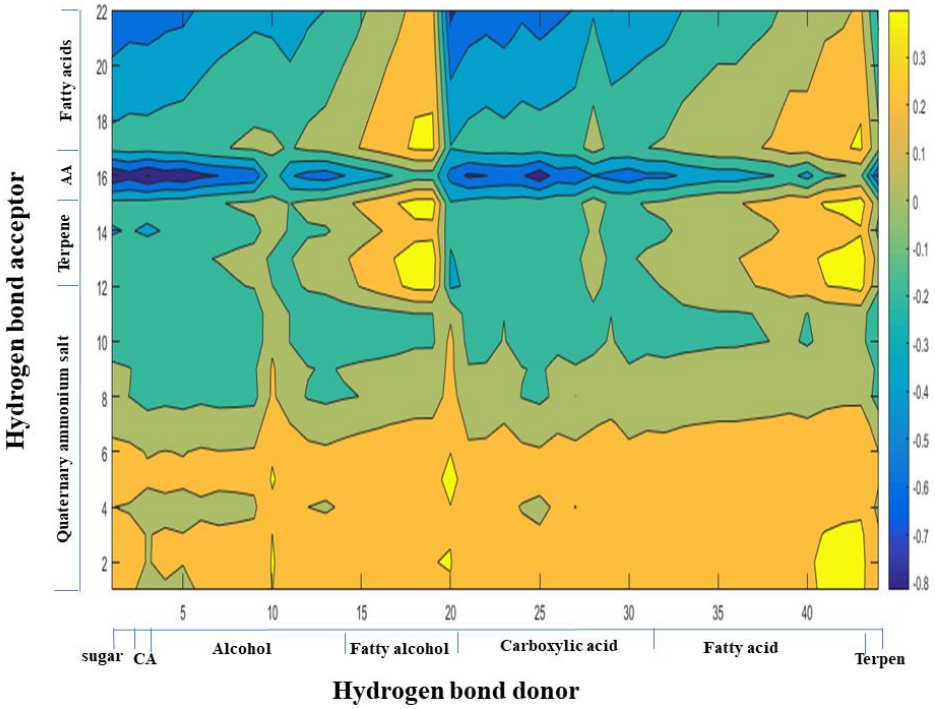


**Figure A.2.** Predicted $\Delta a_w$ in the molar ratio (2:1) and at molalities 7.5 mol/kg: 3.75 mol/kg of the HBA: HBD, at 25 °C using COSMO-SAC.

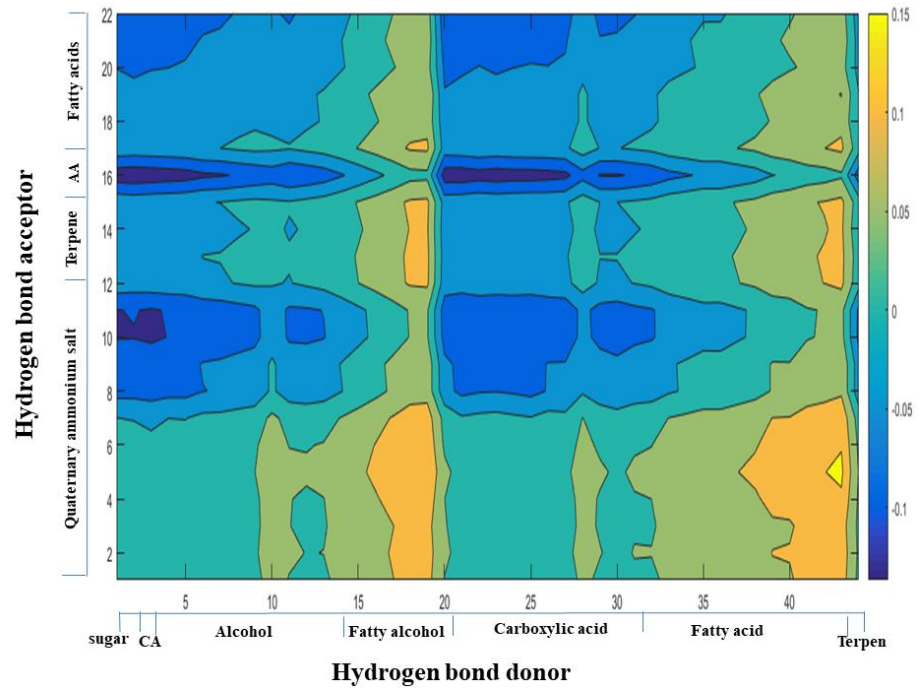


**Figure A.3.** Predicted $\Delta a_w$ in the molar ratio (1:1) and at molalities 1.25 mol/kg: 1.25 mol/kg of the HBA: HBD, at 25 °C using COSMO-SAC.

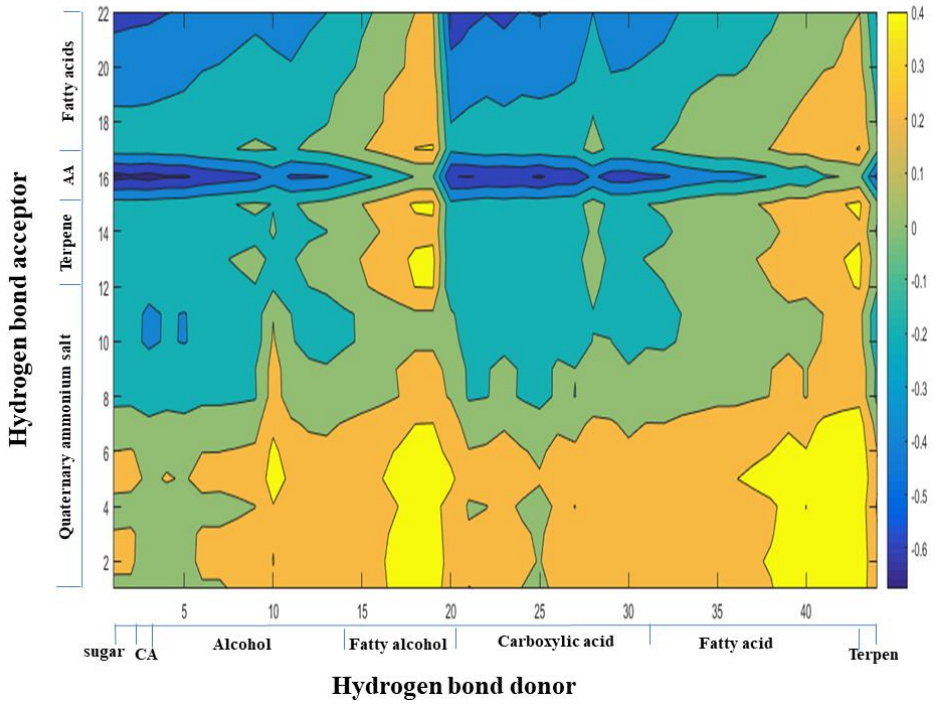


**Figure A.4.** Predicted $\Delta a_w$ in the molar ratio (1:1) and at molalities 3.75 mol/kg: 3.75 mol/kg of the HBA: HBD, at 25 °C using COSMO-SAC.

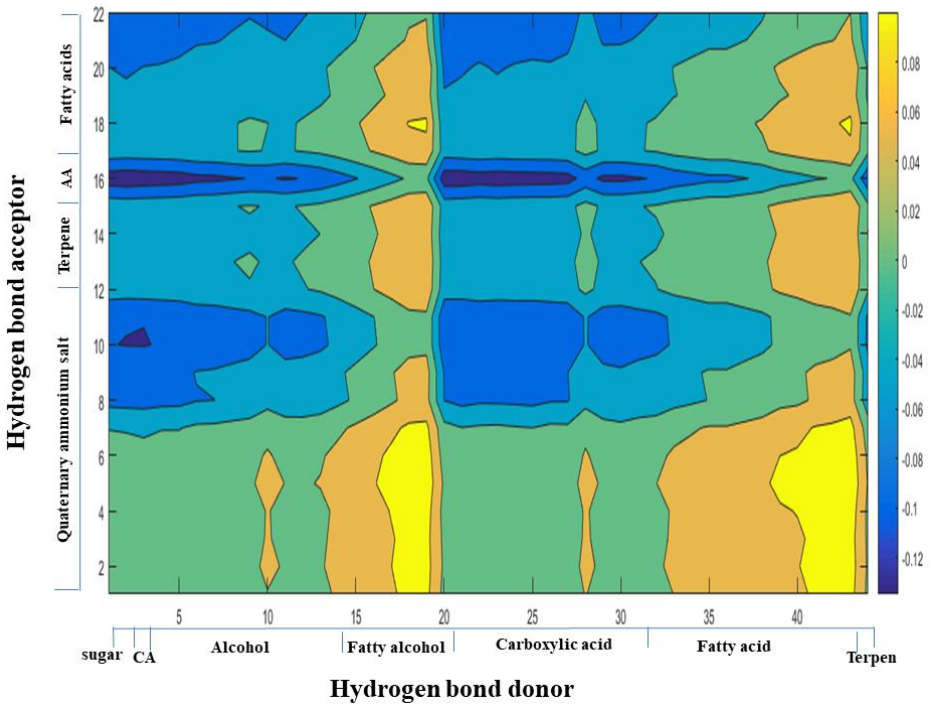


**Figure A.5.** Predicted $\Delta a_w$ in the molar ratio (1:2) and at molalities 0.625 mol/kg: 1.25 mol/kg of the HBA: HBD, at 25 °C using COSMO-SAC.

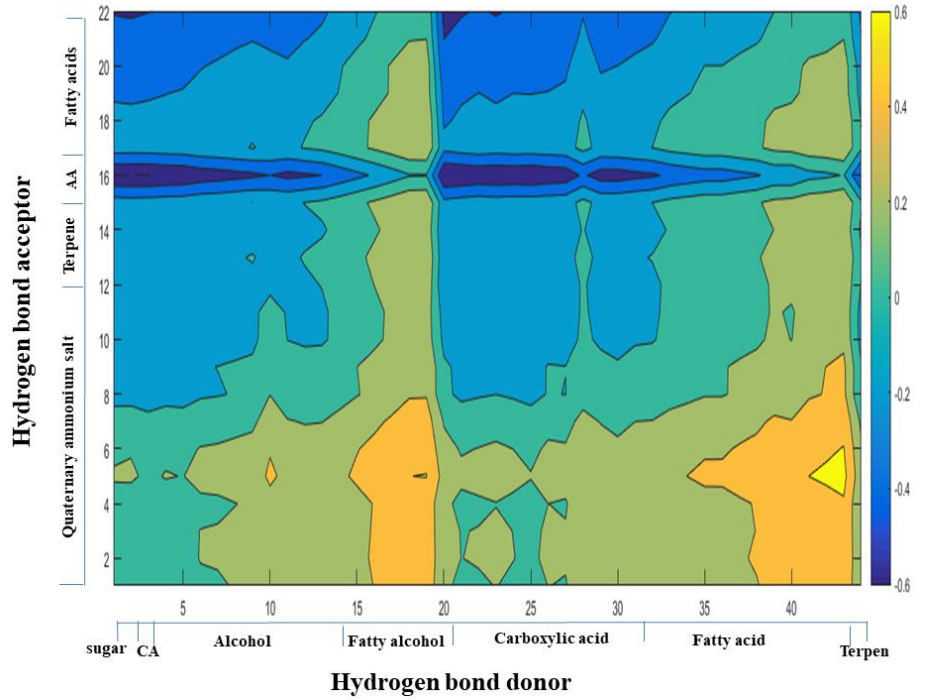


**Figure A.6.** Predicted $\Delta a_w$ in the molar ratio (1:2) and at molalities 1.875 mol/kg: 3.75 mol/kg of the HBA: HBD, at 25 °C using COSMO-SAC.

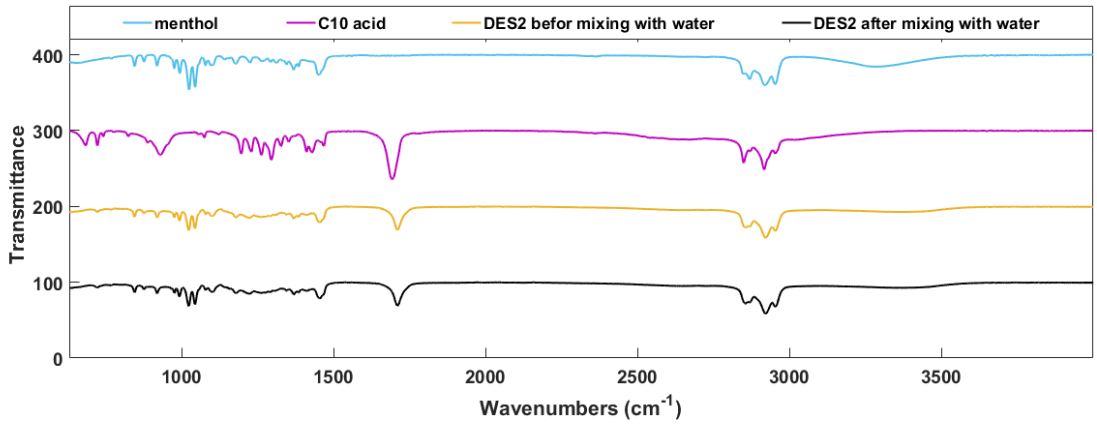


**Figure A.7.** The FT-IR spectra of Menthol: C10 acid and their pure components.

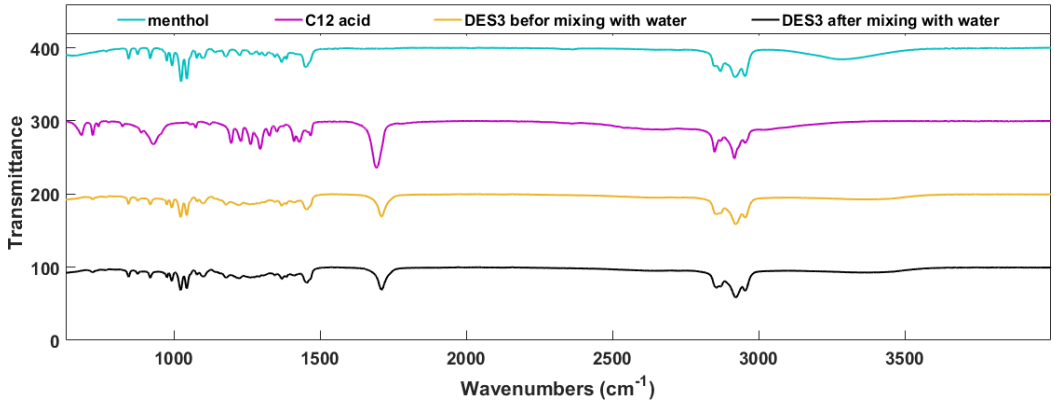


**Figure A.8.** The FT-IR spectra of Menthol: C12 acid and their pure components.

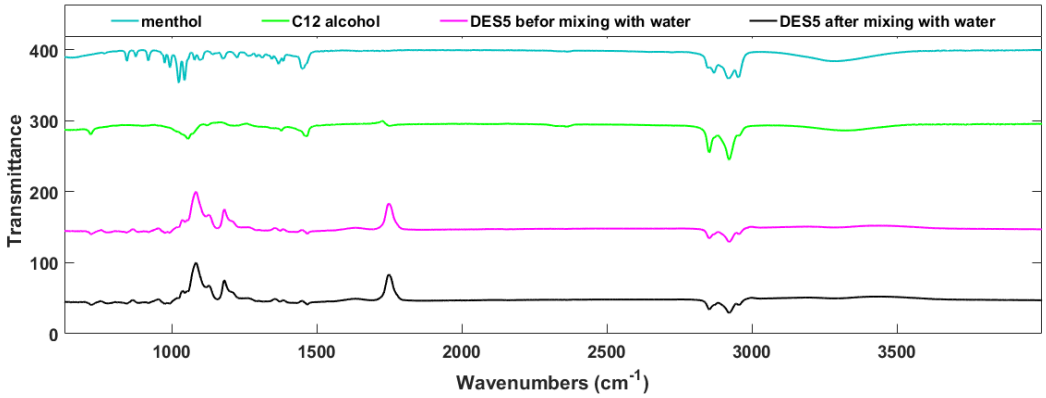


**Figure A.9.** The FT-IR spectra of menthol: C12 alcohol and their pure components.

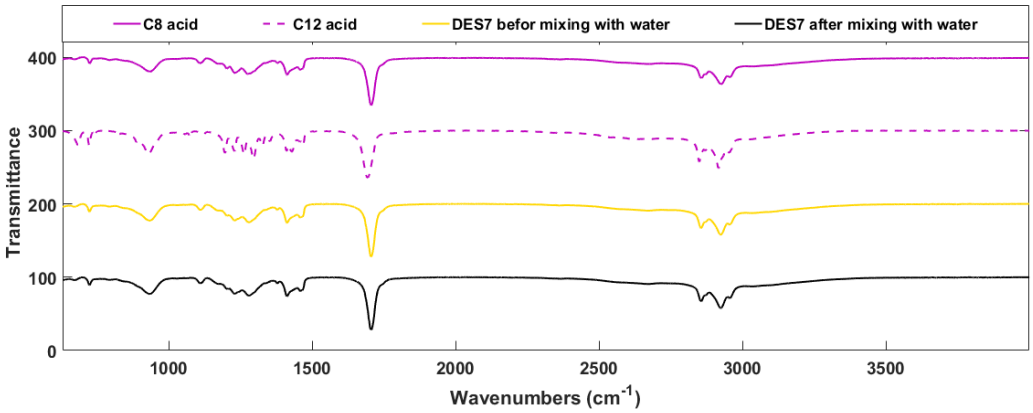


**Figure A.10.** The FT-IR spectra of C8 acid: C12 acid and their pure components.

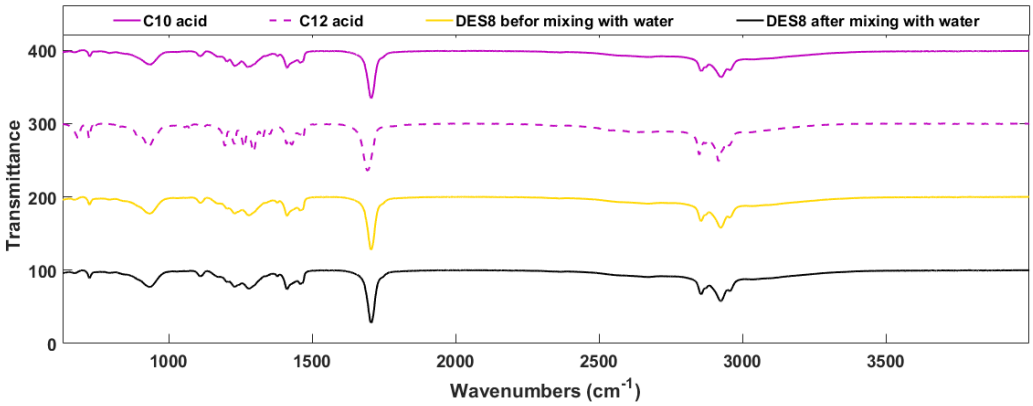


**Figure A.11.** The FT-IR spectra of C10 acid: C12 acid and their pure components.

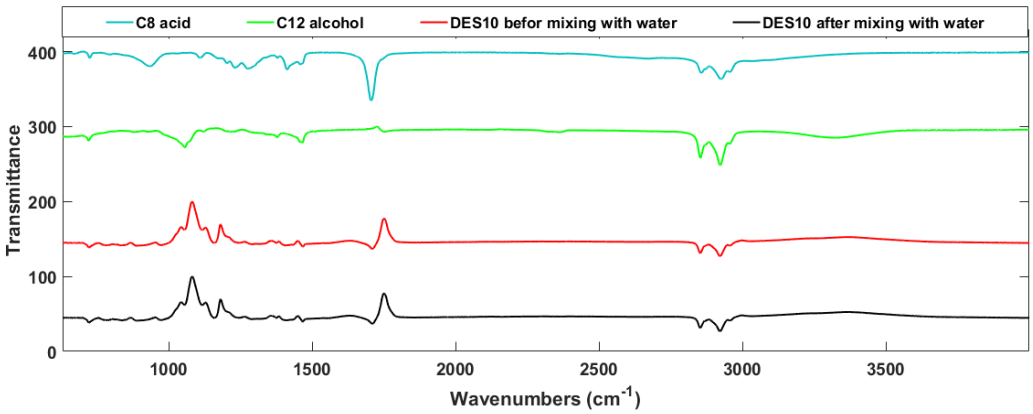


**Figure A.12.** The FT-IR spectra of C8 acid: C12 alcohol and their pure components.

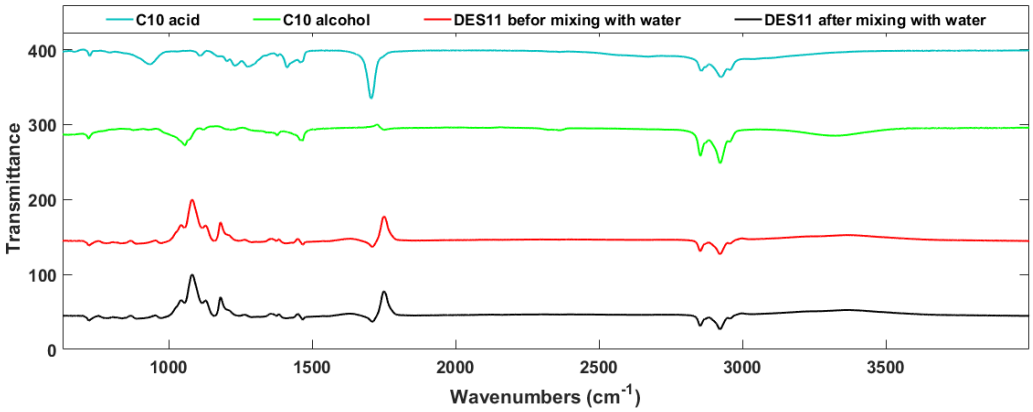


**Figure A.13.** The FT-IR spectra of C10 acid: C10 alcohol and their pure components.

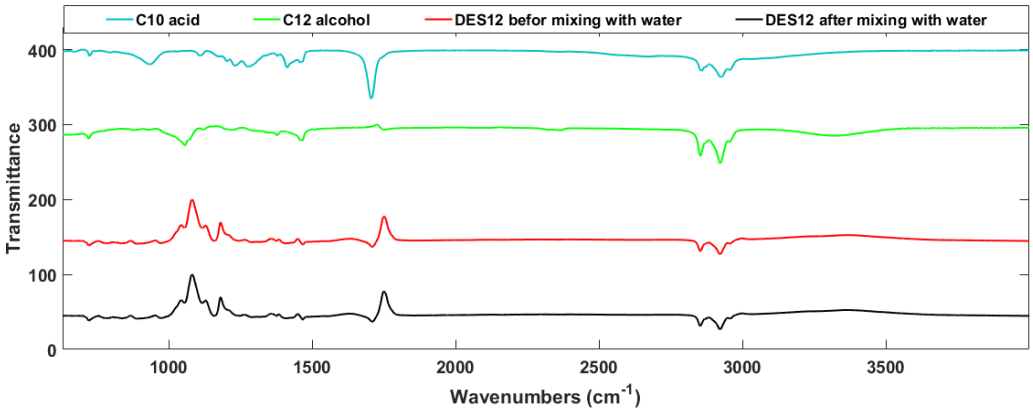


**Figure A.14.** The FT-IR spectra of C10 acid: C12 alcohol and their pure components.

# Appendix B

## Tables

**Table B.1**. Summary of some recent studies employing HDES-based LLE for extracting various pharmaceuticals from water-based samples.

| Analytes | Sample matrix | HDES (mol:mol) | Method | Recovery (%) | Key findings | Ref. |
|---|---|---|---|---|---|---|
| Oxytetracycline, Doxycycline, Tetracycline | Water | Thymol: Octanoic acid (1:1) | Dispersive LLME | 74-113 | Choline chloride: ethylene glycol HDES was used as disperser solvent. Thymol: Octanoic acid HDES was used as extraction solvent. The addition of beta-cyclodextrin (β-CD) to the extraction phase improved extraction efficiencies. | [1] |
| Levofloxacin, Ciprofloxacin | Spiked water | Thymol: Hexanoic acid (2:1) | LLME | 94-110 | Four HDES were used as extraction solvent. The impact of the solution pH, of the phase transition behavior of the HDES was studied. | [2] |
| Salicylic acid, Oxaprozin, Diclofenac, Ibuprofen | Water and Milk | Thymol: 1,1,3,3-tetramethylguanidine chloride (2:1) | Ultrasound-assisted Dispersive LLME | 79–107 | Three HDES composed of guanidinium chloride and thymol, methyltrioctylammonium chloride and thymol, and choline chloride and thymol were used as extraction solvent. | [3] |
| Ofloxacin, Norfloxacin, Ciprofloxacin, Enrofloxacin | Surface water | Thymol: Heptanoic acid (2:1) | LLME | 84–113 | The developed method based on in situ formation of twenty one HDES (composed of thymol, menthol, and camphor and fatty acids) coupled with shaker-assisted LLME (in situ HDES-SA-LLME) was validated. | [4] |
| Sulfamethoxazole, Sulfamethazine, Sulfapyridine | Urine | Vanillin: Menthol (1:1) Vanillin;Thymol (1:1) | LLME | 91–93 | Thymol and Vanillin were used as both media for Schiff bases formation and the precursor of HDES. | [5] |
| Ketoprofen, Diclofenac | Urine | Menthol: Analytes | LLME | 93-97 | The procedure was applied based on in-situ HDES formation and menthol used as extractant solvent. | [6] |
| Terbutaline, Clorprenaline, Tulobuterol, Clenbuterol, Salbutamol | Water | Tetra butyl ammonium chloride: Decanoic acid (1:3) | Dispersive LLME | 56 - 91 | Nine HDES based on quaternary ammonium salts and fatty acids were prepared. | [7] |
| Ciprofloxacin | Water | Decanoic acid: Dodecanoic acid (2:1) | LLE | 90 | Ten HDES based on quaternary ammonium salts, menthol and fatty acids were prepared. | [8] |

| | | | | | | |
|---|---|---|---|---|---|---|
| Tetracycline, Oxytetracycline, Chlortetracycline | Water | Methyltrioctylammonium chloride: Nonanoic acid (1:2) | LLME | 77- 87 | Ten HDES based on quaternary ammonium salts, fatty acids and fatty alcohol as extraction solvents were prepared. | [9] |
| Tetracycline, Doxycycline, Oxytetracycline | Water | Choline chloride: Thymol: Nonanoic acid (1:2:2) | Dispersive LLME | 74–95 | Four new thymol-based ternary HDES were prepared.<br>The HDES hydrophobicity and its effect on the pH of water samples was studied. | [10] |
| Levofloxacin, Ciprofloxacin | Water | Tricaprylylmethylammonium chloride: 1-octanol (1:1) | LLME | 94.8 | Sixteen HDES based on quaternary ammonium salts; fatty acids and fatty alcohol were prepared. | [11] |
| Sulfadiazine, Sulfamerazine, Sulfametoxydiazine, Sulfamethoxazole | Water | Choline chloride: o-cresol<br>Choline chloride: m-cresol<br>Choline chloride: p-cresol (1:2) | Dispersive LLME | 80–93 | The three HDES showed commendable performance for extraction of sulfonamides compared to hydrophilic DESs. | [12] |
| Carbamazepine | Aqueous solution | Menthol: acetic acid (1:1) | Reactive LLE | > 90 | The study used of various carboxylic acid based deep eutectic liquids (DEL) such as menthol: acetic acid / formic acid --Diethyl succinate and DEL were used as diluent and extractant. | [13] |
| Diclofenac | Aqueous solution | DL-menthol: Acetic acid (1:1) | Reactive LLE | 47- 78 | The designed HDES enhanced the removal of diclofenac by more than 2.7 to 4.5 times compared to a conventional solvent.<br>Diethyl succinate and HDES were used as diluent and extractant. | [14] |
| Valsartan | Aqueous solution | L-menthol: (+)-Di-p-toluoyl-D-tartaric Acid (8:1) | LLE | 91 | Four hydrophobic DESs with five hydrophilic DESs were studied for enantioseparation of valsartan. | [15] |

**Table B.2.** Compound, CAS number, molecular weight ($M_w$), supplier, purity, and logarithm of the octanol-water partition coefficients (log$K_{OW}$).

| **Compound** | **CAS number** | **$M_w$ (g/mol)** | **Supplier** | **Purity (wt%)** | **Log$K_{OW}$ [16]** |
|---|---|---|---|---|---|
| Ofloxacin | 82419-36-1 | 361.40 | TCI | 98.0 | 1.56 |
| L-menthol | 1490-04-6 | 156.26 | Acros Organics | 99.5 | 2.66 |
| Octanoic acid | 124-07-2 | 144.21 | Thermo Scientific | 98.0 | 2.7 |
| Decanoic acid | 334-48-5 | 172.26 | Thermo Scientific | 99.0 | 3.59 |
| Dodecanoic acid | 143-07-7 | 200.32 | Acros Organics | 99.0 | 4.48 |
| 1-Decanol | 112-30-1 | 158.28 | TCI | 98.0 | 3.47 |
| 1-Dodecanol | 112-53-8 | 186.33 | Alfa Aesar | 98.0 | 4.36 |

**Table B.3.** Melting points of the selected HDES along with their individual components.

| | Name | Molar ratio (HBA:HBD) | Melting point (°C) | Ref. |
|---|---|---|---|---|
| **Pure compounds** | L-Menthol | - | 42.6 | [17] |
| | 1-Decanol | - | 6.9 | |
| | Octanoic acid | - | 16.4 | |
| | Decanoic acid | - | 31.7 | |
| | Dodecanoic acid | - | 44.4 | |
| **HDES** | L-Menthol: Octanoic acid | (1:1) | -4.35 | [18] |
| | L-Menthol: Octanoic acid | (1:2) | 2.3 | |
| | L-Menthol: Decanoic acid | (1:1) | 13.2 | |
| | L-Menthol: Decanoic acid | (1:2) | 20.1 | |
| | L-Menthol: Decanoic acid | (1:3) | 24.4 | |
| | Octanoic acid: Decanoic acid | (1:1) | 13.84 | [19] |
| | Octanoic acid: Decanoic acid | (2:1) | 6.4 | |
| | Decanoic acid: Dodecanoic acid | (2:1) | 18.1 | [20] |
| | Decanoic acid: Dodecanoic acid | (3:1) | 20.3 | |
| | Octanoic acid: 1-Decanol | (1:1) | -1.3 | [21] |
| | Octanoic acid: 1-Decanol | (2:1) | 3.1 | |
| | Decanoic acid: 1-Decanol | (1:1) | 14.9 | |
| | Decanoic acid: 1-Decanol | (2:1) | 22.4 | |
| | Decanoic acid: 1-Decanol | (3:1) | 24.2 | |

**Table B.4.** Solubility in water of individual components of HDES.

| HDES components | Water solubility (g/100 g water) | Temperature (ºC) | Ref. |
|---|---|---|---|
| L-menthol | 0.038 | 25 | [22] |
| Octanoic acid | 0.079 | 30 | |
| Decanoic acid | 0.018 | 30 | [23] |
| Dodecanoic acid | 0.0063 | 30 | |
| 1-Decanol | 0.0037 | 25 | [24] |
| 1-Dodecanol | 0.0004 | 25 | |

**Table B.5.** $2^3$ factorial planning.

| Run | Coded variables | | |
|---|---|---|---|
| | $X_1$ | $X_2$ | $X_3$ |
| 1 | -1 | -1 | -1 |
| 2 | 1 | -1 | -1 |
| 3 | -1 | 1 | -1 |
| 4 | 1 | 1 | -1 |
| 5 | -1 | -1 | 1 |
| 6 | 1 | -1 | 1 |
| 7 | -1 | 1 | 1 |
| 8 | 1 | 1 | 1 |
| 9 | -1.68 | 0 | 0 |
| 10 | 1.68 | 0 | 0 |
| 11 | 0 | -1.68 | 0 |
| 12 | 0 | 1.68 | 0 |
| 13 | 0 | 0 | -1.68 |
| 14 | 0 | 0 | 1.68 |
| 15 | 0 | 0 | 0 |
| 16 | 0 | 0 | 0 |
| 17 | 0 | 0 | 0 |
| 18 | 0 | 0 | 0 |
| 19 | 0 | 0 | 0 |
| 20 | 0 | 0 | 0 |

**Table B.6.** Coded levels of independents variables used in the factorial planning of response surface methodology.

| Independent variables | Axial | Factorial | Central | Factorial | Axial |
|---|---|---|---|---|---|
| | **-1.682** | **-1** | **0** | **1** | **1.682** |
| **$X_1$ - pH** | 2.0 | 2.8 | 4.0 | 5.2 | 6.0 |
| **$X_2$ - OFX concentration(mg/ml)** | 0.5 | 0.9 | 1.5 | 2.1 | 2.5 |
| **$X_3$ - ES-water ratio (v/v)** | 0.6 | 0.9 | 1.3 | 1.8 | 2.1 |

**Table B.7.** Predicted logarithm of partition coefficient of OFX ($\log(K_{OFX})$) for the HDES in different molar ratios (2:1, 1:1 and 1:2), at 25 ° C using COSMO-RS.

| HDES | Molar ratio | | |
|---|---|---|---|
| | **1:2** | **1:1** | **2:1** |
| Menthol: C8 acid | 2.36 | 2.04 | 1.53 |
| Menthol: C10 acid | 2.53 | 2.18 | 1.66 |
| Menthol: C12 acid | 2.61 | 2.24 | 1.79 |
| Menthol: C10 alcohol | 0.93 | 0.63 | 0.60 |
| Menthol: C12 alcohol | 0.83 | 0.43 | 0.51 |
| C8 acid: C10 acid | 2.93 | 2.58 | 3.33 |
| C8 acid: C12 acid | 3.44 | 3.04 | 3.71 |
| C10 acid: C12 acid | 3.55 | 3.23 | 4.41 |
| C8 acid: C10 alcohol | 1.38 | 1.90 | 3.17 |
| C8 acid: C12 alcohol | 1.34 | 1.73 | 2.91 |
| C10 acid: C10 alcohol | 1.57 | 2.16 | 3.51 |
| C10 acid: C12 alcohol | 1.15 | 1.71 | 2.36 |

**Table B.8.** The measured partition coefficient of OFX and extraction efficiency of OFX along with the initial pH of each system for the selected HDES at 25 °C.

| HDES | Molar ratio | pH | Measured $K_{OFX}$ | Error | Measured $EE_{OFX}$ (%) | Error |
|---|---|---|---|---|---|---|
| Menthol: C8 acid | (1:2) | 3.98 | 3.11 | 0.21 | 75.64 | 1.30 |
| Menthol: C10 acid | (1:2) | 4.55 | 6.58 | 0.31 | 86.80 | 0.54 |
| Menthol: C10 acid | (1:3) | 4.32 | 6.38 | 0.07 | 86.64 | 0.35 |
| C8 acid: C10 acid | (2:1) | 3.80 | 3.75 | 0.22 | 78.95 | 0.72 |
| C8 acid: C12 acid | (2:1) | 3.92 | 4.51 | 0.07 | 81.83 | 0.31 |
| C10 acid: C12 acid | (2:1) | 4.40 | 7.35 | 0.24 | 88.02 | 0.35 |
| C10 acid: C12 acid | (3:1) | 3.93 | 5.50 | 0.04 | 84.62 | 0.09 |
| C8 acid: C10 alcohol | (2:1) | 4.05 | 2.77 | 0.11 | 73.49 | 0.77 |
| C10 acid: C10 alcohol | (2:1) | 4.60 | 7.01 | 0.12 | 82.87 | 1.16 |
| C10 acid: C10 alcohol | (3:1) | 4.10 | 4.66 | 0.33 | 82.30 | 1.04 |

**Table B.9.** Summary of different characteristics and prices of some of the compounds used in LLE of OFX. Prices sourced from official pages of Merck in Portugal (https://www.sigmaaldrich.com/PT/) and Alibaba (https://www.alibaba.com/) as of 19/03/24.

| | | | | | **Merck** | **Alibaba** | |
|---|---|---|---|---|---|---|---|
| **Compound** | **Solvent Type** | **CAS** | **Melting Point (°C)** | **Boiling Point (°C)** | **Price (€/kg or €/L*)** | **Price ($/kg)** | **Price (€/kg)**** |
| **Decanoic acid** | Fatty Acid | 334-48-5 | 31.7 | 268.7 | 72.0 | 0.3 - 20.0 | 0.3 - 17.0 |
| **Dodecanoic acid** | Fatty Acid | 143-07-7 | 44.3 | 297.9 | 52.1 | 1.0 - 10.0 | 0.9 - 8.5 |
| **Heptanoic acid** | Fatty Acid | 111-14-8 | -10.5 | 223 | 147.2 | 1.0 - 5.0 | 0.9 – 4.3 |
| **Nonanoic acid** | Fatty Acid | 112-05-0 | 12.5 | 255.6 | 75.3 | 0.8 - 20.0 | 0.7 - 17.0 |
| **1-ethyl-3-methylimidazolium trifluoromethanesulfonate** | Ionic Liquid | 145022-44-2 | | --- | 1,730.0 | 50.0 - 220.0 | 42.5 - 187.0 |
| **Thymol** | Terpene | 89-83-8 | 47-51 | 232-234 | 178.0 | 1.0- 35.0 | 0.9 - 29.8 |
| **Tetrachloroethane** | Volatile Organic | 79-34-5 | -22.9 | 146.7 | 226.0 | 2.1- 3.5 | 1.8 – 3.0 |
| **L-menthol** | Terpene/Alcohol | 2216-51-5 | 42-45 | | 137.0 | 1.0- 50.0 | 0.9 - 42.5 |
| **Decanol** | Alcohol | 112-30-1 | 9.4 | | 64.3 | 1.0- 10.0 | 0.9 - 8.5 |

*Tetrachloroethan; **Assuming exchange rate of 1 US dollar (USD) being equivalent to 0.85 euros (EUR).

**Table B.10.** Experimental data of the partition coefficient and extraction efficiency of OFX obtained through a central composite design, using C10 acid: C12 acid (2:1) HDES.

| | Real variables | | | |
|---|---|---|---|---|
| **Run** | **pH** | **OFX concentration** | **HDES-water ratio (v/v)** | **OFX extraction efficiency ($EE_{OFX}$%)** |
| 1 | 2.8 | 0.9 | 0.85 | 15.43 |
| 2 | 5.2 | 0.9 | 0.85 | 98.06 |
| 3 | 2.8 | 2.1 | 0.85 | 14.19 |
| 4 | 5.2 | 2.1 | 0.85 | 98.10 |
| 5 | 2.8 | 0.9 | 1.75 | 27.01 |
| 6 | 5.2 | 0.9 | 1.75 | 98.74 |
| 7 | 2.8 | 2.1 | 1.75 | 14.27 |
| 8 | 5.2 | 2.1 | 1.75 | 98.83 |
| 9 | 2.0 | 1.5 | 1.30 | 2.94 |
| 10 | 6.0 | 1.5 | 1.30 | 99.25 |
| 11 | 4.0 | 0.5 | 1.30 | 85.22 |
| 12 | 4.0 | 2.5 | 1.30 | 86.81 |
| 13 | 4.0 | 1.5 | 0.54 | 85.85 |
| 14 | 4.0 | 1.5 | 2.06 | 77.18 |
| 15 | 4.0 | 1.5 | 1.30 | 79.06 |
| 16 | 4.0 | 1.5 | 1.30 | 77.80 |
| 17 | 4.0 | 1.5 | 1.30 | 78.91 |
| 18 | 4.0 | 1.5 | 1.30 | 78.85 |
| 19 | 4.0 | 1.5 | 1.30 | 79.20 |
| 20 | 4.0 | 1.5 | 1.30 | 78.33 |

**Table B.11.** Regression coefficients of the predicted second-order polynomial model for the OFX extraction efficiency obtained from the RSM, $R^2 = 0.94$ and $R_{adj}^2 = 0.89$.

| | Regression coefficients | Standard deviation | t-student (10) | p-value |
|---|---|---|---|---|
| **Mean/Interc.** | -207.03 | 3.55 | -58.25 | <0.0001 |
| **(1) pH (L)** | 100.13 | 0.98 | 101.59 | <0.0001 |
| **pH (Q)** | -8.89 | 0.10 | -91.74 | <0.0001 |
| **(2) $C_{OFX}$ (mg/ml) (L)** | -0.45 | 1.82 | -0.25 | 0.81 |
| **$C_{OFX}$ (mg/ml) (Q)** | -1.27 | 0.39 | -3.29 | 0.02 |
| **(3) HDES-Water ratio (v/v) (L)** | 43.50 | 2.51 | 17.30 | <0.0001 |
| **HDES-Water ratio (v/v) (Q)** | -10.12 | 0.69 | -14.68 | <0.0001 |
| **1L by 2L** | 2.45 | 0.26 | 9.41 | <0.0001 |
| **1L by 3L** | -2.37 | 0.35 | -6.84 | <0.0001 |
| **2L by 3L** | -5.30 | 0.69 | -7.64 | <0.0001 |

**Table B.12.** ANOVA data for the OFX extraction efficiency obtained from the RSM.

| | SS | DF | Mean square | F | p-value |
|---|---|---|---|---|---|
| Regress. | 19657.08 | 9 | 2184.12 | 17.98 | <0.0001 |
| Residual | 1214.58 | 10 | 121.46 | | |
| Total | 20871.66 | | | | |

**Table B.13.** The simulation parameters for RDF analysis.

| **Molecule 1** | **Molecule 2 (HDES)** | **Molar ratio (HBA:HBD)** | **Density ($g/cm^3$)** | **Molecule1:Molecule2** | **Box size A×B×C ($Å^3$)** |
|---|---|---|---|---|---|
| Ofloxacin | L-menthol:C10 acid | (1:2) | 0.896 | 5:100 | 21.5×21.5×21.5 |
| Ofloxacin | L-menthol:C10 acid | (2:1) | 0.896 | 5:100 | 21.3×21.3×21.3 |
| Ofloxacin | C8 acid:C10 acid | (2:1) | 0.901 | 5:100 | 20.9×20.9×20.9 |
| Ofloxacin | C10 acid:C12 acid | (2:1) | 0.892 | 5:100 | 22.1×22.1×22.1 |
| Ofloxacin | C10 acid:C10 alcohol | (2:1) | 0.849 | 5:100 | 21.9×21.9×21.9 |

## Figures

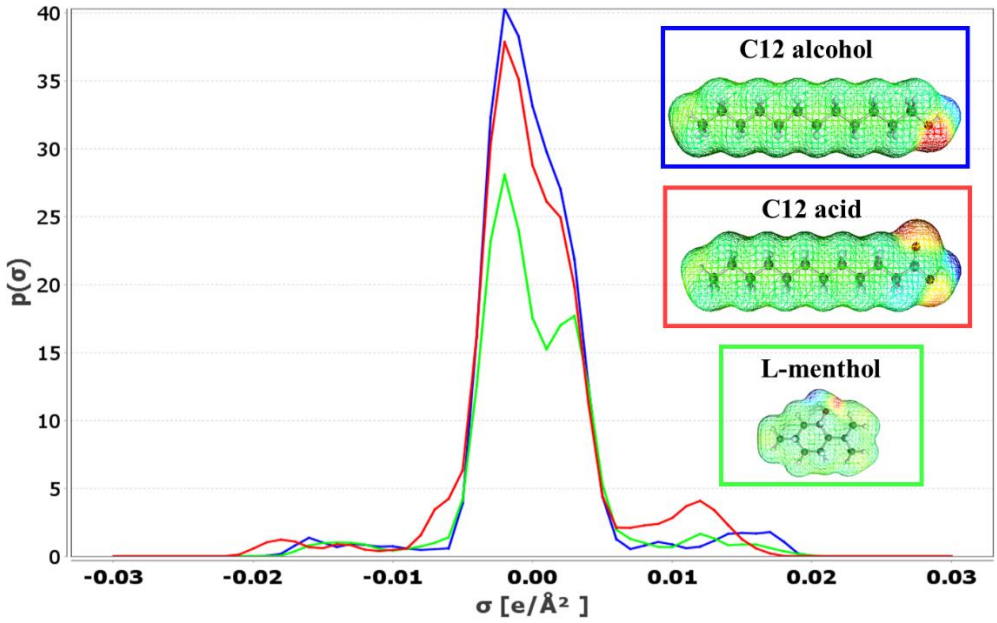


**Figure B.1.** The σ-profiles of the components studied in the HDES formation.

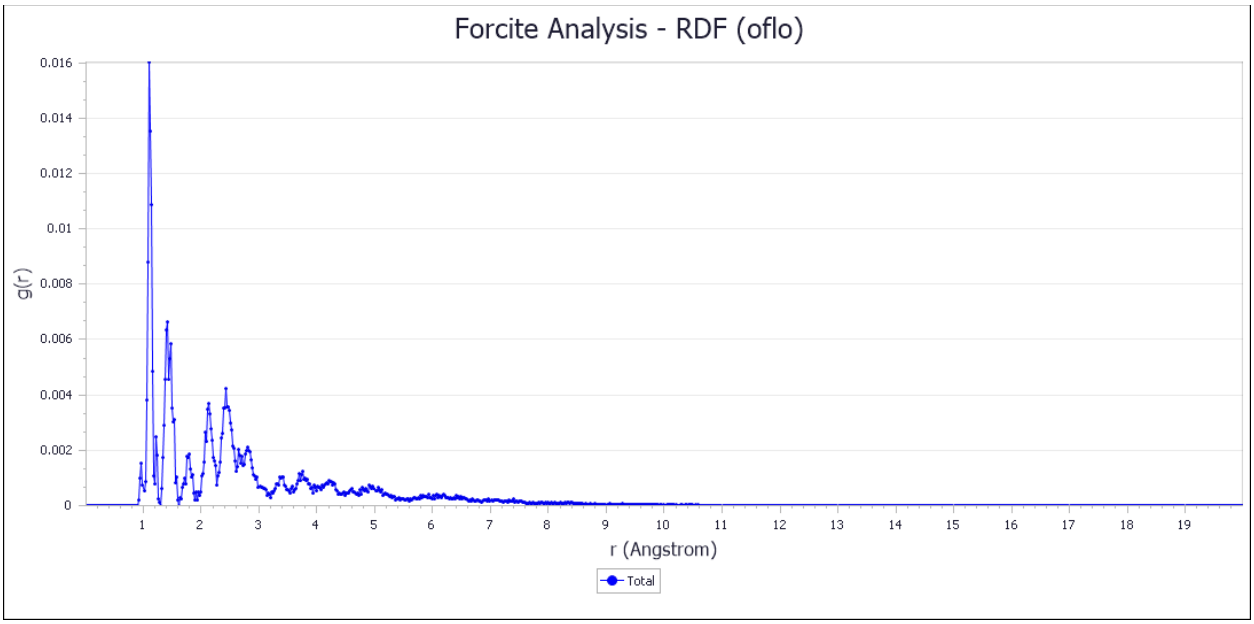


**Figure B.2.** Radial distribution function (RDF) L-menthol:C10 acid (1:2) between the and OFX.

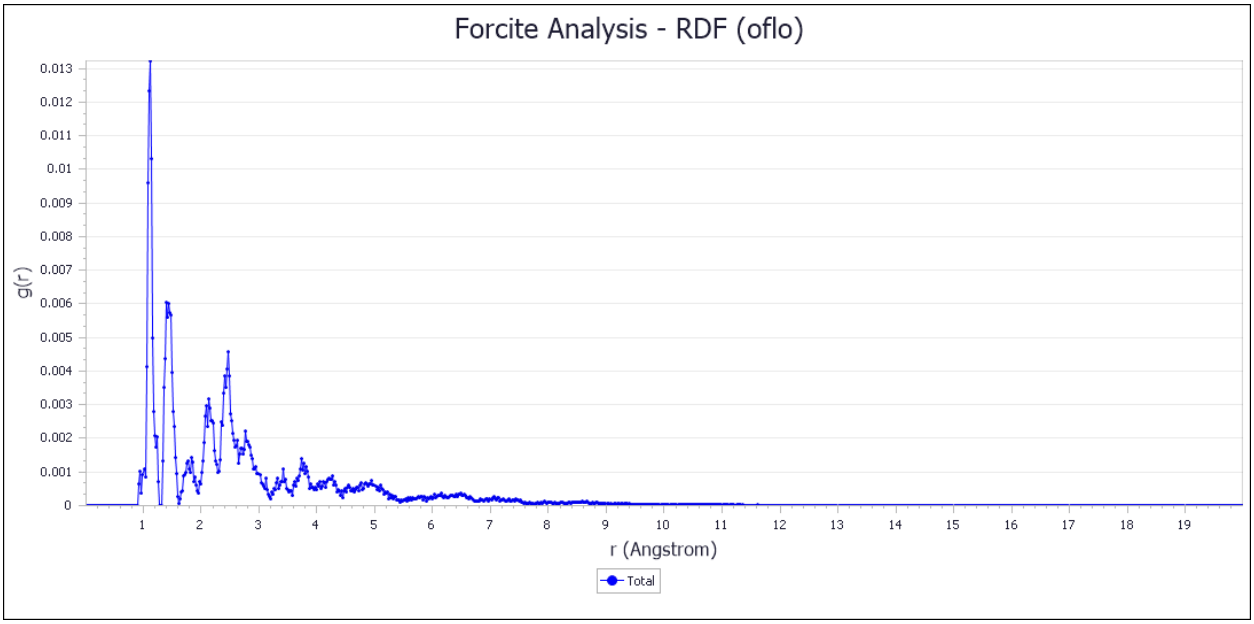


**Figure B.3.** Radial distribution function (RDF) L-menthol:C10 acid (2:1) between the and OFX.

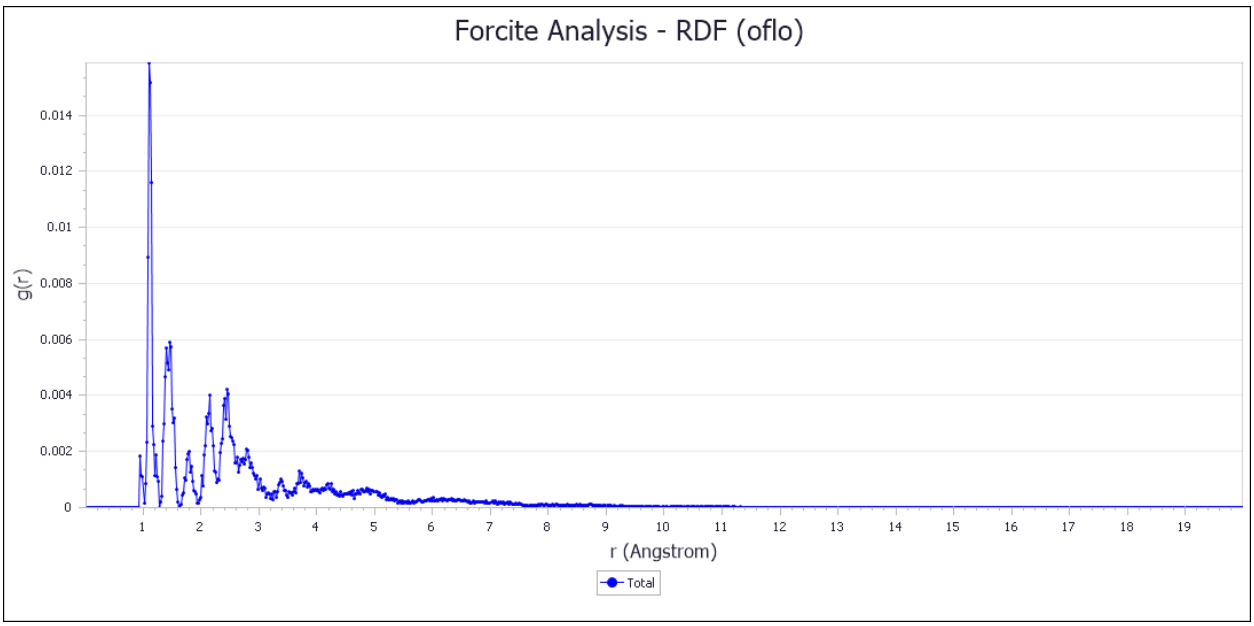


**Figure B.4.** Radial distribution function (RDF) C8 acid:C10 acid (2:1) between the and OFX.

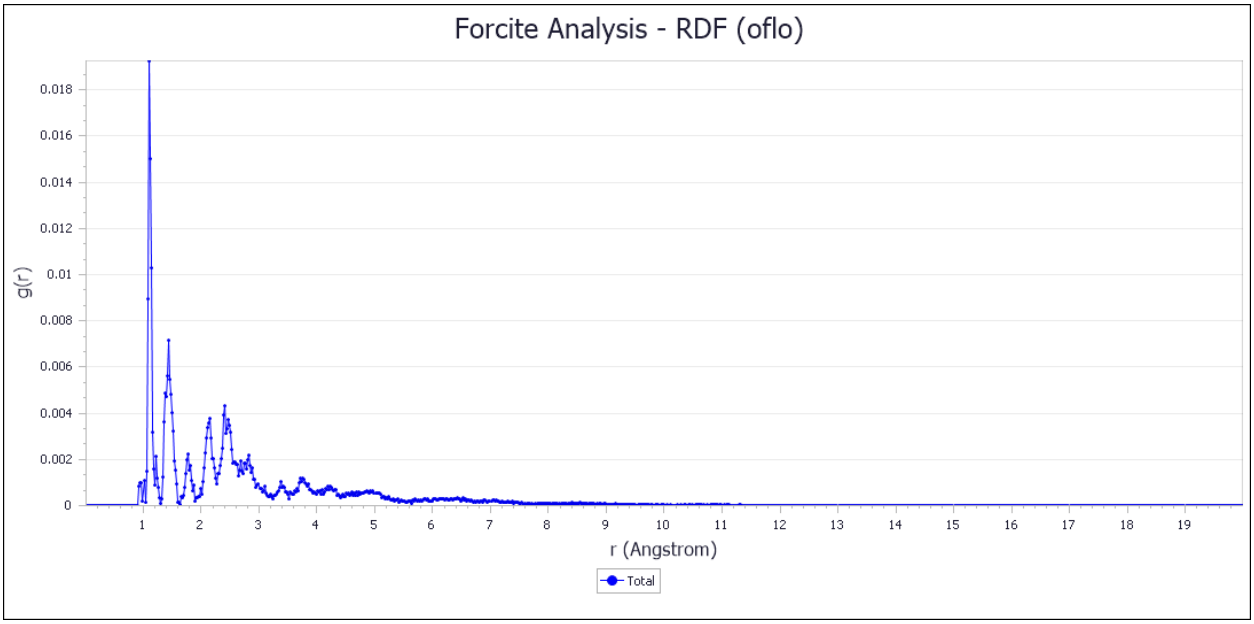


**Figure B.5.** Radial distribution function (RDF) C10 acid:C12 acid (2:1) between the and OFX.

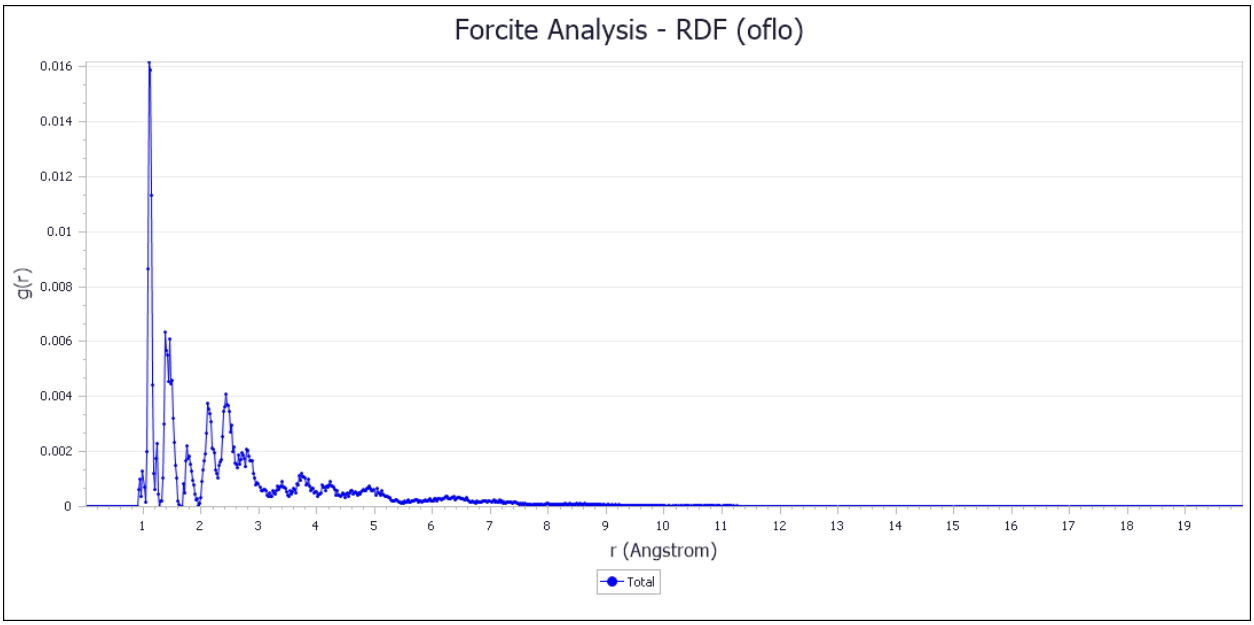


**Figure B.6.** Radial distribution function (RDF) C10 acid:C10 alcohol (2:1) between the and OFX.

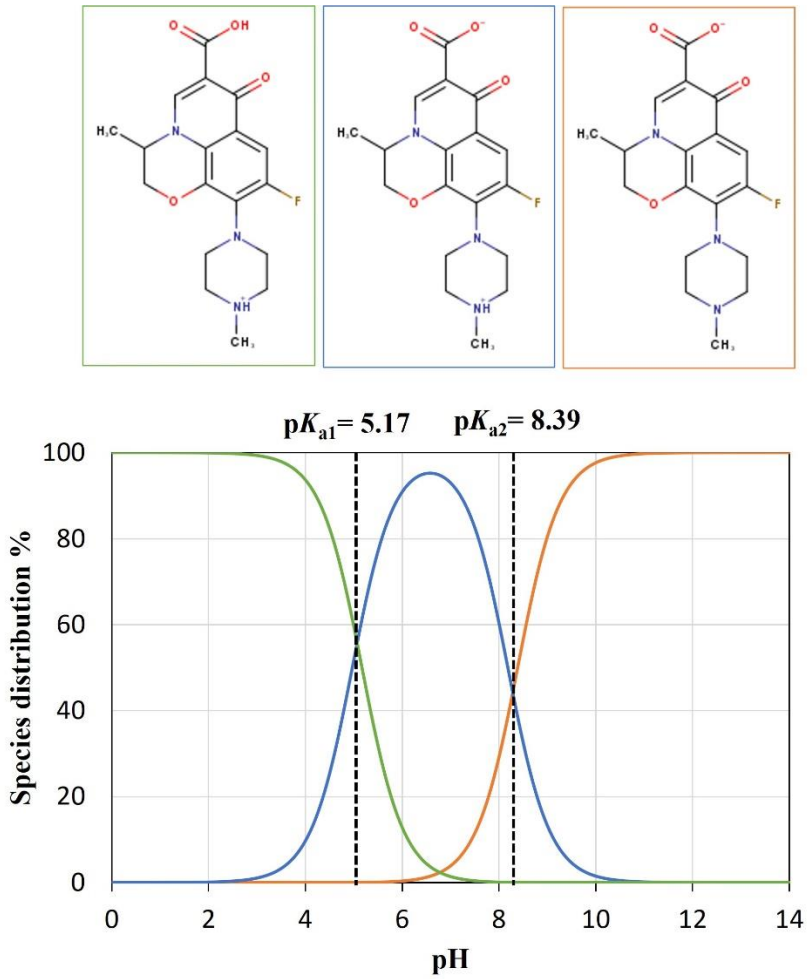


**Figure B.7.** Distribution of distinct forms of OFX at different values of pH [25].

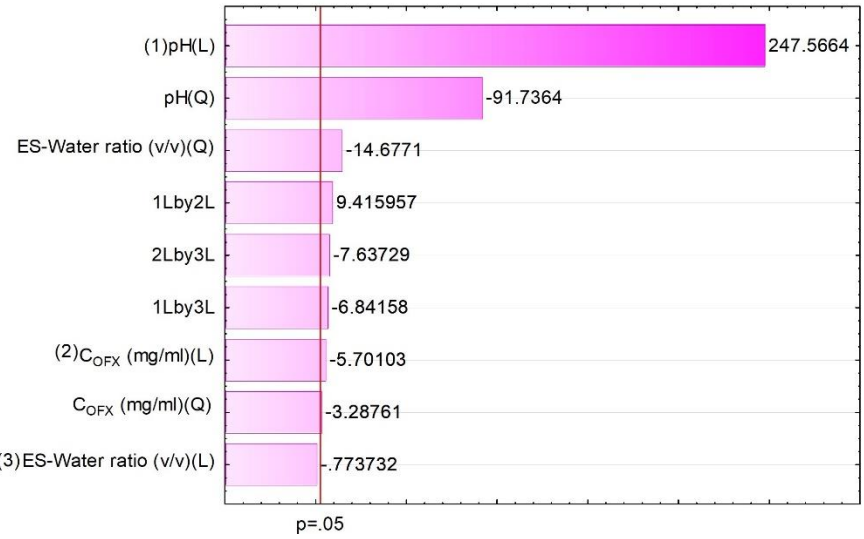


**Figure B.8.** Pareto chart for the standardized main effects in the factor central composite design for the OFX extraction efficiency ($EE_{OFX}$%), with 95% of confidence.

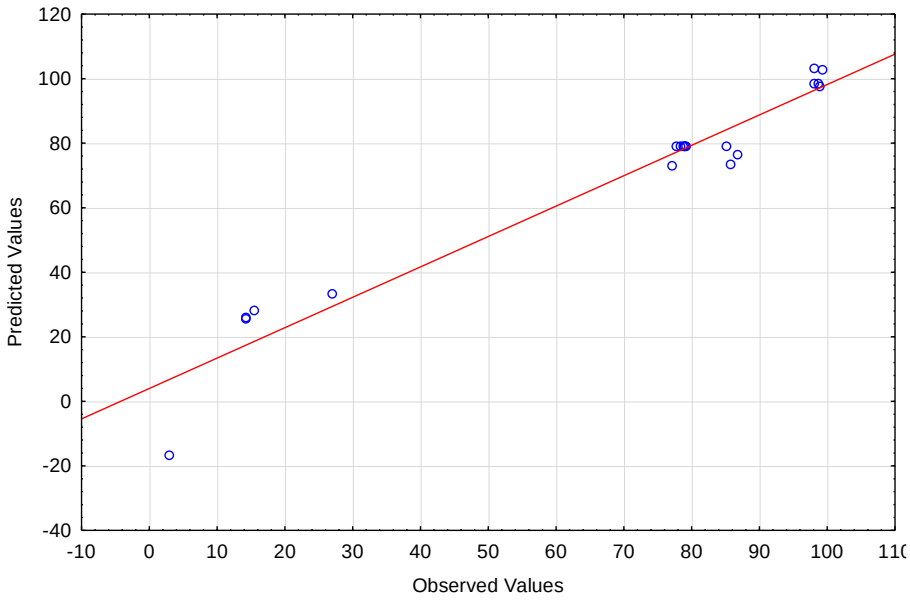


**Figure B.9.** Predict *vs* observed values of the OFX extraction efficiency ($EE_{OFX}$%) from central composite design.

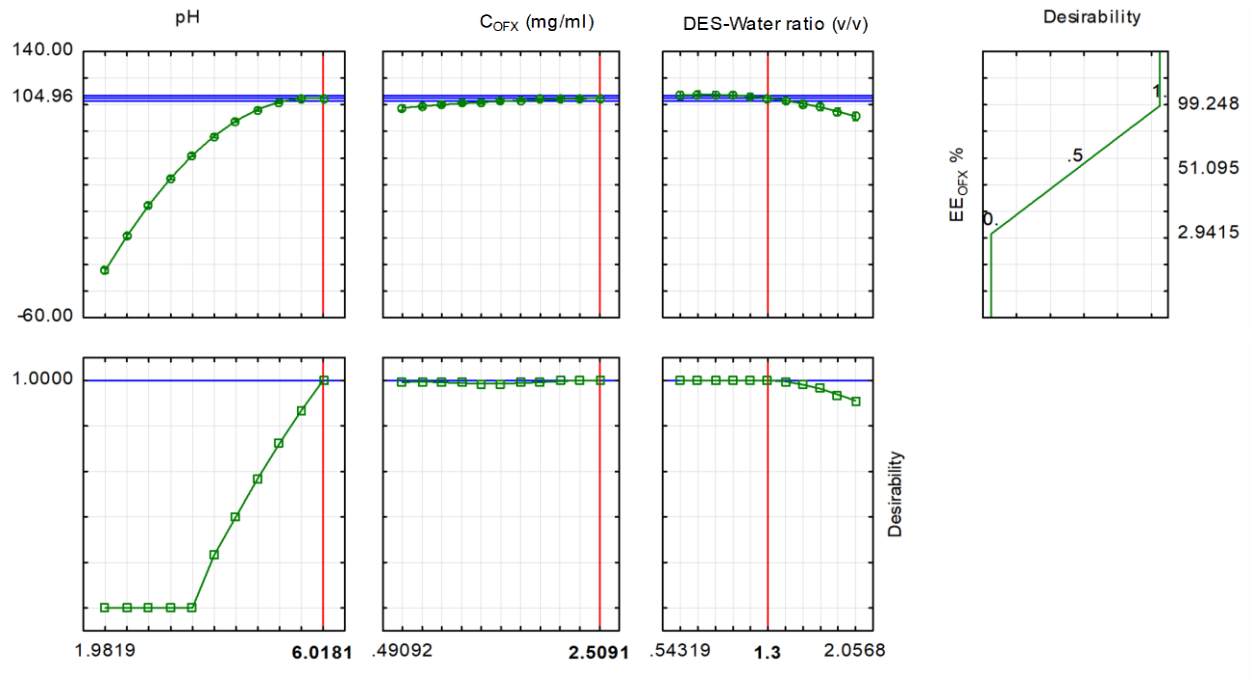


**Figure B.10.** The optimized conditions for maximum partition and extraction of OFX.

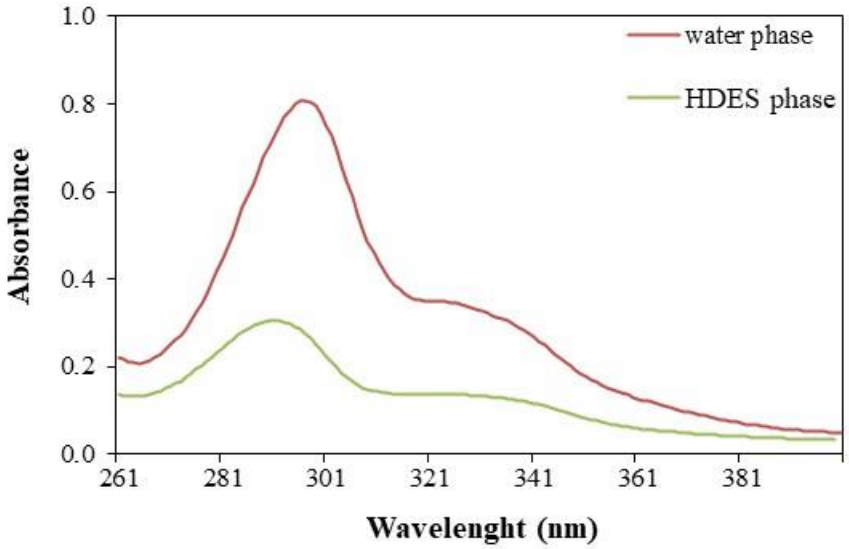


**Figure B.11.** UV-Vis spectra showing the maximum wavelengths of OFX in water and HDES phases.

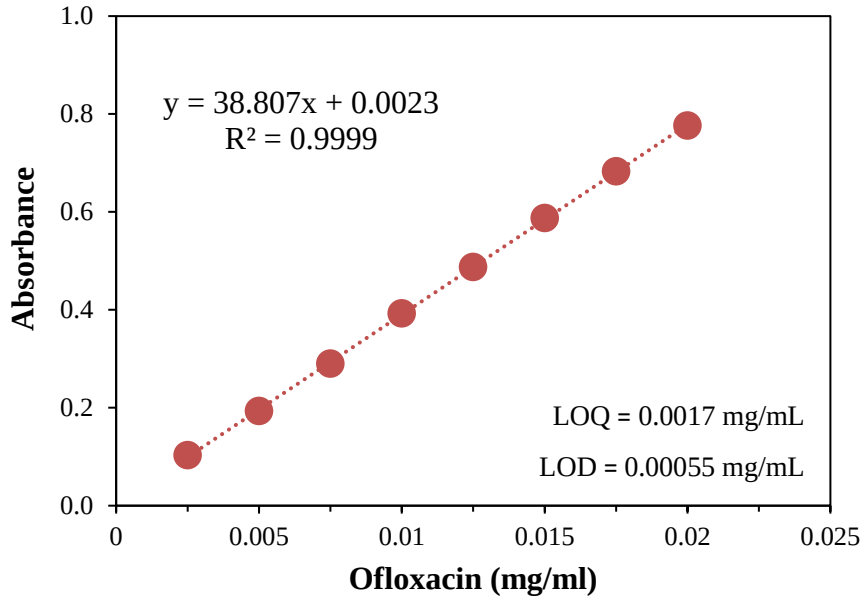


**Figure B.12.** Calibration curve of ofloxacin for water phase, where LOQ corresponds to the limit of quantification and LOD corresponds to the limit of detection.

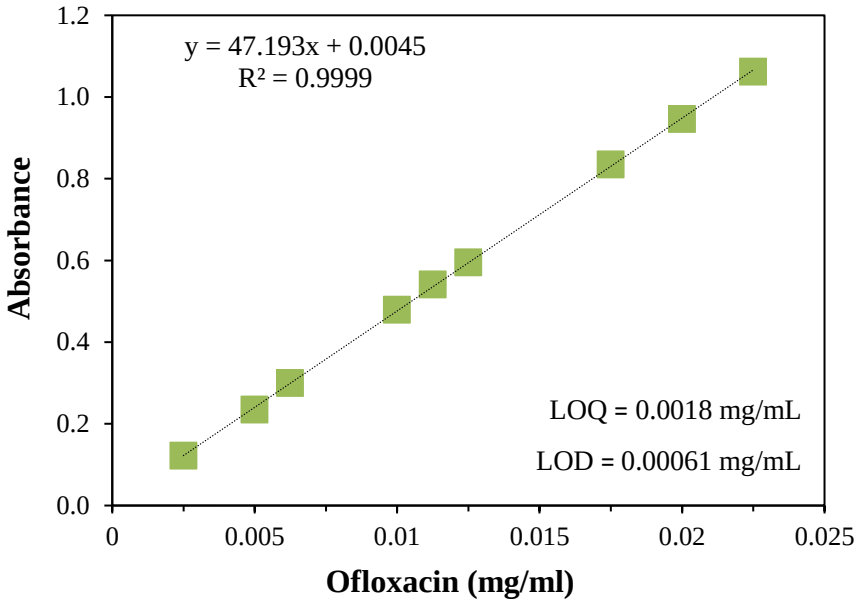


**Figure B.13.** Calibration curve of ofloxacin for HDES phase, where LOQ corresponds to the limit of quantification and LOD corresponds to the limit of detection.

## Procedures

### *Liquid-Liquid Extraction (LLE)*

The extraction was performed by mixing an equal volume of the HDES and an aqueous solution containing OFX at a concentration of 1 mg/ml. The initial mixture was stirred at 50 rpm and (25 ± 1) °C for at least 12 h to promote contact between the two phases. Afterward, the HDES was completely separated from the water phase by centrifugation (at 10000 rpm for 10 min in an Eppendorf 5804 centrifuge). In the studied LLE, the top phase corresponds to the HDES phase, while the bottom phase is the water phase. After a careful separation of phases, the OFX was quantified in both phases by a UV-spectrophotometry utilizing a SYNERGY|HT microplate reader, BioTek, at a wavelength of 297 nm and 292 nm for HDES and water phases (see Figure B.11), respectively, using calibration curves (see Figures B.12 and B.13) previously established. At least three different experiments were performed to determine the average values for partition coefficient and extraction efficiency and their respective standard deviations. In addition, the possible influence of solvents on the quantification method was evaluated using blank control samples.

### *The radial distribution function (RDF) analysis*

The radial distribution function analysis (RDF) for measuring intermolecular interactions was conducted using Material Studio's forcite module, following reported methods from previous studies and Material Studio tutorials [26]. To ensure consistent and accurate results during the simulation, specifying input parameters such as the number of molecules and density is crucial (refer to Table B.13 for these data). Moreover, in Material Studio, the choice of forcefield and step length is pivotal, as their sizes influence the duration of computer simulations and the accuracy of performance. In the present analysis, a step length of 1fs and the COMPASS forcefield were selected through extensive trial and error. Following the replication of 3D structures of molecules, geometry optimization was carried out to attain the stable molecular structure. The initial simulation model in the Materials Studio Software was created using the Amorphous Cell module. Initially, the atoms of the model do not evenly share the cubic unit cell. To address this, geometry optimization is performed in the forcite module to minimize the overall energy of the simulation box. Employing three-dimensional periodic boundary conditions, the cell utilizes the Ewald electrostatic

summation method [26]. Energy minimization is carried out using the smart minimization method. Subsequently, under the NVT ensemble (a simulation protocol where the number of atoms (N), volume (V), and temperature (T) are assumed to be constant), a 200 ps Molecular Dynamics (MD) run is conducted to achieve appropriate cell equilibration [26]. To produce a more realistic model, the amorphous cell or simulation model undergoes annealing. A time step of 1fs is chosen to prevent overlap of molecules within the box. To maintain a constant pressure of 1 atm and attain equilibrium density, the simulation box includes 100 molecules of each HDES and 5 molecules of ofloxacin.

## References


[1] H. Sereshti, F. Karami, N. Nouri, A green dispersive liquid-liquid microextraction based on deep eutectic solvents doped with β-cyclodextrin: Application for determination of tetracyclines in water samples, Microchemical Journal 163 (2021) 105914.

[2] W. Ma, K.H. Row, pH-induced deep eutectic solvents based homogeneous liquid-liquid microextraction for the extraction of two antibiotics from environmental water, Microchemical Journal 160 (2021) 105642.

[3] L. Qiao, R. Sun, C. Yu, Y. Tao, Y. Yan, Novel hydrophobic deep eutectic solvents for ultrasound-assisted dispersive liquid-liquid microextraction of trace non-steroidal anti-inflammatory drugs in water and milk samples, Microchemical Journal 170 (2021) 106686.

[4] K. Li, Y. Jin, D. Jung, K. Park, H. Kim, J. Lee, In situ formation of thymol-based hydrophobic deep eutectic solvents: Application to antibiotics analysis in surface water based on liquid-liquid microextraction followed by liquid chromatography, J Chromatogr A 1614 (2020) 460730.

[5] F. Shakirova, A. Shishov, A. Bulatov, Automated liquid-liquid microextraction and determination of sulfonamides in urine samples based on Schiff bases formation in natural deep eutectic solvent media, Talanta 234 (2021) 122660.

[6] A.Y. Shishov, M. V. Chislov, D. V. Nechaeva, L.N. Moskvin, A. V. Bulatov, A new approach for microextraction of non-steroidal anti-inflammatory drugs from human urine samples based on in-situ deep eutectic mixture formation, J Mol Liq 272 (2018) 738–745.

[7] Y. Liu, W. Xu, H. Zhang, W. Xu, Hydrophobic deep eutectic solvent-based dispersive liquid–liquid microextraction for the simultaneous enantiomeric analysis of five β-agonists in the environmental samples, Electrophoresis 40 (2019) 2828–2836.

[8] C. Florindo, F. Lima, L.C. Branco, I.M. Marrucho, Hydrophobic Deep Eutectic Solvents: A Circular Approach to Purify Water Contaminated with Ciprofloxacin, ACS Sustain Chem Eng 7 (2019) 14739–14746.

[9] X. Di, X. Zhao, X. Guo, Hydrophobic deep eutectic solvent as a green extractant for high-performance liquid chromatographic determination of tetracyclines in water samples, J Sep Sci 43 (2020) 3129–3135.

[10] H. Sereshti, G. Abdolhosseini, S. Soltani, F. Jamshidi, N. Nouri, Natural thymol-based ternary deep eutectic solvents: Application in air-bubble assisted-dispersive liquid-liquid microextraction for the analysis of tetracyclines in water, J Sep Sci 44 (2021) 3626–3635.

[11] W. Tang, Y. Dai, K.H. Row, Evaluation of fatty acid/alcohol-based hydrophobic deep eutectic solvents as media for extracting antibiotics from environmental water, Anal Bioanal Chem 410 (2018) 7325–7336.

[12] Q. Qu, Y. Lv, L. Liu, K.H. Row, T. Zhu, Synthesis and characterization of deep eutectic solvents (five hydrophilic and three hydrophobic), and hydrophobic application for microextraction of environmental water samples, Anal Bioanal Chem 411 (2019) 7489–7498.

[13] A.G. Pekel, E. Kurtulbaş, İ. Toprakçı, S. Şahin, Menthol-based deep eutectic solvent for the separation of carbamazepine: reactive liquid-liquid extraction, Biomass Convers Biorefin 12 (2022) 1249–1256.

[14] E. Kurtulbaş, A.G. Pekel, İ. Toprakçı, G. Özçelik, M. Bilgin, S. Şahin, Hydrophobic carboxylic acid based deep eutectic solvent for the removal of diclofenac, Biomass Convers Biorefin 12 (2022) 2219–2227.

[15] L. Chen, L. Ge, Q. Liang, Z. Zhao, K. Yang, Eutectic solvents formed by (+)-DTTA and L-menthol as novel chiral recognition and separation media for enantioselective extraction of valsartan enantiomers, J Mol Liq 368 (2022) 120818.

[16] ChemSpider, http://www.chemspider.com/ (accessed June 30, 2022).

[17] G. Teixeira, D.O. Abranches, O. Ferreira, J.A.P. Coutinho, Estimating the Melting Temperatures of Type V Deep Eutectic Solvents, Ind Eng Chem Res 62 (2023) 14638–14647.

[18] M.A.R. Martins, E.A. Crespo, P.V.A. Pontes, L.P. Silva, M. Bülow, G.J. Maximo, E.A.C. Batista, C. Held, S.P. Pinho, J.A.P. Coutinho, Tunable Hydrophobic Eutectic Solvents Based on Terpenes and Monocarboxylic Acids, ACS Sustain Chem Eng 6 (2018) 8836–8846.

[19] M.C. Costa, M. Sardo, M.P. Rolemberg, J.A.P. Coutinho, A.J.A. Meirelles, P. Ribeiro-Claro, M.A. Krähenbühl, The solid–liquid phase diagrams of binary mixtures of consecutive, even saturated fatty acids, Chem Phys Lipids 160 (2009) 85–97.

[20] C. Florindo, L. Romero, I. Rintoul, L.C. Branco, I.M. Marrucho, From Phase Change Materials to Green Solvents: Hydrophobic Low Viscous Fatty Acid-Based Deep Eutectic Solvents, ACS Sustain Chem Eng 6 (2018) 3888–3895.

[21] N.D.D. Carareto, T. Castagnaro, M.C. Costa, A.J.A. Meirelles, The binary (solid + liquid) phase diagrams of (caprylic or capric acid) + (1-octanol or 1-decanol), J Chem Thermodyn 78 (2014) 99–108.

[22] S.M. Vilas-Boas, M.C. da Costa, J.A.P. Coutinho, O. Ferreira, S.P. Pinho, Octanol-Water Partition Coefficients and Aqueous Solubility Data of Monoterpenoids: Experimental, Modeling, and Environmental Distribution, Ind Eng Chem Res 61 (2022) 3154–3167.

[23] K. Bober, M. Garus, RP-HPTLC Application in the Investigation of Solubility in Water of Long-Chain Fatty Acids, J Liq Chromatogr Relat Technol 29 (2006) 2787–2794.

[24] C.L. Yaws, J.R. Hopper, S.D. Sheth, M. Han, R.W. Pike, Solubility and henry's law constant for alcohols in water, Waste Management 17 (1998) 541–547.

[25] ChemAxon, MarvinSketch 22.13, (2022). http://www.chemaxon.com (accessed March 20, 2023).

[26] M. Sharif, X. Wu, Y. Yu, T. Zhang, Z. Zhang, Estimation of diffusivity and intermolecular interaction strength of secondary and tertiary amine for CO2 absorption process by molecular dynamic simulation, Mol Simul 48 (2022) 484–494.

# Appendix C

## Tables

**Table C.1.** $2^3$ factorial planning - central composite rotatable design (CCRD).

| Run | Coded variables | | |
|---|---|---|---|
| | $X_1$ | $X_2$ | $X_3$ |
| 1 | -1 | -1 | -1 |
| 2 | 1 | -1 | -1 |
| 3 | -1 | 1 | -1 |
| 4 | 1 | 1 | -1 |
| 5 | -1 | -1 | 1 |
| 6 | 1 | -1 | 1 |
| 7 | -1 | 1 | 1 |
| 8 | 1 | 1 | 1 |
| 9 | -1.68 | 0 | 0 |
| 10 | 1.68 | 0 | 0 |
| 11 | 0 | -1.68 | 0 |
| 12 | 0 | 1.68 | 0 |
| 13 | 0 | 0 | -1.68 |
| 14 | 0 | 0 | 1.68 |
| 15 | 0 | 0 | 0 |
| 16 | 0 | 0 | 0 |
| 17 | 0 | 0 | 0 |
| 18 | 0 | 0 | 0 |
| 19 | 0 | 0 | 0 |
| 20 | 0 | 0 | 0 |

**Table C.2.** Coded levels of independents variables used in the factorial planning - central composite rotatable design (CCRD).

| Independent variables | Axial | Factorial | Central | Factorial | Axial |
|---|---|---|---|---|---|
| | **-1.682** | **-1** | **0** | **1** | **1.682** |
| **$X_1$ - pH** | 3 | 3 | 4 | 5 | 5 |
| **$X_2$ - Excess of chiral selector (CS)** | 19.5 | 40.0 | 70.0 | 100.0 | 120.5 |
| **$X_3$ - HDES-water ratio (v/v)** | 0.5 | 0.9 | 1.3 | 1.8 | 2.1 |

**Table C.3.** Values of interaction energies, including hydrogen bonding (H-bond), electrostatic misfit (misfit), and van der Waals forces (vdW), calculated using COSMO-RS for aqueous mixtures of β-CD, S-β-CD, or CM-β-CD with OFX in either its zwitterionic or positive form, at 20-fold and 120-fold excess of the chiral selector.

| Energy (kcal/mol) | Zwitterionic OFX | | | | | Positive OFX |
|---|---|---|---|---|---|---|
| | 20x | | | 120x | | 120x |
| | β-CD | CM-β-CD | S-β-CD | CM-β-CD | S-β-CD | S-β-CD |
| misfit | 5.61 | 5.62 | 5.52 | 5.59 | 5.77 | 5.90 |
| H-Bond | -10.10 | -10.07 | -9.95 | -12.66 | -9.40 | -12.21 |
| vdW | -13.84 | -13.83 | -13.76 | -14.01 | -13.75 | -13.83 |

**Table C.4.** Selectivity of OFX ($\alpha_{R\text{-}OFX/S\text{-}OFX}$) for each system (bars) and pH (circles), using the chiral selector CM-β-CD at a 120-fold excess. Experiments were conducted at 25°C.

| HDES | Molar ratio | pH | $\alpha_{R\text{-}OFX/S\text{-}OFX}$ | Error |
|---|---|---|---|---|
| L-menthol: C8 acid | (1:2) | 4.8 | 1.19 | 0.03 |
| L-menthol: C10 acid | (1:2) | 4.6 | 1.42 | 0.04 |
| L-menthol: C10 acid | (1:3) | 4.5 | 1.85 | 0.05 |
| L-menthol: C10 alcohol | (2:1) | 6.3 | 0.92 | 0.04 |
| L-menthol: C12 alcohol | (2:1) | 6.2 | 0.97 | 0.08 |
| C8 acid: C10 acid | (2:1) | 4.5 | 1.43 | 0.03 |
| C8 acid: C12 acid | (2:1) | 4.6 | 1.60 | 0.03 |
| C10 acid: C12 acid | (2:1) | 4.4 | 2.01 | 0.06 |
| C10 acid: C12 acid | (3:1) | 4.7 | 1.34 | 0.04 |
| C8 acid: C10 alcohol | (2:1) | 4.7 | 1.26 | 0.05 |
| C8 acid: C12 alcohol | (2:1) | 5 | 1.12 | 0.04 |
| C10 acid: C10 alcohol | (2:1) | 4.5 | 1.36 | 0.04 |
| C10 acid: C10 alcohol | (3:1) | 4.5 | 1.5 | 0.03 |
| C10 acid: C12 alcohol | (2:1) | 5.3 | 1.31 | 0.04 |

**Table C.5.** Experimental data of the selectivity of OFX ($\alpha_{R\text{-}OFX/S\text{-}OFX}$) obtained through a central composite rotatable design, using C10 acid: C12 acid (2:1) as HDES and CM-β-CD as chiral selector.

| Run | variables | | | $\alpha_{R\text{-}OFX/S\text{-}OFX}$ |
|---|---|---|---|---|
| | pH | Excess of chiral selector | HDES-water ratio (v/v) | |
| 1 | 3.4 | 40 | 0.85 | 2.80 |
| 2 | 4.6 | 40 | 0.85 | 1.82 |
| 3 | 3.4 | 100 | 0.85 | 3.44 |
| 4 | 4.6 | 100 | 0.85 | 2.54 |
| 5 | 3.4 | 40 | 1.75 | 2.31 |
| 6 | 4.6 | 40 | 1.75 | 1.33 |
| 7 | 3.4 | 100 | 1.75 | 2.90 |
| 8 | 4.6 | 100 | 1.75 | 1.98 |
| 9 | 3 | 70 | 1.3 | 2.43 |
| 10 | 5 | 70 | 1.30 | 1.51 |
| 11 | 4 | 20 | 1.3 | 1.71 |
| 12 | 4 | 120 | 1.30 | 2.21 |
| 13 | 4 | 70 | 0.54 | 3.76 |
| 14 | 4 | 70 | 2.06 | 1.90 |
| 15 | 4 | 70 | 1.3 | 2.74 |
| 16 | 4 | 70 | 1.3 | 2.80 |
| 17 | 4 | 70 | 1.3 | 2.72 |
| 18 | 4 | 70 | 1.3 | 2.70 |
| 19 | 4 | 70 | 1.3 | 2.77 |
| 20 | 4 | 70 | 1.3 | 2.69 |

**Table C.6.** Regression coefficients of the predicted second-order polynomial model for the selectivity of OFX ($\alpha$) obtained from the central composite rotatable design, $R^2 = 0.92$.

| | **Regression coefficients** | **Standard deviation** | **t-student (10)** | **p-value** |
|---|---|---|---|---|
| Mean | 2.7446 | 0.1409 | 19.4755 | 0.0000 |
| $x_1$ | -0.3628 | 0.0662 | -5.4816 | 0.0009 |
| $x_1^2$ | -0.2500 | 0.0728 | -3.4323 | 0.0110 |
| $x_2$ | 0.2011 | 0.0662 | 3.0391 | 0.0189 |
| $x_2^2$ | -0.2539 | 0.0728 | -3.4861 | 0.0102 |
| $x_3$ | -0.3906 | 0.0662 | -5.9026 | 0.0006 |
| $x_3^2$ | 0.0538 | 0.0728 | 0.7387 | 0.4841 |
| $x_1$ $x_2$ | 0.0989 | 0.0865 | 1.1437 | 0.2903 |
| $x_1$ $x_3$ | 0.0128 | 0.0865 | 0.1477 | 0.8867 |
| $x_2$ $x_3$ | 0.0069 | 0.0865 | 0.0802 | 0.9383 |

**Table C.7.** ANOVA data for the selectivity of OFX ($\alpha$) obtained from the central composite rotatable design.

| | **SS** | **DF** | **Mean square** | **Fcal** | **p-valor** | **Ftab** |
|---|---|---|---|---|---|---|
| Regression | 6 | 5 | 1 | 24.3 | <0.0001 | 3.20 |
| Residuals | 1 | 11 | 0 | | | |
| Fitting | 1 | 9 | 0 | 16.5 | 0.0585 | 19.38 |
| Pure error | 0 | 2 | 0 | | | |
| Total | 6 | 16 | | | | |
| $R^2$ = | 0.92 | | | | | |

## Figures

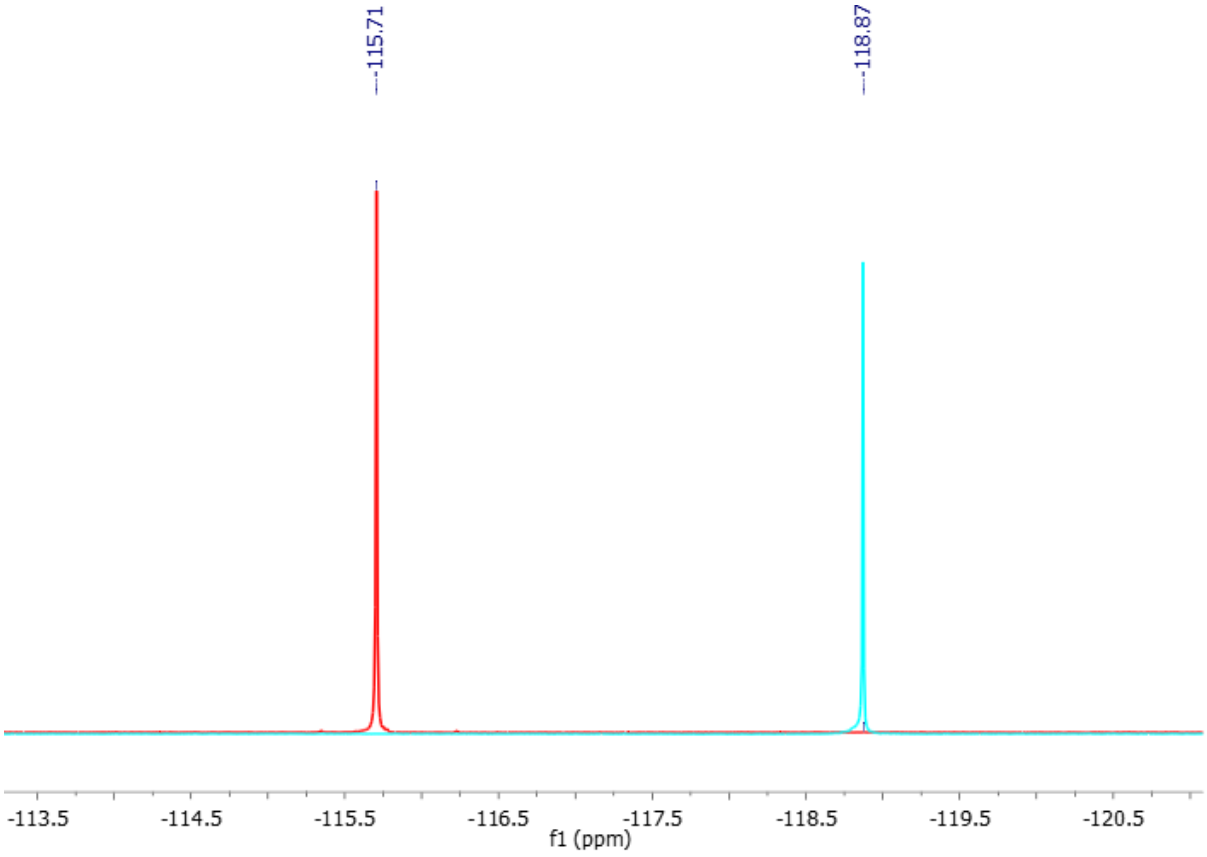


**Figure C.1.** The $^{1}$H-decoupled $^{19}$F NMR spectrum of OFX (red) along with the $^{19}$F NMR spectrum of the internal standard (NaF, blue).

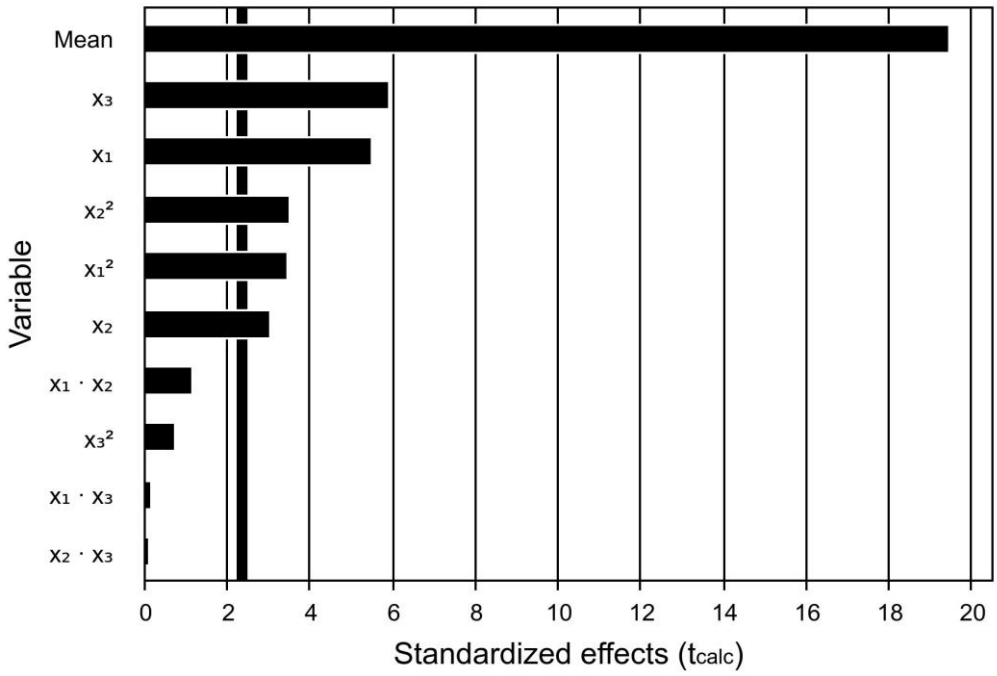


**Figure C.2.** Pareto chart for the standardized main effects in the selectivity of OFX ($\alpha$), with 95% of confidence.

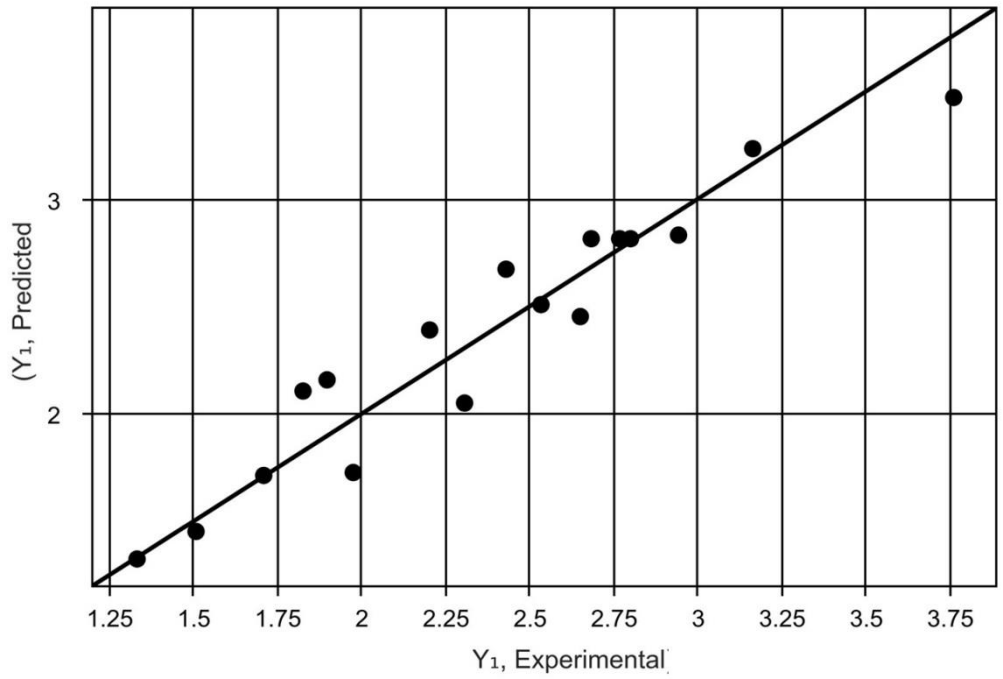


**Figure C.3.** Predict *vs.* observed values of the selectivity of OFX ($\alpha$).